NASA CONTRACTOR REPORT

NASA CR-1786

NASA CR-1786

RADIATION EFFECTS DESIGN HANDBOOK

Section 2. Thermal-Control Coatings

by N. J. Broadway

Prepared by
RADIATION EFFECTS INFORMATION CENTER
BATTELLE MEMORIAL INSTITUTE
Columbus, Ohio 43201
for

NATIONAL AERONAUTICS AND SPACE ADMINISTRATION • WASHINGTON, D. C. • JUNE 1971

1. Report No.	2. Government Accession No.	3. Recipient's Catalog No.
NASA CR-1786		

4. Title and Subtitle	5. Report Date
RADIATION EFFECTS DESIGN HANDBOOK SECTION 2. THERMAL-CONTROL COATINGS	June 1971
	6. Performing Organization Code
7. Author(s)	8. Performing Organization Report No.
N. J. Broadway	
	10. Work Unit No.
*9. Performing Organization Name and Address	11. Contract or Grant No.
RADIATION EFFECTS INFORMATION CENTER Battelle Memorial Institute Columbus Laboratories Columbus, Ohio 43201	NASW-1568
	13. Type of Report and Period Covered
12. Sponsoring Agency Name and Address	Contractor Report
National Aeronautics and Space Administration Washington, D.C. 20546	14. Sponsoring Agency Code

15. Supplementary Notes

16. Abstract

This document contains summarized information relating to steady-state radiation effects on thermal-control coatings. The radiation includes nuclear, charged particles and ultraviolet. The data will provide useful information to the design engineer responsible for choosing thermal-control coatings in space applications.

17. Key Words (Suggested by Author(s))	18. Distribution Statement
Radiation Effects, Thermal-Control Coatings, Ultraviolet Effects, Temperature Control in Space Radiation Damage	Unclassified - Unlimited

19. Security Classif. (of this report)	20. Security Classif. (of this page)	21. No. of Pages	22. Price*
Unclassified	Unclassified	201	$3.00

*For sale by the National Technical Information Service, Springfield, Virginia 22151

PREFACE

This document is the second section of a Radiation Effects Design Handbook designed to aid engineers in the design of equipment for operation in the radiation environments to be found in space, be they natural or artificial. This Handbook provides the general background and information necessary to enable the designers to choose suitable types of materials or classes of devices.

Other sections of the Handbook will discuss such subjects as tran-is sistors, electrical insulators and capacitors, solar cells, structural metals, and interactions of radiation.

ACKNOWLEDGMENTS

The Radiation Effects Information Center owes thanks to several individuals for their comments and suggestions during the preparation of this document. The effort was monitored and funded by the Space Vehicles Division and the Power and Electric Propulsion Division of the Office of Advanced Research and Technology, NASA Headquarters, Washington, D. C., and the AEC-NASA Space Nuclear Propulsion Office, Germantown, Maryland. Also, we are indebted to the following for their technical review and valuable comments on this section:

Mr. A. Reetz, NASA, Hq

Dr. J. B. Schutt, NASA, Goddard SFC

Mr. E. R. Streed, Martin-Marietta, Denver

Our additional thanks are due to Academic Press, Incorporated for permission to use the copyrighted material from References 13 and 19.

TABLE OF CONTENTS

SECTION 2. THERMAL-CONTROL COATINGS

TABLE OF CONTENTS
(Continued)

TABLE OF CONTENTS
(Continued)

TABLE OF CONTENTS
(Continued)

SECTION 2. THERMAL-CONTROL COATINGS

SUMMARY AND CONCLUSIONS

Maintenance of a rather narrow range of temperatures within satellites is essential in both manned and unmanned vehicles. For electronic apparatus, the most suitable temperature range presently is 20 to 40 C. Manned spacecraft must not exceed 110 F (43 C) for periods longer than a few minutes.[1]

Control of temperatures on an operational spacecraft is based on the exchange of radiant energy with the vehicle's environment, and therefore upon the thermal-radiation properties of the exterior surfaces. Thermal-control coatings with the desired radiative properties have been used in the aerospace industry to maintain a predetermined heat balance on space vehicles. Solar absorptance, α_s, and hemispherical emittance, ϵ_h, of the coating have been the prime characteristics with respect to controlling the heat balance of a vehicle.

Design requirements often dictate the use of a surface with low ratios of solar absorptance to emittance, α_s/ϵ. These surfaces are generally susceptible to damage by solar radiation, resulting in an increase in α_s. Considerable effort has been spent in developing coatings which would be stable in a space environment, relatively easy to apply and maintain, and which would have the desired radiative properties.

Ideally, thermal-control surfaces can be divided into four basic classes, solar absorbers, solar reflectors, flat absorbers, and flat reflectors. The solar absorbers are principally metals and are relatively immune to space radiation damage. The flat absorbers [absorbing incident energy from ultraviolet (UV) to the far infrared (IR)] are most easily obtained in general practice, and their stability to space environments presents few problems unique to these coatings. Flat reflectors (reflecting energy incident upon it throughout the spectral range from UV to far IR) have been prepared as paints pigmented with metal flakes or as silver or aluminum vacuum-deposited coatings overlaid with a transparent coating.

The greatest research effort has been expended toward the development of solar reflectors. Some of these have been adapted by suitable pigmentation to provide solar absorber systems.

The principal problem in temperature control is presented by change of the α_s/ϵ ratio of a coating due to degradation by space environments such as UV radiation; proton, alpha particle, and electron bombardment; neutron and gamma radiation; and micrometeoroid impact. These space environmental factors are shown in Table 1. Those environments of importance to coating damage are marked with an asterisk.

TABLE 1. MAJOR PORTIONS OF THE SPACE ENVIRONMENT[2]

	Natural
Particle Radiation	
Protons	Galactic Van Allen* Solar Flare Solar Wind* Auroral
Electrons	Van Allen* Auroral*
Alpha Particles	Solar Wind Solar Flare
Electromagnetic	Solar Emissions*
Physical Impact	Atmospheric Particles Micrometeoroid
	Artificial
Persistent	
Electrons Neutron/Gamma Electron/Gamma	High-Altitude Nuclear Detonations* Spacecraft-Borne Nuclear Reactors* Spacecraft-Borne Isotope Power Supplies
Transient	
Burst Products Plume Contaminants	Nuclear Weapons Rocket Firing in Space

*Considered important with respect to thermal-control coatings.

The following generalizations concerning the effect of space environmental factors on coatings may be made on the basis of a review of presently available data:

(1) The most damaging factor is UV radiation. Of the four basic types of thermal-control surfaces, only the solar reflectors (the white paints primarily) are seriously damaged by space UV.

Specular surfaces and leafing aluminum are resistant to reflectance change in the IR wavelength region, but undergo substantial permanent reflectance losses in the visible and UV wavelength regions. Diffuse coatings are subject to reflectance degradation over much or all of the measured 0.24 to 2.5-micron wavelength region.[3]

(2) Nuclear radiation (gamma and neutron) is also damaging. However, most of the present organic coatings will withstand doses of approximately 10^8 rads (C) without appreciable damage. Inorganic coatings will probably withstand somewhat higher exposures.

(3) Electron bombardment will adversely affect coatings. The damage of particle radiation to organic coatings is similar to that caused by UV. The damage mechanism is, in effect, the same. The better coatings will withstand 10^{15} to 10^{16} e/cm^2 ($E \cong 145$ keV). Higher doses may cause severe damage.

Specular surfaces and leafing aluminum-silicone coatings are, in general, relatively resistant to reflectance degradation due to electron exposure ($E < 50$ keV). Excepting leafing aluminum, the diffuse coatings or paints are, in general, subject to severe, in-air recoverable degradation in the IR wavelength region, and to substantial visible-region reflectance losses which are less recoverable or "bleachable" upon re-exposure to air. Coatings employing methyl silicone binders sustain the greatest degree of reflectance degradation in the IR wavelength region. Coatings using potassium silicate binders suffer the largest electron-induced reflectance losses in the visible region.[3]

It has been found, in a series of tests on various coatings, that over a wide range of fluxes and fluences (4×10^8 to 1.7×10^{12} e/(cm^2 · s), and 10^{13} to 8×10^{15} e/cm^2, no irradiation rate effects from 50-keV electrons are evident.

Electron damage at 77 K (-196 C) is generally less severe than at 298 K (25 C). The combination of UV and electron damage is generally more severe than the sum of the damage caused by the individual factors. However, changes in reflectance of anodized aluminum (both barrier- and sulfuric acid-) and aluminum oxide-potassium silicate coating produced by simultaneous electron-UV irradiations were approximately equal to the sum of the changes produced by separate irradiations to equivalent doses when irradiated in vacuo at 77 K.[4]

(4) Galactic protons are relatively unimportant because of the relatively low flux, but Van Allen and solar-wind protons are damaging to coatings. The limited data available suggest that auroral protons and low-energy solar-flare protons are unimportant with respect to coating damage.

Coatings are available which will withstand about 3×10^{15} p/cm^2 (E = 3 - 468 keV). Above this exposure, damage may be severe. Proton damage has been found to be greater at 77 K (-196 C) in many cases than at 298 K (25 C). Many times, the combination of proton and UV radiation is only slightly more damaging than UV alone. The UV tends to bleach the damage due to proton irradiation.

(5) Solar alpha particles are considered of secondary importance to coating damage when compared to the effects of solar-wind protons and solar UV irradiations. Their numbers are less than those of solar protons. However, their effectiveness on a particle basis is comparable to proton-induced damage.[2]

(6) Residual high-altitude earth-atmospheric particles are considered unimportant in their effects to satellite surfaces. The micrometeoroid environment of space is not important for optical damage, where damage is defined as either a change in α_s or ϵ, or a change in the reflected angular

distribution of solar energy. The latter effect, however, is important for solar concentrator and mirror applications.[2]

(7) Artificial environments such as that caused by the Starfish detonation and spacecraft-borne nuclear sources are damaging.[2] However, the data on electron and nuclear damage are applicable in considering these environments.

(8) Rocket-plume contamination, the products of exhausts from both solid- and liquid-fueled rockets, is a problem with thermal control coatings.[2] More data are needed before conclusions can be reached on this problem.

As was stated in (1) above, the most damaging of the environmental factors is UV radiation. Due to (a) the spectra from available UV sources not matching the solar spectrum, (b) UV damage in vacuum being more severe than UV damage in air, and (c) recovery of damage often being rapid when air is supplied to the coating, it is difficult to forecast UV damage to coatings in space on the basis of laboratory data. As a result, even with "in situ" measurements, i.e., reflectance values of coatings obtained before being removed from the vacuum in which they were irradiated, laboratory data and those obtained from space satellites have not always been in agreement.

Coatings that appear to be most stable to space environment include:

(1) A zinc oxide/potassium silicate coating (Z-93 type) which has shown no measurable damage in over 3000 hours of solar exposure in OSO-II and Pegasus II experiments. This coating suffered somewhat greater damage on the interplanetary flights such as Mariner IV and Lunar Orbiter V. This damage ($\Delta\alpha_s$ = 0.05 after 1000 sun hours in flight on Lunar Orbiter V) was believed due to the solar wind. The coating suffered less damage than the others tested on this flight. The major problems with this coating are the difficulty of application and ease of soiling during preflight operations.

(2) Second surface mirrors which have shown excellent stability to both UV and particle radiation. Silvered Teflon showed no change on the OGO-VI after 4600 ESH. Aluminized 1-mil Teflon showed a $\Delta\alpha_s$ of 0.043 after 5000 hours' exposure on the Mariner V. An SiO_x/Aluminum reflector showed no

TABLE 2. EFFECT OF RADIATION ON

Coating	Binder	α_s	ε	Effect of Ultraviolet + Vacuum	Effect of Nuclear Radiation
S-13 (B1056)	Silicone	0.21	0.88	800 ESH, $\Delta\alpha_s$=0.08 1500 ESH, $\Delta\alpha_s$=0.18 (Pegasus I)	
S-13 G	Silicone	0.19	0.88	1000 ESH, $\Delta\alpha_s$=0.04 (OSO-III)	
(B-1060)		0.19	0.88		
Thermatrol 2A-100	Silicone	0.17	0.86	500 ESH, $\Delta\alpha_s$=0.06-0.16	No change at 10^8 rads(C)
Hughes Organic White (H-10)	Silicone	0.15	0.86		
Silicone (RTV 602) Over Aluminum (1199)		0.20	0.80	1141 ESH, $\Delta\alpha_s$=0.01	
Leafing Aluminum	Phenylated Silicone			1130 ESH, decrease in reflectance at 250 mμ = 24%	

ORGANIC THERMAL CONTROL COATINGS

Effect of Proton Bombardment	Effect of Electron Bombardment	Effect of Temperature	Effect of Combined Environment	Satellite	References
2.1×10^{16} p/cm^2, $\Delta\alpha_s = 0.01$ 1.7×10^{18} p/cm^2, $\Delta\alpha_s = 0.07$			1000 hr $\Delta\alpha_s = 0.14$ (Lunar Orbiter I) 2000 hr $\Delta\alpha_s = 0.20$ (Mariner V) 4600 hr $\Delta\alpha/\varepsilon = 0.40$ ATS-I 6000 hr $\Delta\alpha/\varepsilon \cong 0.30$ (ATS-I)	Lunar Orbiter I Pegasus I Mariner V ATS-I	16, 17, 18, 20, 49
Threshold damage 10^{14} p/cm^2 (E= 20 keV), severe damage at 10^{16} p/cm^2		No evidence of cracking or spalling when cycled 4 times from 260 to -190 C	1300 hr $\Delta\alpha_s = 0.16$ (Lunar Orbiter IV)	Lunar Orbiters II, IV, V	3, 14, 17, 26
	10^{14} e/cm^2 (E=50 keV) $\Delta\alpha_s = 0.01$		1300 ESH $\Delta\alpha_s = 0.12$ (Lunar Orbiter IV)	Lunar Orbiter IV	14, 26
3×10^{15} p/cm^2, $\Delta\alpha_s = 0.01$ 5×10^{16} p/cm^2, (E=10 keV), $\Delta\alpha_s = 0.42$	10^{15} e/cm^2, no effect 10^{16} e/cm^2, $\Delta\alpha_s$= 0.05, bond failure 10^{16} e/cm^2 (E= 80 keV), severe degradation	No serious degradation at ascent temperature, increase in temp increases $\Delta\alpha$	Nuclear +UV, $\Delta\alpha_s$ = 0.08 Proton causes annealing effect with UV. Combined damage greater than sum of separate effects.		21, 27, 38, 57
3×10^{15} p/cm^2 (E=466 keV), $\Delta\alpha_s = 0.01$			1500 sun hr $\Delta\alpha_s$= 0.18 (Lunar Orbiter V)	Lunar Orbiter V	14, 26
			1500 sun hr $\Delta\alpha_s$= 0.13 (Lunar Orbiter V)	Lunar Orbiter V	14, 26
Moderate losses in reflectance after 10^{17} p/cm^2 (E = 20 keV)	Extremely resistant to reflectance change at 10^{16} e/cm^2 (E=20 and 80 keV)				3, 27

TABLE 2.

Coating	Binder	α_s	ϵ	Effect of Ultraviolet + Vacuum	Effect of Nuclear Radiation
Fuller Gloss White	Silicone-alkyd	0.25 0.29	0.90	485 ESH, $\Delta\alpha_s$=0.06 850 ESH, $\Delta\alpha_s$=0.07	Excellent stability at 10^8 rads(C) 4.5×10^7 rads(C), 4.5×10^3 n/cm^2, $\Delta\alpha_s$=0.06 1.8×10^8 rads(C), 1.8×10^{14} n/cm^2, $\Delta\alpha_s$=0.09
PV-100	Silicone-alkyd			162 ESH, $\Delta\alpha_s$=0.17	
White Skyspar	Epoxy	0.22 0.25	0.91	485 ESH, $\Delta\alpha_s$=0.24 850 ESH, $\Delta\alpha_s$=0.39	2.2×10^6 rads(C), no change 5×10^7 rads(C), $\Delta\alpha_s$=0.07; 2×10^8 rads(C), $\Delta\alpha_s$=0.12
Tinted White Kemacryl	Acrylic	0.24 0.28	0.86	485 ESH, $\Delta\alpha_s$=0.11 1000 ESH, $\Delta\alpha_s$=0.12	5×10^7 rads(C), $\Delta\alpha_s$=0.05 2×10^8 rads(C), $\Delta\alpha_s$=0.06, 0.09 $1\text{-}3\times10^8$ rads(C), mechanical failure
Nonleafing Aluminum/Acrylic	Acrylic	0.44	0.48	$\Delta\alpha_s$=0.07 Binder degrades	

(Continued)

Effect of Proton Bombardment	Effect of Electron Bombardment	Effect of Temperature	Effect of Combined Bombardment	Satellite	References
	10^{16}e/cm^2, no change in $\Delta\alpha_s$		UV+Nuclear, 920 ESH, 10^8 rads(C), surface yellowed, paint flaked off		3, 27, 33, 38
3×10^{15}p/cm^2 (E= 466 keV), $\Delta\alpha_s$= 0.03 10^{16}p/cm^2, degraded coating	4×10^{16}e/cm^2, damage approaches saturation level				35
6.4×10^{16} p/cm^2, $\Delta\alpha_s$=0.02 6.4×10^{17} p/cm^2 $\Delta\alpha_s$=0.04 2.1×10^{18} p/cm^2 $\Delta\alpha_s$=0.12	10^{15}e/cm^2, $\Delta\alpha_s$=.03 10^{16}e/cm^2, $\Delta\alpha_s$=0.07			OSO-I OSO-II	33, 34, 38, 49
10^{15}e/cm^2, $\Delta\alpha_s$= 0.02 10^{16}e/cm^2, $\Delta\alpha_s$= 0.06			UV+Nuclear, 920 ESH, 10^8 rads(C), 180 F, paint turned brown and bubbled		33, 38
	10^{16}e/cm^2, $\Delta\alpha_s$=0.01				2, 38

TABLE 3. EFFECT OF RADIATION ON INORGANIC

Coating	Type	α_s	ε	Effect of Ultraviolet + Vacuum	Effect of Nuclear Radiation
Lithafrax/Na_2SiO_3 ($Li/Al/SiO_4$)		0.15	0.86	485 ESH, $\Delta\alpha_s$=0.06 600 ESH, $\Delta\alpha_s$=0.06	$5x10^7$ rads(C), $\Delta\alpha_s$=0.06 $2x10^8$ rads(C), $\Delta\alpha_s$=0.14 Degrades severely $1.3x10^8$ rads(C), $\Delta\alpha_s$=0.10
Synthetic $Li/Al/SiO_4/Na_2SiO_3$		0.16	0.87	485 ESH, $\Delta\alpha_s$=0.09 162 ESH, $\Delta\alpha_s$=0.12	$1.3x10^8$ rads(C), $\Delta\alpha_s$=0.09
Z-93 (Zinc oxide/K_2SiO_3)		0.18 0.20	0.88 0.93	3000 sun hr, $\Delta\alpha_s$=0.00 (OSO-II, OSO-III, Pegasus II)	
Hughes Inorganic White (H-2) (TiO_2/K_2SiO_3)		0.14 0.18	0.89 0.88	1300 sun hr, $\Delta\alpha_s$= 0.14	
Douglas White Inorganic	Z-93			200 ESH, $\Delta\alpha_s$ increased 10 percent	
Zirconium silicate/K_2SiO_3		0.24 0.14	0.87 0.89	485 ESH, $\Delta\alpha_s$=0.04	
Al_2O_3/K_2SiO_3		0.11	0.82	162 ESH, $\Delta\alpha_s$=0.13	

AND COMPOSITE THERMAL CONTROL COATINGS

Effect of Proton Bombardment	Effect of Electron Bombardment	Effect of Temperature	Effect of Combined Environment	Satellite	References
	10^{15}e/cm^2, $\Delta\alpha_s$=0.05 10^{16}e/cm^2, $\Delta\alpha_s$=0.10		Concurrent UV and nuclear more damaging than UV followed by nuclear		36, 38
Low energy protons cause measurable damage. 10^{15}p/cm^2 (E= 466 keV), $\Delta\alpha_s$=0.06	10^{15}e/cm^2, $\Delta\alpha_s$=0.06 10^{16}e/cm^2, $\Delta\alpha_s$=0.09				34, 38
1.6×10^{17}p/cm^2, $\Delta\alpha_s$=0.11 1.9×10^{18}p/cm^2, $\Delta\alpha_s$=0.67	Electrons tend to bleach		1500 sun hrs, $\Delta\alpha_s$= 0.07 (Lunar Orbiter V) 73 hrs, $\Delta\alpha_s$=0.07	Mariner IV Lunar Orbiter V OSO II, III Pegasus II	13, 14, 21, 26, 32, 41, 49
		Thermal cycling 4 times from 533 K to 83 K, $\Delta\alpha_s$=0.03	1000 sun hrs, $\Delta\alpha_s$= 0.09 (Lunar Orbiter IV)	Lunar Orbiter IV Surveyor I	14, 16, 26, 28, 30 47
	10^{16}e/cm^2, $\Delta\alpha_s$= 0.02		10^{16}e/cm^2 and 485 sun hr, $\Delta\alpha_s$=0.06		30, 38
3×10^{15}p/cm^2 (E= 466 keV), $\Delta\alpha_s$= 0.02			Proton+UV only slightly more damaging than UV alone. Electrons+UV enhanced stability of reflectance 4300 ESH, $\Delta(\alpha_s/\varepsilon)$=0.45 (ATS-I) 350 ESH and 5.8×10^{15}e/cm^2 at 77 K, $\Delta\alpha_s$=0.13	ATS-I	4, 19, 20, 41

TABLE 3.

Coating	Type	α_s	ε	Effect of Ultraviolet + Vacuum	Effect of Nuclear Radiation
3M202-A-10					
Anodized Aluminum		0.18 0.23	0.73	162 ESH, $\Delta\alpha_s$=0.04 576 ESH, $\Delta\alpha_s$=0.18 1152 ESH, $\Delta\alpha_s$=0.19 1580 ESH, $\Delta\alpha_s$=0.00 (OSO-III)	$3x10^8$ rads(C), $\Delta\alpha_s$=0.01
SiO on Aluminum		Variable depending on thickness of SiO		Severe degradation	
Rokide C		0.90	0.85	No degradation	
Alodine	Chromate finish on aluminum				
Optical Solar Reflector	No. 1, Ag mirror	0.05	0.81	485 ESH, no change in $\Delta\alpha_s$	
	No. 2, Al mirror	0.10	0.81		
Magnesium fluoride/ Molybdenum/ Magnesium fluoride		0.85 0.91	0.53 0.85	Good UV stability	
Vinyl Silicone on Aluminum		0.16 0.21	0.15 0.90(a)	3800 ESH, no change	
Butvar on Aluminum		0.18 (0.75 mils) 0.22 (3.2 mils) 0.22 (6.5 mils)	0.45 0.85 0.88		

(a) Emittance dependent on coating thickness.

(Continued)

Effect of Proton Bombardment	Effect of Electron Bombardment	Effect of Temperature	Effect of Combined Environment	Satellite	References
10^{16}p/cm^2 (E=3 keV), degraded in visible and IR	$4x10^{16}$e/cm^2 (E= 145 keV) damage approached a saturation level				35
10^{15}p/cm^2 (E= 466 keV), $\Delta\alpha_s$=0.01	$4x10^{16}$e/cm^2 (E= 145 keV)		2000 ESH, $\Delta\alpha$=0.11 (ATS-III)	ATS-III OSO-III	4, 5, 35, 48
10^{16}p/cm^2 (E=3 keV), $\Delta\alpha_s$= no change	No change				
				Vanguard II	2, 8
					9
Emittance changed 0.07					49
$3x10^{15}$p/cm^2, no change	10^{16}e/cm^2, no change in $\Delta\alpha_s$		Stable up to 2 years in all charge and particle environments and combined environments of space		13, 38, 52
					55
			170 ESH, 10^7 rads(C), X-ray, $\Delta\alpha_s$=0.01 1720 ESH, 10^8 rads (C) X-ray, $\Delta\alpha_s$= 0.02		37
			100 ESH, 10^7 rads (C) X-ray, $\Delta\alpha_s$= 0.01 1000 ESH, 10^8 rads (C), X-ray, $\Delta\alpha_s$= 0.02		37

TABLE 3.

Coating	Type	α_s	ε	Effect of Ultraviolet + Vacuum	Effect of Nuclear Radiation
Aluminized FEP Teflon		0.16 0.13- 0.16	0.26- 0.89[a] --		
Silvered FEP Teflon		0.07- 0.09	--	5-mil silvered Teflon 4600 ESH, no change in α_s (OGO-VI)	
Aluminized Polyimide		0.44	0.78 (3 mil Kap-ton)	20,000 ESH $\Delta\alpha$ =0.10	
SiO_x/Al		0.146	0.30		
SiO_2/Al		0.111		1488 ESH $\Delta\alpha_s$= 0.01 to 0.03	
Al_2O_3/Al		0.136	0.25		
SiO-Al-Kaptan				Badly degraded by UV	

(a) Emittance dependent on coating thickness.

(Continued)

Effect of Proton Bombardment	Effect of Electron Bombardment	Effect of Temperature	Effect of Combined Environment	Satellite	References
No change in absorptance to $3x10^{15}p/cm^2$ (E= 40 keV) $1.4\text{-}1.8x10^{16}p/cm^2$ $\Delta\alpha_s$=0.06	$10^{15}e/cm^2$ (E= 80 keV) (2, 5, 10-mil Teflon) only minor reflectance degradation $10^{16}e/cm^2$, significantly altered		1150 ESH, $1.2x10^8$ rads(C) X-ray, $\Delta\alpha_s$ = no change 1-mil aluminized teflon 5000 ESH, $\Delta\alpha_s$=0.04 (Mariner V)	Mariner V	18, 27 37, 50
No change in absorptance to $3x10^{15}p/cm^2$ (E= 40 keV) $1.2\text{-}1.7x10^{16}p/cm^2$, $\Delta\alpha_s$=0.04				OGO-VI	50
$5x10^{14}p/cm^2$ $\Delta\alpha_s$= 0.03		750 F, 30 sec in Vac - no change 7900 F, film visibly darkens			51
			4800 ESHΔ (α/ε)= 0.26 (ATS-I) 3-1/2 yrs, no significant degradation (Explorer XXIII)	ATS-I Explorer XXIII	20, 54
$1x10^{15}e/cm^2$ (E=1 MeV) no change					53
	$10^{17}e/cm^2$ (E= 20 keV) only small changes		4400 ESH $\Delta(\alpha/\varepsilon)$= 0.16 (ATS-I)	ATS-I	20
$10^{16}p/cm^2$ (E= 63 keV), little change	$1.3x10^{16}e/cm^2$ (E=145 keV), slight reduction in spectral reflectance			Apollo	35, 52

degradation after 3-1/2 years on Explorer XXIII. An RTV/silicone coated aluminum showed a $\Delta\alpha_s = 0.08$ after 1100 hours on Lunar Orbiter V.

Optical solar reflectors (OSR), mirrors consisting of vapor-deposited silver or aluminum on fused silica have shown no change in α_s or ϵ for extended missions up to 2 years. These reflectors are ceramic mirrors and therefore are difficult to apply, particularly on irregular surfaces. The mirrors have to be mounted by means of an adhesive or tape and the size of the mirrors is approximately 1 x 1 x 0.008 in.

(3) Coatings that are more easily applied generally have not shown good stability. S-13G (ZnO/silicone) and Thermatrol 2A-100 or Hughes Organic White (both TiO_2/silicone) are representative of the most stable of these coatings. Change in absorptance, $\Delta\alpha_s$, for S-13G was 0.14 in 1200 hours on Mariner V. Absorptance of a TiO_2/silicone apparently increased from 0.24 to between 0.34 and 0.40 on the Apollo 9. The advantages of these coatings are that they are easier to apply and require less prelaunch protection than the above thermal-control materials.

Unfortunately, the more stable coatings are more difficult to apply and to maintain during prelaunch activities. The coatings that do not require elevated-temperature cures and can be repaired easily lack environmental stability. However, some of these latter may be serviceable depending on flight requirements. Continued efforts are needed to develop a stable coating that can be applied easily, cured at room temperature, and is easily repaired or cleaned. The chief difficulty is that easily applied coatings generally require organic binders and these are susceptible to radiation damage.

A summary of the effects of radiation on organic and inorganic coatings is given in Tables 2 and 3.

INTRODUCTION

In a hostile environment such as is encountered in space where vacuum, cryogenic temperatures, solar radiation, and particulate radiation are present, maintaining an operable temperature within a space vehicle is of the utmost importance. The internal temperature of the vehicle must be controlled within rather narrow limits in which its contents will operate efficiently. Many electronic components become inoperative at temperatures above 140 F. Excess heat must be radiated to space or the vehicle will overheat. Conversely, if the vehicle radiates heat faster than it is absorbed, enough heat must be generated internally to maintain the necessary balance.[5]

The temperature of an object in space depends upon several factors. The most important of these are (1) the absorption of radiation by the surface, (2) the radiation or reradiation of energy from the surface, and (3) the generation of heat within the object. Other factors that affect the temperature are the thermal conductivity and specific heat of the spacecraft components, and the absorptance of earth-emitted IR energy and earth-reflected solar radiation.[6] The maintenance of the proper range of temperatures in a space vehicle is one of the more important and complex design problems.

Two techniques are used to regulate the temperature of satellites: active temperature control and passive temperature control. Active control consists of a feedback technique that usually employs electrical power and moving parts. For example, bimetallic strips or thermostats control shutters or vanes to vary the surface in terms of effective optical properties. Passive control relies on the use of surface materials with appropriate thermophysical characteristics. Frequently a combination of both methods is used.

Much research has gone into the study and development of surface materials and coatings which have absorptive and radiative properties useful for controlling temperature. It can be shown that the important parameter in determining the surface equilibrium is the ratio of the solar absorptance (α_s) to the hemispherical emittance (ϵ_h) of the external surface where α_s is the fraction of incident solar energy absorbed and ϵ_h is the fraction of energy radiated as compared to that from a black body at that temperature.[7] Four types of thermal control surfaces are used to maintain a desired temperature range within a space vehicle. These are termed solar reflector, solar absorber, flat reflector, and flat absorber.

A solar reflector is a surface which reflects the incident solar energy while emitting IR energy.[8] It is characterized by a very low α_s/ϵ ratio ranging from 0.065 to 0.34. It has a low α_s and high ϵ. White organic paints with metallic-oxide pigments are representative of this class.

A solar absorber is a surface which absorbs energy while emitting a small percentage of the IR energy. It is characterized by a relatively high α_s/ϵ ratio (greater than 1) and is approximated by polished metal surfaces. It has a high α_s and low ϵ. Such surfaces reflect a relatively large amount of incident solar energy (approximately 70 percent); however, they are much more efficient as solar absorbers than as emitters of IR energy (typical values, $\alpha_s \simeq 0.25$ and $\epsilon \simeq 0.05$) and consequently, when exposed to solar radiation in a vacuum, such surfaces will become hot.[9] The most successful and widely used of the present solar absorbers are aluminum and gold surfaces. Solar absorbers are extremely sensitive to contamination and require careful prelaunch handling.

A flat reflector is a surface which reflects the energy incident upon it throughout the spectral range from UV to far IR.[8] It has a low α_s and low ϵ. This class of surfaces has been the most difficult to develop. The most promising class of materials for this use consists of paints pigmented with metal flakes and very highly polished metal surfaces. These surfaces are generally characterized by a relatively low IR emittance with an $\alpha_s/\epsilon \simeq 1.0$. The most favored flat reflector is nonleafing aluminum silicone paint, $\alpha_s = 0.22$, $\epsilon = 0.24$.[9]

A flat absorber is a surface which absorbs the energy incident upon it throughout the spectral range from UV to far IR.[8] It has a high α_s and high ϵ. Of the four basic surfaces, the flat absorber is the most easily obtained in general practice. Generally, any rough black matte surface will be a good approximation of a flat absorber. Of the available finishes, Black Kemacryl Lacquer and dull-black Micobond paint ($\alpha_s \cong 0.93$, $\epsilon = 0.88$) are most widely used.[9] As a consequence of the relative ease with which a flat absorber can be obtained, the considerations which dictate its choice are those other than the thermal radiation characteristics of the material, such as temperature resistance, mechanical strength, abrasion resistance, adhesive strength, flexibility, cost, and ease of application.

Figure A-1 in Appendix A shows the ideal spectral absorptance of these four types of surfaces and of production materials approximating them. Tables A-1 through A-5 list by types the various materials for which α_s/ϵ have been determined.

Radiation Environments to Which Thermal Coatings May Be Subjected

Thermal coatings in a space environment are subjected to several types of radiation and must be stable to these, or the changes which occur due to radiation must be known so that engineers can consider them in designing space vehicles. The environment which probably affects coatings most seriously is solar radiation, particularly UV. Much information is available on the effects of UV and vacuum, both from laboratory tests and from space flights. However, other electromagnetic and particle radiations will cause changes in thermal-control coatings, and information concerning these effects is comparatively recent. Additional information is being obtained at the present time, and results are not yet available. However, published studies give an indication of what can be expected.

Solar Electromagnetic Radiation

The bulk of the energy in the solar spectrum lies between 0.3 and 4.0 μ, with approximately 1 percent of the energy lying beyond each of these limits.[8] IR and visible radiation do not possess sufficient energy per quantum to break chemical bonds in ordinary reactions. The principal effect of IR radiation is to increase thermal agitation. However, many reactions initiated by the higher energy UV photons proceed at a higher rate because of the temperature increase caused by the IR. Due to differences in absorption coefficients, the effects of radiation in the visible range should be somewhat less than those for the thermal range and are negligible with respect to the possible effects in the UV range.

Both the UV and the soft X-ray components of the solar spectrum possess sufficient energy per quantum to induce rupture of many chemical bonds and thus initiate chemical reactions with organic coatings. The effect of UV radiation on structural metals is negligible except for a static charge that is produced by the removal of electrons by the photoelectric effect.[8]

A great deal of work has been done to determine the effect of UV radiation and the combination of UV radiation and vacuum on thermal-control coatings. However, the first space trips showed much of this information to be unreliable, and the work had to be repeated "in situ". That is, optical measurements had to be made while irradiated samples were still in vacuum. In earlier tests, these measurements were made in air after irradiation in vacuum, and it was found that damage had "healed" when the samples were returned to an air environment.

UV damage to the individual coatings is discussed in other sections of this report. However, it has been shown that of the four basic types of thermal-control surfaces, only the solar reflectors (the white paints primarily) are seriously damaged by space UV radiation.[9]

Penetrating Radiation

The penetrating-radiation environment of space may be due to a variety of sources, of which the most important are cosmic radiation, trapped radiation, auroral radiation, and solar-flare radiation.[8] Those portions of the total space environment which are considered of importance in causing optical damage to spacecraft surface materials are:[9, 10]

Van Allen electrons and protons
Solar-wind and solar-flare protons
Auroral electrons and protons
Artificial electron belt.

Following are discussions of the various types of penetrating radiation and the particle fluxes which may be anticipated. Also, some generalities on the stability of coatings are given.

Primary Cosmic Radiation. Cosmic primaries consist principally of protons (hydrogen nuclei) moving with relativistic or near-relativistic velocities (from 80-90 percent of the velocity of light).[8] Except for magnetic disturbances and variations on the order of ±2 percent with the solar cycle, the cosmic primary radiation field is essentially constant with time.

The effective ionization dose rate due to cosmic primaries is about 10^{-} rad/hr, and the approximate effective dose rate due to secondaries produced in a space vehicle or in the atmosphere is about 10^{-3} rad/hr. Hence, the cosmic-ray-induced damage is regarded as being a very minor hazard.

Geomagnetically Trapped Radiation. For orbits near the earth [up to approximately 20,000 nautical miles (nm) or 23,000 statute miles (sm) in altitude], the Van Allen radiation is of great importance because of the high fluxes The Van Allen radiation belts are usually discussed in terms of an inner and an outer belt. The more stable inner belt is normally considered to consist of those magnetic shells for which $L < 2$ (L = the radial distance of the shell from the center of the earth at the geomagnetic equator), i.e., at altitudes

< 3500 nm, and is populated with penetrating protons (E < 500 MeV) and low-energy electrons (mostly E < 1 MeV). The outer belt includes shells L > 3500 nm and consists almost entirely of slightly more energetic electrons than those in the inner belt.[8]

Trapped Protons. The inner zone proton flux is relatively stable in time although some changes at low altitudes occur over the solar cycle because of atmospheric changes. Farther out in the magnetosphere, the proton distributions are more easily affected by magnetic disturbances, but in general they are more stable than the electron fluxes.[11]

The Van Allen proton environment has been broken up into four energy bands: 4 to 15, 15 to 30, 30 to 50, and > 50 MeV. The contours of the flux levels are shown in Figures A-2 to A-5.[10, 11] Integral flux distributions above 0.4 MeV are shown in Figure A-6.[10] It is evident from the difference in spatial extent between the 0.4-MeV map and the four higher energy maps that it is convenient to think of zones in the proton belt, one with virtually no protons with energies greater than 4 MeV. This is called the "outer radiation" zone and extends between an L value of about 4 (in units of earth radii) to the outer boundary of particle trapping.[10] This zone is characterized by time variations in flux intensities and corresponding changes in energy spectra. The intensities indicated in Figure A-6 probably are not upper limits for this zone, but are more conservative for making predictions of damage to spacecraft. Energy spectra at the magnetic equator for various L values in the inner and outer proton zones are presented in Figures A-7 and A-8. Fluxes of protons at energies lower than the limits shown in Figures A-7 and A-8 exist and may be of importance in producing surface damage in materials. However, data describing these portions of the spectra are limited.

Trapped Electrons. The trapped-electron belt coincides spatially with the proton belt, but has different configurations in its intensity and energy spectrum distributions. The integral flux distribution above 0.5-MeV electron energy as of August, 1964, is given in Figure A-9.[10, 12] This model was derived from data accumulated between late 1962 and 1964. The measurements were made after the creation of the artificial electron belt by beta-decay electrons from the Starfish high-altitude nuclear explosion on July 9, 1962. Since trapped electrons of natural origin were not well measured before 1962, present knowledge does not permit a clean separation in the inner radiation belt between naturally occurring electrons and those of artificial origin.

As with trapped protons, the trapped-electron belt is divided into an inner and outer zone, with the zone boundary being taken at a minimum in the distribution of high-energy electrons at L ~2.5 to 3 earth radii. According to Gaines and Imhof,[10] the inner zone in late 1964 was characterized by energy spectra generally similar to a fission beta spectrum and by monotonic losses in intensity, the loss rate being highest at very low L values and fairly uniform at about a factor of 3 decrease in intensities each year for $L \lesssim 1.3$. Thus for the main portion of the inner zone, the fluxes of artifically injected electrons should have been about two orders of magnitude lower in late 1968 than those shown in Figure A-9.[10, 12]

The electron flux in the outer zone ($L \gtrsim 2.5$) shown in Figure A-9 are approximate mean values from data taken from 1962 to 1964, near a period of minimum solar activity. Intensities throughout this zone show fluctuations of as much as two orders of magnitude over time periods of weeks or a few months.[10] Since changes in spectral shape might be expected to accompany the intensity fluctuations, the spectra shown for L = 3.4 and 5 in Figure A-10 are typical only.[10]

Trapped Alpha Particles. Alpha particles trapped in the geomagnetic field have been observed. However, their integral intensities are low as compared with protons and electrons and they are considered unimportant with respect to radiation effects.

Calculation of Accumulated Fluxes. It can be seen that the calculation of particle fluxes accumulated by a particular spacecraft at a given time involves many variables and is not simple to perform. The Government maintains an "Environmental Science Services Administration" at Goddard Space Flight Center, Greenbelt, Maryland, 20771, where James I. Vette and staff maintain an up-to-date computerized facility for determining the fluxes for a spacecraft orbit for any required period of time. Lockheed Palo Alto Research Laboratory has a similar facility. Figures A-11 and A-12 can be used to determine upper limits for low-altitude circular orbits.

Solar Particles. The geomagnetic field deflects charged particles incident on it from interplanetary space and thus provides very effective shielding to the region of space between about 60 degree north and south magnetic latitudes within the magnetosphere. Near the magnetic poles, and in interplanetary space outside the boundary of the magnetosphere, the direct charged-particle radiation from the sun can be observed. This radiation consists of

two components: high-energy particles that occur sporadically, usually in correlation with visible disturbances on the surface of the sun or solar flares; and low-energy protons and electrons, which are present more continuously.

Solar-Flare Radiation. Protons from solar flares present perhaps the most important source of damaging particles for many orbital configurations. Since solar-proton events occur sporadically and vary widely in peak proton flux and duration, the total flux of protons expected within a particular time period is treated statistically.[10] Fluxes may be as high as 10^4 p/(cm^2. s); average dose rates may range from 1 to 100 rads/hr; and the total dose per flare would range from 10 to 10^3 rads.[8]

Electrons in the energy range 40 to 150 keV have been measured when accompanying a number of small solar flares during solar minimum. The fluxes of electrons observed in all cases were small from a damage standpoint.

Alpha particles and charged nuclei of higher atomic number accompany the fluxes of protons from solar flares. In several cases where both alphas and heavier nuclei have been observed, the ratio between their numbers has been constant at about 60. The ratio of protons to alphas within the same energy range appears to vary considerably, the number ranging from about 10 to several hundred.[10]

Solar Wind. The solar wind is a plasma consisting of protons, electrons, and alpha particles which continuously streams radially outward from the sun. The particle velocity in the vicinity of the earth was found to vary with solar modulation between about 350 and 700 km/sec, which corresponds to energies of approximately 0.6 to 2.6 keV for protons. The particle flux intensity varied between about 3×10^7 and 1×10^9 particles/(cm^2. s).[10] Breuch states that the solar wind is seldom less than 500 eV or greater than 3000 eV and that an average of 1250 eV for the solar wind over the past 30 years is suggested.[2] The surface dose rate will be approximately 10^6 rads/hr.[8] Fluxes are large, but since the energy per particle is small, the damage to materials from solar-wind particles will be confined to surfaces.[10]

It has been demonstrated that solar-wind energies must be used in the laboratory when studying solar-wind effects on thermal-control surfaces. Major recovery effects exist in coatings exposed to simulated solar-wind protons and to combined simulated solar-wind protons plus solar-UV radiation. Combined irradiation produces major synergistic effects and bleaching effects which are coating dependent.[2]

Laboratory data including UV, 2 and 10-keV proton, and UV + proton exposures were used to predict the changes in α_s of three coatings which might have been expected on the OSO-III had the satellite's orbit been in the solar wind.[13] The values were then compared with data from interplanetary experiments (Lunar Orbiters IV, V, and Mariner V). The degradation in space was greater than that predicted from the laboratory data.[13] Differences between the degradation of these coatings in near-earth orbits and those in interplanetary orbits are attributed primarily to differences in environmental parameters between the two types of orbits.[14] It is believed that the electrons, protons, and solar UV in the lunar or interplanetary environment have a synergistic effect which results in a degradation rate higher than that from solar UV exposure alone.[14]

Auroral Radiation. Intense fluxes of protons and electrons have been observed in the auroral regions from about 60 to 70 geomagnetic latitude with somewhat lower fluxes at higher latitudes up to the magnetic poles. The particle intensities fluctuate over several orders of magnitude but may always be present in these regions at altitudes to at least 500 nm. The exact origin of these fluxes and the mechanisms of their trapping or storage and precipitation into the atmosphere are not well understood. They seem to be correlated with solar activity, however; and the most reasonable source with sufficient total energy to produce the observed fluxes is the solar wind.[10]

The average energies of electrons observed in the auroral regions is of the order of a few kilovolts to tens of kilovolts. A rough estimate based on the highest activity data and assuming an average energy of 10 keV gives approximately 10^{12} electrons/($cm^2 \cdot$ day) for a low-altitude polar-orbiting satellite.[10]

Observations of precipitating protons in the auroral regions in 1965 showed average particle energies of 10 to 20 keV and peak fluxes greater than 10^6 protons/($cm^2 \cdot s \cdot$ steradian) for energies greater than 20 keV. A rough estimate for protons would be approximately 10^{10} protons/($cm^2 \cdot$ day), with an average energy of 15 keV.

Man-Made Radiation. The most intense man-made radiations in space have originated from high-altitude nuclear-device detonations. The intensities of electron fluxes and the length of time they remain trapped after injection depend on the yield of the device and the altitude and geomagnetic location of the detonation. As a result of a nuclear detonation, high fluxes of electrons

can be injected into low-altitude regions of space where the fluxes of naturally trapped electrons and protons are rather low.

Miscellaneous Natural Sources. These include thermal-energy atoms, solar X-rays, neutrons, and albedo protons. Of these, the solar X-rays are probably the most impoerant with respect to thermal coatings.[8]

Thermal-Energy Atoms in Space. In intergalactic space there exists a density of about 1 atom/cm^3 of thermal energies (~125 K). These atoms are predominantly protons. For a space vehicle traveling at 10^8 cm/sec (0.003 x velocity of light), the effective flux would be 10^8 p/(cm^2. s) in intergalactic space. At this velocity, the apparent proton energy is about 0.5 keV, and the surface dose rate would be approximately 10^5 rads/hr. The internal dose rate would be negligible. The population of thermal-energy atoms in the solar system is estimated to be about 10^2 protons/cm^3.[8]

Solar X-Rays. Although the major portion of the electromagnetic radiation from the sun which makes up the solar constant [2 cal/(cm^2. min)] is not ionizing in nature, a very small portion (~0.1 percent) lies in the solar X-ray region of a few kilovolts. On this basis, the surface dose rate is estimated to be about 10^6 rads/hr. Since this X-ray energy is absorbed strongly by materials, the interior dose rate is not important.[8]

Neutrons. Except for cosmic-ray interaction with matter such as the earth's atmosphere, there appears to be no major natural source of neutrons. The flux of neutrons from the cosmic-ray effects on the earth's atmosphere is about 1 n/(cm^2. s) and poses no problem.[8]

Albedo Protons. Impingement of cosmic particles on the earth's atmosphere also produces a scattered flux of protons which has an intensity of about 1 p/(cm^2. s). The energy range is 1 to 10 MeV, and the dose per year is probably less than 100 rads.[8]

Alpha Particles. Solar alpha particles are considered of secondary importance in coating damage when compared to the effects of solar-wind protons and solar UV irradiations. Their numbers are less than those of solar

protons; their effectiveness on a particle-to-particle basis in producing optical damage is comparable to proton-induced damage.[2]

It should be noted that the charged-particle space environment has increased importance for coatings over that normally associated with the degradation of other satellite components and systems. The charged-particle environment of space has been found to increase in intensity at the lower energies and, at these lower energies, the particles are almost entirely stopped in the satellite surface. This results in significant energy deposition in the external thermal-control surfaces. The important radiations are the Van Allen and solar-wind particles.[2] A summary of the various radiation sources is given in Table 4.[15]

TABLE 4. EXTERNAL RADIATION SOURCES[15]

Radiation Source	Type of Radiation	Energy, E	Flux, particles/($cm^2 \cdot s$)	Peculiar Characteristics
Galactic cosmic rays	Protons (~90%) Alpha (~10%)	10 MeV - 10^{13} MeV	2	Least significant
Solar wind	Protons (~95%)	~1 keV	2×10^8 at 1 AU[b]	Low energy restricts hazard to surface effects
Solar cosmic ray events (solar flares)	Protons (95%)	Spectrum is very steep above 30 MeV ($\sim E^{-5}$); below 10 MeV, spectrum $\sim E^{-1.2}$	(c)	Energy and number of particles released per event varies; 10^8 particles/cm^2 for medium flare
Solar electromagnetic	Infrared, visible, ultraviolet, soft X-rays	6000 K black body radiator, erratic below 1200 A[a]		Spectrum below 1200 A[a] depends strongly on solar cycle
Trapped radiations				
Inner belt (1.2 to 3.2 earth radii)	Protons and electrons	Energy of protons (E_p) < 30 MeV (90%) Energy of electrons (E_e) < 5 MeV (90%)	Protons: 5×10^5 (E > 1 MeV); Electrons: 2×10^7 (E > 0.5 MeV)	Flux varies with magnetic latitude; electron populations of both belts subject to perturbations due to high-altitude nuclear bursts; outer-belt protons are non-penetrating
Outer belt (3 to 7 earth radii)	Protons and electrons	Virtually all protons less than 1 MeV	Protons: (E > 10 keV): 10^9 Electrons: $5.2 \times 10^7 e^{-5E}$ (E in MeV)	
Aurora	Electrons and protons	E_e between 2 and 20 keV; E_p between 80 and 800 keV	10^{10} (electrons) during auroral storms; < 10^7 protons	Observed between 65° and 70° north and south magnetic latitudes at altitudes between 100 and 1000 km

(a) A = 0.1 nm.
(b) AU ≈ 149.6 Gm.
(c) Precise prediction of solar-flare activity cannot now be made.

ORGANIC COATINGS

This section describes the principal coatings that have been studied for use as thermal-control surfaces. A summary of available data on the effects of space environment on these coatings is presented.

Zinc Oxide/RTV-602 Dimethyl Silicone Binder (S-13)

One of the coatings which looked promising as a thermal-control material was developed by the Illinois Institute of Technology Research Institute. It consists of a high-purity zinc oxide (New Jersey Zinc Company, SP 500) in a dimethyl silicone binder (General Electric, RTV-602), with SCR-05 (GE) catalyst. Earlier tests had indicated that the (S-13) coating could be expected to have good stability when exposed to UV radiation. However, space tests showed that the coating did not have the expected stability. Further investigation showed that the coating was affected by UV in vacuum, but that it quickly recovered or bleached in the near-IR region when exposed to air. Thus, the tests in which optical properties were measured in air after vacuum irradiation had been misleading. It was deemed necessary, therefore, to measure optical properties of thermal-control coatings in situ, that is, while in a vacuum and before being reexposed to air.

Confirmation of this "bleaching" effect may be seen in tests conducted in support of the Lunar Orbiter project.[16] The reflectances of coatings were measured (1) in air, (2) in vacuum before UV irradiation, (3) in vacuum after various intervals of irradiation, (4) in vacuum at varying time periods after irradiation, (5) in an argon atmosphere after vacuum irradiation, (6) in air under reduced pressure after vacuum irradiation, and (7) in air at atmospheric pressure after vacuum irradiation. One of the coatings used in these tests was B-1056 produced by the Boeing Company and based on the S-13 formulation.

In two of the tests, argon was bled into the chamber prior to admitting air.[16] In neither experiment did the B-1056 coating bleach. The maximum exposure to argon was 30 minutes at 0.5 torr. Upon admission of air, two samples "bleached", showing no permanent change in solar absorptance. Two samples retained a +1 percent change. This increase resulted from nonbleachable damage in the visible-wavelength region near the absorption edge (0.4-0.5 microns).

Figure B-1 shows the relative reflectance of samples of the B-1056 coating before UV exposure, after 350 ESH in vacuum, and after air was let into the system. A similar effect was reported at IITRI and is shown in Figure B-2. A reflectance decrease of about 35 percent at a 2-micron wavelength was noted after approximately 800 ESH in vacuum. Recovery when exposed to the atmosphere was almost total after 2 minutes.[17] Major damage occurred at wavelengths greater than 1 micron and was maximum at about 2 microns (see Figure B-1). The damage bleached out upon exposure to air. It was noted also that no gross bleaching occurred when air pressure was less than 10^{-2} torr.[16]

Pegasus reported data on the degradation of S-13 for at least 1800 sun hours. As is shown in Figure B-3, there was good agreement between the laboratory (vacuum) data and that obtained on space flights of both Orbiter I and Pegasus I. Data from OSO-III showed a trend with S-13 coating of continuous change with exposure to sunlight.[13] The results compared favorably with data from Pegasus I and OSO-II, both near-earth experiments. Changes in α_s measured in the near-earth space environment generally were much less than those measured in interplanetary space.

Results from the Mariner V experiment, which was continuously exposed to the solar wind are shown in Figures B-4 and B-5. This flight was launched on June 14, 1967, encountered Venus on October 19, 1967, and obtained information on interplanetary space. The TCR (temperature control reference) assemblies were continuously sunlit, and normal to incident solar radiation to within less than ± 1/2 degree.[18] Data on apparent solar absorptance versus mission duration were obtained for the first 48 days of flight, at which time the temperature reached the upper limit of the sensor range and no further data were obtained (Figure B-5). Since it was the change in temperature which was monitored, solar absorptance was obtained by assuming a constant emittance of 0.86 and a solar intensity of 126.4 W/ft^2 at 1 AU (this value was indicated by early results from the black TCR). Absorptance changed from about 0.23 (less than 1 hour after sun acquisition) to approximately 0.41. This degradation was more rapid than was expected based on laboratory tests.[18]

The S-13 coating was also tested on the ATS-I flight and, again, degradation was more rapid than was expected.[19, 20] Data are shown in Figure B-6.

Work has shown that the sensitivity of the S-13 coating to UV increases very rapidly as the wavelength of irradiation decreases below 300 mμ.[21]

See Table B-1 and Figures B-7 and B-8. During UV irradiation in vacuum S-13 increases in spectral absorptance near the absorption edge of ZnO. In addition, it increases considerably in spectral absorptance in the IR region which, as stated above, bleaches out when the sample is returned to the atmosphere. As seen in Figure B-9, IR absorption is wavelength sensitive. For approximately the same degradation near the absorption edge, the short-wavelength UV (250 mμ) is more effective in producing the near IR degradation than is the longer wavelength UV (350 mμ).

Effect of UV and Electron Exposure

An S-13 coating was subjected to four types of exposure: UV only, electron only, UV followed by electron, and simultaneous UV and electron exposure.[3] All UV exposures were 18 ESH and all electron exposures were 5×10^{14} e/cm^2. Samples receiving sequential exposure remained in situ between exposures. All reflectance measurements were made in situ. Table B-2 shows the spectral-reflectance changes after the four types of exposure. It may be seen that initial UV exposure preconditions the S-13 coating so that later electron exposure leaves it less degraded in reflectance than an electron-only exposure dose.[3] The extent of degradation also appears to depend on the ratio of exposure rates of electron and UV radiation.

Effect of UV and Proton Exposure

An S-13 coating was subjected to UV, 10 keV proton, and combined (sequential) UV and proton exposure at room temperature (298 K) and 10^{-7} torr.[22] The effects of proton radiation are shown in Figures B-10 and B-11. The characteristic curve for zinc oxide susceptibility to proton damage may be seen. There appears to be no rate effect. Also shown in Figure B-10 is the fact that the coating showed a bleaching in the IR after remaining in the vacuum chamber for approximately 74 hours. Increasing the dose from 10^{15} to 10^{16} p/cm^2 almost doubled the peak change in absorptance with approximately 5 percent greater damage in the IR range. The effect of ultraviolet radiation (750 sun hours) was slight. There was a slight absorptance peak near 0.4μ and less change in the IR than had been found with the zinc oxide/potassium silicate coating. See Figure B-12.

The effects of the combined (sequential) environment are shown in Figures B-13 to B-16.[22] After a dose of 10^{15} p/cm^2, there is little difference between the sum of the individual environments and the combined environments except in the IR, where the effect of the sum is greater than the

effect of the combined environments. Figure B-15 shows that the absorptance peak around 0.4μ was considerably greater for the low dose rate than for the higher dose rate with approximately the same damage in the IR range.

Zinc Oxide [SP-500] Coated With Potassium Silicate/RTV-602 Silicone (S-13G)

Illinois Institute of Technology Research Insititute (IITRI) developed a formulation using a potassium silicate protected ZnO in RTV-602 silicone binder and designated the coating as S-13G. This is more resistant to UV in a vacuum than the S-13. The coating, catalyzed with GE's SRC-05 catalyst at a 0.4 percent by weight level based on the RTV-602 solids, cures to the touch in 4 to 6 hours and can be handled in 16 hours. The uncured paint possesses a shelf life in excess of 3 months. An 8-mil film of S-13G has an α_s of 0.19 ± 0.02 and an emittance of 0.88 ± 0.05. $\Delta\alpha_s$ is 0.03 for 1000 ESH employing in situ postexposure reflective measurements and AH-6 lamp irradiation.[17]

An S-13G specimen employing a sifted pigment that was not dry ground prior to a 3-hour paint-grinding operation exhibited an increase in solar absorptance of 0.01 in 1400 ESH of irradiation.[23] A specimen employing pigment that was first hand mulled and then wet ground for 3 hours exhibited a $\Delta\alpha_s$ of 0.05; a specimen prepared from hand-mulled pigment that was wet ground 5-1/2 hours exhibited a $\Delta\alpha_s$ of 0.06 in 1400 ESH. Since sifting as a method of insuring sufficiently deagglomerated particles is highly inefficient, a compromise method is employed consisting of wet grinding unsifted, unground silicate-treated pigment for 7 hours in the RTV-602 vehicle. A coating prepared in this way exhibited a $\Delta\alpha_s$ of 0.02 in the 1400 ESH test.[23] A grinding period of 4 to 5 hours is usually required to produce a satisfactory coating. The presence of potassium silicate on the zinc oxide severely retards the formation of IR absorption bands (2.12 microns). However, in processing this material, considerable color center sites are formed leading to damage under UV irradiation in the visible-wavelength region.[16] This illustrates the importance of the methods used for preparing the coating.

There has been almost a continual development of S-13G regarding its manufacture and mechanical treatment in its manufacture. The formula for this paint as reported at the 3rd AIAA Thermophysics conference, was:[24]

Components	Weight, lbs
Silicate-treated SP500 ZnO	25
RTV-602 silicone resin (GE)	12
S-13G mixed thinner	14
(Comprising, percent)	
Toluene	40
Xylene	20
n-butanol	15
Isopropanol	20
Butyl acetate	5

The treatment of the ZnO involved a reaction of the pigment, SP-500 ZnO (New Jersey Zinc Co.), with PS-7 potassium silicate (Sylvania Electric Co.) at a temperature of 165 F. After the reaction, the filtered cake was wrapped in Mylar and allowed to "sweat" for 18 hours. The pigment aggregates were deliberately kept large, around 80 mesh, to prevent damage to the optical properties of the pigment and (for the same reason) a minimum of grinding was used in preparing the paint.[24]

Figure B-17 shows the spectral reflectance of the S-13G coating before exposure, after exposure to UV while still in a vacuum, and after air was admitted to the chamber.[16] The effect of UV exposure to S-13G may be seen also in Figure B-18. Decreases in reflectance in the UV, visible, and IR wavelength regions after UV irradiation were as follows:[25]

UV Exposure,	Decrease (Increase) in Reflectance, $\Delta R = R_i - R_f$ (%)		
ESH	250 mμ	425 mμ	2100 mμ
135	(3)	10	6
250	(2)	14	8
490	(2)	19	8
770	--	23	--
1130	0	25	6

Figure B-19 shows the laboratory data and those obtained from Lunar Orbiter II flight. It will be noted that there was not good agreement for the S-13G coating between laboratory-test and flight data. The reported laboratory tests were conducted near 70 F. Lunar Orbiter II deck temperature experienced considerable thermal cycling due to the orbit of the spacecraft. The orbit about the moon was 3-1/2 hours, with about 30 percent of the time in the dark. It was believed that this changing thermal input might have

caused failure of the adherence or cracking in the top coat. In either case, the thermal properties would change. Another reason for the discrepancy between the flight and laboratory data is the fact that the latter did not include the effects of particulate radiation. Figure B-19 also shows the increase in $\Delta\alpha_s$ for the S-13 coating (Boeing B-1056) which occurred on Lunar Orbiter I so that a comparison may be made of the behavior in space of the two coatings, S-13 and S-13G.[16]

Coating S-13G was also tested on Lunar Orbiter IV and tested over B-1056 (Boeing) on both Lunar Orbiters IV and V. The latter coatings were used as a reference because the equipment-mount decks (EMD) of these two spacecraft were painted with S-13G over B-1056 and it was desired to have a test coupon of the same coating system as the EMD.[26] The S-13G coating was 10 mils in thickness and had an absorptance value, $\alpha_s = 0.184$. With the S-13G over the B-1056, the undercoat was 10 mils, while the S-13 G overcoat was 2 mils. Initial absportance was $\alpha_s = 0.191$. Initial reflectance versus wavelength is given in Figures B-20 and B-21. Also in Table B-3 are the initial absorptance/emittance ratios from flight measurements. Figures B-22 and B-23 show the changes in α_s/ϵ of these coatings during the Lunar Orbiters IV and V flights.

Figure B-24 shows the degradation of test coatings on Lunar Orbiter IV and the comparative test on Lunar Orbiter V for S-13G/B-1056. Figure B-25 shows the degradation of coatings on Lunar Orbiters I, II, and V. A comparison of these figures will show:

(1) Differences between Orbiter V test coupon and EMD's on Orbiters I and II are no greater than differences between the Orbiter IV and Orbiter V coupons.

(2) S-13G coating over B-1056 lessened degradation experienced by B-1056 alone up to about 800 sun hours. After that time the S-13G/B-1056 curve for Orbiter II merged with the B-1056 curve for Orbiter I.

(3) The calorimetric UV test predicted much less degradation on B-1056 than was experienced in flight. It is suggested that temperature of the paint during exposure may be partially responsible for this disparity. The specimen temperature in the calorimetric test was from 9 to 30 F, whereas Lunar Orbiter deck temperatures ranged from 40 to over 100 F.

Comparing the results of the S-13G coatings tested on the Mariner V with those obtained from Lunar Orbiter IV (see Figure B-26), it will be seen that the increase in solar absorptance for each coating was approximately equal. The solar absorptance of the S-13G on the Lunar Orbiter was initially lower than that on the Mariner.[14]

Preliminary results of the OSO-III flight experiment indicated only a 0.04 increase in solar absorptance in 1000 ESH. When compared to the 0.12 increase for the same exposure time on the Lunar Orbiter, a substantial difference in the results of these two flight experiments is clearly shown.[14] The OSO experiments were in a near-earth environment, below the earth's Van Allen belt, and therefore exposed primarily to UV radiation and micrometeoroids. The Mariner and Lunar Orbiter experiments passed through the Van Allen radiation belts and thus were exposed to all the listed environmental parameters. Although there were variations in the processing parameters among the versions of S-13G prepared for testing on the three flight experiments, a consideration of these variations does not show a significant reason why the OSO experiments should record much lower degradation rates; therefore the change must be attributed to the environmental parameters.[14] There appears to be a definite difference in the degradation rate of thermal-control coatings between the near-earth orbital environment and the interplanetary or lunar environment.

Effect of Electron Bombardment

When irradiated with 50-keV electrons at 22 C, zinc oxide-, ethyl silicone sample types (S-13, S-13G, and a zinc oxide-Dow Corning Q92-016 methyl silicone coatings) had their greatest reflectance losses in the IR region. These showed the greatest loss of reflectance in the IR region of the various coatings tested. The S-13G appears to be the most sensitive of the ZnO-methyl silicone specimens. However, the loss of reflectance in the visible region was much less than that of many other sample types.[3] Figure B-27 shows the effect of 50-keV electrons on an early formulation of S-13G coating after electron bombardment.[25] The decrease in reflectance was 11 percent at 590 mμ after 6×10^{14} e/cm^2, and 20 percent at 2100 mμ after the same dose. Initially a rapid decrease of reflectance in the IR region occurred, which eventually tended to saturate. However, in the visible region, the buildup of damage was slow at first and then more rapid at high exposure.[25]

Coatings S-13, S-13G, and Goddard 101-7 (treated ZnO/methyl silicone) were exposed to 20-keV, 50-keV, and 80-keV electrons separately to

doses of 10^{16} e/cm^2.[27] It may be seen in Figures B-28 to B-30 that these coatings are susceptible to electron damage, particularly at the higher energy levels. It was found that after exposure to 20-keV electrons, samples (maintained in a vacuum and not exposed to light) partially recovered in reflectance values. However, exposures to the same dose had the same reflectance values regardless of whether or not exposure was continuous.[27]

Proton Damage

The S-13G coating was exposed to proton bombardment (E= 20 keV) and sustained threshold degradation at 10^{14} p/cm^2, moderate degradation at 10^{15} p/cm^2. and severe damage at 10^{16} p/cm^2.[3] It was also exposed to 10-keV proton, UV, and combined (sequential) proton and UV[22] at room temperature and 10^{-7} torr. The effect of proton radiation on this material is shown in Figure B-31. The coating showed the characteristic damage curve for ZnO with about the same affects as the S-13 irradiated with continuous low current. The effect of UV only is shown in Figure B-32. The change in solar absorptance is greater (around 0.4 micron) than for the S-13 or the ZnO/K_2SiO_3 with virtually no damage in the IR range. The effect of combined (sequential) environment simulation is shown in Figure B-33. Bleaching of the proton damage in the IR range has apparently occurred.

The S-13G coating was tested for the effects of thermal cycling. Test cycle consisted of holding at test temperature, 395 K or 533 K, for 1/2 hour, cooling to near-liquid-nitrogen temperature for 6 hours, and then letting the sample slowly increase to ambient temperature (300 K) over a period of 17.5 hours. Coatings were thermally cycled 4 times before examination. No evidence of cracking or spalling of the coatings was observed by the unaided eye or at 100X magnification.[28]

B-1060

A modification of the S-13G is B-1060 produced by the Boeing Company. According to their work, the sensitivity of their B-1056 paint to damage under UV vacuum exposure was dependent upon catalyst concentration and differed from batch to batch. Boeing then developed a paint using the silicate-treated zinc oxide, RTV-602 (GE silicone binder), and 1,1,3,3-tetramethyl guanidine (TMG) as catalyst.[26] The formulation follows:

Pigment	ZnO (potassium silicate-treated SP-500)
Resin	RTV-602 (GE)
Catalyst	0.2 percent 1,1,3,3-tetramethyl guanidine (TMG)

The stability of the paint to ultraviolet is indicated in the following data:[26]

Initial absorptance	0.194
$\Delta\alpha_s$ after 0.55 ESH UV	0.003
$\Delta\alpha_s$ after 2.2 ESH UV	0.005
$\Delta\alpha_s$ after 8.8 ESH UV	0.007
$\Delta\alpha_s$ after 125 ESH UV	0.028
$\Delta\alpha_s$ after 10^{14} 50-keV electrons/cm^2	0.007

Reflectance curves showing the wavelength at which damage occurs are shown in Figures B-34 and B-35.

Initial absorptance/emittance of flight coupons carried on Lunar Orbiter IV are given in Table B-3. The increase in absorptance on exposure to the sun during flight is shown in Figure B-24. Laboratory in situ degradation of B-1060 is also shown in Figure B-24. In this case, the laboratory data indicated greater degradation than was experienced in flight. Most of the change in absorptance ($\Delta\alpha_s$ = 0.028) experienced by the B-1060 in the laboratory was due to increase in absorptance in the short-wavelength region around 400 mμ, and not due to the zinc oxide "IR anomaly".

The coatings tested on Lunar Orbiters IV and V are listed below in order of increasing degradation experienced in 1000 equivalent full sun hours of flight:[26]

Coating		$\Delta\alpha_s$ After 1000 Sun Hours
Z-93 (McDonnell)	SP-500 ZnO dispersed PS-7 potassium silicate	0.049
Silicone Over Aluminum (Boeing)	RTV-602 over aluminum foil, 0.15% TMG	0.081
Hughes Inorganic H-2	TiO_2 in PS-7	0.089
B-1060 (Boeing)	Modification of S-13 paint	0.091
Hughes Organic H-10	Calcined china clay dispersed in RTV-602	0.120
S-13G (IITRI)	--	0.123
S-13G B-1056	--	0.168

Flight data for these coatings are given in Figures B-22 and B-23.

Titanium Dioxide-Silicone Coatings (Thermatrol White Paint)

Based on the properties of the ZnO-silicone coatings, it would be anticipated that work would also be directed toward the development of a titanium dioxide-silicone coating. Such has been the case. However, difficulty has been encountered in obtaining a coating stable to UV and/or ascent heating.[9] In general, these coatings show good stability in the UV and IR wavelengths of the solar spectrum, but when subjected to UV radiation, their reflectance in the visible wavelengths is considerably decreased. They are resistant to electron bombardment up to 10^{15} e/cm^2, but are susceptible to proton degradation. The pigment is very susceptible to proton damage.[22] The coating is resistant to nuclear radiation (10^8 rads) and to a combined nuclear and UV environment.

Lockheed developed a coating known as Thermatrol 2A-100 which consisted of a 1:1 weight ratio of Titanox RA-NC pigment and Dow Corning Q92009 silicone binder. This binder is a polymethyl vinyl silicone and the pigment is a rutile TiO_2 which has been given a surface treatment. The pigment consists of 94 percent TiO_2, 1.8 to 2.4 percent Al_2O_3, 0.6 to 2.0 percent SiO_2, and 0.5 to 1.4 percent ZnO.[28,29,30] The α_s/ϵ ratio of the paint is 0.19. It can be applied as a paint and cured at room temperature or used as a precured tape with a pressure-sensitive silicone adhesive.

Several modifications have been made to improve the coating, and some of the data which follow are for earlier formulations. However, on the basis of available information, it is believed that the conclusions are applicable to the current commercial product. It is known that the surface treatment of the pigment is important to the UV stability of the paint, and one of the problems is to incorporate the pigment into the binder without affecting the surface of the pigment particles.

Thermatrol 2A-100 was exposed to a xenon source (AH-6 lamp) at a 1-sun level (0.20 to 0.40 μ) for 500 hours in a vacuum at a temperature of 395 K (122 C). In situ values of before and after exposure were α_s = 0.18 and 0.32, respectively.[27] The total hemispherical emittance remained essentially constant at 0.85 ± 0.003 for the two samples tested. The change in solar absorptance appeared to reach a saturation value of 0.14 after 300 to 400 hours of exposure at this temperature.[28]

In another test, only slight damage was found when a TiO_2/silicone (Ti Pure R-960 in RTV 602 silicone) coating was subjected to 190 sun hours UV at room temperature and 10^{-7} torr.[22] See Figure B-36.

A rutile TiO_2/methyl silicone (GE RTV 602) coating was found to offer the best stability of the white diffuse coatings to an electron environment (20 keV, 50 keV, and 80 keV), providing a dose above 10^{15} e/cm^2 was not encountered.[27] However, at 10^{16} e/cm^2 (E=80 keV) catastrophic degradation occurred. An anatase TiO_2/methyl silicone (Q92009) degraded more at lower fluences, but did not degrade to as great an extent at 10^{16} e/cm^2. Compare Figures B-37 and B-38. Titanium dioxide-methyl silicones were found to be less sensitive to a reflectance change in the IR region than the zinc oxide-methyl silicone samples when exposed in situ to 50-keV electrons. They suffered more significant reflectance loss in the visible region, however.[3] The most radiation resistant of this type coating were the rutile titanium dioxide-GE RTV 602 methyl silicone and rutile TiO_2-Dow Corning XR 6-3488 methyl silicone coatings. However, the TiO_2GE RTV 602 appeared to craze when subjected to 10^{15} p/cm^2 at 22 C. Figure B-39 shows the effect of proton radiation on the Ti-Pure R-960/RTV 602 silicone coating. At 3 x 10^{15} p/cm^2, the spectral curve has the characteristic peak of ZnO but does not return to near zero in the visible range as does the ZnO.[22]

An anatase titanium dioxide-methyl phenyl silicone (OAO Pyromark Standard White) coating was subjected to four types of exposure: UV only, electron only, UV followed by electron, and simultaneous UV and electron exposure. All UV exposures were 18 ESH and all electron exposures were 5 x 10^{14} e/cm^2 (E = 50 keV). Samples receiving sequential exposure remained in situ between exposures. All reflectance measurements were made in situ.

As may be seen in Table B-4, reflectance changes from combined exposures are less than additive, with consecutive exposure (UV followed by electron) causing significantly less damage than simultaneous exposure. In much of the wavelength region measured, simultaneous exposure resulted in less degradation than electron-only exposure.[3]

The effect of UV radiation only on this coating is shown in Figure B-40. Changes after 1130 ESH for this coating were 3 percent at 250 mμ, 67 percent at 425 mμ, and 2 percent at 2100 mμ (UV, visible, and IR wavelengths).[25]

This coating when subjected to 20-keV protons reached threshold damage at 10^{14} p/cm^2, moderate damage at 10^{15} p/cm^2, and sustained severe degradation at 10^{16} p/cm^2.[3]

Thermatrol 2A-100 was exposed to nuclear radiation, 1.3 x 10^8 rads (C), 1.9 x 10^{13} n/cm^2 (E<0.48 eV), and 5.6 x 10^{14} n/cm^2 (E>2.9 MeV).

No change in solar absorptance was noted, the value remaining at 0.16. Also there was no change in hemispherical emittance.[31]

A titanium dioxide-silicone white paint which is used on the outer shell of the service-module fuel-cell bay of the Apollo spacecraft was mounted on the service module and command module of Apollo 9.[32] During the extra-vehicular activity period, the astronauts removed the samples along with samples of ZnO/K_2SiO_3 and chromic acid anodized aluminum. These specimens were the first to be returned to earth from space unaffected by reentry conditions. Exposure to space was approximately 73 hours.

The sources of contamination to which these samples were exposed included:[32]

Plume impingement

Boost heating effects

Outgassing products of ablative materials

Pyrotechnic discharge products

The natural space environment.

Degradation of the titanium dioxide-silicone coating resulted in a 42 to 67 percent in absorptance increase, and in a slight increase in emittance. Absorptance increased from 0.24 to between 0.34 and 0.40. Emittance increased from 0.86 to 0.88. Although degradation occurred, the absolute values were well within acceptable limits for the Apollo lunar-landing missions.[32] It should be noted, however, that samples were not brought back to earth in vacuum and therefore the effect of solar exposure in space may not be accurately reflected in the above figures.

An anatase TiO_2 (Titanox AMO) in Dow Corning Q92-090, a methyl silicone, was tested on the ATS-I satellite.[19,20] In this flight, α/ϵ for this coating increased over 200 percent. See Figure B-41. This was more than had been anticipated from laboratory measurements.

Hughes Organic White Paint (H-10)

This coating is made with a calcined china clay (Plasmo clay, which is primarily aluminum silicate) dispersed in General Electric RTV-602 silicone resin. Initial solar absorptance as a function of wavelength is shown in Figure B-42. It was tested on the Lunar Orbiter V and found to be equivalent

to the S-13G coating. Initial absorptance/emittance values are given in Table B-3. Solar absorptance, α_s, obtained in the laboratory was 0.147 and, after 1000 sun hours of flight on the Lunar Orbiter V. $\Delta\alpha_s = 0.120$.[26] Changes in α/ϵ during the Lunar Orbiter V flignt are shown in Figure B-23.[14]

Leafing Aluminum/Phenylated Silicone

Leafing aluminum in a phenylated silicone binder showed moderate losses in reflectance after exposure to 10^{17} p/cm^2 (E = 20 keV). Exposure was at 22 C. The losses were confined to wavelengths shorter than 0.7 microns. On the other hand, reflectance as measured in situ increased at wavelengths longer than 0.7 microns. Thus a determination of solar absorptance would show little change due to proton exposure.[3]

This coating was also subjected to 10^{16} e/cm^2 (E = 20 keV and E = 80 keV) and found to be extremely resistant to reflectance change.[27] See Figures B-43 and B-44.

Exposed to 50-keV electrons, this coating underwent practically no reflectance changes throughout the measured region to a dose of 8×10^{14} e/cm^2 and only small changes were observed after 8×10^{15} e/cm^2. At 2100 mμ, reflectance decreased 3 percent after exposure to 6×10^{14} e/cm^2, and 8 percent after 8×10^{15} e/cm^2.

Exposure to UV resulted in the following decreases in reflectance:[3]

Exposure, ESH	Decrease (Increase) in Reflectance, percent		
	250 mμ	425 mμ	2100 mμ
135	10	1	(2)
250	13	1	1
490	17	2	1
770	--	3	--
1130	24	4	1

Silicone Over Aluminum

Lunar Orbiter V carried a specimen of 1/4-mil 1145-0 aluminum-alloy foil over which was applied 3.8 mils of RTV-602 silicone catalyzed

with 0.15 percent TMG (1, 1, 3, 3-tetramethyl guanidine). Figure B-45 shows the reflectance of the foil substrate as a function of wavelength and the initial reflectance of the silicone-aluminum composite as a function of wavelength.

Evaluation of UV stability, in situ, was made on a film of RTV-602 silicone.[26] The film was 2.6 mils thick over 2024 clad aluminum and was catalyzed with 0.15 percent TMG. Figure B-46 shows the reflectance of the silicone-aluminum composite unexposed, and after 336 and 1141-ESH UV exposure measured in situ. The data show no measurable degradation of the silicone after 336 ESH of UV. The 1141-ESH exposure resulted in an increase in absorptance below 540 millimicrons and a decrease in absorptance above 540 millimicrons, with a net $\Delta\alpha$ of 0.012. Laboratory in situ degradation of the silicone-aluminum coating is plotted in Figure B-47. It may be noted that there is a large disparity between the in situ value and the flight values obtained from Orbiter V. However, the silicone over aluminum has about the same stability as Hughes inorganic coating and as B-1060, but it is less costly to apply than any of the other coatings tested on Lunar Orbiters IV and V. The change in absorptance, $\Delta\alpha_s$, after 1000 sun hours in flight was 0.081, which was surpassed only by the Z-93 coating. Flight data for Orbiter V are shown in Figure B-23.

Silicone-Alkyd-Modified Paints

Fuller Gloss White

Fuller Gloss White is a TiO_2-pigmented silicone-modified alkyd coating in production use that requires a 465 F cure. Its initial solar absorptance is 0.25 while its initial hemispherical emittance is 0.90. It has fair optical stability in an UV environment, but good optical stability in electron, gamma, and neutron environments. It degraded more than the algebraic sums of the two individual environments in sequential exposure (UV followed by electron).

Lockheed found that absorptance changed by 0.09 ± 0.05 after 2000 sun hours. Tested for thermal-cycling resistance, the coating cracked and showed a loss of adhesion after 170 cycles of -240 to 70 F, taking 18 minutes per cycle.[33]

Ascent temperature is limited to 650 F.[33] The effect of ascent heating is shown in Figure B-47.[9]

Fuller Gloss White showed excellent stability when irradiated (gamma and neutron) to 10^8 rads (C) in vacuum at 100 F.[33] Solar absorptance before and after irradiation was 0.26. Hemispherical emittance, 0.84, was unaffected.[31]

An exposure of 850 sun hours in vacuum caused a change of solar absorptance from approximately 0.25 to 0.32. (See Figure B-48). Optical property degradation was marginal in the UV-only environment.[31]

PV-100 (TiO_2 in a Silicone Alkyd Vehicle)

General Dynamics tested PV-100 coating, manufactured by Vita-Var Paint Company, and found that it was degraded by 10^{16} p/cm^2 (E=3 keV) in the visible and IR regions.[34] See Figure B-49. Spectral reflectance also decreased in these regions when the coating was subjected to electron irradiation (145 keV). See Figure B-50. Damage is not proportional to dose, but approaches a saturation level at a dose not much greater than 4×10^{16} e/cm^2 (145 keV).[34]

Acrylic Paints

The best known acrylic paint used as a thermal-control material is White Kemacryl, a TiO_2-pigmented acrylic flat paint manufactured by Sherwin-Williams. The paint is cured at room temperature and has an initial solar absorptance of 0.24. Initial total hemispherical emittance is 0.86. It has good optical stability in an electron environment, but poor optical stability in an UV environment.[35] Some mechanical damage was observed after this coating had been subjected to an electron environment. When exposed to electron and then UV irradiation, the paint degraded more than the results of the two environments separately would predict. Small blisters were formed on the Kemacryl coating. It was believed that these were most likely caused by electron-induced decompositon products. It was concluded that these surface alterations had no detrimental effect on the mechanical integrity of the coating. It was also estimated that the blisters had no measurable effect on solar absorptance.

Lockheed exposed the coating to 100 and 850 sun hours of UV and reported α_s/ϵ as increasing from 0.30 to 0.35 after 100 hours and 0.40 after 850 sun hours, respectively. The maximum allowable ascent temperature was given as 450 F providing alterations in surface finish, and solar absorptance due to bubbling can be tolerated. Otherwise the maximum temperature

encountered must be less than 200 F.[9] See Figure B-51 for the effect of ascent heating on solar absorptance.

Tinted white Kemacryl lacquer (Sherwin-Williams M49WC17, room-temperature cured) was subjected to nuclear radiation in vacuum.[25] Emittance did not change. Data shown in Figure B-52 indicate an increase in α_s from 0.28 to 0.32 after an exposure of 5×10^7 rads (C), but no further change at 2.5×10^8 rads (C).[31] However, degradation of optical properties was considered unsatisfactory after 10^8 rads.

UV exposure of 1000 sun hours increased α_s from approximately 0.26 to approximately 0.38.[31] See Figure B-48. In combined nuclear and UV radiation, this paint turned brown and bubbled.[31] Exposure was 920 sun hours of UV and 7.1×10^{13} n/cm^2 (E< 0.48 eV), 4.6×10^{14} n/cm^2 (E > 2.9 MeV), and 1.1×10^8 rads (C) gamma. Temperature was 180 F.

A MgO/Acrylic coating supplied to General Dynamics by Wright-Patterson Air Force Base was subjected to 10^{16} p/cm^2 (E=3 keV), and some loss in reflectance was noted in the UV and visible regions.[34] See Figure B-53.

Polyvinyl Butyral

Butvar (polyvinyl butyral) has been considered for use as a thermal-control finish because of its excellent film-forming characteristics and good UV stability.[36] It surpasses the acrylic polymers in adhesion and flexibility, but its stability to the heat which may be encountered during ascent conditions rules it out as a good candidate for a surface coating for outer space use. Its softening point is approximately 125 C. A further limitation is the existence of two moderately strong absorption bands at 1.7 and 2.3 microns which tend to make the solar absorptance dependent on thickness as well as the emittance. The change in solar absorptance and emittance with film thickness on an aluminum backing is shown in Table B-5.

Epoxy Coatings

White Skyspar

White skyspar is an enamel consisting of a TiO_2-pigmented epoxy-base paint which is in commercial production (Andrew Brown Co.). It cures at

room temperature and has an initial solar absorptance of 0.25 and an initial total hemispherical emittance of 0.91.[37] It is stable to electron bombardment, but degrades under UV irradiation. Lockheed reports initial α_s/ϵ as 0.24; change in absorptance ($\Delta\alpha_s$) is reported as 0.35 ± 0.06 after 2000 sun hours.[9] The maximum allowable ascent temperature is 450 F.[9]

Skyspar was flown aboard OSO-I and OSO-II Satellites. Agreement between laboratory tests and flight tests was extremely poor, varying several orders of magnitude. However, agreement between the OSO-I and OSO-II data was excellent.[21] The main cause of coating degradation during near-earth satellite experiments can be attributed to absorbed solar-UV radiation since low-energy solar-wind protons are effectively shielded from the orbits of the satellites, OSO-I and -II and Pegasus I, II, and III, by the earth's magnetosphere. It is believed that inadequate simulation of solar-UV radiation is the main factor in the presently observed discrepancy between flight and laboratory data. Another factor is the lack of temperature control in the laboratory tests.

The threshold wavelength for degrading the reflectance of TiO_2/epoxy coatings is between 260 and 290 mμ (4.7 and 4.2 eV)[21]. Olson, McKellar, and Stewart reported that photons with energies less than 4.2 eV resulted in increased absorption primarily in the visible and IR, whereas photons of greater energy produced damage primarily near the UV absorption edge.[38] Figure B-54 shows the absorptance changes due to irradiation with a band centered at 260 mμ and with a band centered at 350 mμ. The two curves have been normalized to equal change in solar absorptance. It will be noted that with the 260-mμ irradiation, the induced solar absorptance occurred primarily near the absorption edge of TiO_2, and the degraded sample had a yellow appearance. For the 350-mμ incident radiation, the induced absorptance extended through the visible and near-IR regions, and the sample exhibited a grayer appearance. The absorption edge of the epoxy binder is located at about 290 mμ. Thus the high absorptance and poor stability of the epoxy resin undoubtedly have a strong effect on the sensitivity to wavelengths shorter than 300 mμ.

Skyspar enamel was subjected to nuclear radiation in a vacuum. As seen in Figures B-48 and B-52, this coating showed poor stability to UV and only fair stability to nuclear radiation. It was tested for nuclear-radiation stability at temperatures of -100, 0, 100, and 200 F to an exposure dose of 2.2×10^6 rads (C), 0.6×10^{13} n/cm^2 ($E < 0.48$ eV), 1×10^{14} n/cm^2 ($E > 2.9$ MeV). Changes in α_s are shown in Table B-6. The greatest increase was $\Delta\alpha_s = 0.06$ at 200 F. At 0 and -100 F, there was no change. There was no change in hemispherical emittance.[31]

At a dose of 5×10^7 rads (C), α_s of this material changed from 0.23 to 0.30 and at a dose of 2×10^8 rads (C), α_s changed to 0.35. Temperature was about 100 F.[31]

Epoxy Flat Black ("Cat-a-lac")

Another epoxy coating is "Cat-a-Lac" flat black which consists of a carbon pigment in an epoxy binder. It is widely used as a spacecraft black coating. Its reflectance does not vary with wavelength, thus the coating is insensitive to spectral discrepancies between the sun and a solar simulator.[18] It was one of the test surfaces on the Mariner IV absorptivity standard, and data indicated good coating stability in the space environment. On the Mariner V flight, this coating showed an unexpected apparent bleaching of approximately 4 percent. It was significantly larger than anything observed in the laboratory. Simulation testing indicated a change of the order of 1 percent in solar absorptance for equivalent exposure. This bleaching is unexplained. Although it probably is not serious from a thermal-control standpoint, it adds to the discrepancies found between laboratory and flight data.[18]

Polyurethane Coatings

A Magna-Laminac X-500 polyurethane flat chromium green paint has thermal properties similar to the flight-type solar cells.[39] Their optical properties are as follows:

Coating	Absorptance (α)	Emittance (ϵ)	α/ϵ
Flight-type solar cell	0.71	0.82	0.865
X-500 polyurethane paint	0.71	0.85	0.835

No information was reported on its stability in a space environment.

INORGANIC AND COMPOSITE COATINGS

Inorganic coatings in general are more resistant to space radiation than are organic coatings. However, they generally are not as convenient to apply, and in many cases require an elevated-temperature cure.

Silicates

Probably the inorganic binder most frequently used for coatings is sodium silicate. Of these silicate coatings the most important has been lithium aluminum silicate paint.

Lithium Aluminum Silicate Paint (Lithafrax)

This coating consists of commercial lithium aluminum silicate (Lithafrax 2123) in a silicate binder (sodium silicate D). It requires a 390 F cure and has the composition $4(Li_2O \cdot Al_2O_3 \cdot 8SiO_2)Na_2SiO_3$. Initial absorptance and emittance values are reported as 0.15 and 0.87, respectively.[37]

Spraying gives excellent coatings, but brushing or dipping results in poor adhesion and poor coverage. Minute amounts of contamination seriously alter both the initial α_s/ϵ ratio and the UV resistance of the paint. In addition, the paint cannot be adequately cleaned once it is contaminated or soiled after application. Consequently, extreme care must be taken to prevent contamination of both the paint itself prior to application and the painted surface after application. After application, the resultant surface should be treated as an optical surface with protection provided from dirt and contamination. The surface should be handled only with clean, white cloth gloves.

The method of application, temperature of cure, and susceptibility to soiling limits the use of this paint. However, its UV resistance is good, having an initial absorption of 0.13 ± 0.03; $\alpha_s = 0.19 \pm 0.03$ after exposure to 600 sun hours of UV irradiation. It will survive a 230 C ascent heating environment with no change in optical properties.

Although Lithafrax is stable under UV-vacuum radiation, it degrades severely under electron-vacuum bombardment (E = 0.80 MeV).[37]

The Lithafrax coating bleached when exposed to UV after being exposed to electron bombardment, and α_s after the sequential exposure of electron and UV was less than the sum of the separate effects of electron bombardment and UV radiation.

A Lithafrax/sodium silicate coating was subjected to nuclear radiation and to a combination of UV and nuclear radiation while in a vacuum. Irradiated to a dose of 5×10^7 rads, this coating changed in α_s from 0.14 to 0.20. At a dose of 2×10^8 rads, α_s was equal to 0.28.[31] Hemispherical emittance, ϵ_h, did not change. Figures B-48 and B-52 show that the Lithafrax/silicate coating is relatively stable in an UV environment, but it degrades severely in a nuclear environment. It was found that there was no isotope dependence in optical degradation.[31] Figure C-1 shows a comparison of the separate effects of UV and nuclear irradiation with the effect of concurrent irradiation for the Lithafrax/sodium silicate system. Although the exposure doses were not given, based on related data, it is probably that the nuclear exposure was 1.5×10^{13} n/cm^2 ($E < 0.48$ eV), 4.3×10^{14} n/cm^2 ($E > 2.9$ MeV), and 1.4×10^8 rads (C) gamma. The UV exposure was 500 to 640 sun hours. The combined UV and nuclear radiation consisted of 920 sun hours and 7.1×10^{13} n/cm^2 ($E < 0.48$ eV), 4.6×10^{14} n/cm^2 ($E > 2.9$ MeV), and 1.1×10^8 rads (C) gamma.[31] These curves show a strong interdependence of the effects of ultraviolet and nuclear radiations and, more importantly, they show that the degradation sustained in separate irradiations cannot be used to predict degradation when the two radiations are concurrent.

Synthetic $Li/Al/SiO_4$ Coating. Lockheed reported a research coating that contained synthetic $Li/Al/SiO_4$ and cured at room temperature.[37] Initial solar absorptance was 0.16, and initial total hemispherical emittance was 0.87. In general there was not much difference between this coating and the commercial Lithafrax coating. Its advantage lies in its room-temperature cure.

The effect of nuclear radiation in vacuum on the synthetic $Li/Al/SiO_4$/sodium silicate system was similar to that on Lithafrax. A dose of 1.3×10^8 rads (C) gamma, 8.2×10^{12} n/cm^2 ($E < 0.48$ eV), and 5.3×10^{14} n/cm^2 ($E > 2.9$ MeV) changed α_s for the synthetic pigment from 0.14 to 0.23. For Lithafrax, the change was 0.16 to 0.26.[31]

Hughes Inorganic White Coating
($Al\text{-}SiO_4/K_2SiO_3$)

The prime white finish used in Surveyor I[16] consisted of naturally occurring China Clay (Plasmo clay), which is primarily aluminum silicate, in Sylvania PS-7 electronic-grade potassium silicate.[30] The pigment contains approximately 3.0 percent impurities consisting of 0.42 titanium, 0.05 calcium, 1.28 magnesium, 0.42 sodium, and 0.11 potassium. The clay is calcined at 1275 C, then ball milled for 12 hours with water. The coating is applied with an air brush; the first two coatings are each baked for 1 hour at 225, and the third coating baked for 1 hour at 260 F.

As tested by Lockheed, solar absorptance for this coating was 0.14 ± 0.02 (Gary spectrometer) or 0.14 ± 0.01 (Gier-Dunkle spectrometer) and emittance was 0.89 ± 0.04.[30] The coatings were thermally cycled 4 times from 533 K to 83 K. There was no evidence of cracking or spallation. However, several areas of a slightly brown color appeared. The increase in solar absorptance, $\Delta\alpha_s$, was between 0.04 and 0.07.[16] After 540 solar hours in vacuum, solar absorptance of a 6.4-mil sample increased from 0.18 to 0.22, and exposure to the same number of hours in air gave a solar absorptance of 0.21.[16]. Figure C-2 shows the reflectance of the coating before and after UV exposure in vacuum. Minimum damage was noted in the IR region.[16] The spectral damage found in this test corresponds to that found in normal measurement tests in air.[16]

Aluminum Oxide-Potassium Silicate

Aluminum oxide/potassium silicate coatings were subjected to 20-keV and to 80-keV electrons. The visible-region absorption band was deeper and more sharply defined after 80-keV exposure than after 20-keV exposure. In contrast, damage in the near UV was greater after 20-keV electron exposure.[27] See Figure C-3.

Another aluminum oxide-potassium silicate coating was exposed in situ to particulate radiation (protons alone or protons plus electrons) and to combined electromagnetic and particulate radiation (UV with protons alone or UV + protons + electrons).[40] Test conditions are given in Table C-1 and data are shown in Figure C-4. In this work there were no significant differences found between ambient and in situ measurements. A predominant reflectance change was observed between 0.30 and 0.40 microns. Protons and UV had the effect of coloring this region, and electrons had the effect of

bleaching it. As with zinc oxide, the pattern was that the addition of electrons enhanced the stability of reflectance.

The 0.4-micron region in aluminum oxide is not at the band gap. The reflectance change has the characteristics of a color center in that the magnitude of change is an apparent function of radiation. It could be either a "physics" color center, i.e., belonging to the general F or V center classification, or a "chemical" color center, i.e., a function of the appearance of a new chemical impurity formed as a result of ionization, oxidation, or migration of an original impurity in the material. Thus in an aluminum oxide (dielectric) pigmented potassium silicate coating, the major effect of the addition of thermal electrons to proton and UV exposure is bleaching of what is probably a color center in the near UV.

Three coatings, Al_2O_3/K_2SiO_3 , $(TiO_2 + Al_2O_3)/K_2SiO_3$, and $(ZnO + TiO_2 + Al_2O_3)/K_2SiO_3$ were tested for stability to space environment on the ATS-I satellite. Absorptance increased considerably; much more than was anticipated from laboratory tests.[19, 20] Data are shown in Figures C-5 to C-10.

Zirconium Silicate Paints

Lockheed produces a zirconium silicate coating (LP10A) having a pigment-binder ratio of 3.5:1 by weight. The pigment is Metals and Thermit Corp. 1000 W grade, "Ultrox" zirconium silicate, acid leached and calcined by Lockheed. The binder is potassium silicate. The coating is applied by standard spray-gun techniques and cures at room temperature in approximately 12 hours.[30] The original coating has a solar absorptance of 0.14 ± 0.02 (Gary) or 0.14 ± 0.01 (Gier Dunkle) and a hemispherical emittance of 0.89 ± 0.03 according to Smith and Grammer.[30]

Samples to be tested for UV and electron stability had an initial $\alpha_s = 0.24$ and $\epsilon = 0.87$. The coating remained optically stable when subjected to either electron bombardment or UV radiation.[37] It should be noted, however, that this work was not done in situ and therefore is only indicative of the stability of this coating. After an exposure of 10^{16} e/cm^2, $\alpha_s = 0.26$; and when exposed to 10^{16} e/cm^2 followed by 485 sun hours in vacuum, $\alpha_s = 0.30$.

A $ZrO_2 \cdot SiO_2$ pigment has been synthesized by Lockheed and has been optimized with respect to calcination conditions, purification, and grind properties. Radiation stability of this pigment combined with potassium

silicate has been claimed to be excellent under exposures to laboratory simulated solar UV, solar-wind protons, and combined UV and 230-keV protons, Van de Graaff protons, and 1-MeV electrons. It has also demonstrated resistance to neutron/gamma radiation.[41]

Zinc Oxide in Potassium Silicate (Z-93)

This coating is very stable in the UV and electron environment,[42] but is damaged by proton bombardment.[13] Its use with satellites has been limited because of difficulties encountered in its application and to the difficulty of keeping it clean during preflight construction and activities.[42] However, it is used where surfaces are irregular, and on nuts and bolts and other hardware on which it is difficult to apply coatings other than paint. Although it soils easily it can be touched up.

Experiments in OSO-II, OSO-III, and Pegasus II have shown no measurable damage to this coating after over 3000 hours of solar exposure.[13, 21] Laboratory tests also indicate high stability although there are indications of increases in solar absorptance after 3000 ESH. Flight data from OSO-III indicated that the coating showed marked stability over the 1580 ESH for which data were analyzed.[13] A change in α_s of about 0.005 was noted after 1580 ESH. This is in good agreement with the data obtained from the OSO-II and the Pegasus II. The temperature of all three of the coatings was less than 0 C.

Data from Mariner IV and Lunar Orbiter V showed that the Z-93 coatings suffered greater degradation on these interplanetary flights than on those in the near earth environment. The cause of the increased degradation was apparently the solar wind.[13] Both spacecraft were exposed to the solar wind continuously. Data from the Mariner IV and Lunar Orbiter V are shown in Figure C-11. The initial solar absorptance as a function of wavelength is shown in Figure C-12, and initial absorptance/emittance values are given in Table B-3. For this paint, α_s was 0.184. After 1000 sun hours in flight on the Lunar Orbiter V, $\Delta\alpha_s$ was 0.049, the lowest value obtained in the Lunar Orbiter IV and V flights. Absorptance/emittance ratios, α_s/ϵ_h, as a function of sun exposure are shown in Figure C-13. Orbiter V flight data are shown in Figure B-23.

Specimens of a ZnO/K_2SiO_3 coating along with two ther coatings (TiO_2/K_2SiO_3 and a chromic acid-anodized aluminum) were retrieved from their mountings by astronauts during their extravehicular-activity period on

Apollo 9.[32] The samples had received approximately 73 hours of space exposure and were the first to be returned to earth from space unaffected by reentry conditions. Samples were subjected to the following sources of contamination:

Plume impingement from the tower jettison and Saturn II retromotors and from the service-module and lunar-module reaction-control-system engines

Boost heating effects

Outgassing products of ablative materials

Pyrotechnic discharge products

The natural space environment.

A comparison of preflight and postflight results show that the degradation of the ZnO/K_2SiO_3 coating ranged from 25 to 40 percent increase in absorptance. Absorptance, α_s increased from 0.20 to 0.25 - 0.28. See Table C-2. No appreciable change in emittance was evidenced. Although degradation occurred, the absolute values were well within acceptable limits for the Apollo lunar-landing missions.[32] It should be noted, however, that the retrieved samples were not returned under vacuum conditions and therefore degradation under solar exposure may not be entirely reflected in the measurements obtained.

Using a xenon lamp (which has a smooth continum between 200 and 400 mμ) and a short-wavelength cut-off technique, the effect of various regions of the UV on the solar absorptance of Z-93 coating was determined.[21] Table C-3 and Figure C-14 show the changes in $\Delta\alpha_s$ caused by the various regions of UV radiation. As is the case for many coatings, wavelengths shorter than 300 mμ were relatively much more damaging to Z-93 than those longer than 300 mμ.

Stability to Proton Bombardment. The Z-93 coating was exposed to 8-keV protons along with the S-13 (ZnO/silicone) and a barrier-layer anodized aluminum coating.[43] A plot of the change in solar absorptance versus integrated proton flux of 8-keV protons is shown in Figure C-15. It may be noted that the Z-93 coating was more susceptible to damage by the 8-keV protons than were the other two coatings. The threshold of significant

damage for the white coatings (a change in solar absorptance greater than 0.01) was in the order of 3 to 7 x 10^{14} p/cm^2.

In another experiment, the coating was exposed in situ to particulate exposure (protons alone or protons plus electrons) and to combined electromagnetic and particulate exposure (UV with protons or UV with protons and electrons).[40] Test conditions are given in Table C-1 and data are shown in Figures C-16 and C-17. The reflectance changes occurring with the coating varied considerably with wavelength. An increase in reflectance below the band gap was noted. Protons alone produced coloration at all wavelengths except below the band gap. The addition of electrons to the proton beam increased coloration at the band gap, but it also bleached the visible and near IR. The same general tendency was observed in the combined-environment exposures. However, specimen overheating was suspected in the test where electrons were added in the combined-environment test. In these tests, the addition of electrons was seen to cause less change in reflectance than when the particulate radiation was all protons.

There is evidence that the rate at which protons are applied to ZnO/K_2SiO_3 coatings has a definite effect on the amount of damage to the material, especially in the IR portion of the spectrum.[22].

In the proton-only environment, damage to the silicate-coated zinc oxide is both temperature and energy dependent, with the greatest damage occurring with the lower energy.[44]

A comparison of individual proton, UV and combined irradiations of equal exposure conditions and fluxes is shown in Figures C-18 to C-20 for temperatures of 233 K (-40 F), 298 K (77 F), and 422 K (300F).[45] The induced absorption for the combined exposures at 233 K and 298 K exhibits less changes in absorptance than the sum of the individually produced absorption changes. However, at 422 K, the sum of the individual environment exposures is approximately the same as the value obtained by the combined-environment exposure. A comparison of the proton-only spectral changes at 422 K with the combined environment changes at 298 K shows almost identical changes. Apparently, the temperature annealing produces an effect similar to that of the UV radiation to reduce the induced absorption of the proton radiation.

The changes in spectral absorptance for combined 750 ESH of solar radiation and an integrated exposure of 2 x 10^{15} p/cm^2 (E = 10 keV) at the three temperatures are shown in Figure C-21.[45] The dominating influence

of the ultraviolet radiation at elevated temperatures results in the greatest change in absorptance for the specimen exposed at 422 K (300 F).

The degradation, α_s, of the ZnO/K_2SiO_3 coating is about 25 percent less when simultaneously exposed to 10-keV protons and simulated solar-UV radiation than when exposed to protons only at 298 K (77 F).

Douglas White Inorganic Paint (Z-93 Type). This was coated 5 mils thick on 0.016-inch 6061 aluminum sheet. After 200 hours UV (compact-arc xenon source, irradiation intensity of 1 ESH) in vacuum, solar absorptance increased 10 percent. No change was observed when air was introduced.[46]

Titanium Dioxide in Potassium Silicate

Hughes Inorganic White (H-2) is made with Cabot RF-1 titanium dioxide dispersed in Sylvania PS-7 potassium silicate. Initial solar absorptance as a function of wavelength is shown in Figure C-22. It was tested on Lunar Orbiter IV and was found to be about equivalent to the silicone-aluminum and B-1060 coatings.[26] Initial absorptance and emittance values, both laboratory and flight values, are given in Table B-3. Absorptance, α_s, was 0.178 (laboratory value) and after 1000 sun hours (flight), $\Delta\alpha_s = 0.089$. Only two coatings had lower $\Delta\alpha_s$ values after 1000 sun hours' exposure on the Lunar Orbiter IV and V flights. (See page 36.) Flight data for Lunar Orbiter IV are given in Figure B-22.

Lanthanum Oxide in Potassium Silicate

This coating is susceptible to UV damage, but is less susceptible to proton damage. Increasing the total proton exposure by a factor of 5 did not increase the damage, indicating a very good resistance to proton damage. In contrast to the ZnO/K_2SiO_3, the La_2O_3/K_2SiO_3 shows a definite damage effect, principally due to UV exposure. Combined environment tests including both proton and UV radiation produced comparable damage to the sum of the individual environments.[22] However, so drastic is the UV-only degradation that it completely dominates the combined environments picture.[44]

Oxide Coatings

Rokide C

Rokide C is essentially chromic oxide (85 percent Cr_2O_3) flame sprayed by Norton Abrasive Company[9] at room temperature, $\alpha_s = 0.90$ and $\epsilon = 0.85$. The green coating is extremely hard and is very inert chemically. There is no degradation of optical properties resulting from UV exposure.

However, because of differential thermal expansion between the oxide coating and metal substrates, adhesion is a problem during rapid changes of temperature. One method of overcoming this difficulty is the use of a nichrome undercoat on René 41 nickel alloy. This Rene 41-nichrome-Rokide C combination thermal-control system has been checked for thermal-shock damage. Heating complex shapes to 1640 F within 5 minutes followed by a 5-minute cooling period has resulted in no coating failures.

The bonding between the substrate material, nichrome, and Rokide C is believed to be purely mechanical. Rokide C may be used on other metallic substrates; however, thermal-shock stability should always be checked experimentally for any new substrate. Because of the mechanical bonding, all substrates must be grit blasted prior to coating application.[9]

Bright Anodized Coatings

Aluminum is an excellent reflecting material for radiation in all parts of the spectrum while continuous films of aluminum oxide are transparent to radiation in the visible region and "black" in the IR. Therefore, polished aluminum which has been anodized is expected to have a double surface effect because the polished aluminum reflects the solar radiation which is permitted to penetrate the aluminum oxide coating.[5] An oxide coating of sufficient thickness is opaque in the long-wavelength IR region. Figure C-23 shows the optical properties of polished aluminum which has been anodized. Figure C-24 shows the effect of temperature on the total hemispherical emittance. Emittance appears to be highest in the cryogenic-temperature range.

Vacuum-thermal exposure produces two major results. Water present in the oxide is partially driven out as is evidenced by the reduction of the absorption band at 3 microns. A decrease in the reflectance in the visible spectrum was the most pronounced effect.[5] See Figures C-25 and C-26.

Since the distribution of energy of a 65 C surface (based on black-body radiation) peaks at approximately 8.4 microns, the reduction of the water-absorption band has very little effect on the emittance of the anodized-aluminum coating used at this temperature.

The optical properties of the bright anodized-aluminum system were only slightly altered by UV radiation in air.[5] However, the combined vacuum-UV radiation was very detrimental to the solar absorptance of bright anodized coatings prepared by the usual methods. The color centers formed during exposure caused a gradual increase in yellowing up to 120 hours' exposure. There appears to be a leveling-off beyond the 120 hours. This yellowing causes the α/ϵ ratios to double (0.19 to 0.42) after exposures up to 120 hours. Table C-4 and Figures C-27 and C-28 show the effect of vacuum-UV on 0.5-mil sheet.

Preliminary data indicate there is only a slight change in the optical properties of bright anodized aluminum when exposed to 3×10^8 rads (C) of nuclear radiation.[5] Table C-5 shows the changes in absorption and emittance for various coating thicknesses after irradiation.

Anodized aluminum was unaffected by a dose of 10^{16} p/cm^2 (E = 3 keV) and unaffected by electron exposure as far as spectral reflectance at a dose of 4×10^{16} e/cm^2 (E = 145 keV).[34]

The synergistic effects of simultaneous 145-keV electron and UV radiation on the spectral reflectance of barrier-anodized aluminum and sulfuric acid-anodized aluminum along with aluminum oxide-potassium silicate thermal-control coatings were investigated at 77 K.[4] Damage to the sulfuric acid-anodized aluminum specimens was produced primarily in the wavelength region below 0.7 microns, with only small changes evident at longer wavelengths. An increase in α_s of 40 percent was induced by 350 ESH of UV, while 5.8×10^{15} e/cm^2 produced no change in α_s. Simultaneous irradiation to approximately the same doses resulted in a 35 percent increase in α_s.

Barrier-anodized aluminum was found to be very resistant to both UV and electron radiations.[4] An increase of 12 percent in α_s was produced by 350 sun hours of UV, while 5.8×10^{15} e/cm^2 resulted in an 18 percent increase in α_s. These changes were again exhibited primarily in the wavelength region less than 0.7 micron.

The effects of electron and UV radiations on these materials are shown in Table C-6. Samples were prepared on 10-mil 1199 aluminum substrates.

Charged-particle and gamma-radiation tests were run on barrier-layer anodized aluminum having emittances up to 0.31.[43] It was found that charged-particle radiation (proton and alpha particle) exposures up to 1×10^{16} particles/cm^2 and cobalt-60 gamma-radiation doses up to 1.3×10^6 rads (C) did not degrade the anodized aluminum surfaces. Following are the energy levels employed and the changes in absorptance which occurred:

Type of Radiation	Energy, MeV	Integrated Flux, particles/cm^2	Dose, roentgens	$\Delta\alpha_s$ at Maximum Exposure
Protons	$1 - 9 \times 10^{-3}$	$10^{14} - 10^{16}$	--	0.005
Protons	2.5	7×10^{12} to 2×10^{15}	--	0.0
Alphas	$2 - 16 \times 10^{-3}$	$10^{13} - 10^{16}$	--	0.031
Alphas	5.0	$10^{13} - 4 \times 10^{14}$	--	0.0
Gamma (Co-60)	1.17 and 1.33	--	1.3×10^6	0.0

The barrier-layer anodized aluminum was found stable to abrasion, salt-spray, weatherometer, and UV.[43]

Alzak, the result of an anodic oxidation of aluminum sheets that have been electrobrightened, is produced commercially by the Aluminum Company of America. The thick, porous oxide layer is formed by an extensive dissolution of aluminum in a fluoboric acid solution and is then sealed in an oxide hydration using deionized water. Its resultant α_s/ϵ depends on the thickness and purity of the Al_2O_3 layer, and values comparable to a white paint may be achieved. The quality of this coating is dependent on the purity of the components used in the various stages of processing. Since it is produced commercially in large quantities, variation in UV stability from sheet to sheet has been observed and the initial optical properties are not yet predictable. This coating has been considered for the Orbiting Astronomical Observatory satellite program. The coating forms the entire outer shell of the spacecraft and therefore its stability is of critical importance.[47]

The coating was tested on the ATS-3 and it was found that most of the damage was caused by UV irradiation ($\lambda > 160$ mμ). The loss in reflectance

was restricted to wavelengths less than 1200 mμ, and laboratory testing has shown that this is caused by an increase in the absorptance of the Al_2O_3 film which begins in the near UV and progresses toward longer wavelengths with increased exposure. See Figures C-29, C-30, and C-31. The original values of α_s and ϵ were 0.15 and 0.77, respectively (7.7-μm-thick coating). As the stability of this commercially produced coating varies from batch to batch, these results are not generally applicable, but they serve as a good indication of what may be expected of this material.[47]

Alzak coatings were subjected to 20 and 80-keV-electron radiation. It was found that it sustained more degradation from 20-keV electrons than from 80-keV electrons. Reflectance losses were chiefly in the UV region.[27] See Figure C-32.

The effect of UV irradiation on a 0.29-mil anodized aluminum (Alzak) is shown in Figure C-33. Changes in the UV, visible, and IR portions of the spectrum with irradiation are as follows:[25]

Exposure ESH	Decrease (Increase) in Reflectance, percent with UV Exposure ($\Delta R = R_i - R_f$)		
	250 mμ	425 mμ	2100 mμ
135	51	20	(1)
250	54	27	1
490	59	32	1
770	--	35	--
1130	60	38	1

Anodized aluminum was tested in the OSO-III flight experiment.[13] The 1199 aluminum alloy substrate was chemically brightened, electropolished in a solution of fluoboric acid, and anodized in a solution of ammonium tartrate. This coating showed no change in α_s in 1580 ESH.

Chromic acid-anodized aluminum was exposed to space radiation on Apollo 9 spacecraft. Samples were retrieved in space for postflight tests. Absorptance increased from 0.70 to 0.73, an increase of 4 percent. Emittance decreased from 0.73 to 0.70.[32] (Note: samples exposed to air before changes in absorptance determined.)

Chromate Coatings (Alodine)

Alodine A-1 and A-2, two chromate finishes on aluminum, were subjected to ion bombardment from plasma bombardment systems in an effort to simulate solar-wind damage.[48] Peak bombardment potentials were close to 1 keV. The Alodines showed absorptance decreases of 0.01 to 0.04 over the entire 0.26 to 2.6-μ range. The conditions of high vacuum and plasma caused changes in the coating because of volatile constituents such as water. The changes did not follow definite patterns.

The total normal emittance, ϵ_n, for IR radiation changed a maximum of 7 percent with hydrogen-ion bombardment.[48] It should be pointed out, however, that the data obtained were not in situ.

Composite Coatings

Several composite systems show promise as thermal-control coatings. In general, these consist of a reflecting substrate coated with a semitransparent dielectric film. The reflectance of the metal substrate controls the solar absorptance, and the thickness of the transparent or semitransparent dielectric film governs the emittance.[36] These films are frequently prepared as tapes which are bonded to the surface of the space vehicle by means of a pressure-sensitive adhesive.

Second-Surface Mirrors

Transparent or semitransparent films with a reflecting substrate are known as second-surface mirrors. Some are ceramic mirrors having dimensions about 1 x 1 x 0.008 inch and are applied to the substrate with an adhesive. Others are flexible films with a reflective metal backing which has been applied to the film by vapor deposition. Following are discussions of several types of second-surface mirrors.

Series-Emittance Thermal-Control Coatings. General Electric developed a series of such coatings.[36] The films suggested include Teflon, a vinyl silicone (GE 391 - 15 - 170, formerly known as PJ 113), and Butvar (polyvinyl butyral). Metals examined for the reflective surfaces were aluminum,

silver, gold, and copper. These metals were applied to the films by vapor deposition or the dielectric was coated on the metal foil. The adhesive which passed the ascent-heating-simulation test satisfactorily was General Electric's SR 527 (a silicone adhesive). However, two other adhesives also have been evaluated and appear to have merit. These are Dow Corning's DC 281 silicone adhesive and Minnesota Mining's Y9050U. The latter is a double-faced pressure-sensitive tape. It is essentially a silicone-impregnated fiber-glass cloth which is laminated to the metal surface.[36] These latter two adhesives failed not in shear, but by peeling as a leading edge was raised when subjected to a simulated ascent heating.

According to Linder it is theoretically possible to achieve any α_s/ϵ ratio between 0.05 and 5.0 with this system, although practical limitations on minimum coating thickness and lack of complete transparency to the solar spectrum somewhat limit this selection.[36]

Additional advantages of this type of system include (1) the ability to select coatings having lower emittances with the same α_s/ϵ ratio will minimize the radiant-heat loss from the vehicle and therefore will reduce the power requirement and (2) an improved UV stability of the Teflon-metal and silicone-metal systems which makes this type coating very attractive for use on long-life missions.

Table C-7 and Figure C-34 show the variation in total normal emittance with the thickness of Teflon over vapor-deposited aluminum while Table B-5 shows similar information for Butvar on aluminum. Spectral absorptance of silver-coated Teflon is given in Figure C-35. The reflectance curves for 0.5-mil Mylar metallized with silver, aluminum, gold, and copper are shown in Figure C-36.

The experimental vinyl silicone, GE 391-15-170, has been shown to be extremely resistant to UV degradation. A program to develop a technique for applying this material in controlled thicknesses to a metal foil is being developed. It is anticipated that emittance values between 0.15 and 0.90 may be obtained, depending on the thickness of the silicone coating.

Teflon and vinyl silicone (GE 391-15-170) have been exposed to the combined effects of UV and X-rays. No significant changes in solar absorptance of either of these systems were observed with exposures up to 1000 ESH and 100 megarads (C). There are indications, however, that as exposure is continued, the absorption edge of the dielectric tends to shift to longer wave lengths. A typical curve of UV reflectance after exposure to UV and X-rays

for Butvar and GE 391-15-170 (PJ 113) is shown in Figures C-37 and C-38. A summary of data obtained on UV and high-energy exposure is shown in Table C-8.

Silver- and Aluminum-Coated Teflon. These have shown excellent stability to UV and to particulate radiation. Generally, FEP Teflon is used because its radiation stability in air is better than that of TFE Teflon. In vacuum, FEP is only slightly better than TFE, but both are stable to approximately 10^6 rads (C) when not exposed to air or oxygen.

Six Teflon-based coatings were subjected to 80-keV electrons.[27] These included 2-, 5-, and 10-mil aluminized Teflon and 2-, 5-, and 10-mil silvered Teflon. After exposure to 10^{15} e/cm^2 (E = 80 keV), the exposed surfaces still retained a specular appearance and, except at the shortest wavelengths measured, sustained only minor reflectance degradation. Exposure to 10^{16} e/cm^2, however, left each Teflon coating significantly altered. The plastic assumed a light gray appearance so that the vapor-deposited metal was masked. Some crazing and a considerable amount of mottling of each Teflon surface was also evident.[27]

Similar samples and also silvered samples were subjected to proton bombardment.[49] No change in solar absorptance (α_s) was detected until after a dose of 3×10^{15} p/cm^2 (E = 40 keV). At the maximum doses, 1.2 to 1.8×10^{16} p/cm^2, changes in absorptance ($\Delta\alpha_s$) averaged 0.04 for the silvered Teflon and 0.06 for the aluminized Teflon. See Table C-9. The temperature of the Teflon coating substrates throughout the test period was 10 ± 1 C, based on water-exit temperature from the chamber. Vacuum levels during the exposures were 1 to 2×10^{-7} torr. Magnetic analysis of the proton beam eliminated masses > 1 from the beam before it entered the exposure chamber. Exposure rates were between 1 and 4×10^{10} p/(cm^2-s).

Aluminized Teflon was used as the outer portion of a thermal shield on Mariner II and Mariner V. The thermal shield consisted of 18 layers of aluminized Mylar and was attached to the sunlit surface of the spacecraft to reduce the influence of increasing solar intensity during the mission. The outer layer was aluminized 1-mil FEP Teflon and was used as a second-surface mirror with $\alpha/\epsilon = 0.13/0.55 = 0.24$. The shield for Mariner II was similar except that it utilized 5-mil Teflon. With the Mariner V, a temperature transducer was taped to the bottom side of the aluminized Teflon. The reported data were assumed to be the measured temperature of the sunlit FEP Teflon sheet. This assumption appeared to be supported by the data obtained.

Early mission data shown in Figure C-39 show that the FEP Teflon degradation followed a typical rate characteristic of low α/ϵ materials, with an initial relatively high rate, decreasing as degradation progressed. However, approximately 45 days after launch, the rate began to increase again as can be seen in the shape of the curve in Figure C-39. The beginning of this increase in rate was coincident with a Class-2 solar flare, the radiation products of which were seen at the spacecraft. However, a second flare did not produce any increase in degradation rate. The increase in rate following the first flare could not be attributed directly to radiation damage since the rate increased gradually and the higher rate persisted too long.[18]

A 5-mil silvered Teflon sample was flown on the OGO-VI (approximately 400 to 1100-km polar orbit). Prior to launch, α_s measured as 0.085. After approximately 4600 hours of solar exposure, no increase in α_s was detectable.[49]

Polyimide/Aluminum. Kapton H-film (polyimide) with an aluminum backing was also tested for use similarly to aluminized Teflon. This material has excellent high-temperature properties, good radiation resistance, but it is affected by UV. Although this film shows some reflectance loss in the UV, its moderate reflectance changes, both increases and decreases, in the visible and IR regions when exposed to UV radiation in vacuum are considered important. See Figure C-40. Exposed to UV in situ for 20,000 hours, α_s changed from 0.305 to 0.41.[50]

Aluminized Kapton was subjected to 20 and 80-keV-electron radiation. With the 20-keV exposure, reflectance changes were minimal at fluences below 10^{15} e/cm^2. The largest reflectance changes at 10^{16} e/cm^2 were in the UV wavelengths just longer than the visible-region absorption band. Decreases were much more severe than those after exposure to the 20-keV electrons. See Figure C-41. Reflectance damage after exposure to 10^{16} e/cm^2 (E = 80 keV) was considered "catastrophic".[27]

In another experiment, a 2-mil Kapton H-film over a thin aluminum coating on an aluminum substrate was subjected to 50-keV electrons. The greatest losses were in the visible and near-IR regions. Decreases in reflectance were as follows:[25]

Dose, e/cm^2	Decrease in Reflectance, percent ($\Delta R = R_i - R_f$) 590 mμ	2100 mμ
1×10^{13}	0	--
2×10^{14}	4	0
6×10^{14}	13	0
8×10^{15}	60	--

When subjected to UV radiation alone (in situ), decreases in the reflectance changed as follows:[25]

Exposure ESH	Decrease (Increase) in Reflectance, percent ($\Delta R = R_i - R_f$) 250 mμ	425 mμ	2100 mμ
135	3	(2)	(2)
250	5	(2)	2
490	6	(2)	2
770	--	(2)	--
1130	7	(2)	1

Kapton showed no change in properties when exposed to 750 F for 30 seconds in vacuum. Above 900 F, it visibly darkened.[50]

Polyimide film has also been used as a backing for a second-surface mirror, SiO on aluminum. This composite consists of a 10,500 A SiO overcoat on 1200 A aluminum vapor deposited on 1.5-mil Kapton (polyimide), an experimental film supplied by G. T. Schjeldahl Company, Northfield, Minnesota. It was subjected to proton and electron radiation, exhibiting little change in reflectance in the UV and visible regions after receiving a dose of 10^{16} p/cm^2 (E = 3 keV).[34] (See Figure C-42.) There was a slight reduction in spectral reflectance in the UV when exposed to 1.3×10^{16} e/cm (E = 145 keV). It is badly degraded in UV irradiation, appearing slightly yellow-brown.[34] (See Figure C-43.)

Silicon monoxide coatings are more susceptible to 320 ESH of UV radiation than to either 1.3×10^{16} e/cm^2 (E = 145 keV) or 1×10^{16} p/cm^2

(E = 3 keV). This type coating is being used in the Apollo program and is also being considered for Air Force satellites.[51]

Coated, Vapor-Deposited Aluminum. Vacuum-deposited aluminum coated with surface layers of dielectric materials gives highly reflecting and protected mirror surfaces which have been successfully used for controlling the temperature of many satellites. Coatings generally used over the aluminum are silicon oxide (SiO_x), silicon dioxide (SiO_2), aluminum oxide (Al_2O_3), and magnesium fluoride (MgF_2).

Silicon Oxide (SiO_x). The most frequently used surface film for controlling the temperature of satellites has been silicon oxide (SiO_x) produced by evaporation of silicon monoxide in the presence of oxygen or air. Recommended deposition parameters are rates of 3 to 5 A/sec at about 8 x 10^{-5} torr of oxygen or 1 to 2 A/sec at 1 x 10^{-4} torr of air. Films of this material show rather high absorptance in the near and far UV. However, this undesired absorptance is claimed to be eliminated by UV irradiation in air.[52, 53]

By increasing the thickness of reactively deposited silicon oxide (SiO_x) on aluminum from zero to 32 quarter-wavelengths ($\lambda/4$), ϵ increases from 0.017 to 0.53 and α/ϵ can be varied from about 5 to 0.2.[53] Exposure to UV in air virtually eliminates the initially high UV absorptance of this coating without changing the IR reflectance appreciably. The total emissivity of this coating is unchanged by the UV treatment. With this treatment, α will decrease. After 18 hours of UV irradiation in air, α was found to change from 0.128 to 0.110. These coatings have been used as temperature-control surfaces on many satellites, and there are ample laboratory and flight data to show their high stability in space environment.[53]

Temperature data from Explorer XXIII over a 3-1/2 year period have indicated no significant degradation of its SiO_x coating.[53] However, a 1200-mμ SiO_x coating tested on the ATS-3 proved to be very unstable.[47] It was believed that the SiO_x coating tested on the ATS-3 was not typical of these coatings. Vapor-deposited SiO_x (1.5μ) over opaque evaporated aluminum showed excellent stability when tested on the ATS-I. Initial α/ϵ was 0.48. Changes in α/ϵ which occurred in flight on the ATS-I are shown in Figure C-44. This coating was about equivalent with the Al_2O_3/Al coating and was one of the more stable materials.

The thermal-control coatings for the surfaces of the Vanguard satellites are based on the same principle. The exterior thermal-control surface

consisted of evaporated aluminum covered with a 0.65-μ film of silicon monoxide.[8] The film is essentially transparent to solar radiation but has a strong absorption band at about 10μ. By controlling the film thickness of this system, one exercises control over IR emittance independently of solar absorptance. The α_s/ϵ ratio can be varied from about 4.0 to about 0.5. For the system employed in Vanguard, $\alpha_s/\epsilon = 1.3$.

This system, however, if not properly prepared, has been shown to be subject to severe degradation by solar UV exposure.[2] It appears that the degradation is related to the change in stoichiometry of the silicone oxide film under irradiation. The dielectric film is produced by evaporation of SIO in an oxidizing atmosphere or by subsequent oxidation of an evaporated SiO layer. Upon irradiation the transparent SiO_x film loses oxygen and reverts to the straw-colored SiO with resulting increase in solar absorptance.

Silicon Dioxide (SiO_2). SiO_2 films have strong absorption bands in the IR region with maxima in the 8.5 to 9.5-μ and the 23 to 25-μ regions. SiO_2 films of thicknesses up to about 0.2 μ have, even in the 8.5 to 9.5-μ wavelength region, very little effect on the normal incidence reflectance of aluminum. However, if thicker films of SiO_2 are applied to aluminum, very large reflectance decreases can be observed in the IR region. Figure C-45 shows the IR reflectance from 5 to 40 μ for aluminum coated with 0.40, 0.97, and 2.59-μ films of SiO_2.

Figure C-46 shows that interference effects produce a maximum α of 0.13 with SiO_2 films that are effectively one-quarter wavelength thick at λ = 550 mμ, and that for thicker films, α becomes essentially independent of the SiO_2 thickness and has a value of 0.111 ± 0.04 in a thickness range of 0.36 to 1.9 μ. In addition, the α values of SiO_2/Al coatings determined in air were found to be identical with those measured in vacuum.[52]

For the temperature control of satellites, films of aluminum coated with about 6 to 14 $\lambda/4$ of SiO_2 are most frequently used (λ = 550 mμ). For this range of SiO_2 thickness, ϵ and ϵ_n (normal emissivity) of SiO_2/Al increase with increasing temperature in the temperature range measured. This is a very desirable property for a temperature-controlling coating since it provides a certain amount of self-regulation of the satellite temperature. For a satellite coated with Al and 6 $\lambda/4$ of SiO_2, an increase of the shell temperature from 10 to 20 C may be predicted to occur during 1400 hours of exposure to sunlight.[52]

Aluminum coated with various thicknesses of SiO_2 were exposed to 1-Mev electrons using a dose of 1×10^{15} e/cm^2. No changes in the optical properties from the UV to the far IR were observed. It appears that UV irradiation is the main cause for the degradation of SiO_2-coated aluminum films in outer space. SiO_2 over aluminum was exposed to 20 and 80-keV electrons in situ and was found to be very resistant to reflectance change.[27] See Figures C-47 and C-48. This coating undergoes significant improvement in reflectance in the 0.25 to 0.3-μ-wavelength region during electron irradiation, similarly to that observed with UV irradiation.

SiO_2-coated aluminum samples were subjected to UV irradiation in vacuum. Figure C-49 shows the decrease in reflectance experienced by two SiO_2-coated samples subjected to xenon arc lamp in a vacuum of 1×10^{-7} torr. The films were 6.2 and 13.4 $\lambda/4$ thick, and the irradiation was performed in two stages using first one and then five times the equivalent solar energy. Reflectance values were determined while the samples were kept in vacuum at about 1×10^{-5} torr. For both samples, the reflectance decrease was most pronounced at shorter wavelengths and became negligible for wavelengths longer than 700 mμ, but the damage suffered by the thicker coating was approximately twice that experienced by the thinner one. The IR reflectance and ϵ of the SiO_2-coated aluminum were found to be unaffected by UV irradiation.

SiO_2- and Al_2O_3-coated aluminum samples tested on the ATS-3 were more stable than the other dielectric coatings, although their degradation was more severe than that observed in the laboratory.[47] UV radiation was responsible for most of the damage although a significant degradation was caused by other factors acting in combination.

A technique for producing UV transparent films of Al_2O_3 and SiO_2 by evaporation with an electron gun has been developed. Because of their hardness, chemical stability, and excellent adherence, these two film materials are suitable as protective layers for aluminum, front-surface mirrors, especially if high reflectance in the UV is required.[52] The fact that the optical properties of vacuum-deposited Al_2O_3 and SiO_2 are less dependent on the preparation conditions than those of SiO_2 prepared from SiO makes these film materials more suitable for many optical applications.

Aluminum Oxide (Al_2O_3). Aluminum overcoated with Al_2O_3 degrades less than that with SiO_2 under identical UV irradiations.[52] Aluminum oxide over aluminum was also exposed to electrons (E = 20-keV and

E = 80 keV) and found to be extremely resistant to reflectance change.[27] See Figures C-50 and C-51.

Vapor-deposited aluminum oxide (11,000 A) on 1000 A of aluminum evaporated onto a buffed, chemically cleaned, and glow-discharge cleaned substrate, and silicon dioxide deposited in vacuum onto a buffed and degreased aluminum substrate exhibited only small changes in reflectance from 0.25 to 2.5 μ for exposures as great as 10^{17} e/cm^2.[3] Exposure was to 20-keV electrons at 22 C.

Vapor deposited Al_2O_3 (1.1 μ) on opaque evaporated aluminum was tested for UV stability in the laboratory and on the ATS-I. The initial α_s/ϵ was 0.54 as measured in the laboratory, and 0.59, measured 48 hours after launch.[19] The changes which occurred in flight on the ATS-I are shown in Figure C-52. This coating along with SiO_x on aluminum was the most stable of those tested on this flight.

Magnesium Fluoride Over Evaporated Silver. This material is not used as a thermal-control coating, but is a potential surface coating for a solar concentrator mirror. The thin (2 x $\lambda/4$ at 550 mμ) overcoat of MgF_2 serves to protect the silver from atmospheric contaminants. It was included in the ATS-3 tests. The substantial loss in reflectance that occurred in the 300 to 650-mμ region can be attributed to both a broadening of the interference minimum band and a decrease at the interference maximum position due to substantial damage taking place within the body of the MgF_2 film.[47] The relative stability of the shielded sample (fused-silica shield) indicated that most of the damage to the unshielded sample was caused by low-wavelength (160 mμ) UV and electron or proton irradiation acting in combination.

The ATS-3 data have shown that MgF_2-coated silver is not the best choice for a solar-concentrator-mirror coating. However, it will continue to be used as both a protective and reflectance-increasing flim for front-surface aluminum mirrors used in far UV, orbiting telescopes. Therefore it is important that the correlation between preparation techniques and environmental stability of MgF_2 be thoroughly defined.[47]

Uncoated Aluminum. The uncoated aluminum samples tested on the ATS-3 were least susceptible to damage by UV ($\lambda > 160$ mμ) irradiation as indicated by the shielded-sample data.[47] The unshielded samples, however, degraded severely, and the loss in reflectance increased with decreasing wavelength. The change showed no signs of saturating after 1 year

in orbit and may be increasing as time goes on. These results did not agree with earlier findings of the OSO-III Thermal Control Coatings Experiment which showed aluminum to be very stable. Differences in the orbital environment may explain some of the disagreement.

Optical Solar Reflector. Two versions of the optical solar reflector have been developed at Lockheed Missiles and Space Co.[2] The first consists of vapor-deposited silver on Corning 7940 fused silica with an overcoating of vapor-deposited Inconel. The second is vapor-deposited aluminum on Corning 7940 fused silica with an overcoating of vapor-deposited silicon monoxide. The front surface of these mirrors consists of the high-purity fused silica, the second or reflecting surface is the silver or aluminum which has been vapor-deposited on the fused silica. The silver or aluminum coating is protected from corrosion or damage while being handled with the vapor-deposited Inconel or silicon monoxide. These mirrors, 1 x 1 x 0.008 inch thick, are applied to the substrate with RTV-615 silicone adhesive.[2,9] The adhesive requires a minimum cure of 14 days at room temperature to minimize outgassing during ascent. Reflective properties are as follows:[9,51]

Optical Solar Reflector	Sample Temperature, R	α_s	ϵ	α_s/ϵ
Silver	325-530	0.050 ± 0.005	0.81	0.062
	260		0.744 ± 0.01	
	360		0.800 ± 0.01	
	460		0.807 ± 0.015	
	560		0.795 ± 0.02	
	660		0.790 ± 0.02	
Aluminum	325-530	0.100 ± 0.005	0.81	0.124
	260		0.744 ± 0.01	
	360		0.800 ± 0.01	
	460		0.807 ± 0.015	
	560		0.795 ± 0.02	
	660		0.790 ± 0.02	

These optical solar reflectors (OSR) are fragile and should be protected from mechanical dámage during storage and shipping. Surface contamination, including fingerprints, oil, dust, and atmospheric weathering, does not cause permanent degradation after application. However, contaminants must be removed prior to launch. Panels with OSR applied to them have successfully passed sinusoidal and random-vibration tests.

There has been no measurable change in α/ϵ due to near UV, and these coatings have been stable for extended missions up to 2 years in all charged-particle environment and combined environments of space. These coatings have been extensively investigated and have never been damaged.[2, 9, 13] (See Table C-10.) Also, data from the OSO-III flight showed no change in α_s of the OSR (vapor-deposited silver on fused silica and Inconel overcoat) in 1580 ESH.[13]

Solar-Thermoelectric Systems

Another composite is the solar-thermoelectric system reported by Schmidt and Park at Honeywell, Inc.[54] These multilayer coatings consist of transparent molybdenum films between nominally quarter-wavelength-thick dielectric spacers of such materials as magnesium fluoride (MgF_2) and aluminum oxide (Al_2O_3). The solar absorbers are prepared by evaporating the multilayer optical coatings on highly reflective substrates.

The primary criteria for material selection are:

(1) Substrate – high reflectance in the IR, high melting temperature, low vapor pressure, low electrochemical potential to provide chemical stability with the dielectric layers

(2) Dielectric films – high transmission in the IR, high melting temperature, low vapor pressures, and high electrochemical potential

(3) Metal films – high transmission in the IR, high melting temperature, low vapor pressure, and low electrochemical potential. Selective absorption in the solar spectrum is often advantageous.

One of the best samples reported was prepared with depositions of CeO_2, molybdenum, and MgF_2 (magnesium fluoride). This sample demonstrated very good high-temperature stability up to 538 C in vacuum. Another sample showed excellent high-temperature, high-vacuum, and UV stability. All the films passed the Scoth tape test for adhesion. They do not possess high abrasion resistance; however, they can be washed in acetone or alcohol.[54] Unfortunately, there has been difficulty in reproducing these materials.

Miscellaneous Coatings

Several coatings were reported for which available information is very meager. In many cases only the solar absorptance and hemispherical emissivity were given. Composition of some of these was not available. The reported information on such coatings follows.

3M 202-A-10

A Minnesota Mining and Manufacturing Co. coating (202-A-10) was subjected to proton and electron irradiation in a vacuum. It was degraded by 10^{16} p/cm^2 (E = 3 keV) in the visible and IR spectral regions (Figure C-53). Spectral reflectance in these regions decreased as a result of electron irradiation. Damage approached a saturation level at doses not much greater than 4×10^{16} e/cm^2 (E = 145 keV). (See Figure C-54.) Specimens appeared somewhat darker after electron irradiation.[34]

Aluminized Mylar

Mylar, 5 mils thick, with 2×10^{-6} inch of aluminum on both surfaces (available from Hastings & Co., Inc., Philadelphia, Pa.) was unaffected by a dose of 10^{16} p/cm^2 (E = 3 keV) and 4×10^{16} e/cm^2 (E = 145 keV). The specimen blistered during irradiation, but blistering was believed to be due to outgassing of the epoxy used to attach the film to the stainless steel disk.[34]

Cameo Aluminum 2082 Porcelain Enamel

Type 6061 aluminum sheet, 16 mils thick, coated with 1.5 mils porcelain enamel, increased in solar absorptance only 4 percent after 200 ESH of UV in vacuum.[46]

Bismuch Sulfide (Bi_2S_3)-Dyed
Anodized Aluminum [1100 (2-S)Al]

The Bi_2S_3-dyed anodized aluminum was somewhat unstable. It had relatively low absorptance values and was somewhat undesirable as a high absorber for space applications.[55]

Cobalt Sulfide (CoS)-Dyed
Anodized Aluminum [1100(2-S)Al]

The CoS-dyed anodized aluminum was stable with relatively high absorptance values over the entire wavelength region considered.[55] (See Figures C-55 and C-56.)

Nickel Sulfide (NiS)-Dyed
Anodized Aluminum [1100(2-S)Al]

NiS-dyed anodized aluminum was stable with relatively high absorptance values over the entire wavelength region considered.[55] (See Figures C-57 and C-58.)

Lead Sulfide (PbS)-Dyed Anodized Aluminum,
Sandoz Black BK-Dyed Anodized Aluminum,
and Sandoz Black OA-Dyed Anodized Aluminum

These dyes on [1100(2-S)] aluminum had relatively low solar absorptance and showed slight changes of solar absorptance when exposed to simulated space environment. They would have limited usefulness as thermal-control coatings.[55]

Black Nickel Plate on Aluminum [1100(2-S)Al]

Black nickel plate on aluminum was very stable over the solar region of the spectrum for exposures to a simulated space environment of simultaneous high vacuum and UV radiation of 3800 ESH plus electron radiation of 10^{15} e/cm^2 (E = 1 MeV), and showed no significant change of solar absorptance from the initial high value of 0.959. However, the room-temperature emittance at the longer wavelengths (from 3 to 25 mμ) was relatively low, 0.686, and was reduced even further to 0.598 by exposure to the simulated space environment. This 12 percent change of thermal emittance was the largest of any of the black coatings tested.[55] (See Figures C-59 and C-60.)

Du-Lite-3-D on Type 304 SS (Grit Blasted)

Du-Lite-3-D on Type 304 SS is a good flat absorber in the solar spectral region. Solar absorptance is relatively high and thermal emittance is relatively low. It was stable to simulated space environment. Thermal emittance changed 4.1 percent.[55] (See Figures C-61 and C-62.)

Westinghouse Black on Inconel, Sodium Dichromate-Blackened SS (Type 347), Sodium Dichromate-Blackened Inconel, and Sodium Dichromate-Blackened Inconel X

Various other combinations of "blackened" metals are good flat absorbers in the solar spectral region. Solar absorptance of these is relatively high, while thermal emittance is relatively low. They are stable to simulated space environment. The major disadvantage to these may be the high temperatures required during the coating process. The thermal emittance of sodium dichromate-blackened Inconel changed only 2.7 percent after being subjected to 4770 solar hours in vacuum and 10^{15} e/cm^2. Sodium dichromate-blackened Inconel X showed negligible change after 2560 solar hours in vacuum plus 10^{15} e/cm^2.[55] See Figures C-63 to C-70. Chemically blackened Inconel and beryllium with α_s and ϵ greater than 0.80 were used on the Gemini spacecraft for maintaining lower temperatures during reentry.[51]

Pyromark Black Refractory Paint on Aluminum [1100(2-S)Al] and Pyromark Black Refractory Paint on Inconel

These cannot be considered as flat reflectors because solar absorptance and emittance are relatively high. However, the paints are unaffected by prolonged exposure to simulated space environment.[55] See Figures C-71 to C-74.

PIGMENTS

Because of the convenience of painting a surface, particularly an irregular structure, efforts have continued to develop a paint which would be stable to space environment. The major task in developing low-solar-absorptance, pigmented, thermal-control coatings has been to effect a stability to UV radiation and to charged particles. The approach to this problem at the present time is to determine mechanisms of UV degradation in specific materials, particularly pigments. Knowing the mechanism of degradation, methods of protection from such degradation can then be developed.[56] In connection with this approach, efforts have been made to determine the effect of particle size on reflectance. It has been found, for example, that the contribution of voids (between discrete particles and between agglomerates) is an important factor because voids increase spectral reflectance and yet tend to mitigate the absorption effect of intrinsic absorbers.[56] Also, studies have been conducted to characterize degradation in terms of solid-state parameters. Efforts have been made to detect and identify the defect centers produced by UV irradiation. Considerable effort has been made to determine the reasons for the instability of pigments to UV radiation and to develop methods of improving their stability.

Zinc Oxide

Probably the major studies have centered on zinc oxide (ZnO), not only because of the results of previous coating studies, but also because it has lended itself for study and analyses. Several models have been offered to describe the degradation of zinc oxide that manifests itself by an increase in the optical-absorption coefficient in two spectral regions, the 0.39 to 0.8 and the 1.0 to 2.4-μ range.

One general model that has been advanced to describe the degradation of zinc oxide is as follows.[57] UV photons, which are absorbed near the surface, produce free electrons and holes. The photoproduced holes that diffuse to the surface recombine with electrons at surface oxygen, thereby neutralizing the surface oxygen. The neutralized surface oxygen is then evolved from the zinc oxide surface if the ZnO is in a vacuum environment. The first oxygen to be evolved is chemisorbed oxygen, but as the irradiation is continued, surface lattice oxygen is also evolved.

The evolution of oxygen leaves the surface zinc rich, and the excess zinc diffuses into the bulk of the zinc oxide. Thus, the net result of the UV irradiation is the generation of excess zinc and an increase in the concentration of free electrons.

The mechanisms by which the above actions cause the increased visible- and IR-region absorption are not clearly defined.[57] Some believe that the enhanced IR absorption is a result of additional free-carrier absorption which is caused by the increase in the free-electron concentration. Others believe that the enhanced IR absorption is a result of an increase in the density and population of defect levels lying near the conduction band.

The increased visible absorption is likewise not clearly understood. It has been explained by some workers that this is the result of the excess zinc precipitating out at dislocations, causing severe lattice strain in the neighborhood of the dislocation.[57] Such strain could result in a decrease in the separation between the conduction- and valence-band extrema and, in effect, decrease the band gap in the neighborhood of the precipitation. This would produce a low-energy tail on the fundamental absorption edge, similar to the visible degradation observed. Another explanation to the increased visible absorption is that it is a result of defect centers whose energy levels lie just above the valence band.

A series of experiments involved studies of changes in electrical properties of thin films and of crystals with UV irradiation, and studies on the effect of radiation on electron paramagnetic resonance, magnetic susceptibility, and luminescence.[57] These studies have shown that UV irradiation of ZnO results in the production and population of defect centers with energy levels near the conduction band and that these centers are sensitive to IR radiation. UV irradiation also increases the free-electron concentration to such a density that free-carrier absorption in the near IR region should become appreciable. The luminescence studies demonstrated that luminescent defect levels were present in untreated SP-500 ZnO and that UV irradiation enhanced the population and density of those levels.

These photoproduced holes and electrons can undergo chemical reaction.[58] Such chemical reactions change the structure of the coating, leading eventually to coloration. One approach to prevent optical degradation is to find surface additives that act as recombination centers, alternately capturing the holes and electrons and thus removing the photoproduced carriers with no net chemical change. In studies with ZnO,

single-crystal measurements have shown improvement up to a factor of 10^6 in rate of conductivity degradation, and powder measurements have shown photodamage protection from 10^{-2} monolayers of additive.[58]

In these studies, it was concluded that suitable surface additives, acting as electron-hole recombination centers, could prevent degradation of thermal-control coatings by preventing irreversible chemical reactions at the surface of the pigment grains. It was indicated that the surface additive will be effective if it has the following properties: (1) it must be nonvolatile and chemically inert toward its environment and toward photolysis, (2) it must exist in two stable oxidation states separated by one electron, (3) the energy level occupied by this electron should be just below the bottom of the conduction band of the pigment in order that both the hole and electron-capture cross sections be high, (4) the additive must be present in both oxidation states, and (5) it must uniformly cover the surface of each grain of pigment material.

The material showing the most promise with ZnO was the redox couple, a 1:1 ferrocyanide-ferricyanide combination.[59] Tests of this additive have been made using two test procedures. These were (1) monitoring vacuum photolysis of ZnO by measurement of the increase in dark conductance of the ZnO crystals and (2) monitoring of vacuum photolysis by electron-spin resonance (ESR) of a signal at $g \sim 1.96$ associated indirectly with donors in ZnO.[58] This latter method is applicable to powdered ZnO.

More work needs to be done before satisfactory results may be achieved with thermal-control coatings. However, a promising approach has been made and theoretical considerations have been advanced which should lead to the development of stabilized pigments for thermal-control paints.

Two principal optical effects are found with ZnO. One, induced by UV in vacuum (only), appears as an increasing IR absorption which increases with increasing irradiation. The other effect, induced only by mechanical and thermal treatments, appears as an absorption band very near the optical absorption edge.[60]

It has been found that solar radiation-induced degradation of particulate ZnO reflectance occurs in two spectral regions – the visible adjacent to the band-edge and the near IR between 0.8 and 2.8 μ. Visible degradation is most effectively produced by photons of wavelength less than 0.3 μ.

It is not certain, but probable, that the occurrence of IR degradation is a necessary precondition for production of visible degradation. The kinetics of IR degradation are strongly dependent on the irradiation intensity as well as the total irradiation.[61] The visible degradation is primarily dependent on the total irradiation. One of the aspects noted was that the glow discharge which accompanies start-up of an electronic vacuum (VacIon) pump may cause significant IR degradation, but none in the visible wavelengths of sintered ZnO.

The IR degradation is strongly affected by surface preparation of the ZnO particles. Samples sintered, sintered and exposed to VacIon start-up, and milled into a paint exhibit progressively more total degradation during irradiation.[61]

Titanium Dioxide

Some preliminary fundamental studies have been initiated with rutile titanium dioxide pigments containing various impurity levels in an effort to determine damage mechanisms when the pigment is exposed to solar radiation, electron irradiation, or combined environments.[62] Electrical-conductivity measurements and gas-evolution experiments under exposure to UV excitation were conducted to investigate the role of the surface of the pigment particles.

Pigments used for this work included a high-purity rutile (220 ppm silicon, 60 ppm aluminum, 100 ppm nickel, 10 ppm magnesium, and 21 ppm carbon) prepared by a proprietary colloidal process by W. R. Grace and Company, and a stabilized rutile pigment, Du Pont Ti-Pure R-910 (4000 ppm aluminum, 1000 ppm silicon, 10 ppm magnesium, and 87 ppm carbon). Binderless samples of the pigment were prepared by a spray technique and by a casting method. Also, pigmented silicone samples were prepared. The silicone was General Electric's RTV-602 cured with tetramethyl guanidine.

In the course of the work, the effect of exposure to UV from an unfiltered xenon arc (Spectralab X-25 solar-spectrum-simulation source of 4 suns) was determined. See Figure C-75. The pigment was the high-purity rutile which had been dry pressed to a density of 1.5 g/cm^3. Samples were also exposed to electron radiation (Figures C-76 and C-77) and to simultaneous UV and electron irradiation (Figures C-78 and C-79).

The conclusions reached were:[62]

The diffuse reflectance spectra of all irradiated specimens degraded.

UV irradiation produced significantly more degradation in the visible than in the IR region, while electron irradiation produced a relatively uniform degradation across the spectrum.

The saturated magnitudes of the UV and electron degradations were about the same.

All the damaged samples showed recovery at room temperature in vacuum (about 10^{-6} torr). The UV-damage recovery tended to destroy all the defect centers, whereas the electron-damage recovery is more rapid in the IR and small in the visible region. In both, recovery essentially ceased in about 4 to 6 hours.

Renewed irradiation with electrons following recovery produced new absorbing centers in the visible region, but the IR reflectance degradation for the second irradiation was about the same as for the first.

Simultaneous UV and electron irradiation resulted in saturation behavior only near 1 micron, indicating a synergistic effect in the IR

Recovery from simultaneous UV and electron bombardment lead to almost complete recovery in the IR within a day, whereas little recovery in the visible was observed at this stage.

Recovery after exposure to air 53 days later was essentially complete to the preirradiation vacuum characteristic for all specimens.

Titanates

Zinc orthotitanate (Zn_2TiO_4) is a spinel that is formed from 2 moles of ZnO and 1 mole of anatase TiO_2. The most stable product to date is formed at 1050 C. The extraordinarily hard product requires considerable energy to grind into a suitable powder. It is believed that the grinding is largely responsible for the random instability that has been observed in space-simulation tests employing in situ reflectance measurements.[23] Zinc orthotitanate exhibits bleachable degradation in the 0.4 to 1.5-μ region, with the damage centered at about 0.9 μ.

The extraction of all residual, unreacted zinc oxide with acetic acid has been found to be necessary for the elimination of a strong absorption in zinc orthotitanate at 3500 A wavelength. Unextracted zinc oxide and excess titania are believed to be in part responsible for the bleachable IR damage observed.[23] This pigment appears promising as a stable material when properly prepared. Work is continuing on developing methods for producing a stable material.[63, 64] Other titanates such as iron titanate are also being investigated.

Zirconium Silicate

A series of zirconium silicates ($ZrO_2 \cdot SiO_2$) have been synthesized and examined for use as pigments in thermal control coatings.[8] Calcination temperature, purification, and grinding conditions are important for stability in a space environment. A thermal-control coating consisting of $ZrO_2 \cdot SiO_2$ in potassium silicate (K_2SiO_3) has shown excellent stability when subjected to 485 sun hours in vacuum. $\Delta\alpha_s$ for one coating was 0.04. The coating has shown excellent stability to proton and combined UV-proton environments. After exposure to 2×10^8 rads (C), gamma, and 4×10^{14} n_fvt, neutron, $\Delta\alpha_s$ was 0.03.[8] Work is continuing on the development of this pigment.

BINDERS

Silicone Binders

Polydimethyl siloxanes are the most stable polymers available in terms of UV irradiation in vacuum. Both elastomeric and rigid cross-linked silicone polymers are stable. Since they are essentially transparent to UV, their stability is primarily a function of their purity; thus the amount of amine catalyst used to cure the linear polymers greatly influences the stability of the system.[6]

General Electric methyl silicone RTV-602 coated over 1199 aluminum reflector sheet was tested as part of the Lunar Orbiter V flight experiment. The increase in α/ϵ of this coating can be considered to indicate the "true stability" of the binder. This was the degradation of an unprotected binder, and therefore the damage incurred by the RTV-602 can be considered a maximum degradation for this material. The addition of a pigment to this binder would generally lower the quantity of solar-UV radiation that the binder would be exposed to and, as a result, lower the degree of binder damage. Figure C-80 shows the change in solar absorptance of a thermal-control coating, Hughes H-10 [calcined (mono 90) clay/RTV-602] and the RTV-602 over 1199 aluminum. Since the H-10 contained a relatively stable pigment, and with the change in absorptance of the RTV-602 as shown in Figure C-80, it is considered that a significant portion of the damage to the H-10 coating can be attributed to the degradation of the binder. There was, of course, some attenuation of the binder damage due to the presence of the pigment.[14]

Phenylmethyl silicones undergo considerably greater optical damage when irradiated with similar doses of UV in a vacuum. The difference between aromatic and aliphatic silicones is believed to be due principally to the relative degree to which they absorb near-UV radiation. The phenyl groups absorb UV preferentially, whereas the entire methyl silicone molecule is comparatively transparent. The predominant mechanism is thought to be dehydrogenation, whether it be methyl or phenyl segments that are affected.

REFERENCES

(1) Plunkett, J. D., "Technology Survey: NASA Contributions to the Technology of Inorganic Coatings", Denver Research Institute, University of Denver, NASA SP-5014, National Aeronautics and Space Administration, Washington, D. C., 1964.

(2) Breuch, R. A., and Greenberg, S. A., "Recent Coating Developments and Exposure Parameters", Paper presented at Thermal Control Working Group Meeting, Dayton, Ohio, August 16-17, 1967.

(3) Fogdall, L. B., Cannaday, S. S., and Brown, R. R., "In Situ Electron, Proton, and Ultraviolet Radiation Effects on Thermal Control Coatings", Final Report, Boeing Aerospace Group, Seattle, Washington, NASA-CR-100146, D2-84118-9, Final Report, Sept. 15, 1965 - July 15, 1968. Avail: NASA; N69-23865 and CFSTI.

(4) Miles, J. K., Cheever, P. R., and Romanko, J., "Effects of Combined Electron-Ultraviolet Irradiation on Thermal Control Coatings in Vacuo at 77 K", General Dynamics/Ft. Worth, Paper presented at the AIAA 3rd Thermophysics Conference, Los Angeles, California, June 24-26, 1968. Avail: AIAA, Paper No. 68-781. Progress in Astronautics and Aeronautics, Volume 21, "Thermal Design Principles of Spacecraft and Entry Bodies", J. T. Bevans, editor, Academic Press, New York, 1969, pp. 725-740.

(5) Weaver, J. H., "Bright Anodized Coatings for Temperature Control of Space Vehicles", Plating, 51 (19), 1165-1172 (December, 1964).

(6) Zerlaut, G. A., Carroll, W. F., and Gates, D. W., "Spacecraft Temperature-Control Coatings: Selection, Utilization, and Problems Related to the Space Environment", IIT Research Institute, Technology Center, Chicago, Illinois, Paper presented at 16th International Astronautical Congress, International Astronautical Federation, Athens, Greece, September 13-18, 1965.

(7) Boebel, C. P., and Babjak, S. J., "Recent Developments in External Coatings for Spacecraft", Paper presented at Aeronautics and Space Engineering and Manufacturing Meeting, Los Angeles, California, October 3-7, 1966, Published by the Society of Automotive Engineers, Inc., Paper No. 660653.

(8) Goetzel, C. G., Rittenhouse, J. B., and Singletary, J. B., Editors, "Space Handbook", Lockheed Missiles and Space Co., Sunnyvale, California, ML-TDR-64-40, March, 1964, Tech. Doc. Rpt., AF 33 (657)-10107.

(9) Breuch, R. A., "Handbook of Optical Properties for Thermal Control Surfaces", Final Report, Vol. III of High-Performance Insulation Thermal Design Criteria, LMSC-A847882, Vol. III, Lockheed Missiles and Space Co., June 25, 1967.

(10) Rittenhouse, J. B., and Singletary, J. B., Editors, "Space Materials Handbook. Third Edition", Lockheed Missiles and Space Company, Palo Alto, California, AFML-TR-68-205, NASA SP-3051, July, 1968. Avail: N70-11113, AD 692353.

(11) Vette, James I., "Models of the Trapped Radiation Environment. Volume I: Inner Zone Protons and Electrons", Aerospace Corporation, NASA SP-3024, 1966. Avail: NASA, N66-35685. Also avail: Clearinghouse for Federal Scientific and Technical Information, Springfield, Virginia 22151.

(12) Vette, J. I., Lucero, A. B., and Wright, J. A., "Models of the Trapped Radiation Environment. Volume II: Inner and Outer Zone Electrons", Aerospace Corporation, El Segundo, California, NASA SP-3024, 1966. Avail: N66-35685, AD 659723.

(13) Millard, John P., "Results From the Thermal Control Coatings Experiment on OSO-III", Ames Research Center, Moffett Field, California, Paper presented at AIAA 3rd Thermophysics Conference, Los Angeles, California, June 24-26, 1968. Avail: AIAA, Paper No. 68-794. Progress in Astronautics and Aeronautics, Volume 21, "Thermal Design Principles of Spacecraft and Entry Bodies, J. T. Bevans, editor, Academic Press, New York, 1969, pp. 769-795.

(14) Slemp, W. S., and Hankinson, T. W. E., "Environmental Studies of Thermal Control Coatings for Lunar Orbiter", NASA Langley Research Center, Paper presented at AIAA 3rd Thermophysics Conference, Los Angeles, California, June 24-26, 1968. Avail: AIAA, Paper No. 68-792. Progress in Astonautics and Aeronautics, Volume 21, "Thermal Design Principles of Spacecraft and Entry Bodies", J. T. Bevans, editor, Academic Press, New York, 1969, pp. 797-817.

(15) Shulman, H., and Ginell, W. S., "Nuclear and Space Radiation Effects on Materials", Teledyne Isotopes and McDonnell Douglas Corporation, NASA SP-8053, NASA Space Vehicle Design Criteria (Structures), June, 1970.

(16) Blair, P. M., Jr., Pezdirtz, G. F., and Jewell, R. A., "Ultraviolet Stability of Some White Thermal Control Coatings Characterized in Vacuum", Paper presented at AIAA Thermophysics Specialist Conference, New Orleans, Louisiana, April 17-20, 1967. Avail: AIAA, Paper No. 67-345.

(17) Zerlaut, G. A., and Rogers, F. O., "The Behavior of Several White Pigments as Determined by in Situ Reflectance Measurements of Irradiated Specimens", IIT Research Institute, Technology Center, Chicago, Illinois, Paper presented at Proceedings of the Joint Air Force-NASA Thermal Control Working Group, August 16-17, 1967, Dayton, Ohio, AFML-TR-68-198, August, 1968, Tech. Rpt.

(18) Carroll, W. F., "Mariner V Temperature Control Reference Design, Test, and Performance", Jet Propulsion Lab., Pasadena, California, Paper presented at the AIAA 3rd Thermophysics Conference, Los Angeles, California, June 24-26, 1968.

(19) Reichard, P. J., and Triolo, J. J., "Preflight Testing of the ATS-1 Thermal Coatings Experiment", NASA Goddard Space Flight Center, Paper presented at AIAA Thermophysics Specialist Conference, New Orleans, Louisiana, April 17-20, 1967. Avail: AIAA, Paper No. 67-333, Progress in Astronautics and Aeronautics, Vol. 20, "Thermophysics of Spacecraft and Planetary Bodies", B. G. Heller, editor, Academic Press, New York, 1967, pp 491-513.

(20) Data received from J. J. Triolo, NASA Goddard Space Flight Center, Greenbelt, Maryland, June, 1970.

(21) Arvesen, J. C., "Spectral Dependence of Ultraviolet-Induced Degradation of Coatings for Spacecraft Thermal Control", Paper presented at the AIAA Thermophysics Specialist Conference, New Orleans, Louisiana, April 17-20, 1967. Avail: AIAA, Paper No. 67-340. Progress in Astronautics and Aeronautics, Volume 20, "Thermophysics of Spacecraft and Planetary Bodies", G. B. Heller, editor Academic Press, New York, 1967, pp. 265-280.

(22) Holland, W. R., "Stability of Thermal Control Coatings Exposed to Combined Space Environments", AVCO, Electronics Division, Tulsa, Oklahoma, NASA-CR-73160, December, 1967. Avail: NASA, N68-16904 and CFSTI.

(23) Zerlaut, G. A., Noble, G., and Rogers, F. O., "Development of Space-Stable Thermal-Control Coatings", Report No. IITRI-U6002-55 (Triannual Report), March 1-July 31, 1967, IIT Research Institute, George C. Marshall Space Flight Center, NASA, Huntsville, Alabama.

(24) Zerlaut, G. A., Rogers, F. O., and Noble, G., "The Development of S-13G-Type Thermal Control Coatings Based on Silicate-Treated Zinc Oxide", IIT Research Institute, Paper presented at the AIAA 3rd Thermophysics Conference, Los Angeles, California, June 24-26, 1968. Avail: AIAA, Paper No. 68-790. Progress in Astronautics and Aeronautics, Volume 21, "Thermal Design Principle of Spacecraft and Entry Bodies, J. T. Bevans, editor, Academic Press, New York, 1969, pp. 741-766.

(25) Brown, R. R., Fogdall, L. B., and Cannaday, S. S., "Electron-Ultraviolet Radiation Effects on Thermal Control Coatings", The Boeing Co., Seattle, Washington, Paper presented at the AIAA 3rd Thermophysics Conference, Los Angeles, California, June 24-26, 1968. Avail: AIAA, Paper No. 68-779. Progress in Astronautics and Aeronautics, Volume 21, "Thermal Design Principles of Spacecraft and Entry Bodies", J. T. Bevans, editor, Academic Press, New York, 1969, pp. 697-724.

(26) Caldwell, C. R., and Nelson, P. A., "Thermal Control Experiments on the Lunar Orbiter Spacecraft", The Boeing Company, Seattle, Washington. Paper presented at AIAA 3rd Thermophysics Conference, June 24-26, 1968, Los Angeles, California, Avail: AIAA, Paper No. 68-793. Progress in Astronautics and Aeronautics, Volume 21, "Thermal Design Principles of Spacecraft and Entry Bodies," J. T. Bevans, editor, Academic Press, New York, 1969, pp. 819-852.

(27) Fogdall, L. B., and Cannaday, S. S., "Dependence of Thermal Control Coating Degradation Upon Electron Energy", The Boeing Co. Seattle, Washington, NASA-CR-103205, D2-126114-1, May, 1969, Final Report. Avail: NASA, N69-30549 and CFSTI.

(28) Smith, F. J., and Grammer, J. G., "Emissivity Coatings for Low-Temperature Space Radiators", Quarterly Progress Report No. 42 for quarter ending June 30, 1966, NASA-CR 72059, Lockheed Missiles and Space Company, Sunnyvale, California. Report prepared for National Aeronautics and Space Administration, Lewis Research Center, Cleveland, Ohio.

(29) Smith, F. J., Olson, R. L., and Cunnington, G. R., "Emissivity Coatings for Low-Temperature Space Radiators", Quarterly Progress Report No. 1 for quarter ending September 30, 1965, NASA-CR-54807, Aerospace Sciences Laboratory, Lockheed Palo Alto Research Laboratory, Lockheed Missiles and Space Company, Sunnyvale, California. Report prepared for National Aeronautics and Space Administration, Lewis Research Center, Cleveland, Ohio, NAS-7630.

(30) Smith, F. J., and Grammer, J. G., "Emissivity Coatings for Low-Temperature Space Radiators", Quarterly Progress Report No. 2 for quarter ending December 31, 1965, NASA-CR 72059, Lockheed Missiles and Space Company, Sunnyvale, California. Report prepared for National Aeronautics and Space Administration, Lewis Research Center, Cleveland, Ohio.

(31) Breuch, R. A., and Pollard, H. E., "Nuclear Environmental Effects on Spacecraft Thermal Control Coatings", Lockheed Missiles and Space Company, Palo Alto, California, Paper presented at Symposium on Thermal Radiation of Solids, San Francisco, California, March 4-6, 1964, National Aeronautics and Space Administration, NASA SP-55, ML-TDR-64-159, N65-26895, 1965.

(32) Smith, J. A., and Luedke, E. E., "Apollo 9 Thermal Control Coating Degradation", Manned Spacecraft Center, Houston, Texas, TRW Systems, Redondo Beach, California, May, 1969.

(33) Rittenhouse, J. B., and Singletary, J. B., "Space Materials Handbook, Supplement 1 to the Second Edition Space Materials Experience", Lockheed Palo Alto Research Laboratory, NASA SP-3025, ML-TDR-64-40, Supp. 1, 1966.

(34) Cheever, P. R., Miles, J. K., and Romanko, J., "In Situ Measurements of Spectral Reflectance of Thermal Control Coatings Irradiated in Vacuo", Paper presented at AIAA Thermophysics Specialist Conference, New Orleans, Louisiana, April 17-20, 1967, Avail: AIAA Paper No. 67-342, Progress in Astronautics and Aeronautics, Vol. 20, "Thermophysics of Spacecraft and Planetary Bodies", B. G. Heller, editor, Academic Press, New York, 1967, pp. 281-296.

(35) Gilligan, J. E., and Caren, R. P., "Some Fundamental Aspects of Nuclear Radiation Effects in Spacecraft Thermal Control Materials", Research Laboratories, Lockheed Missiles and Space Company, Palo Alto, California, Paper presented at Symposium on Thermal Radiation of Solids, San Francisco, California, March 4-6, 1964, National Aeronautics and Space Administration, NASA SP-55, ML-TDR-64-159, N65-26894, 1965.

(36) Linder, B., "Series Emittance Thermal Control Coatings", Paper presented at Thermal Control Working Group Meeting, Dayton, Ohio, August 16-17, 1967.

(37) Breuch, R. A., Douglas, N. J., and Vance, D., "Effect of Electron Bombardment on the Optical Properties of Spacecraft Temperature Control Coatings", AIAA Journal, 3 (12), 2318-2327 (December, 1965).

(38) Olson, R. L., McKellar, L. A., and Stewart, J. V., "The Effects of Ultraviolet Radiation on Low α_s/ϵ Surfaces", NASA-SP-55, 1965.

(39) Glenn, E. E., and Munoz-Mellowes, A., "Thermal Design and Testing of the Pioneer Spacecraft", TRW Systems Group, TRW Inc., Redondo Beach, California.

(40) Farnsworth, D., "Exploratory Experimental Study on Neutral Charge Low Energy Particle Irradiation of Selected Thermal Control Coatings", Martin Marietta Corp., Denver, Colorado, NASA-CR-73290, January, 1969, NAS2-4962. Avail: NASA, N69-16965 and CFSTI.

(41) Bailin, L. J., "Effects of Combined Space Radiation on Some Materials of Low Solar Absorptance", Materials Sciences Laboratory, Lockheed Palo Alto Research Laboratory, Paper presented at the 11th National SAMPE Symposium and Exhibit, St. Louis, Missouri, April 19-21, 1967. Avail: DDC, AD 666364.

(42) Slensky, A. F., MacMillan, H. F., and Greenberg, S. A., "Solar-Radiation-Induced Damage to Optical Properties of ZnO-Type Pigments", Lockheed Palo Alto Research Laboratory, Lockheed Missiles and Space Company, Palo Alto, California, LMSC-4-17-68-1, NASA-CR-98174, February, 1968. Avail: NASA, N69-13059 and CFSTI.

(43) Clarke, D. R., Gillette, R. B., and Beck, T. R., "Development of a Barrier-Layer Anodic Coating for Reflective Aluminum in Space", The Boeing Company, Seattle, Washington. Paper presented at the AIAA/ASME 8th Structures, Structural Dynamics and Materials Conference, Palm Springs, California, March 29-31, 1967, Progress in Astronautics and Aeronautics, Volume 20, "Thermophysics of Spacecraft and Planetary Bodies", G. B. Heller, editor, Academic Press, 1967, pp 315-328.

(44) McCargo, M., Greenberg, S. A., and Breuch, R. A., "Study of Environmental Effects Upon Particulate Radiation Induced Absorption Bands in Spacecraft Thermal Control Coating Pigments", Lockheed Palo Alto Research Laboratory, Palo Alto, California, LMSC-6-78-68-45, NASA-CR-73289, January, 1969. Avail: NASA, N69-16868 and CFSTI.

(45) Streed, E. R., "An Experimental Study of the Combined Space Environmental Effects on a Zinc-Oxide/Potassium-Silicate Coating", Ames Research Center, Moffett Field, California, Paper presented at the AIAA Thermophysics Specialist Conference, New Orleans, Louisiana, April 17-20, 1967. Avail: AIAA, Paper No. 67-339, Progress in Astronautics and Aeronautics, Volume 20, "Thermophysics of Spacecraft and Planetary Bodies", G. B. Heller, editor, Academic Press, 1967, pp. 237-264.

(46) Rawuka, A. C., "In Situ Solar Absorptance of Ultraviolet Degraded Inorganic Coatings", Materials and Process Engineering Laboratory Report, Serial No. MP 50, 749, Catalog No. RD 28700, October 5, 1967.

(47) Heaney, James B., "Results From the ATS-3 Reflectometer Experiment", NASA Goddard Space Flight Center, Greenbelt, Maryland, Paper presented at the AIAA 4th Thermophysics Conference, San Francisco, California, June 16-18, 1969. Avail: AIAA No. 69-644.

(48) Jorgenson, G. V., Wenner, G. K., KenKnight, C. E., Eckert, E. R. G., Sparrow, E. M., and Torrance, K. E., "Solar-Wind Damage to Spacecraft Thermal Control Coatings", Surface Physics Laboratory of the Applied Science Division of Litton Systems, Inc., Report No. 2842, Summary Report, October 20, 1965.

(49) Personal Communication from A. L. Fitzkee, NASA Goddard Space Flight Center, Greenbelt, Maryland, June 3, 1970. Proton irradiation performed by The Boeing Company, Aerospace Group, Seattle, Washington, under the direction of L. B. Fogdall, R. R. Brown, and R. S. Caldwell.

(50) Luedke, E. E., and Miller, W. D., "Kapton Base Thermal Control Coatings", Thermophysics Section, TRW Systems Group, Redondo Beach, California, Paper given at Symposium on Coatings in Space, Cosponsored by ASTM E-10 Sub VI on Space Radiation Effects and NASA, in Cooperation with ASTM E-21 on Space Simulation, Cincinnati, Ohio, December 11-12, 1969.

(51) Borson, E. N., "System Requirements for Thermal Control Coatings", Aerospace Corporation, El Segundo, California, SAMSO-TR-67-63, September 1967, June 1967-August 1967, FO4695-67-C-0158, 30 pp. Avail: DDC, AD 661963.

(52) Hass, G., Ramsey, J. B., Heaney, J. B., and Triolo, J. J., "Reflectance, Solar Absorptivity, and Thermal Emissivity of SiO_2-Coated Aluminum", Applied Optics, 8 (2), 275-281 (February, 1969).

(53) Bradford, A. P., Hass, G., Heaney, J. B., and Triolo, J. J., "Solar Absorptivity and Thermal Emissivity of Aluminum Coated with Silicon Oxide Films Prepared by Evaporation of Silicon Monoxide", Applied Optics, 9 (2), 339-344 (February, 1970).

(54) Schmidt, R. N., and Park, K. C., "High-Temperature Space-Stable Selective Solar Absorber Coatings", Applied Optics, 4 (8), 917-925 (August, 1965).

(55) Wade, W. R., and Progar, D. J., "Effects of a Simulated Space Environment on Thermal Radiation Characteristics of Selected Black Coatings", Langley Research Center, Langley Station, Hampton, Virginia, NASA TN D-4116, National Aeronautics and Space Administration, Washington, D. C., September, 1967.

(56) Gilligan, J. E., and Brzuskiewicz, J., "A Theoretical and Experimental Study of Light Scattering in Thermal Control Materials", IIT Research Institute, Chicago, Illinois, Paper presented at the AIAA 5th Thermophysics Conference, Los Angeles, California, June 29-July 1, 1970. Avail: AIAA, Paper No. 70-831.

(57) Kroes, R. L., Kulshreshtha, A. P., Wegner, U. E., Mookherji, T., and Hayes, J. D., "Effects of Ultraviolet Irradiation on Zinc Oxide", NASA Marshall Space Flight Center and Brown Engineering Co., Huntsville, Alabama, Paper presented at the AIAA 5th Thermophysics Conference, Los Angeles, California, June 29-July 1, 1970. Avail: AIAA, Paper No. 70-829.

(58) Morrison, S. R., and Sancier, K. M., "Effect of Environment on Thermal Control Coatings", Stanford Research Institute, Final Report SRI Project PAD-6146, October 15, 1969.

(59) Morrison, S. R., "Iron Cyanide as a Surface State to Prevent ZnO Photolysis in Vacuum", J. of Vacuum Science and Technology, 7 (1), 84-89 (1970).

(60) Gilligan, J. E., "The Optical Properties Inducible in Zinc Oxide", IIT Research Institute, Chicago, Illinois. Paper presented at the AIAA 5th Aerospace Sciences Meeting, New York, New York, January 23-26, 1967, Avail: AIAA, Paper No. 67-214, Progress in Astronautics and Aeronautics, Volume 20, G. B. Heller, editor, "Thermophysics of Spacecraft and Planetary Bodies", Academic Press, 1967, pp. 329-347.

(61) Greenberg, S. A., and Cuff, D. F., "Solar-Radiation-Induced Damage to Optical Properties of ZnO-Type Pigments", Lockheed Palo Alto Research Laboratory, Lockheed Missiles and Space Corporation, Technical Summary Report for Period 27 June 1966 to 27 March 1967, NAS 8-18114, L-92-67-1, June 1967.

(62) Firle, T. E., and Flanagan, T. M., "Mechanisms of Degradation of Polymeric Thermal Control Coatings. Part II. Effects of Radiation on Selected Pigments", Gulf General Atomic Incorporated, AFML-TR-68-334, Part II, March, 1970.

(63) Zerlaut, G. A., and Ashford, N., "Development of Space-Stable Thermal-Control Coatings", IIT Research Inst., IITRI-U6002-73, January 31, 1969.

(64) Campbell, W. B., Cochran, J. K., Hinton, J. W., Randall, J. W., Versic, R. J., and Burroughs, J. E., "Preparation of Pigments for Space-Stable Thermal Control Coatings", The Ohio State University Research Foundation, July, 1969.

(65) "Advanced Papers of the ASM 1962 Golden Gate Metals Conference on Materials Science and Technology for Advanced Applications", 1962 Golden Gate Metals Conference, San Francisco, California, February 15-17, 1962.

INDEX

APPENDIX A

THERMAL CONTROL MATERIALS FOR SOLAR AND FLAT ABSORBERS AND REFLECTORS

and

CONTOURS OF CONSTANT FLUX ELECTRONS AND PROTONS

TABLE A-1. THERMAL-CONTROL MATERIALS FOR SOLAR ABSORBERS(9, 33, 65)

Note: Unless otherwise indicated, these materials show no significant change in absorptance or emittance in penetrating nuclear radiation in vacuum.

Material	Substrate	α_s/ϵ	Absorptance and Emittance, 70 F	Ascent Temperature Limits, F	Ultraviolet Resistance	Thermal-Cycling Resistance	Remarks
6061 Aluminum, chemically cleaned	As-rolled	2.7±0.05	α_s = 0.16±0.04 ϵ = 0.07±0.03	Structural limits only	No effect	No effect	The surface is very susceptable to increases in α_s and ϵ caused by contamination.
6061 Aluminum, chemically cleaned	Sheet sanded before processing	2.7	α_s = 0.16±0.05 ϵ = 0.06±0.03	Structural limits only	No effect	No effect	Ditto
6061 Aluminum, chemically cleaned	Forging	3.2±0.08	α_s = 0.29±0.06 ϵ = 0.09±0.06	Structural limits only	No effect	No effect	
	Weld area	2.6±0.08	α_s = 0.26±0.06 ϵ = 0.10±0.06				
2024 Aluminum, chemically cleaned (non-clad)	As-rolled, hand sanded	3.7±0.06	α_s = 0.20±0.05 ϵ = 0.06±0.03	Structural limits only	No effect	No effect	The surface characteristics of the sheet materials are subject to variations depending on fabrications operations.
2024 Aluminum, sheet (clad)			α_s = 0.22±0.05 ϵ = 0.06±0.03				
Aluminum		14.35	α_s = 0.387 ϵ = 0.027				
Aluminum		4.28	α_s = 0.218 ϵ = 0.051				
Aluminum, sandblasted (120 size grit)		1.50	α_s = 0.600 ϵ = 0.410				
Aluminum foil, dry-annealed			α_s = 0.12±0.04 ϵ = 0.04±0.02				
Aluminum foil, dull side		7.43	α_s = 0.223 ϵ = 0.030				
Aluminum foil, bright side		6.81	α_s = 0.218 ϵ = 0.032				
Aluminum foil, shiny side		5.33	α_s = 0.192 ϵ = 0.036				
Aluminum foil type		5.54	α_s = 0.238 ϵ = 0.043				
Aluminum foil, plain (MIL-A-148)	Not applicable	$3.0^{+0.05}_{-0.04}$	α_s = 0.12±0.04 ϵ = 0.05±0.02	Structural limits only	No effect	No effect	Subject to degradation from pre-launch environment. Adhesive is limiting factor in space environment.
Fasson Foil (Rubber-based adhesive backed bright aluminum foil. Type I has a clear protective coating. Type II is base only.)	Any clean rigid surface	$3.0^{+0.05}_{-0.04}$	α_s = 0.12±0.04 ϵ = 0.05±0.02	375	No effect	No information	Must not be external during ascent. Foil should be perforated (1/32-in. diam. on 1/2-in. centers) to prevent lifting due to gas evolution in vacuum.

TABLE A-1. (Continued)

Material	Substrate	α_s/ϵ	Absorptance and Emittance, 70 F	Ascent Temperature Limits, F	Ultraviolet Resistance	Thermal-Cycling Resistance	Remarks
Mystik 7402, silicone based adhesive backed aluminum foil	Any clean, rigid surface	$3.0^{+0.05}_{-0.04}$	$\alpha_s = 0.12 \pm 0.04$ $\epsilon = 0.04^{+0.02}_{-0.01}$	750	No effect	No information	If applied externally, the tape should have mechanical fastening on both ends to prevent ascent forces from peeling the tape from substrate. Subject to handling degradation.
Quilted Inconel Foil (H. I. Thompson Specification No. TPS 0101B) MIL-N-6840	Not applicable	3.17 ± 0.07	$\alpha_s = 0.38 \pm 0.05$ $\epsilon = 0.12 \pm 0.05$	2200	No effect	No effect	Very susceptible to increase in α_s and by fingerprints and oxidation in prelaunch environment. Primarily for engine heat shield usage.
Inconel X Foil, MIL-N-7786	Not applicable	4.40 ± 0.10	$\alpha_s = 0.66 \pm 0.09$ $\epsilon = 0.15 \pm 0.05$	1500	No effect	No effect	Subject to handling degradation.
QMV Beryllium, chemically polished	Not applicable	5.00 ± 0.08	$\alpha_s = 0.50 \pm 0.06$ $\epsilon = 0.10 \pm 0.06$	1700 (test maximum)	No effect	No effect	High ascent temperature has no effect on α_s or ϵ if at pressure of 0.05 torr or less.
Hanovia Gold 6518 on René 41	René 41	6.0 ± 0.08	$\alpha_s = 0.53 \pm 0.06$ $\epsilon = 0.09 \pm 0.06$	900 (no change)	No effect	No effect	May be suitable for other substrates. At 1700 F, values changed to $\alpha_s = 0.8 \pm 0.06$ $\epsilon = 0.40 \pm 0.10$.
Gold, plated on stainless steel	Stainless steel	10.77	$\alpha_s = 0.301$ $\epsilon = 0.028$				
Gold over titanium with resin undercoat	Titanium	9.10	$\alpha_s = 0.300$ $\epsilon = 0.033$				
Gold, vacuum deposited		8.29	$\alpha_s = 0.282$ $\epsilon = 0.034$				
Molybdenum, slug		3.94	$\alpha_s = 0.480$ $\epsilon = 0.122$				
Chrome-aluminized Mylar		2.90	$\alpha_s = 0.247$ $\epsilon = 0.085$				
Electroless nickel		2.60	$\alpha_s = 0.450$ $\epsilon = 0.170$				
Pure tantalum		5.46	$\alpha_s = 0.442$ $\epsilon = 0.081$				
René 41, vapor honed and buffed		3.86	$\alpha_s = 0.398$ $\epsilon = 0.103$				
Production Dow 15 on HM21A magnesium	HM21A magnesium	11.98	$\alpha_s = 0.359$ $\epsilon = 0.030$				

TABLE A-2. THERMAL-CONTROL MATERIALS FOR FLAT ABSORBERS[9, 33, 65]

Material	Substrate	α_s/ϵ	Absorptance and Emittance, 70 F	Ascent Temperature Limits, F	Ultraviolet Resistance	Thermal-Cycling Resistance	Remarks
Black Kemacryl Lacquer (Sherwin Williams M49BC 12), room-temp cure	Any clean rigid substrate; primer required	1.06±0.04	α_s = 0.93±0.03 ϵ = 0.88±0.03	No effect at 450	$\Delta\alpha_s$<0.05 after 600 sun hr UV	No failure in 385 cycles -150 to 70 F, 18-min cycles	1.5-mil dry film thickness required for solar and infrared opacity.
Fuller Black Silicone Paint (W. P. Fuller 517-B-2)	HM21A-T8 Mg, Hm 21A-O Mg, Al, Ti, stainless steels, super-alloys, and other rigid substrates capable of withstanding cure cycle	1.01±0.07	α_s = 0.89±0.05 ϵ = 0.88±0.05	No effect at 1070	$\Delta\alpha_s$<0.05 after 600 sun hr UV	**Cracking and loss of adhesion in 170 cycles -240 to 70 F, 18-min cycles**	1-mil dry film thickness required for solar and infrared opacity; peak cure-cycle temperature, 465 F.
Rokide C (chromic oxide, flame sprayed by Norton Abrasive Co., 85% Cr_2O_3)	René 41 with a 2-mil coating of Nichrome	1.06±0.06	α_s = 0.90±0.04 ϵ = 0.85±0.04	No effect at 1660	No effect	No failure; 70 to 1600 F in 5 minutes	The bonding between Rokide C and the substrate is purely mechanical and thermal shock is a potential problem.
Platinum Black (deposit of finely divided platinum on OMV beryllium)	QMV beryllium	1.11±0.08	α_s = 0.94±0.03 ϵ = 0.85±0.07	No effect at 1200	No effect	No information; probably no effect	Possesses stable high-temperature emittance.
Dow 17 (Anodized on HM 21A Magnesium Alloy)	HM21A Mg Alloy	1.11±0.10	α_s = 0.78±0.08 ϵ = 0.70±0.06	No effect at 500	No effect	No effect	Proprietary process of Dow Chem. Co.; thermal stability >500 F doubtful.
Dull Black Micobond (Midland Industrial Finishes)		1.11	α_s = 0.93±0.04 ϵ = 0.89±0.04				
Dull Black Micobond, vinyl (phenolic) Paint		1.10	α_s = 0.930 ϵ = 0.840				
Carbon-Black Pigment		1.16	α_s = 0.908 ϵ = 0.780				
Cermet (ceramic containing sintered metal)		1.10	α_s = 0.650 ϵ = 0.580				

TABLE A-3. THERMAL-CONTROL MATERIALS FOR SOLAR REFLECTORS[9, 33, 36, 49, 50, 65]

Material	Substrate	α_s/ϵ	Absorptance and Emittance, 70 F	Ascent Temperature Limits, F	Ultraviolet Resistance	Thermal-Cycling Resistance	Remarks
Tinted White Kemacryl Lacquer (Sherwin Williams M49WC17), room-temp cured	Any clean, rigid surface, primer required	0.33±0.05	$\alpha_s = 0.28 \pm 0.04$ $\epsilon = 0.89^{+0.03}_{-0.06}$	450	$\Delta\alpha_s$ = 0.18±0.04 after 2000 sun hr	No failure in 385 cycles -150 to 70 F, 18-min cycles	5-mil dry film thickness required for opacity to solar; 1-mil thickness sufficient for opacity in IR. Requires 14 days at room-temperature cure to minimize blistering during ascent heating. Used where maximum ascent temperature is <450. If no change in surface can be tolerated, max temperature <200 F.
Full r Gloss White Silicone Paint (517-W-1), cured at 465 F	HM21A-T8 Mg, Hm21A-O Mg, Al, Ti, SS, superalloys, and other rigid substrate capable of withstanding cure cycle	$0.28^{+0.04}_{-0.07}$	$\alpha_s = 0.25 \pm 0.03$ $\epsilon = 0.90^{+0.03}_{-0.06}$	650	$\Delta\alpha_s$ = 0.09 ±0.05 after 2000 sun hr	Cracking and loss of adhesion in 170 cycles -240 to 70 F, 18-min cycles	5-mil dry film thickness required for opacity to solar; 1-mil thickness for opacity in IR.
White Epoxy Paint (A. Brown Skyspar SA 9185)	Any rigid surface	$0.24^{+0.05}_{-0.07}$	$\alpha_s = 0.91^{+0.03}_{-0.06}$ $\epsilon = 0.22 \pm 0.04$	450 200 to 450 F; α_s increases by 0.04 (constant) maximum allowed	$\Delta\alpha_2$ = 0.35 ±0.06 after 2000 sun hr	No failure in 385 cycles -150 to 70 F, 18-min cycles	α_s highly susceptible to change from prelaunch sunlight and fluorescent lights. Not recommended where α_s/ϵ is critical.
Optical Solar Reflector (OSR), vapor-deposited silver on Corning 7940 fused silica with an overcoating of vapor-deposited Inconel		0.062	$\alpha_s = 0.50 \pm 0.005$ $\epsilon = 0.795 \pm 0.02$ (-135 to +70 F)	500			4-mil dry film, 14-day cure to minimize outgassing of adhesive during ascent. 500 F limit due to adhesive.

TABLE A-3. (Continued)

Material	Substrate	α_s/ϵ	Absorptance and Emittance, 70 F	Ascent Temperature Limits, F	Ultraviolet Resistance	Thermal-Cycling Resistance	Remarks
Optical Solar Reflector (OSR), vapor-deposited aluminum on Corning 7940 fused silica with an over-coating of vapor-deposited silicon monoxide		0.124	α_s = 0.100±0.005 ϵ = 0.795±0.02	500			14-day cure to minimize out-gassing during ascent.
Aluminum, coated with silicon monoxide		0.73	α_s = 0.510 ϵ = 0.700				
White Porcelain Enamel		0.31	α_s = 0.256 ϵ = 0.828				
Thermatrol 2A-100), white air drying silicone paint (TiO_2 pig-mented dimethyl siloxane)		0.19	α_s = 0.16±0.03 ϵ = 0.95±0.03	650			Surface is soft and rubbery. Material is electrostatic. 24-hr cure at room temperature re-quired.
Magnesium, coated with silica oxide		0.25	α_s = 0.210 ϵ = 0.830				
Lithiated Aluminum Silicate Inorganic Paint		0.21	α_s = 0.180 ϵ = 0.870				
White Silicate Paint (LMSC)	1100 Al	0.17	α_s = 0.13±0.03 ϵ = 0.85±0.04	600	$\Delta\alpha_s$ = 0.04 after 2000 sun hr	No effect	Cured at 400 F.
White Silicone Air-Dry Paint (LMSC)	Any rigid sub-strate	0.16	α_s = 0.14 ϵ = 0.86	700	$\Delta\alpha_s$ = 0.03 after 2000 sun hr	No effect	
Metal films (silver, aluminum, gold) with dielectric overlay (SiO_2, Al_2O_3) Solar absorptance controlled by choice of metal film, emittance deter-mined by thickness of dielectric layer			α_s = 0.05±0.02 (silver) α_s = 0.14±0.02 (aluminum) α_s = 0.20±0.02 (gold) ϵ = 0.03 (500 angstrom dielectric overlay) to ϵ = 66 (60,000 angstrom dielectric overlay)				
Aluminized FEP Teflon, emissivity dependent on thick-ness of Teflon			α_s = 0.13 to 0.16 ϵ = 0.26 to 0.89				
Silvered FEP-Teflon			α_s = 0.07-0.09 ϵ dependent on thickness				
Aluminized Polyimide (3 mil Kapton)			α_s = 0.44 ϵ = 0.78				

TABLE A-4. THERMAL-CONTROL MATERIALS FOR FLAT REFLECTORS[9, 33, 65]

Material	Substrate	α_s/ϵ	Absorptance and Emittance, 70 F	Ascent Temperature Limits, F	Ultraviolet Resistance	Thermal-Cycling Resistance	Remarks
Fuller Aluminum Silicone Paint (172-A-1)		0.89±0.10	α_s = 0.25±0.07 ϵ = 0.28±0.07		$\Delta\alpha_s$ increases by 0.09±0.04 after 600 sun hr, ϵ is unaffected		Baked at 465 F. No change observed at 885 F.
Fuller Aluminum Silicone Paint (171-A-152)		0.92±0.08	α_s = 0.22±0.04 ϵ = 0.24±0.04		$\Delta\alpha_s$ increases by 0.09±0.04 after 600 sun hr, ϵ is unaffected		No change to 880 F.
Fuller Aluminum Silicone Paint (not identified)		1.2	α_s = 0.230 ϵ = 0.200				
Nonleafing Aluminum Acrylic Paint		0.85±0.08	α_s = 0.41±0.03 ϵ = 0.48±0.05	650 where bubbling can be tolerated, otherwise 240 F maximum			Requires 14-day cure to minimize blistering.

TABLE A-5. MISCELLANEOUS THERMAL-CONTROL MATERIALS[9]

Material	Substrate	α_s/ϵ	Absorptance and Emittance, 70 F	Ascent Temperature Limits, F	Ultraviolet Resistance	Thermal-Cycling Resistance	Remarks
LMSC Silicone Tape (1A48)	Any rigid substrate	0.18	$\alpha_s = 0.16$ $\epsilon = 0.86$	700	$\Delta\alpha_s = 0.04$ after 2000 sun hr	No effect	
Rokide A, aluminum oxide, flame sprayed by Norton Abrasive Co., San Jose, Calif.	Any metallic substrate	0.36±0.05	$\alpha_s = 0.27 \pm 0.04$ $\epsilon = 0.75 \pm 0.03$				This material was used on Explorers 1, 3, and 7 and Tiros 2. Total area covered by this material small; actual performance of material cannot be evaluated. Tiros 2 transmitted 1 yr, Explorer 7 transmitted about 2 yr.
Stainless Steel AISI 410, sandblasted	Not applicable	0.88	$\alpha_s = 0.75$ $\epsilon = 0.85$		No information		This material with Rokide A stripes was primary thermal-control surface of Explorers 1, 3, and 4.
Aluminum (2024), sandblasted	Al alloy (2024)	2.0	$\alpha_s = 0.42$ $\epsilon = 0.21$		No information		Material used in Explorer 7 as support for solar cells and as stiffener ring between glass reinforced polyester conical sections of spacecraft structure. Thermal design was 0 to 60 C. While in orbit inments in spacecraft were never lower than 16 C or higher than 41 C. Transmitted from 10/13/59 to 8/24/61.
LMSC White Silicone Air Dry Paint	Any rigid substrate	0.16	$\alpha_s = 0.14$ $\epsilon = 0.86$	700	$\Delta\alpha_s \pm 0.03$ after 2000 sun hr	No effect	

TABLE A-5. (Continued)

Material	Substrate	α_s/ϵ	Absorptance and Emittance, 70 F	Ascent Temperature Limits, F	Ultraviolet Resistance	Thermal Cycling Resistance	Remarks
Black Micobond (L6X962) Midland Industrial Finishes Co., Waukegan, Ill.	Any metal surface	1.11±0.05	α_s = 0.93±0.04 ϵ = 0.84±0.03	No information	No effect after 500 sun hr	No information	
Reynolds Wrap Foil, smooth	Not applicable	Dull side 5.0; shiny side 6.3	α_s = 0.20 ϵ = 0.04 α_s = 0.19 ϵ = 0.03	Structural limits only	No effect	No effect	
Lockspray Gold	Anodized Mg or Al alloys coated with clear or white, glossy or matte epoxy	7.3 to 4.8	α_s = 0.22 to 0.24 ϵ = 0.03 to 0.05	No effect to 400 F	No information	No effect	Material used as coating on visor of face plate on Astronaut White's helmet during extra-vehicular activity in the Gemini 4 mission; used as coating on interior of Gemini 5 adapter section with substrate of white epoxy on Dow 17 treated Mg alloy HK31A-H24.

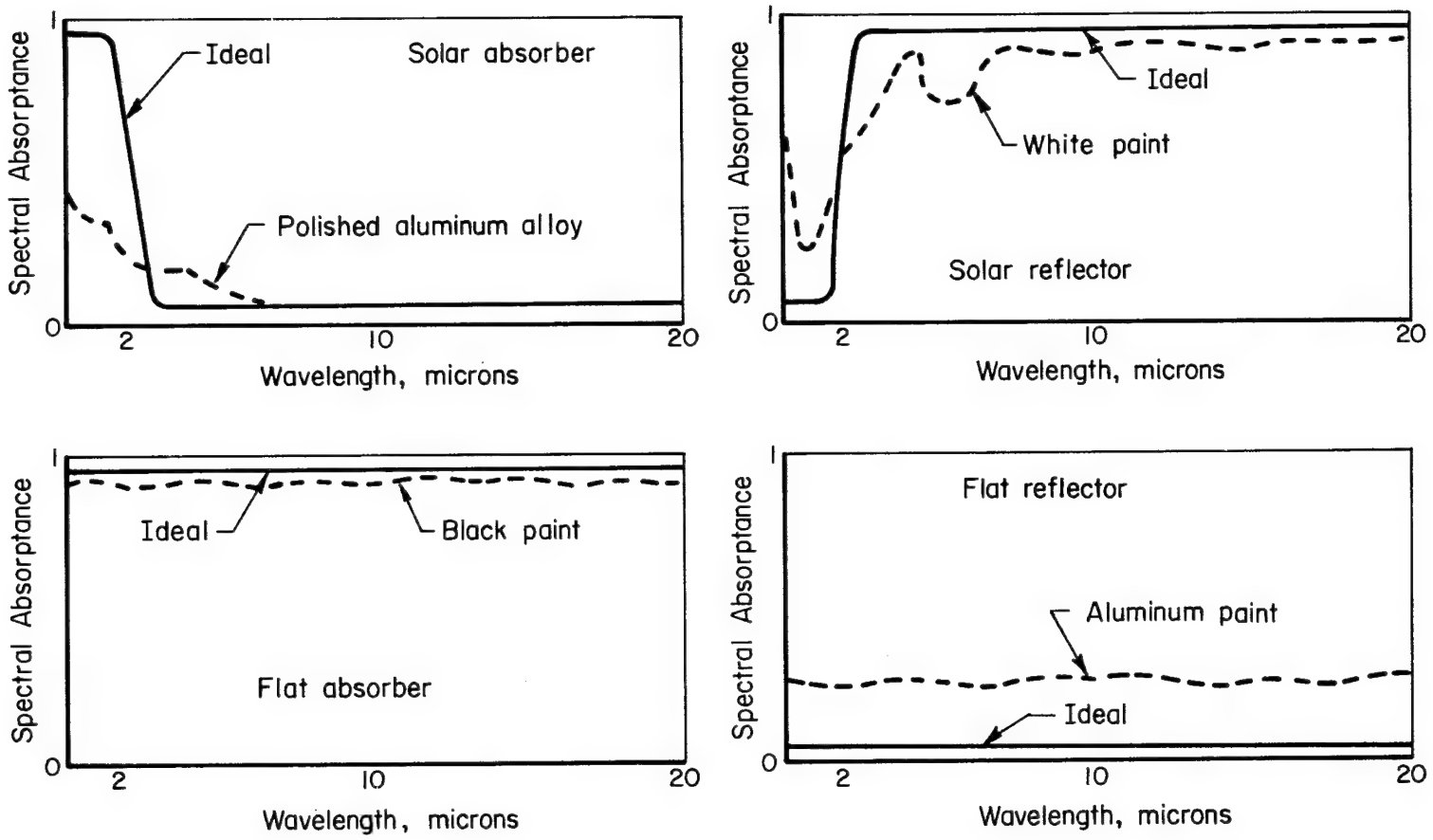

FIGURE A-1. IDEAL REPRESENTATION OF FOUR BASIC SURFACES AND PRODUCTION MATERIALS APPROXIMATING THEM[2]

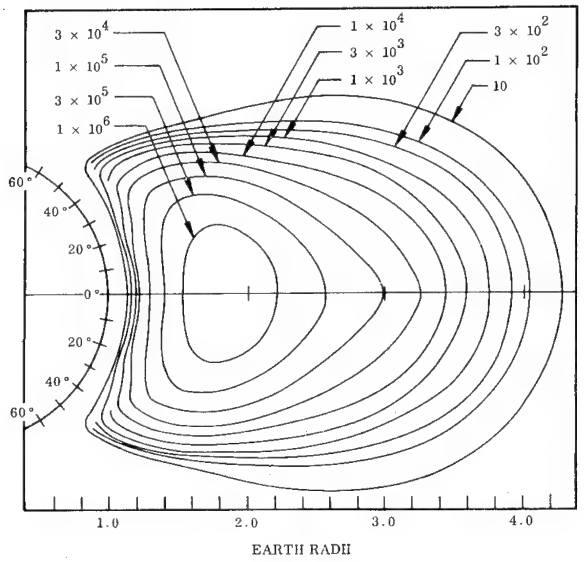

FIGURE A-2. PROTON ISOFLUX CONTOURS (E > 4 MeV)

Contours are labeled in units of protons/ cm^2-sec, R_E = 3440 nm.[10,11]

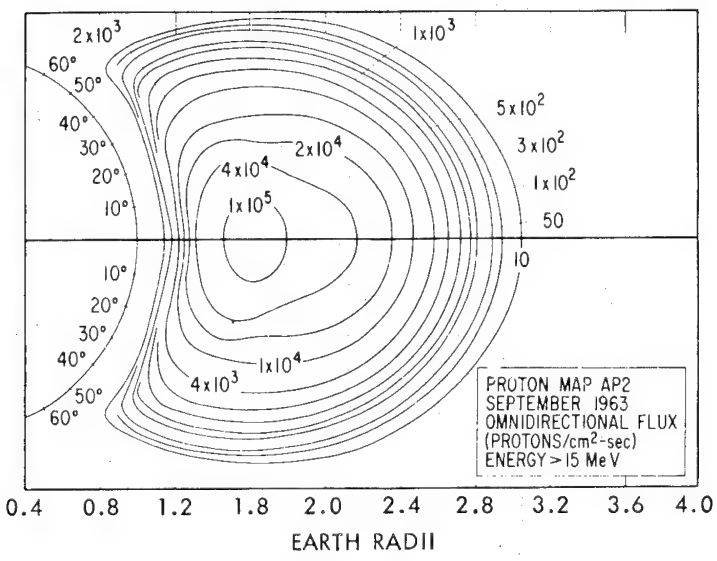

FIGURE A-3. PROTON ISOFLUX CONTOURS (E > 15 MeV)

Contours are labeled in units of protons/ cm^2-sec, R_E = 3440 nm.[11]

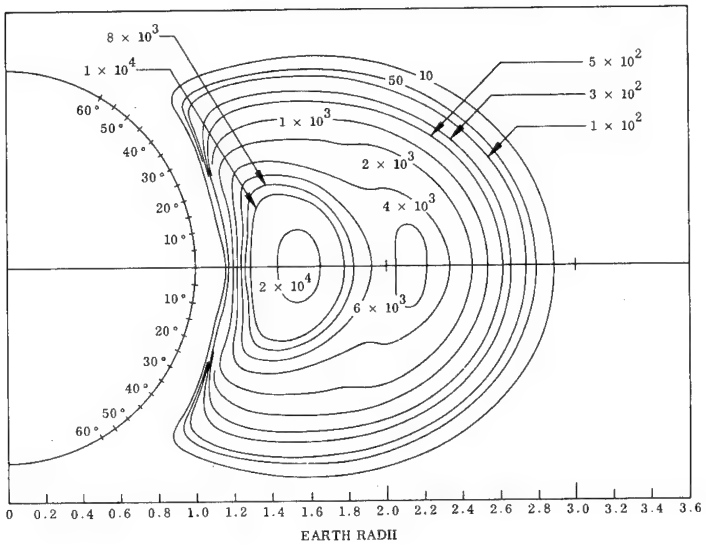

FIGURE A-4. PROTON ISOFLUX CONTOURS (E > 34 MeV)

Contours are labeled in units of protons/ cm^2 - sec, radial distance is in earth radii, R_E = 3440 nm.(10, 11)

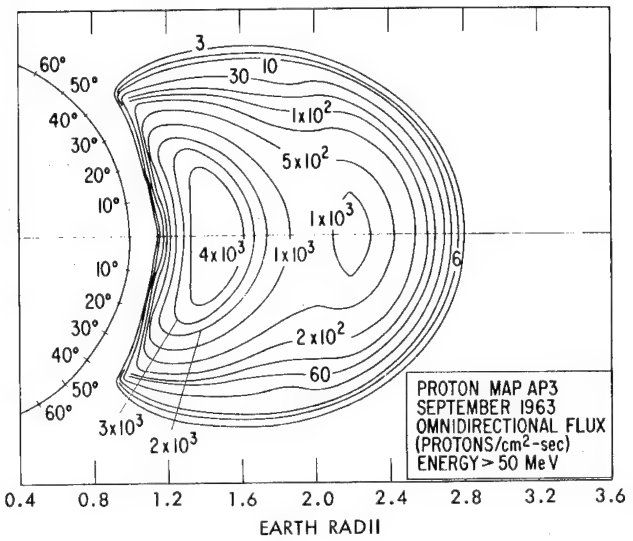

FIGURE A-5. PROTON ISOFLUX CONTOURS (E > 50 MeV)

Contours are labeled in units of protons/ cm^2-sec, R_E = 3440 nm.(11)

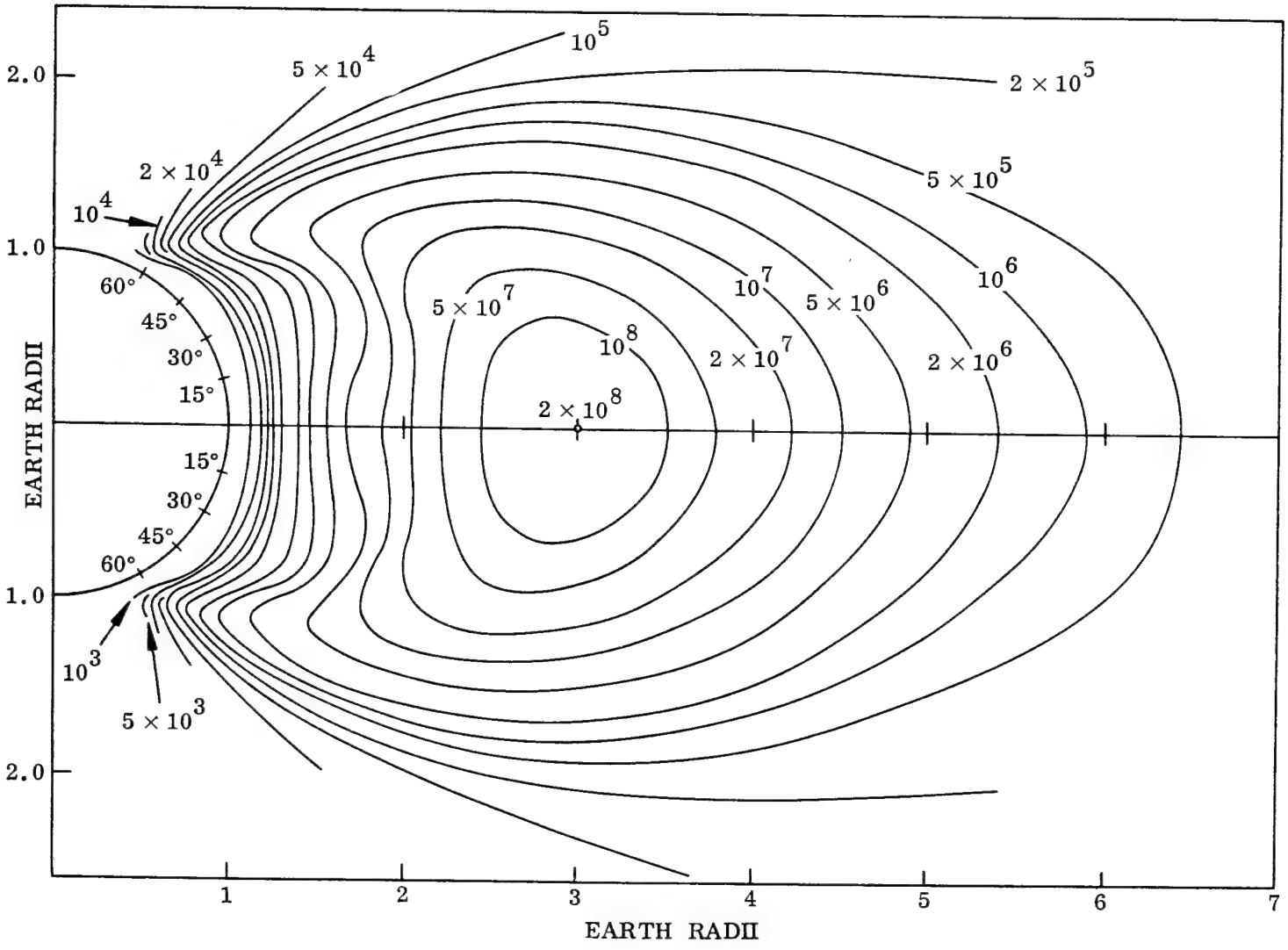

FIGURE A-6. PROTON ISOFLUX CONTOURS (E > 0.4 MeV)

Contours are labeled in units of protons/ cm^2-sec. (10)

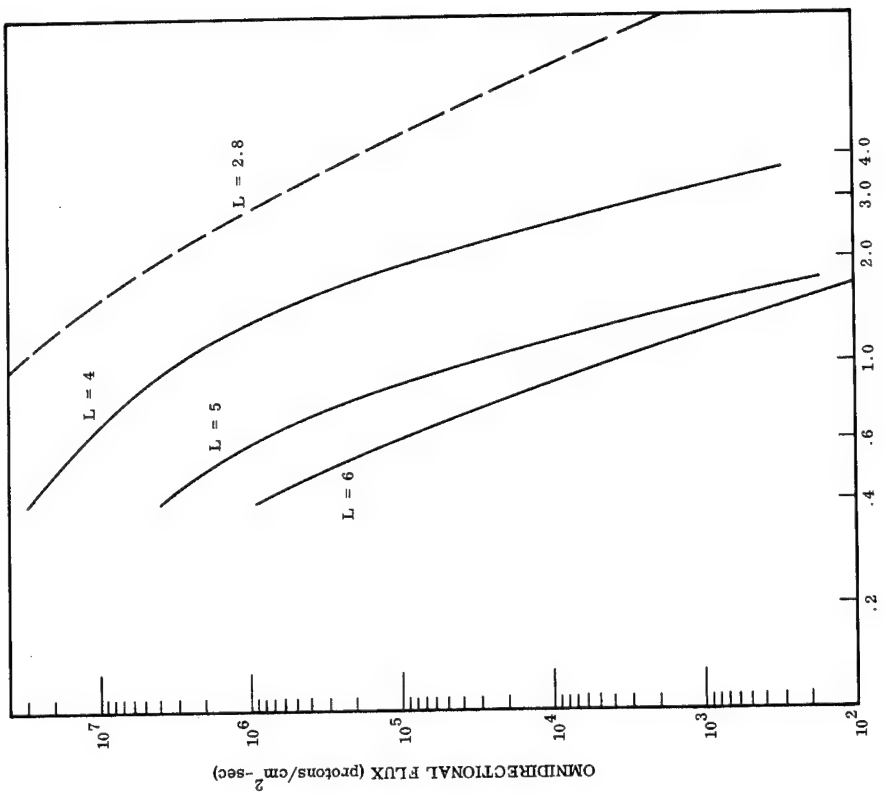

FIGURE A-8. OUTER ZONE PROTON SPECTRA(10)

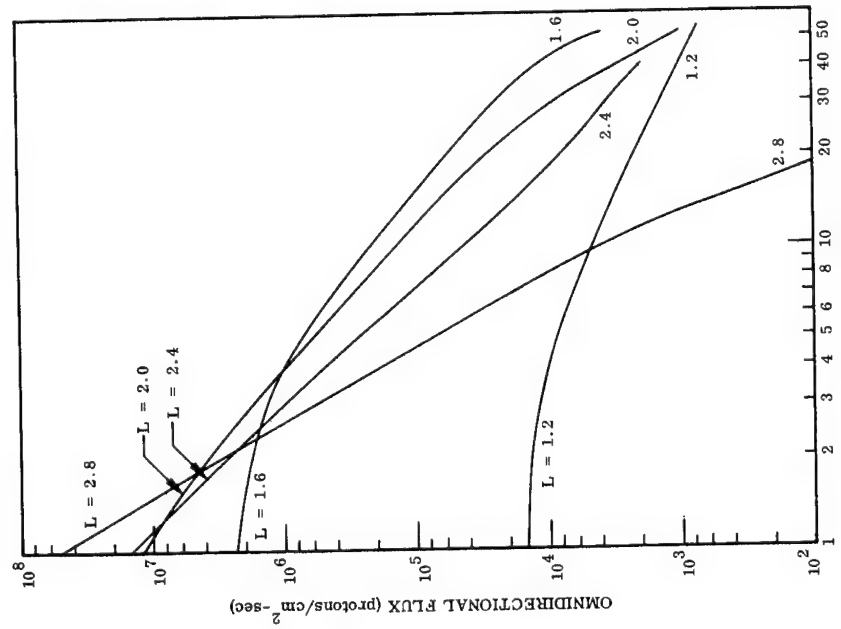

FIGURE A-7. INNER ZONE PROTON SPECTRA(10)

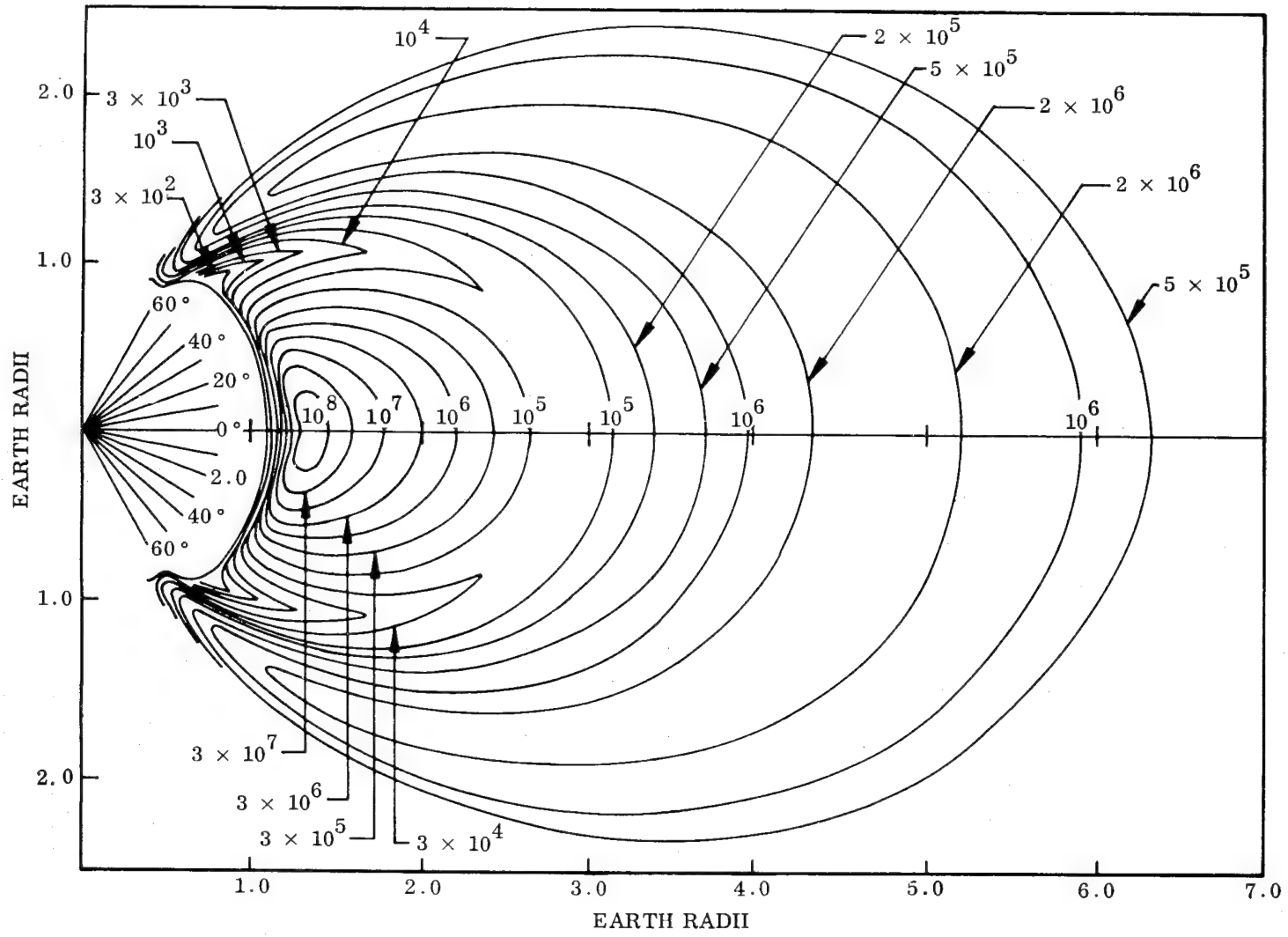

FIGURE A-9. TRAPPED ELECTRON ISOFLUX CONTOURS (E > 0.5 MeV) AS OF AUGUST 1964

Contours are labeled in units of electrons/cm^2-sec. (10,12)

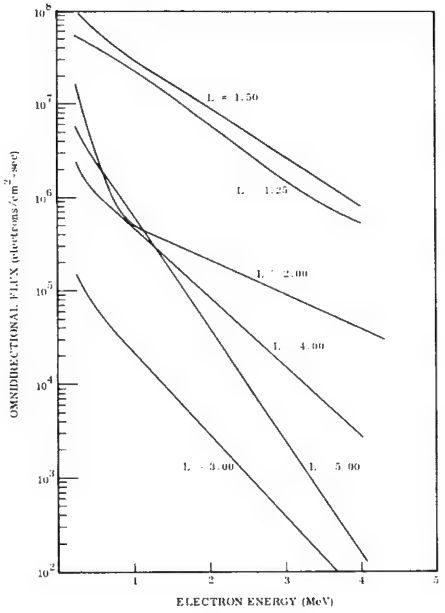

FIGURE A-10. TRAPPED ELECTRON SPECTRA[10]

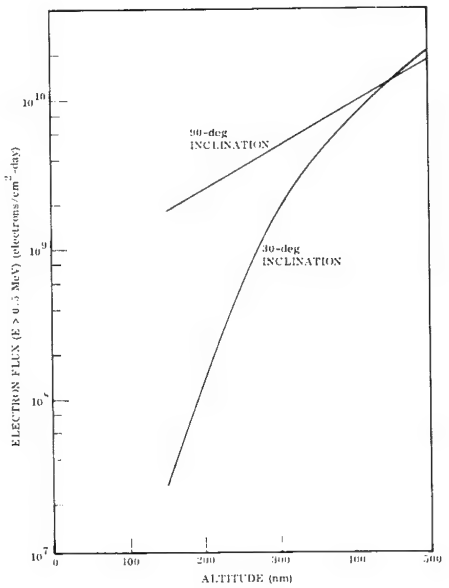

FIGURE A-11. ELECTRON FLUX PER DAY ENCOUNTERED IN CIRCULAR ORBITS FOR DECEMBER 1968[10]

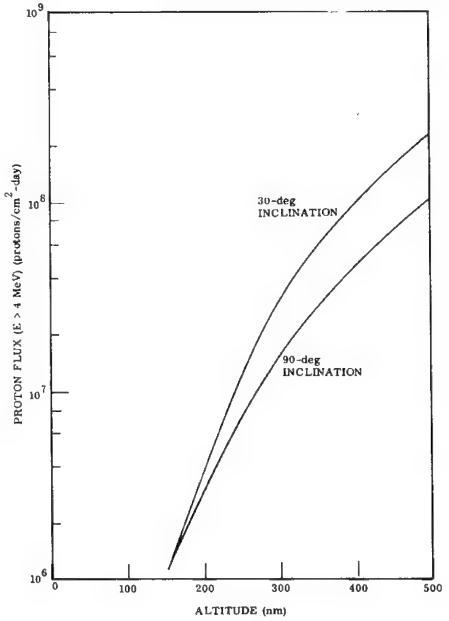

FIGURE A-12. PROTON FLUX PER DAY ENCOUNTERED IN CIRCULAR ORBITS[10]

APPENDIX B

TABLES AND FIGURES FOR ORGANIC THERMAL-CONTROL COATINGS

TABLE B-1. EFFECT OF WAVELENGTH OF ULTRAVIOLET ON SPECTRAL ABSORPTANCE OF S-13 COATING[21]

Peak Irradiation Wavelength, mμ	Energy Absorbed by Sample, 10^6 joules/m^2	$\Delta\alpha_s$[a]	$\phi\lambda$, 10^{-8} joules/m^2
255 (4.86 eV)	7.3	0.035	0.48
273 (4.54 eV)	14.6	0.038	0.26
293 (4.23 eV)	21.7	0.026	0.12
350 (3.54 eV)	60.0	0.015	0.03

(a) Initial α_s = 0.200.

TABLE B-2. DECREASE IN REFLECTANCE IN S-13 (TYPE B)[3]

Measured After Exposure to:	$\Delta R = R_i - R_f$(°C) at Selected Wavelengths						
	425 mμ	590 mμ	950 mμ	1,200 mμ	1,550 mμ	2,100 mμ	2,500 mμ
UV only	1	1	3	6	10	22	14
Electrons only	0	2	6	11	20	37	26
Arithmetic Sum of above	1	3	9	17	30	59	40
Consecutive exposure to UV, then to electrons	0	2	4	7	15	30	19
Simultaneous UV-electron exposure	0	2	7	12	24	43	30

UV exposure = 18 ESH.
Electron exposure = 10^{14} e/cm^2.

TABLE B-3. INITIAL ABSORPTANCE/EMITTANCE OF FLIGHT COUPONS[26]

Coating	α_s (lab)	E_{ir} (lab)	α_s/E_{ir} (lab)	α_s/E_{ir} (flight)	α_s/E_{ir}-α_s/E_{ir} (lab)	α_s/E_{ir}-α_s/E_{ir} (flight)
S-13-G over B-1056 (L. O. IV)	0.191	0.860	0.222	0.200	0.022	
S-13-G over B-1056 (L. O. V)	0.191	0.860	0.222	0.187	0.035	
S-13-G	0.184	0.879	0.209	0.203	0.006	
B-1060	0.178	0.855	0.208	0.193	0.015	
Hughes Inorganic (H-2)	0.178	0.876	0.203	0.216	0.013	
Hughes Organic (H-10)	0.147	0.860	0.171	0.162	0.009	
Silicone-over-Aluminum	0.197	0.800	0.246	0.239	0.007	
Z-93 (McDonnell)	0.184	0.880	0.209	0.183	0.026	

TABLE B-4. DECREASE IN REFLECTANCE IN TiO_2 - METHYL PHENYL SILICONE[3]

Measured After Exposure to:	$\Delta R = R_i - R_f$ (%) at Selected Wavelengths							
	425 mμ	500 mμ	590 mμ	950 mμ	1,200 mμ	1,550 mμ	2,100 mμ	2,500 mμ
UV only	36	17	8	4	3	2	2	2
Electrons only	9	10	12	18	19	17	12	6
Arithmetic sum of above	45	27	20	22	22	19	14	8
Consecutive exposure to UV, then to electrons	36	19	9	5	4	3	2	1
Simultaneous UV-electron exposure	40	22	15	16	16	14	13	6

UV exposure = 18 ESH.
Electron exposure = 5×10^{14} e/cm^2.

TABLE B-5. RADIATIVE PROPERTIES OF BUTVAR ON ALUMINUM[36]

Thickness, mils	Solar Absorptance	Emittance
0.75	0.18	0.45
3.2	0.22	0.85
6.5	0.22	0.88

TABLE B-6. EFFECT OF SAMPLE TEMPERATURE DURING NUCLEAR IRRADIATION ON THE OPTICAL PROPERTIES OF THERMAL-CONTROL COATINGS[31]

Material	Temperature During Irradiation, F ± 10	α_s Initial	α_s Final	Dose
Skyspar epoxy-based coating	-100	0.22	0.22	2.2×10^6 rads (C)
	0	0.22	0.22	0.6×10^{13} n/cm^2, E<0.48 eV
	+100	0.22	0.23	1×10^{14} n/cm^2, E>2.9 MeV in vacuum
	+200	0.22	0.28	
$ZrSiO_4$–K_2O/SiO_2	70	0.11	0.13	2.2×10^6 rads (C)
	-320	0.11	0.22	2.26×10^{14} n/cm^2, E<0.48 eV 4.72×10^{14} n/cm^2, E>2.9 MeV in vacuum
$Na_2O \cdot Al_2O_3 \cdot 4SiO_2$ – Na_2O/SiO_2	70	0.17	0.24	
	-320	0.17	0.34	

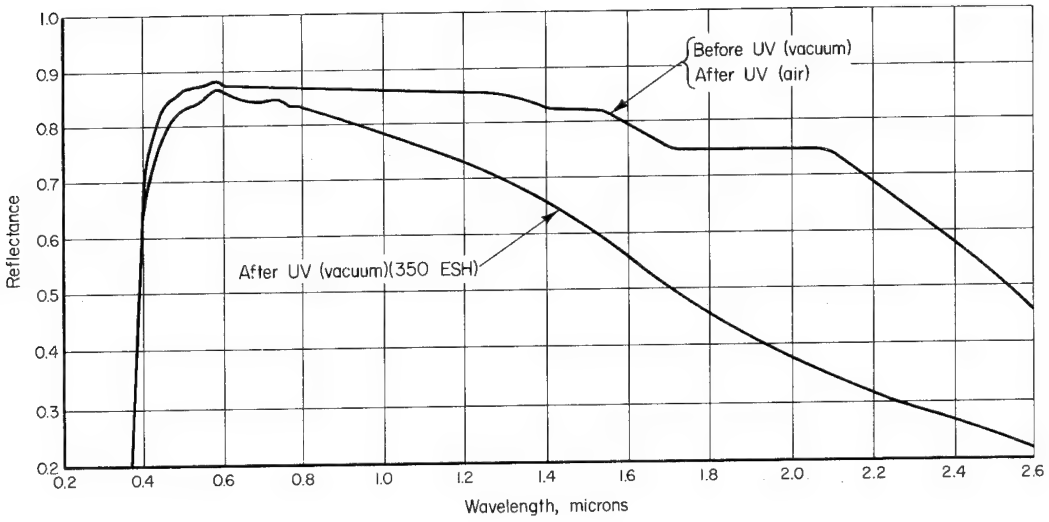

FIGURE B-1. SPECTRAL REFLECTANCE OF B1056 COATING[16]

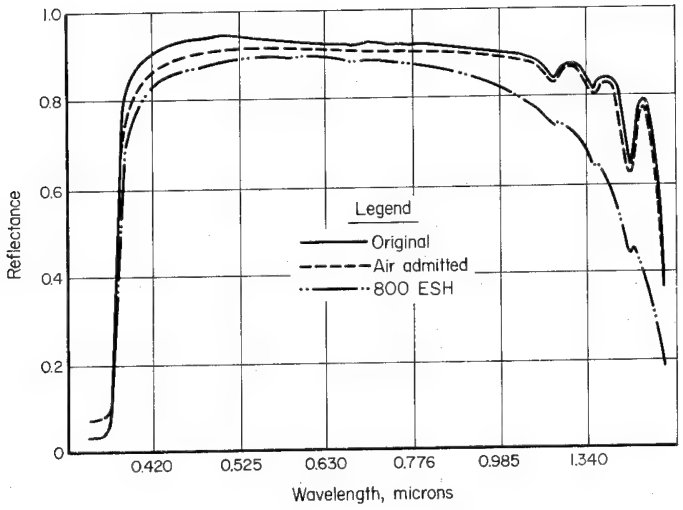

FIGURE B-2. EFFECT OF UV IN VACUUM ON S-13 COATING[17]

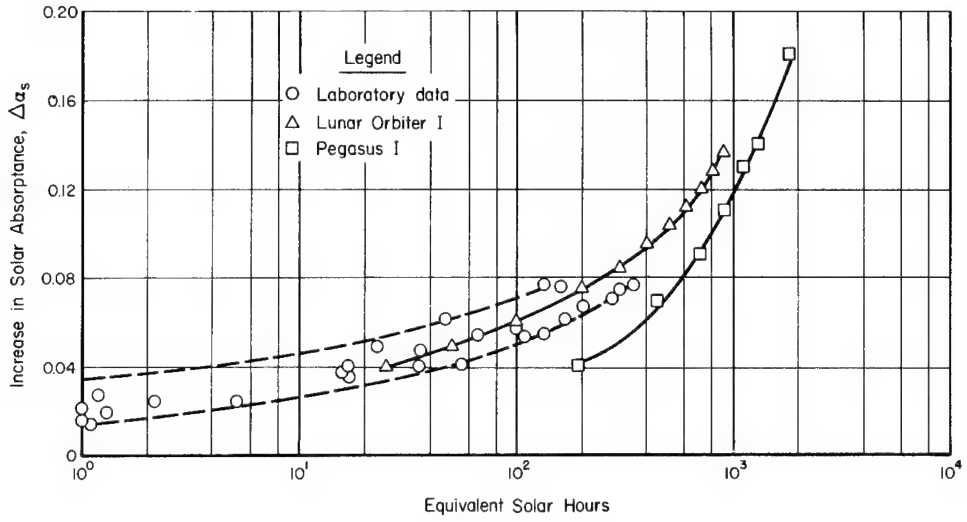

FIGURE B-3. CHANGE IN SOLAR ABSORPTANCE OF B1056 COATING; LABORATORY DATA AND FLIGHT DATA[16]

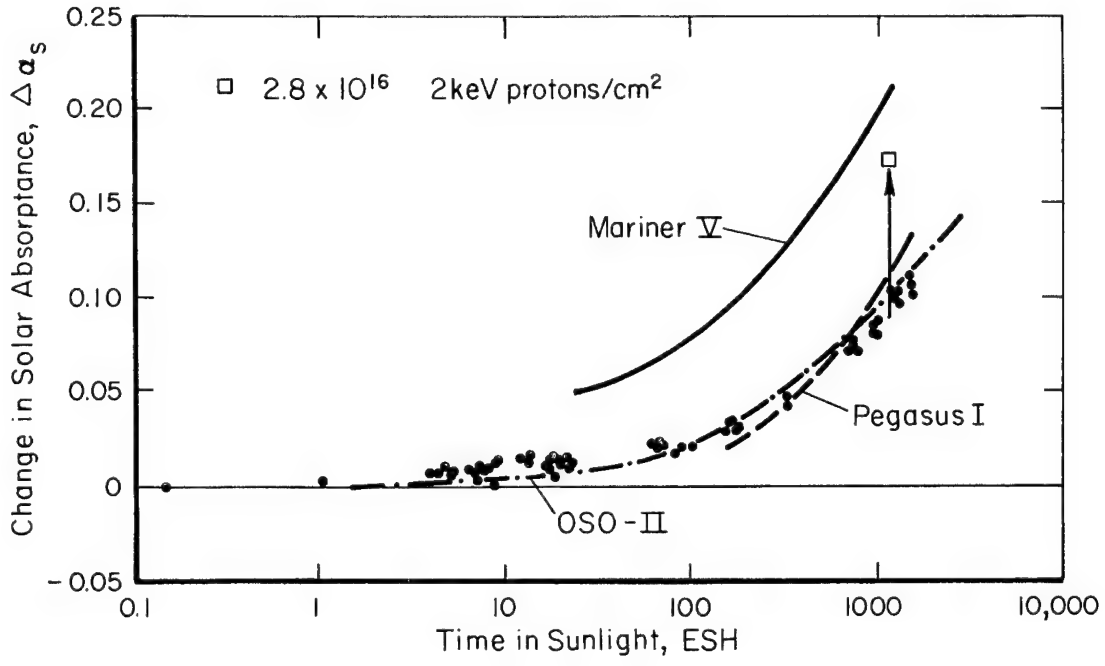

FIGURE B-4. ZINC OXIDE IN SILICONE (S-13)

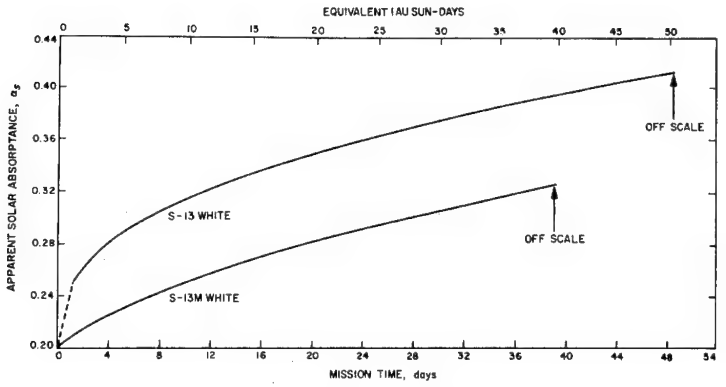

FIGURE B-5. SOLAR ABSORPTANCE OF S-13 AND S-13M WHITE COATINGS ON MARINER V TCR[18]

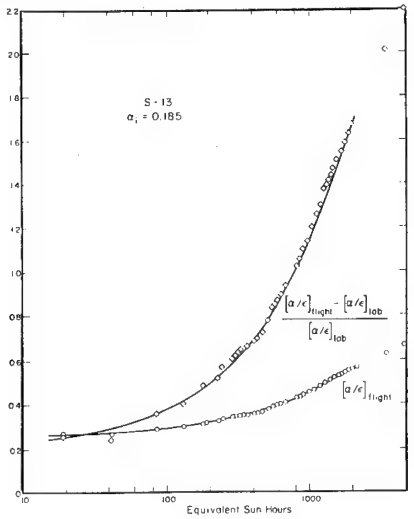

FIGURE B-6. ATS-1 FLIGHT DATA FOR S-13 COATING[20]

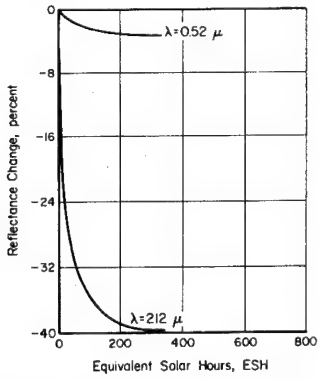

FIGURE B-7. REFLECTANCE CHANGE OF B1056 AS A FUNCTION OF UV EXPOSURE AT TWO WAVELENGTHS[16]

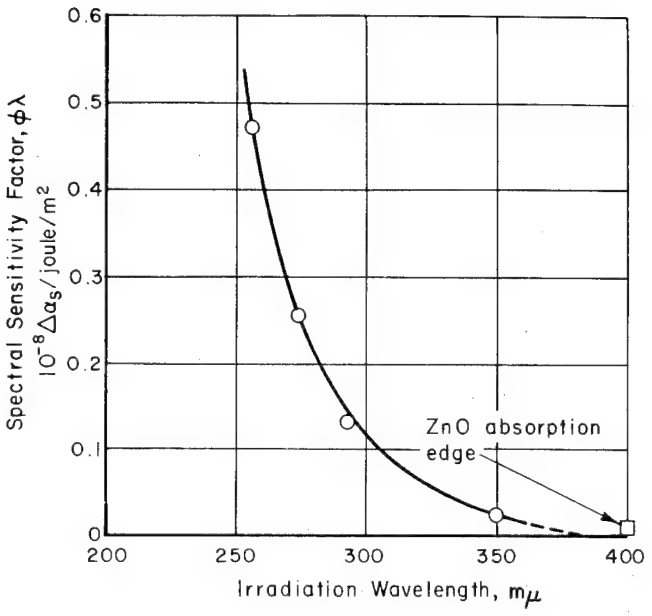

FIGURE B-8. EFFECT OF IRRADIATION WAVELENGTH ON SPECTRAL SENSITIVITY OF S-13 COATING[21]

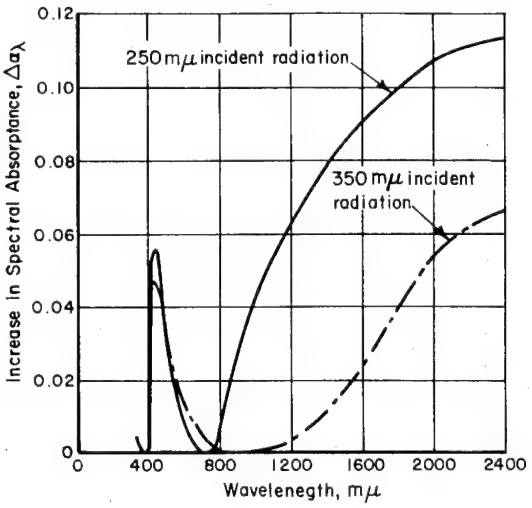

FIGURE B-9. EFFECT OF WAVELENGTH ON SPECTRAL ABSORPTANCE OF S-13 COATING[21]

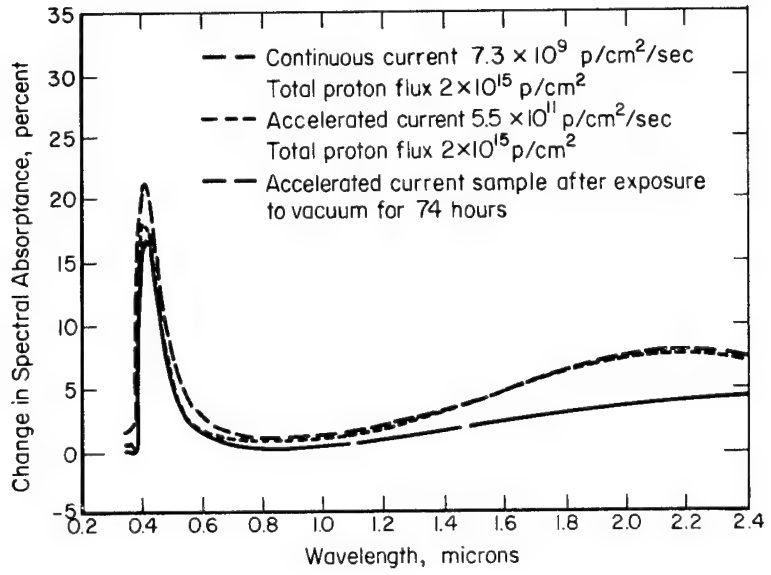

FIGURE B-10. RATE AND VACUUM EFFECT OF PROTON RADIATION ONLY - ZnO/SILICONE[22]

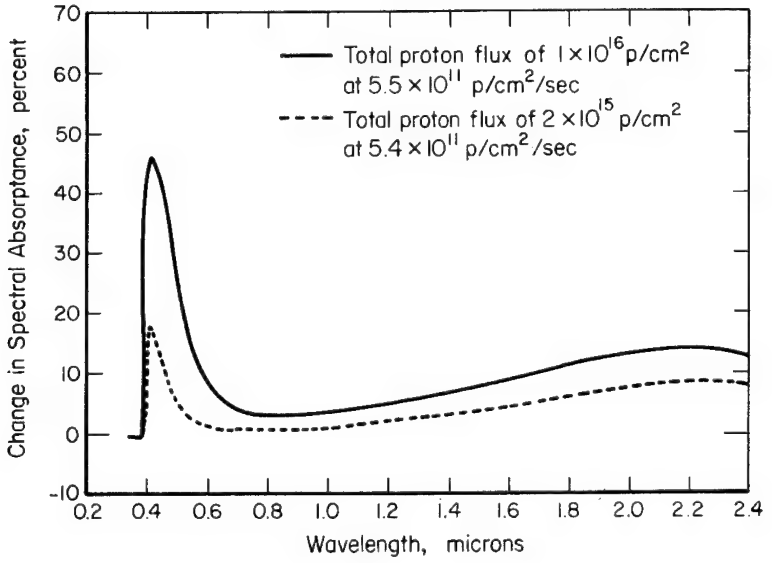

FIGURE B-11. EFFECT OF INCREASING TOTAL PROTON FLUX FROM 2×10^{15} P/CM^2 TO 1×10^{16} P/CM^2 - ZnO/SILICONE[22]

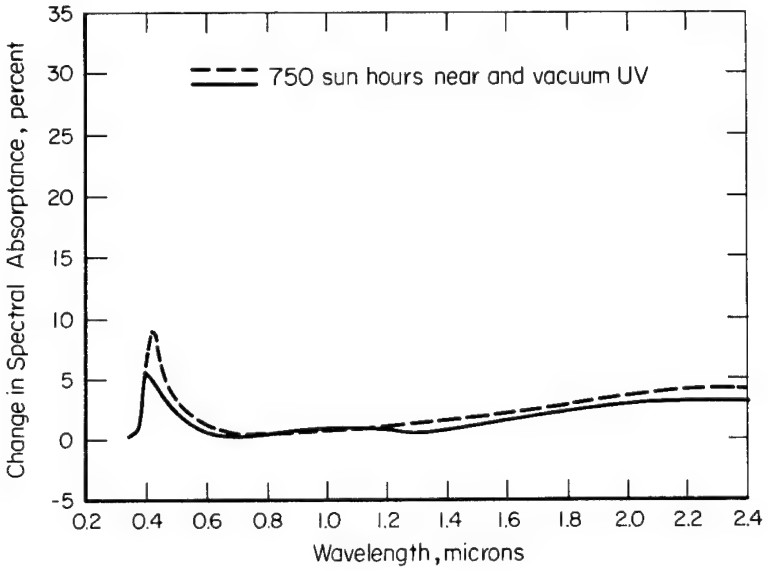

FIGURE B-12. EFFECT OF UV RADIATION ONLY - ZnO/SILICONE[22]

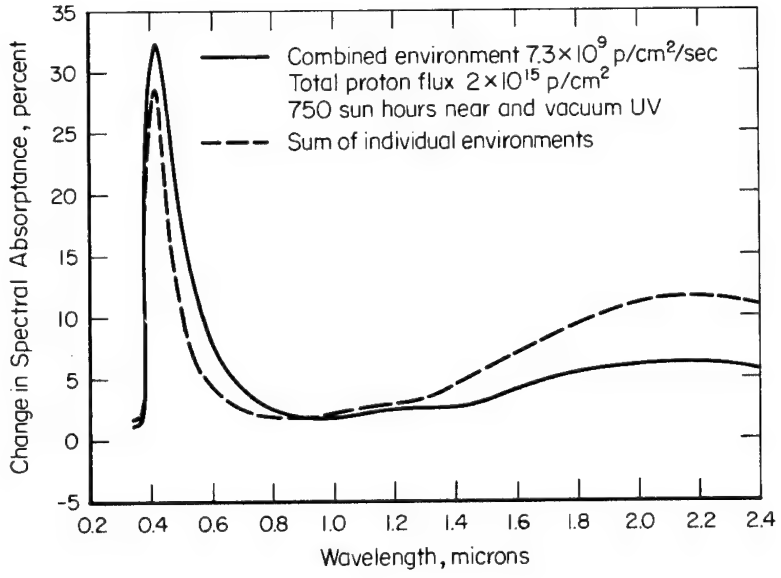

FIGURE B-13. COMBINED EFFECTS VERSUS SUM OF INDIVIDUAL EFFECTS. CONTINUOUS LOW CURRENT - ZnO/SILICONE[22]

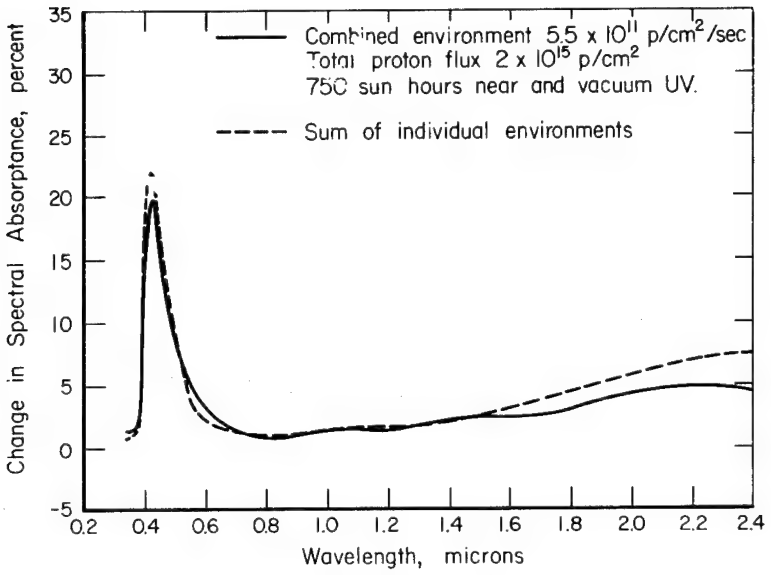

FIGURE B-14. COMBINED EFFECTS VERSUS SUM OF INDIVIDUAL EFFECTS. ACCELERATED CURRENT - ZnO/SILICONE[22]

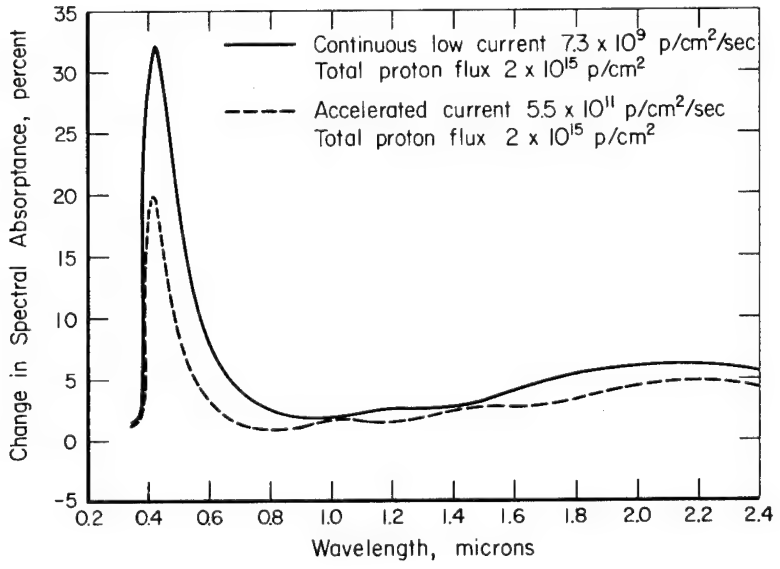

FIGURE B-15. COMBINED EFFECTS WITH CONTINUOUS CURRENT VERSUS COMBINED EFFECTS WITH ACCELERATED CURRENT - ZnO/SILICONE[22]

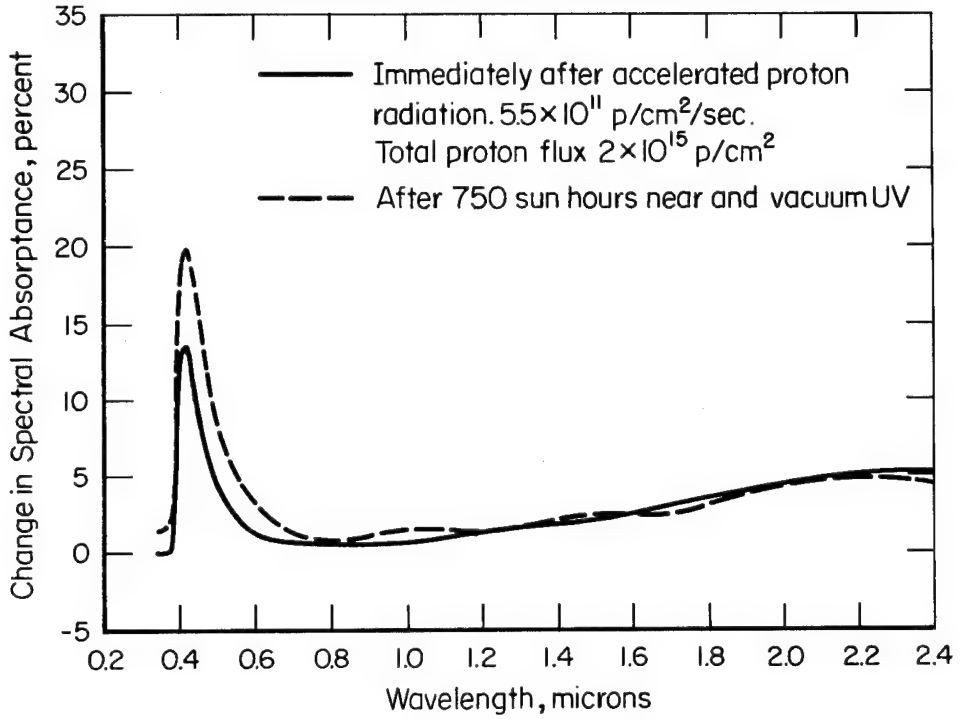

FIGURE B-16. EFFECT OF COMBINED ENVIRONMENT IMMEDIATELY AFTER ACCELERATED PROTON EXPOSURE AND AT END OF TEST - ZnO/SILICONE[22]

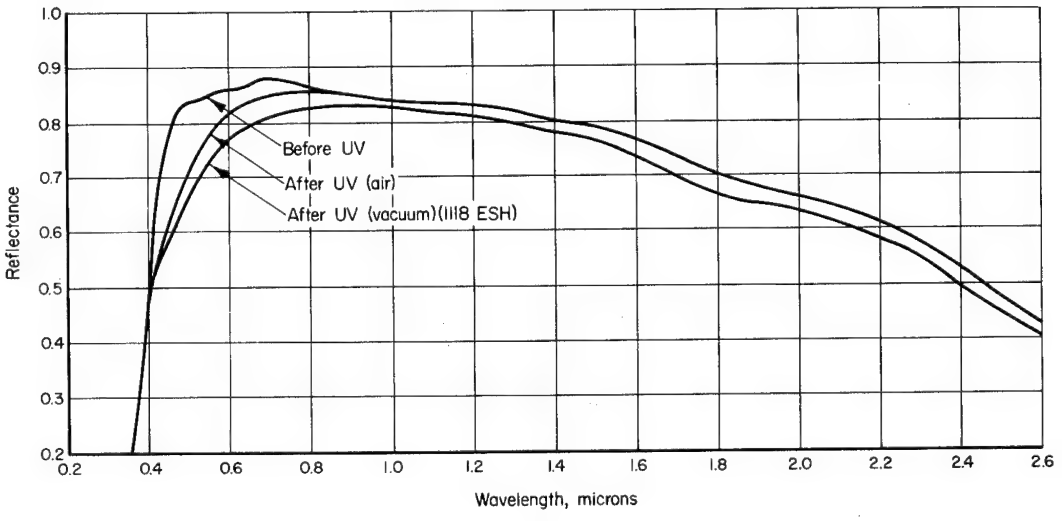

FIGURE B-17. SPECTRAL REFLECTANCE OF S-13G COATING[16]

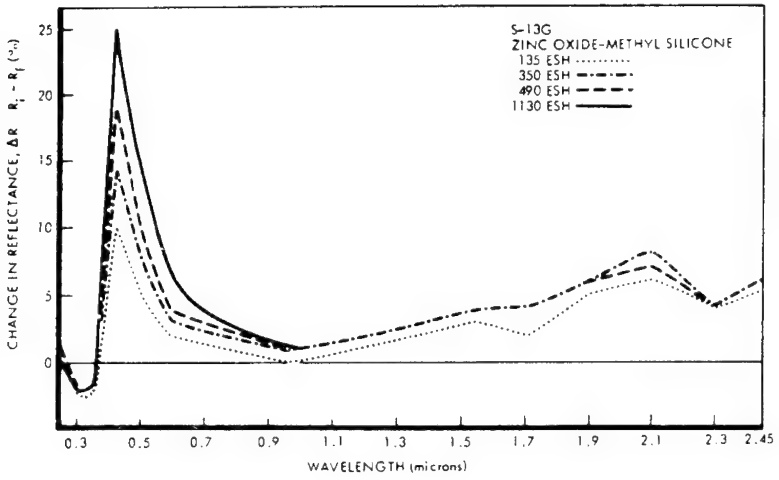

FIGURE B-18. REFLECTANCE CHANGES IN AN EARLY FORMULATION OF S-13G[25]

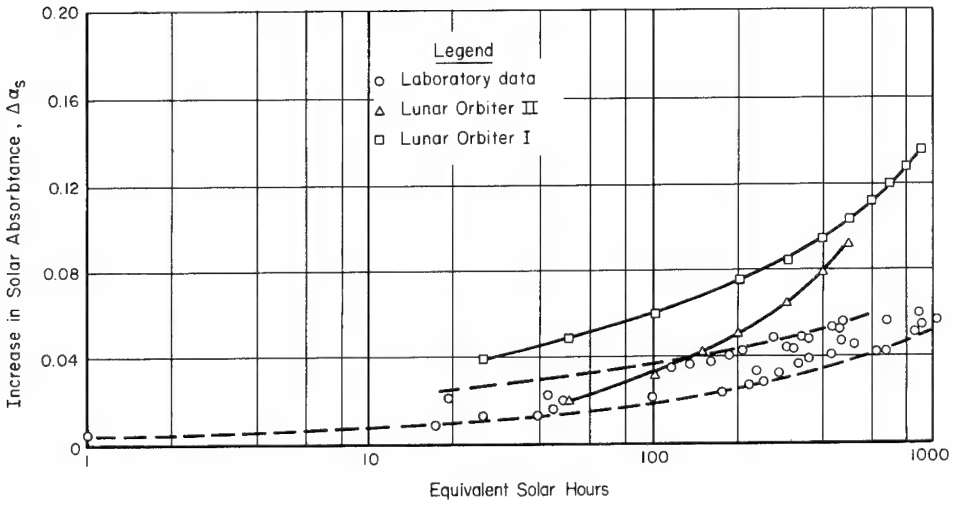

FIGURE B-19. CHANGE IN SOLAR ABSORPTANCE OF S-13G COATING: LABORATORY DATA AND FLIGHT DATA[16]

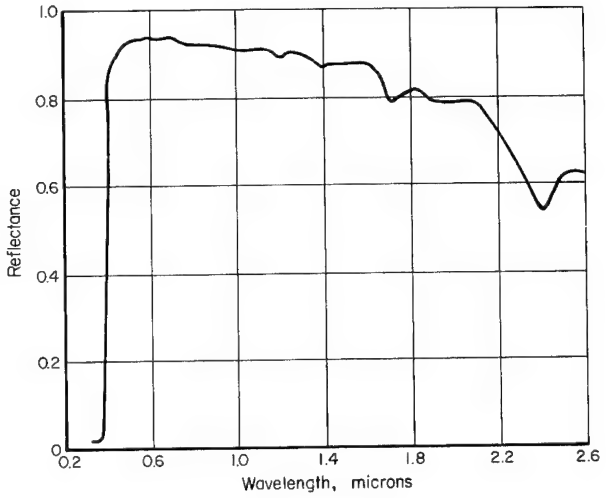

FIGURE B-20. INITIAL REFLECTANCE S-13G USED ON LUNAR ORBITER IV[26]

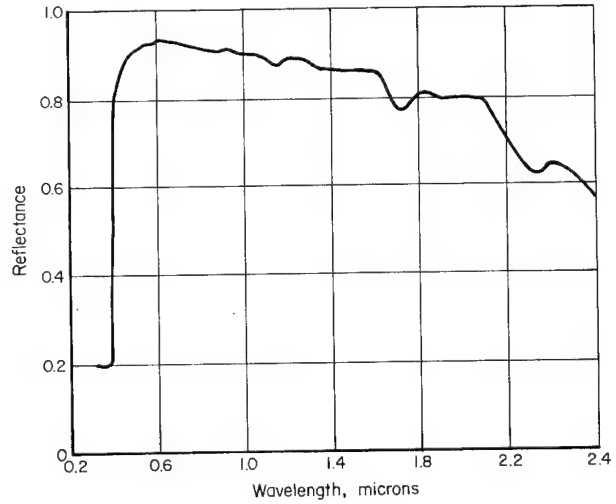

FIGURE B-21. INITIAL REFLECTANCE S-13G OVER B-1056 USED ON LUNAR ORBITERS IV AND V[26]

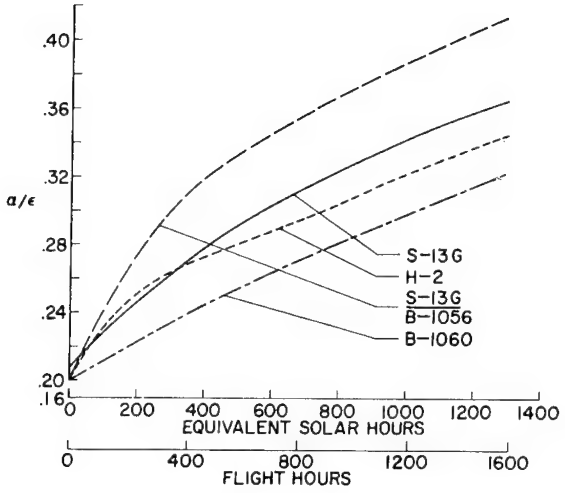

FIGURE B-22. RESULTS OF THE THERMAL CONTROL COATING FLIGHT EXPERIMENT ON LUNAR ORBITER IV[14]

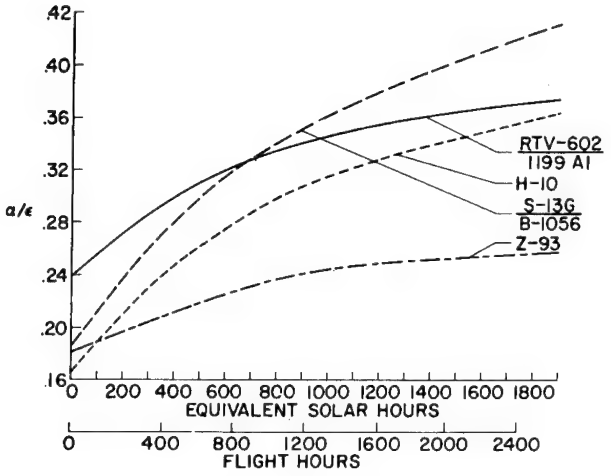

FIGURE B-23. RESULTS OF THE THERMAL CONTROL COATING FLIGHT EXPERIMENT ON LUNAR ORBITER V[14]

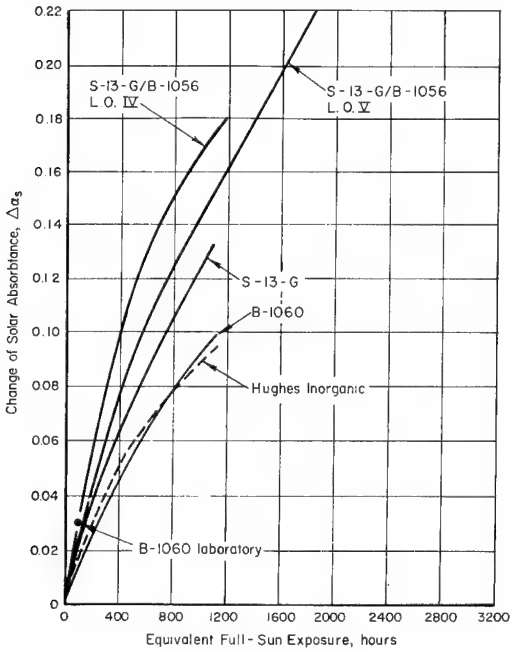

FIGURE B-24. DEGRADATION OF COUPONS ON LUNAR ORBITER IV WITH COMPARISONS TO LUNAR ORBITER V[26]

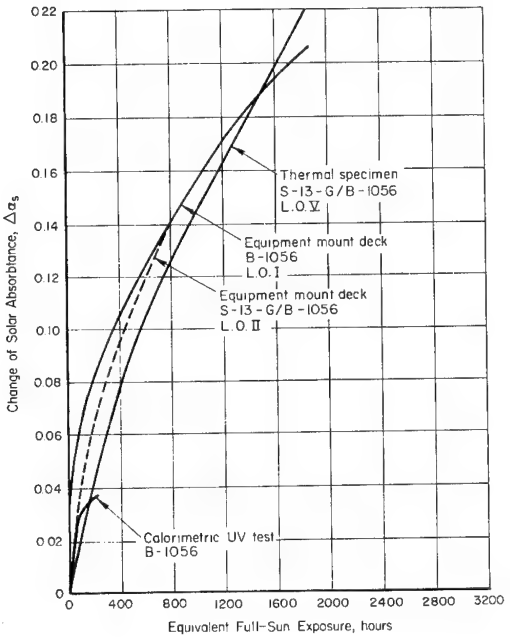

FIGURE B-25. DEGRADATION OF COATINGS ON LUNAR ORBITERS I, II, AND V[26]

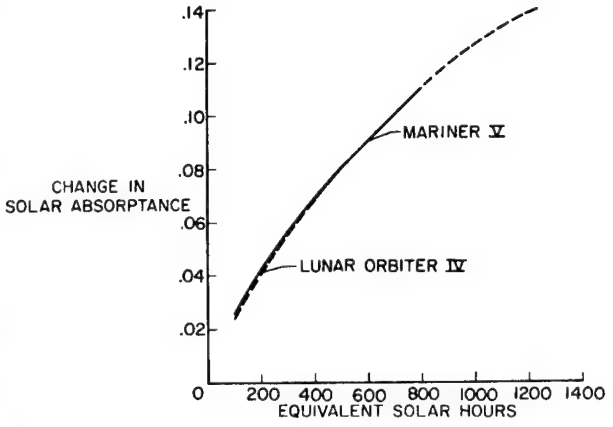

FIGURE B-26. COMPARISON OF THE CHANGE IN SOLAR ABSORPTANCE OF S-13G COATINGS IN TWO FLIGHT EXPERIMENTS[14]

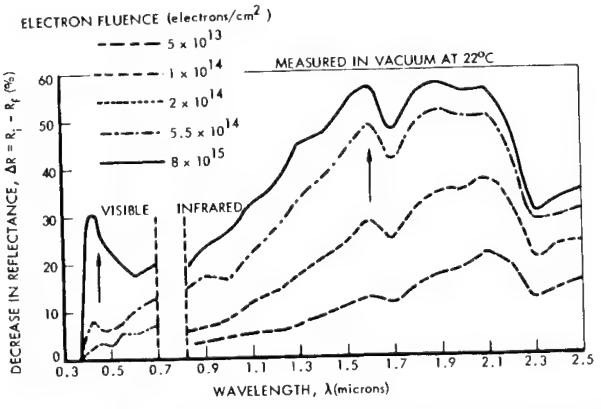

FIGURE B-27. IN SITU REFLECTANCE LOSS IN TREATED ZINC OXIDE-METHYL SILICONE FOLLOWING EXPOSURE TO 50 KEV ELECTRONS[25]

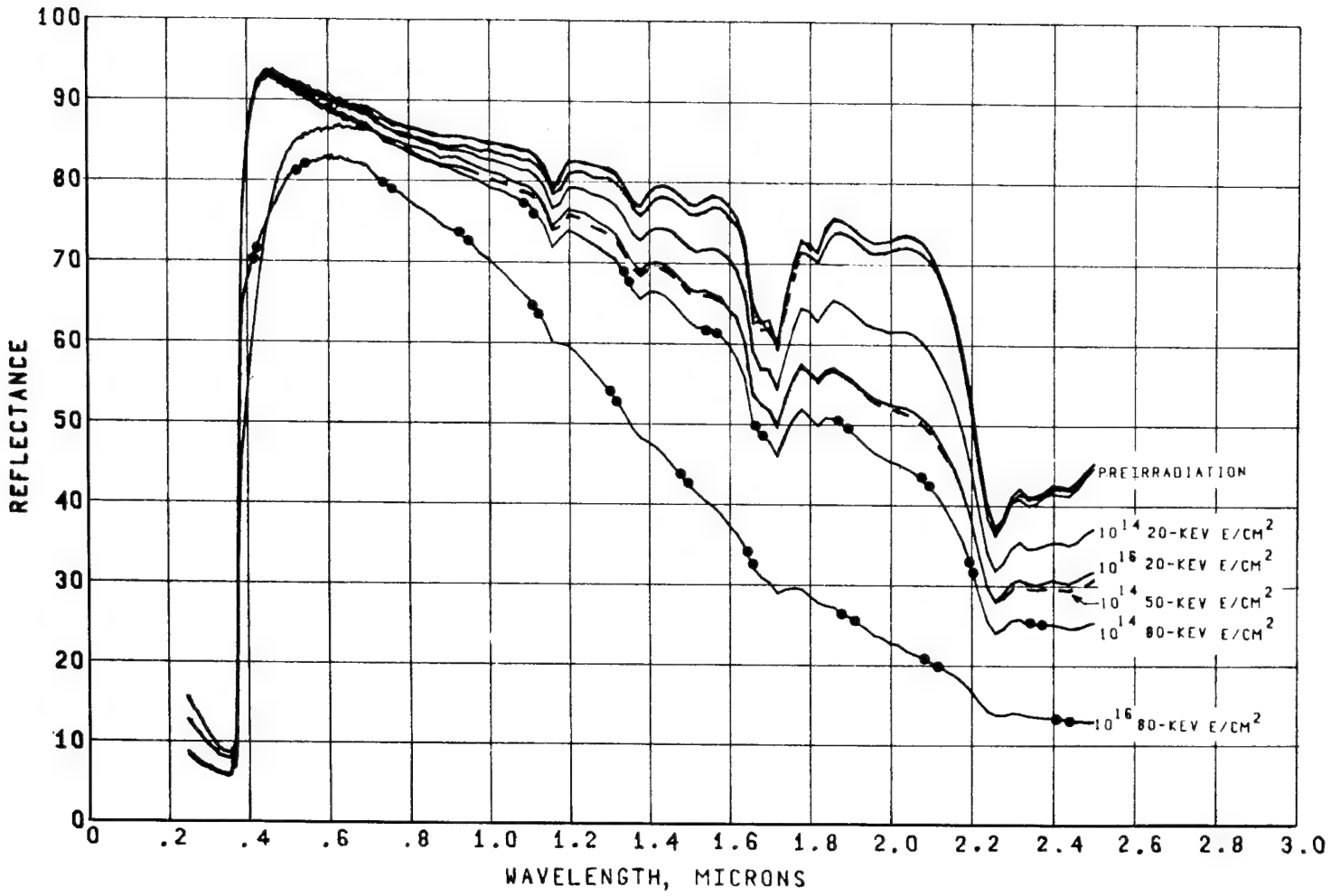

FIGURE B-28. DEPENDENCE OF REFLECTANCE DEGRADATION IN S-13 UPON ELECTRON ENERGY[27]

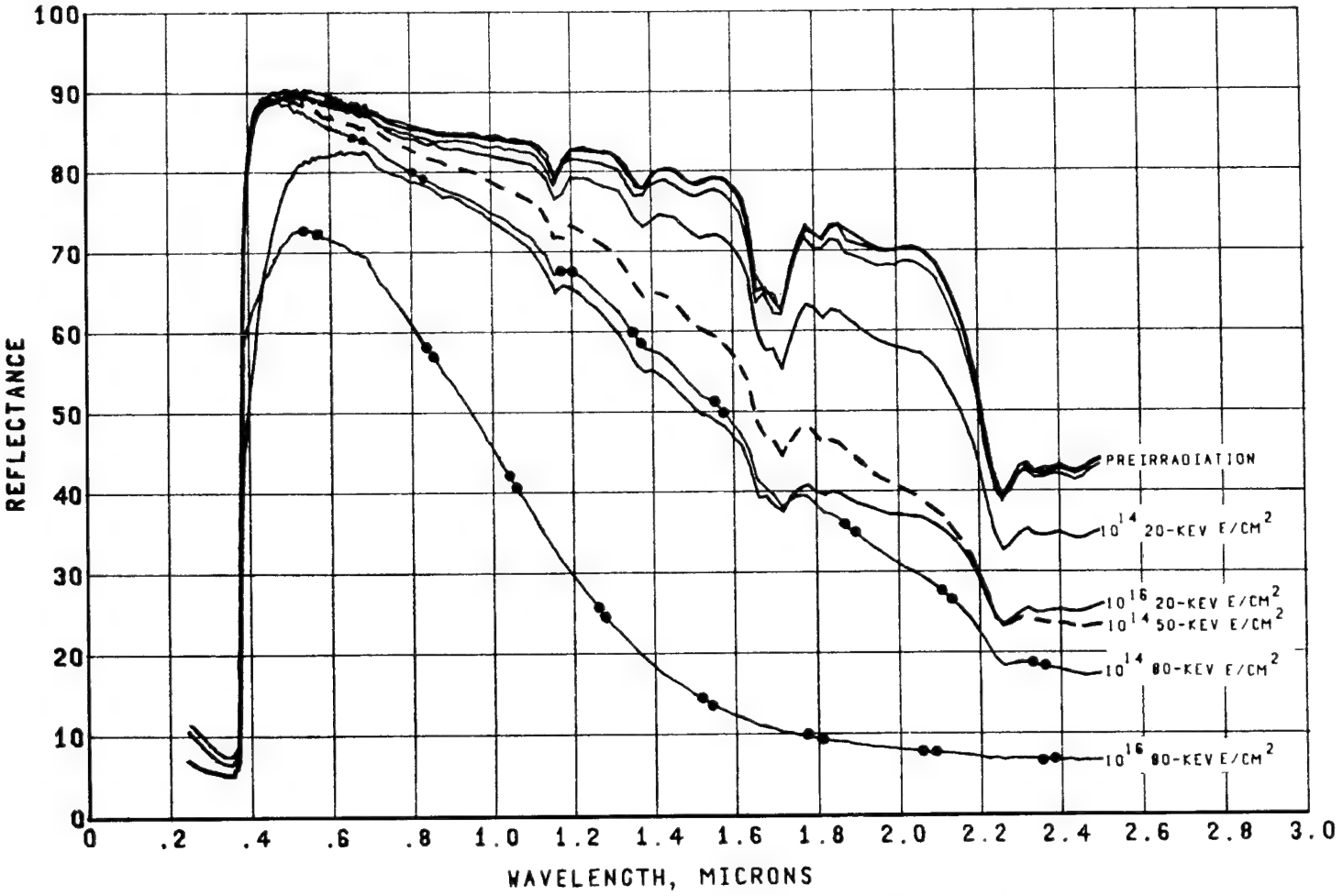

FIGURE B-29. DEPENDENCE OF REFLECTANCE DEGRADATION IN S-13G UPON ELECTRON ENERGY[27]

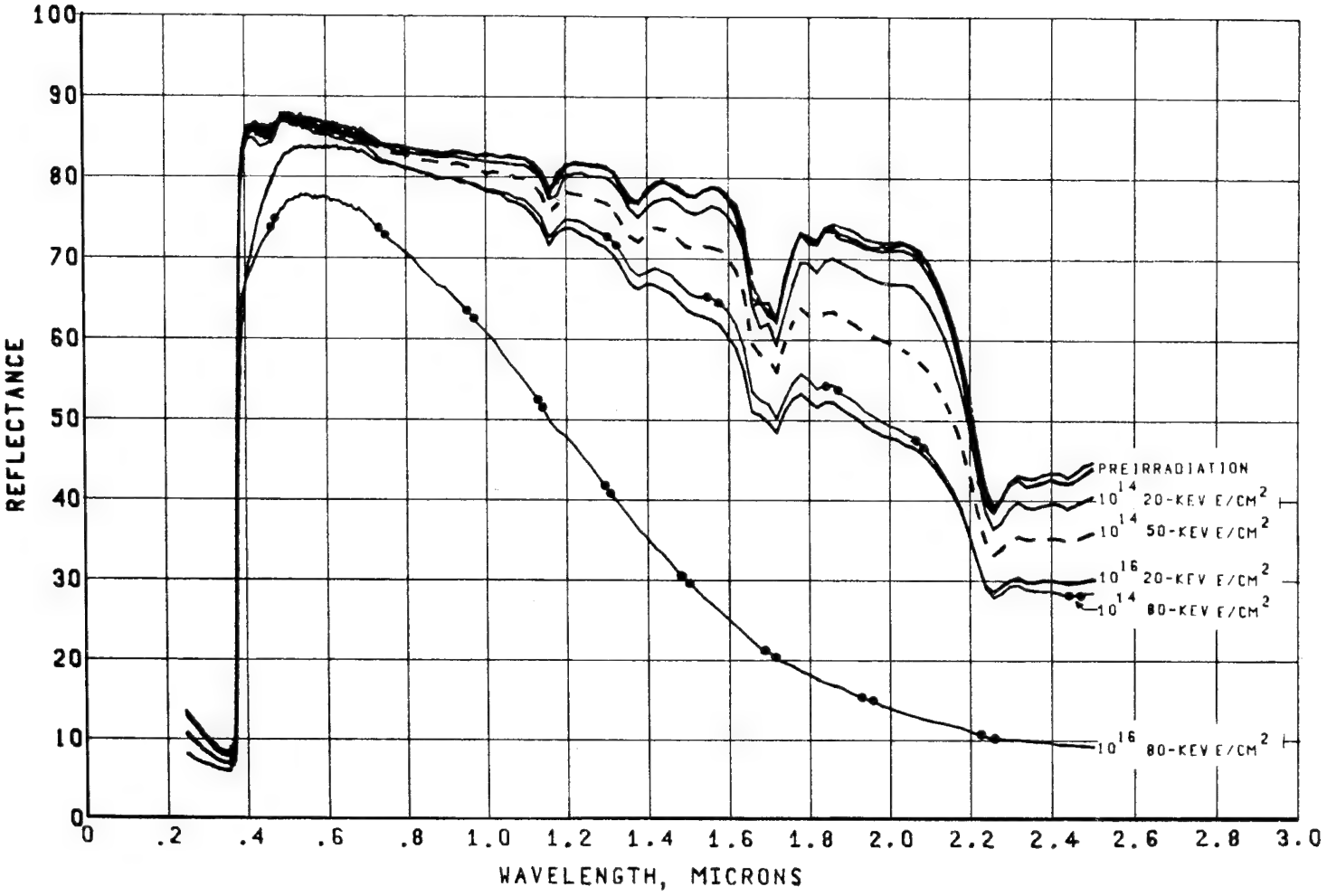

FIGURE B-30. DEPENDENCE OF REFLECTANCE DEGRADATION IN TREATED ZINC OXIDE-METHYL SILICONE (GODDARD SERIES 101-7-1) UPON ELECTRON ENERGY[27]

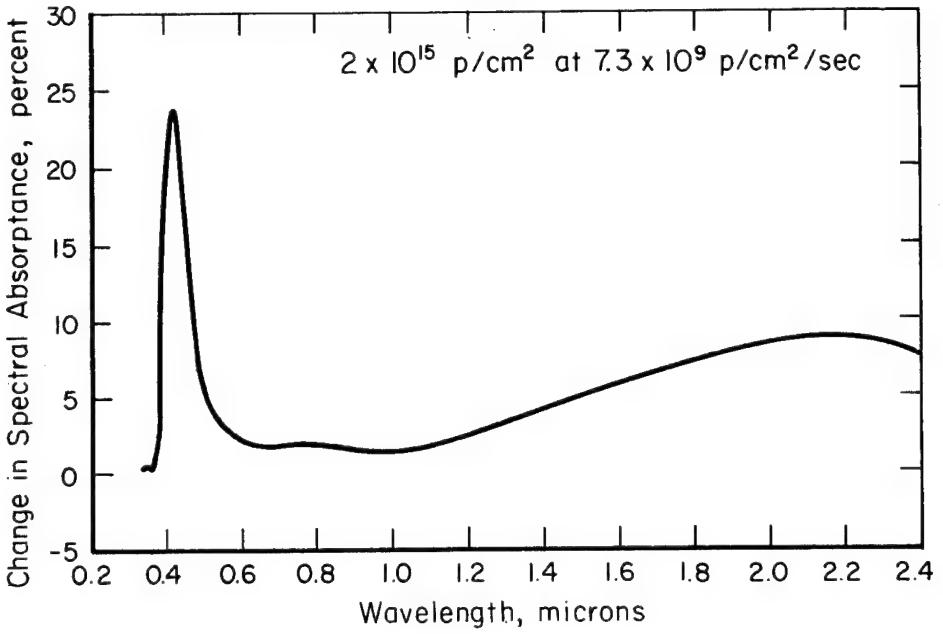

FIGURE B-31. EFFECT OF PROTON RADIATION ONLY (S-13G)[22]

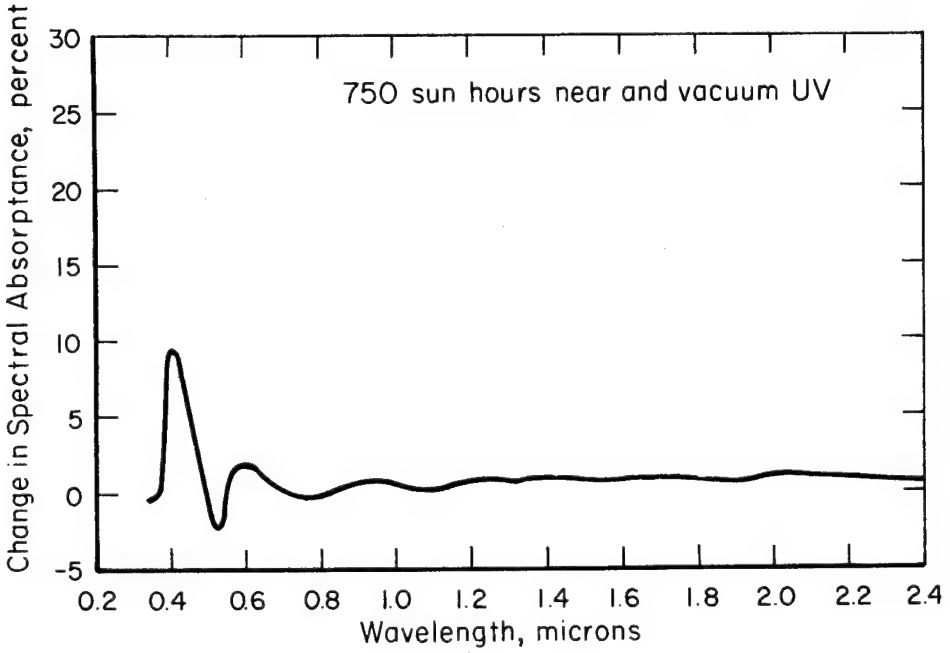

FIGURE B-32. EFFECT OF UV RADIATION ONLY (S-13G)[22]

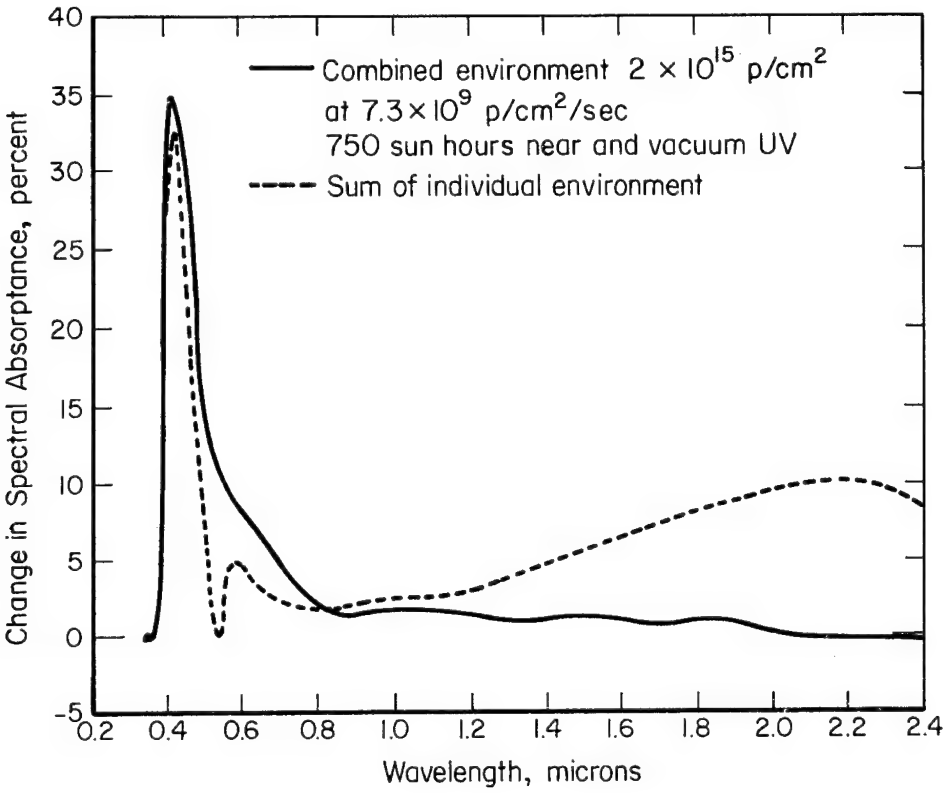

FIGURE B-33. COMBINED EFFECT VERSUS SUM OF INDIVIDUAL EFFECTS (S-13G)[22]

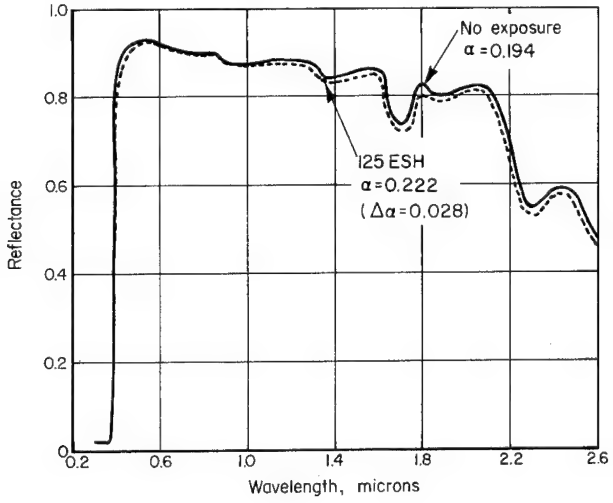

FIGURE B-34. B-1060 (10.1 MILS), DEGRADATION FROM ULTRAVIOLET, MEASURED IN SITU[26]

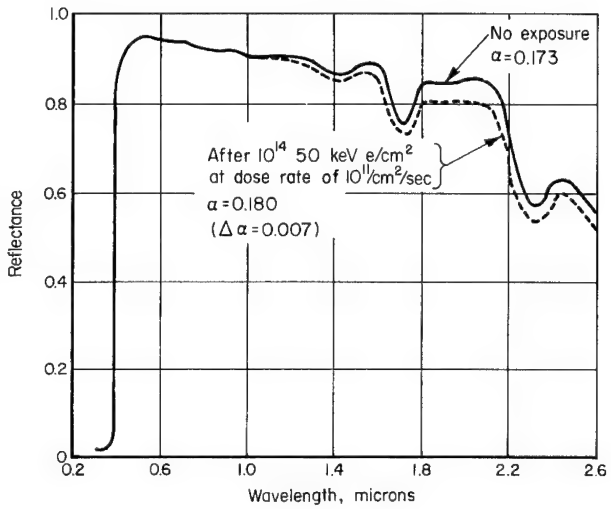

FIGURE B-35. B-1060 (9.4 MILS), DEGRADATION FROM 50-keV ELECTRONS, IN SITU MEASUREMENTS[26]

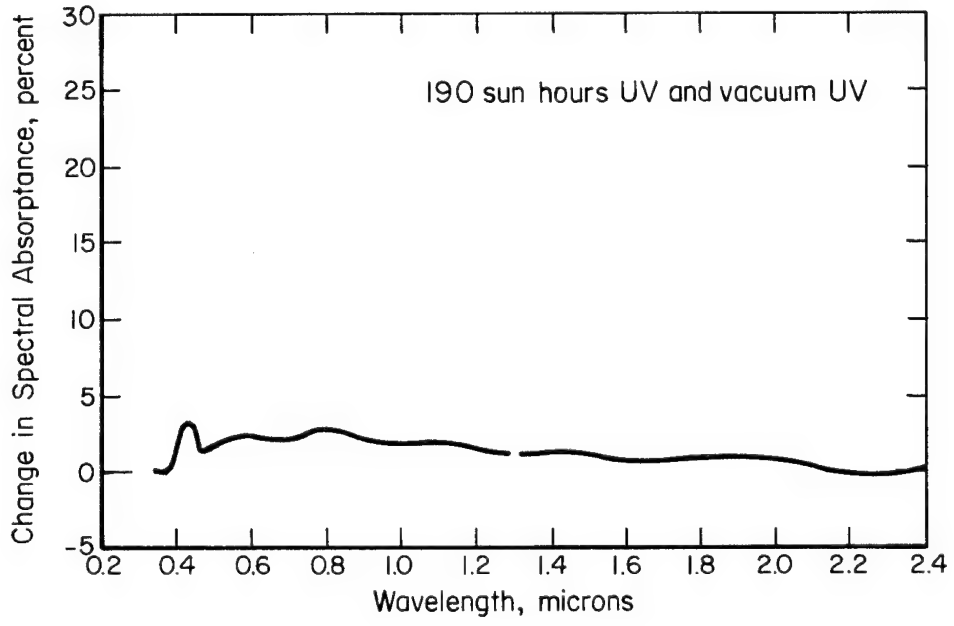

FIGURE B-36. EFFECT OF UV RADIATION ONLY (TiO_2 SILICONE)[22]

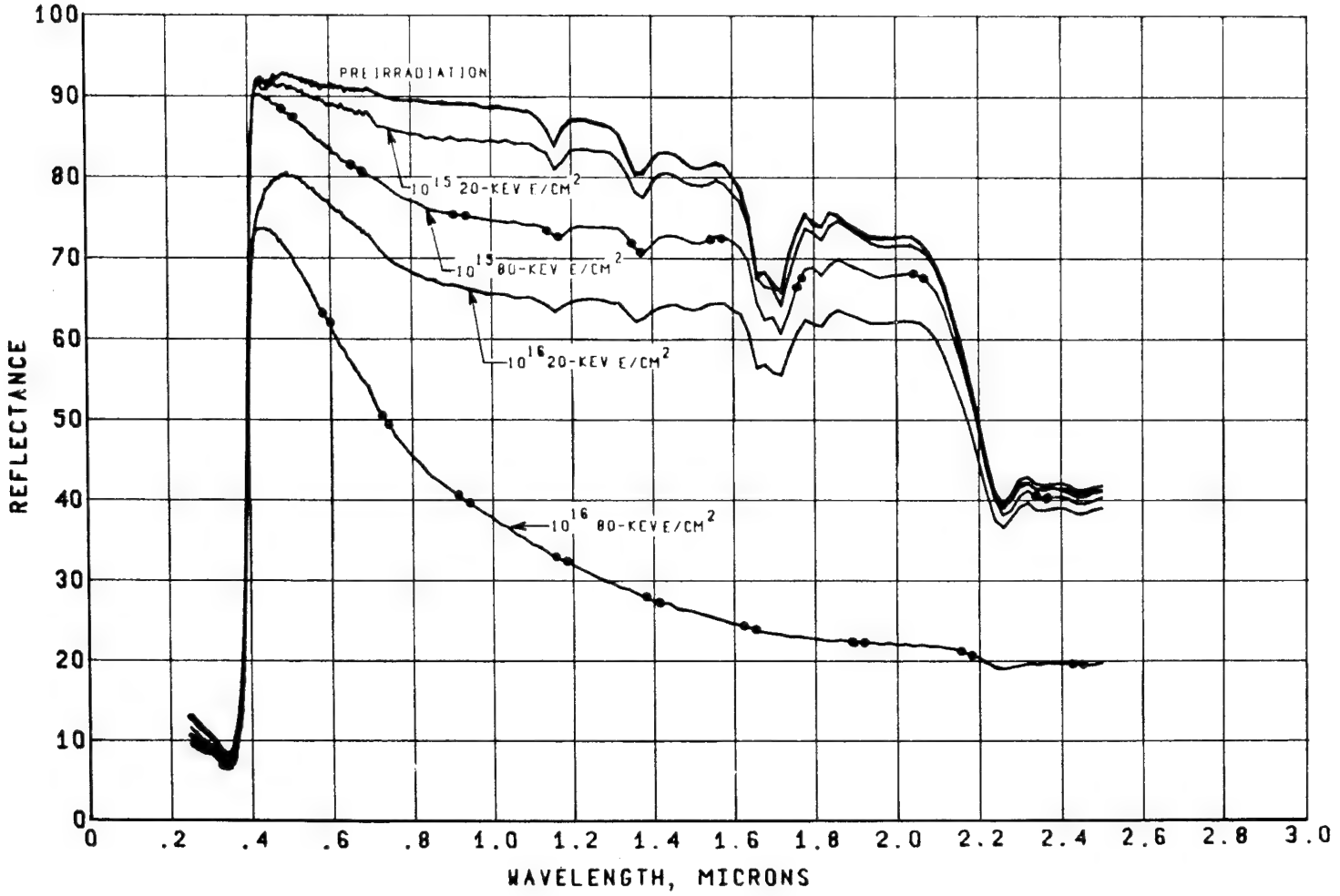

FIGURE B-37. DEPENDENCE OF REFLECTANCE DEGRADATION IN RUTILE TiO_2-METHYL SILICONE UPON ELECTRON ENERGY[27]

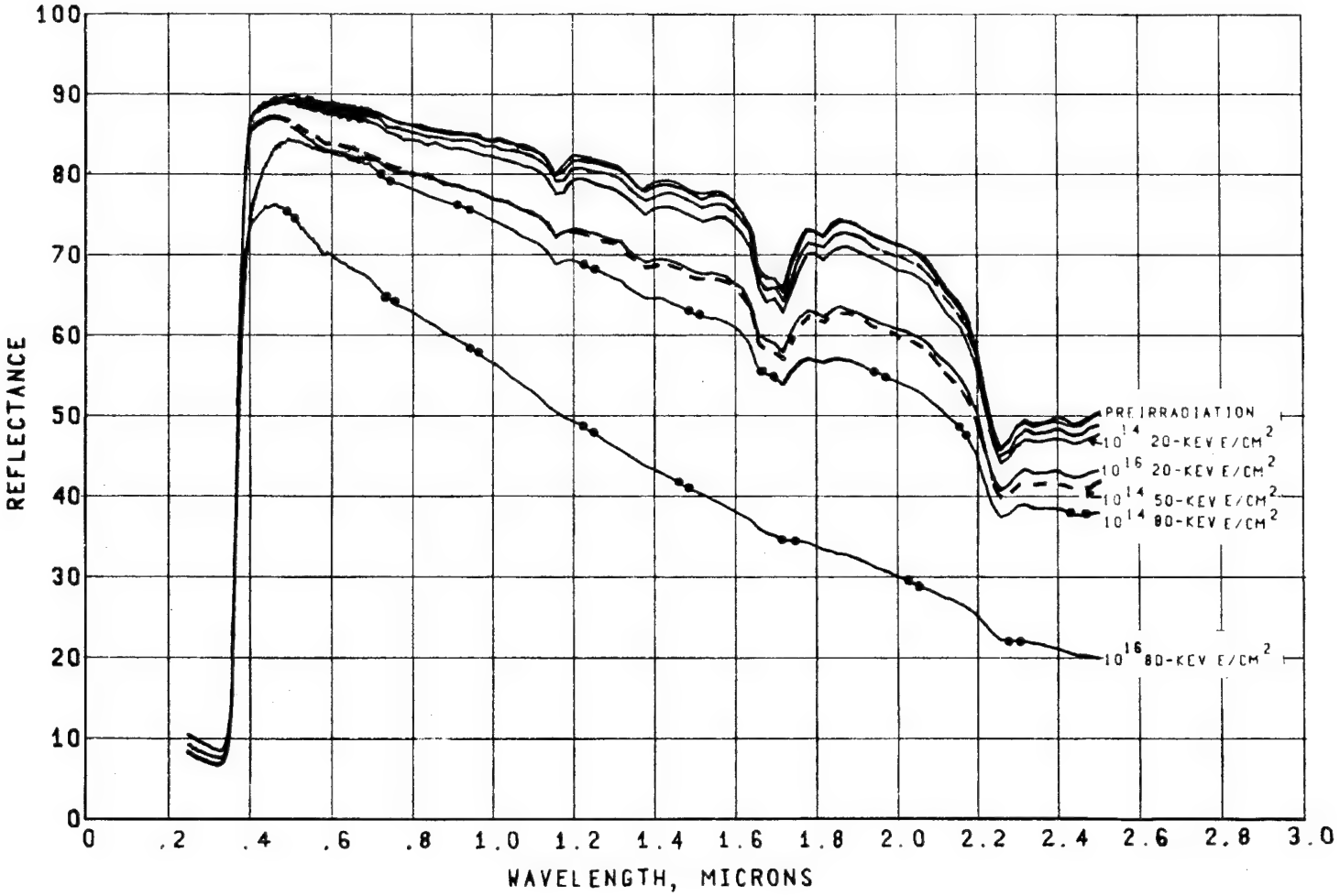

FIGURE B-38. DEPENDENCE OF REFLECTANCE DEGRADATION IN ANATASE TiO_2-METHYL SILICONE UPON ELECTRON ENERGY[27]

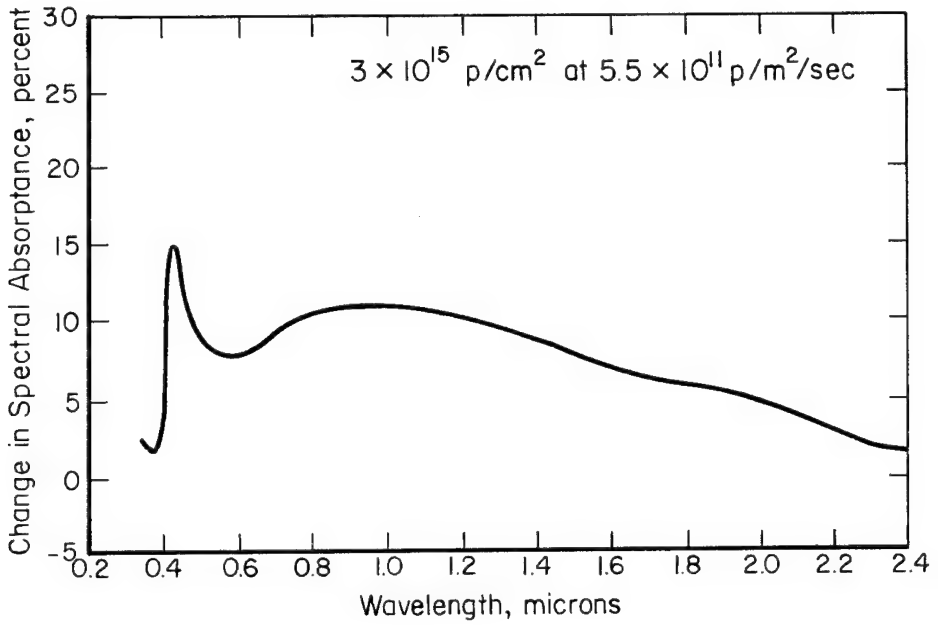

FIGURE B-39. EFFECT OF PROTON RADIATION ONLY (TiO_2 SILICONE)[22]

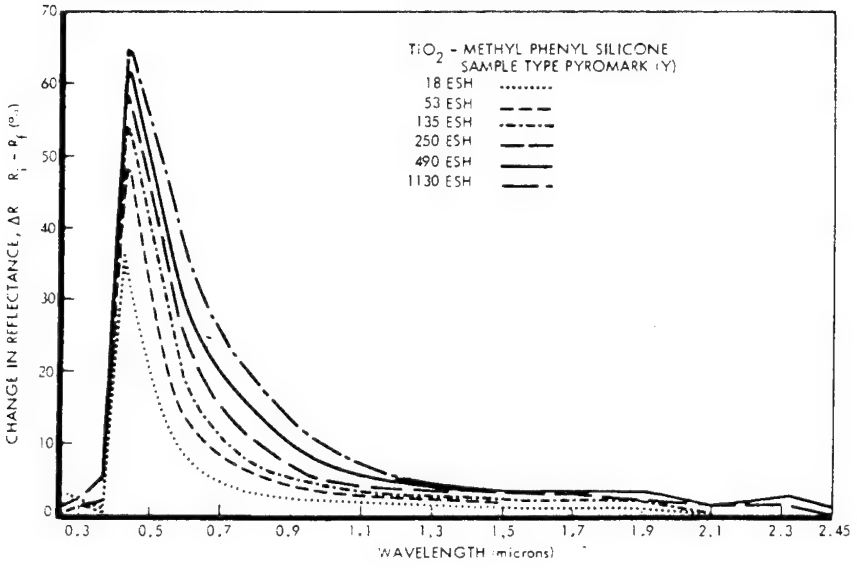

FIGURE B-40. REFLECTANCE CHANGES FOR SAMPLE TYPE PYROMARK[25]

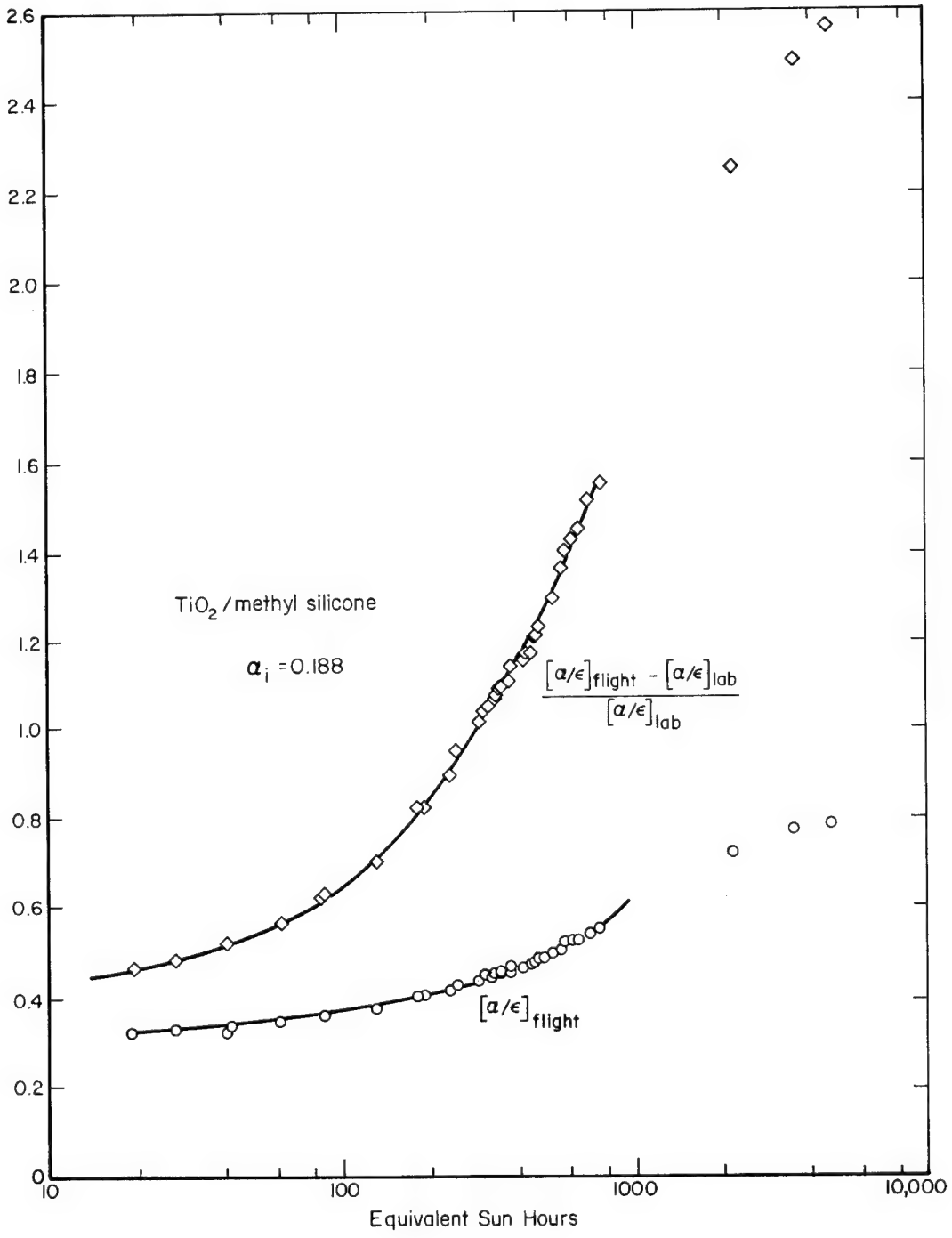

FIGURE B-41. ATS-1 FLIGHT DATA FOR TiO_2/METHYL SILICONE COATING[20]

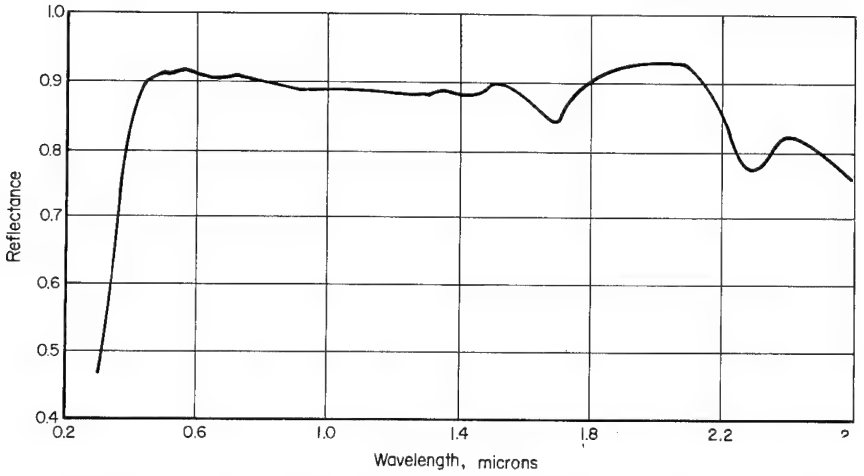

FIGURE B-42. INITIAL REFLECTANCE H-10 HUGHES ORGANIC COATING USED ON LUNAR ORBITER V[26]

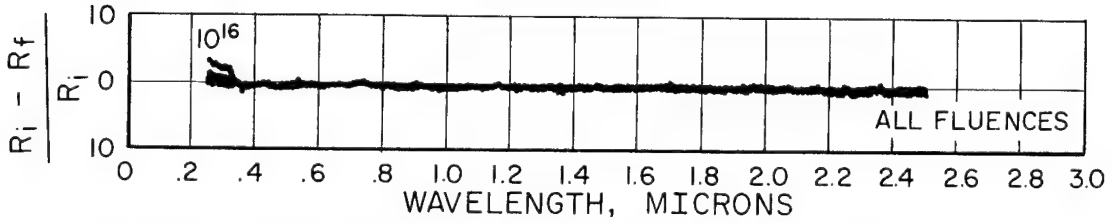

FIGURE B-43. REFLECTANCE CHANGES IN LEAFING ALUMINUM-SILICONE DUE TO 20-keV ELECTRON EXPOSURE[27]

R_i = initial reflectance
R_f = reflectance after irradiation

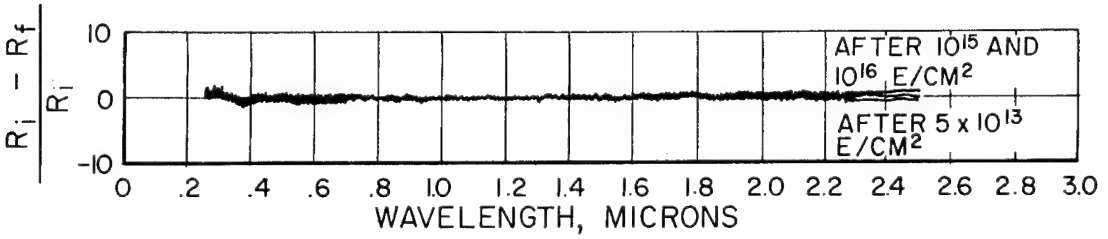

FIGURE B-44. REFLECTANCE CHANGES IN LEAFING ALUMINUM-SILICONE DUE TO 80-keV ELECTRON EXPOSURE[27]

R_i = initial reflectance
R_f = reflectance after irradiation

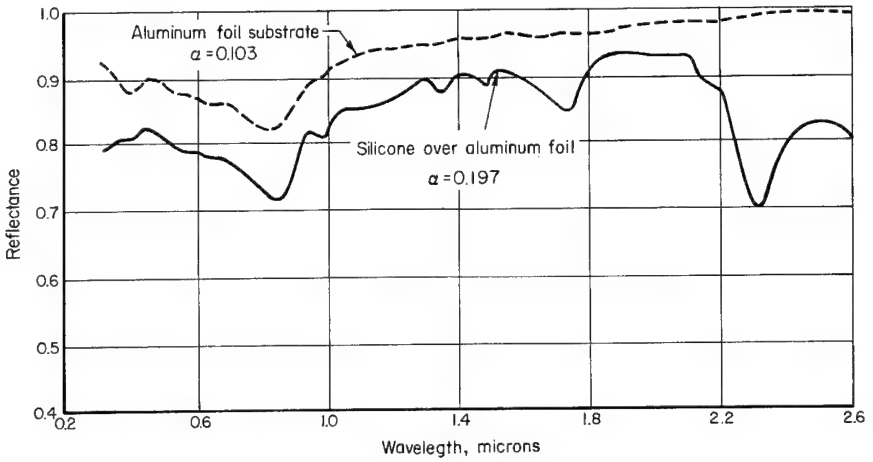

FIGURE B-45. INITIAL REFLECTANCE RTV-602 SILICONE (3.8 MILS) OVER ALUMINUM FOIL USED ON LUNAR ORBITER V[26]

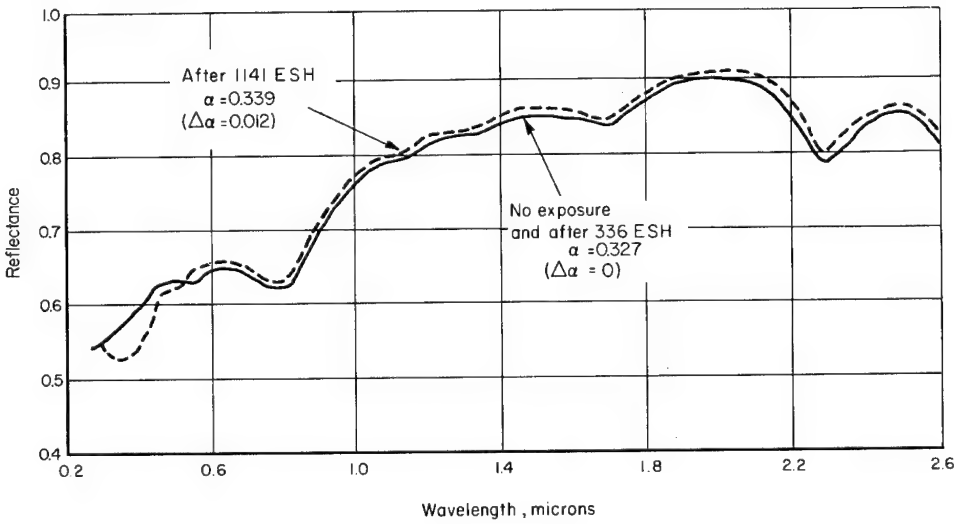

FIGURE B-46. RTV-602 SILICONE (2.6 MILS) OVER CLAD ALUMINUM; DEGRADATION FROM ULTRAVIOLET, MEASURED IN SITU[26]

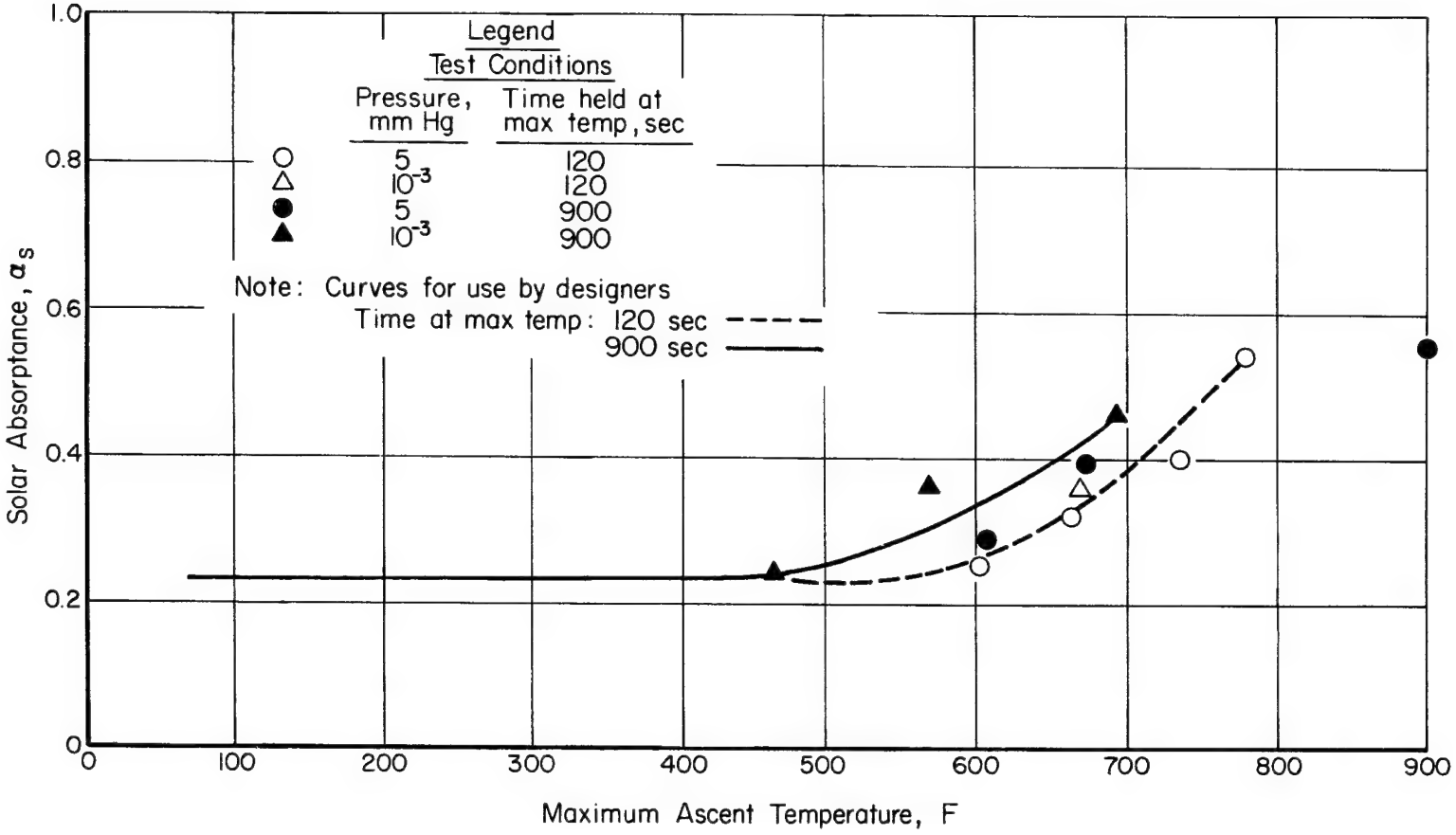

FIGURE B-47. EFFECT OF ASCENT HEATING ON SOLAR ABSORPTANCE OF FULLER (S17-W-1) GLOSS WHITE PAINT ON DOW 17 OR HM21A MAGNESIUM[9]

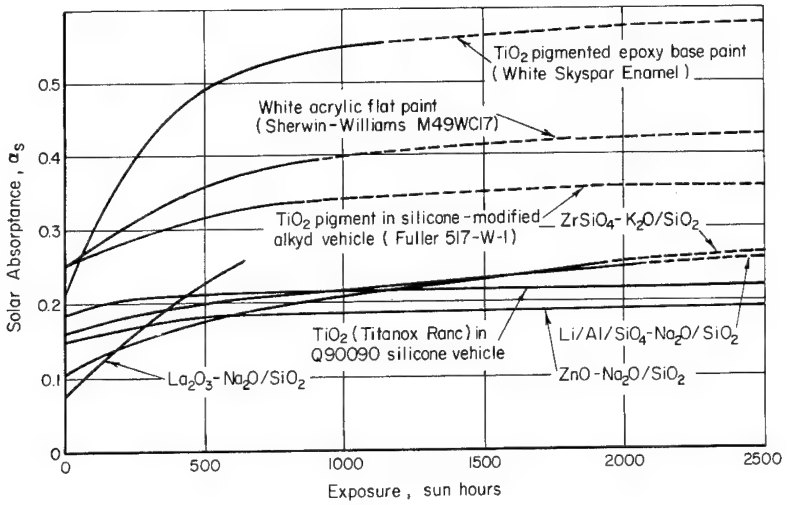

FIGURE B-48. EFFECT OF NEAR-ULTRAVIOLET RADIATION IN VACUUM ON THE SOLAR ABSORPTANCE OF SELECTED SOLAR REFLECTOR COATINGS[31]

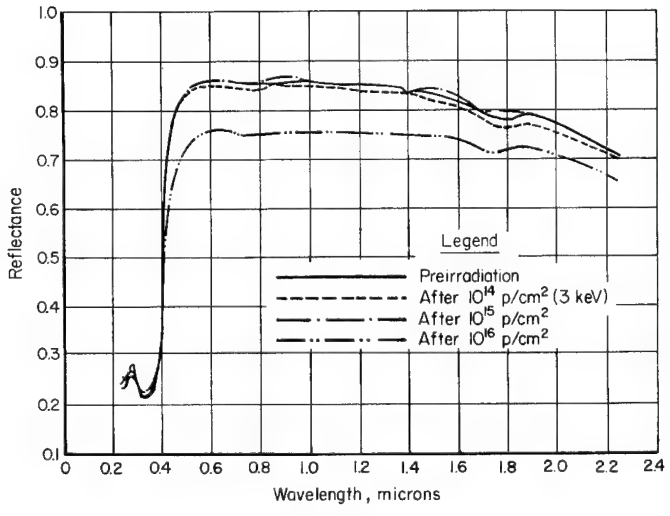

FIGURE B-49. SPECTRAL REFLECTANCE OF PV-100 (9-2) IN VACUO[34]

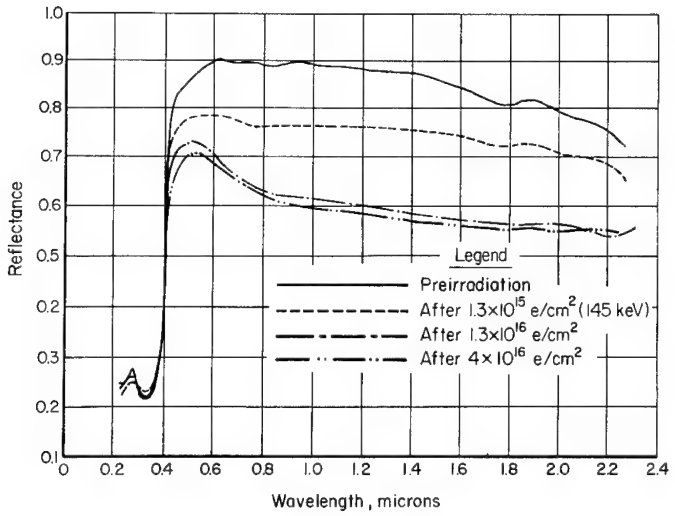

FIGURE B-50. SPECTRAL REFLECTANCE OF PV-100 (8-2) IN VACUO[34]

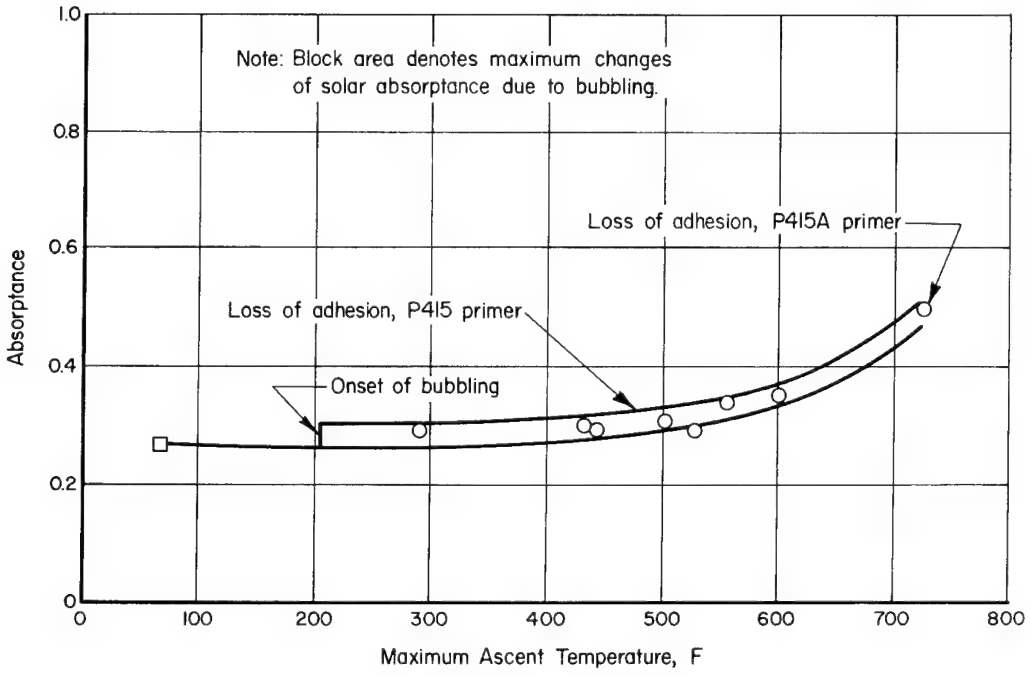

FIGURE B-51. EFFECT OF ASCENT HEATING OR SOLAR ABSORPTANCE OF SHERWIN WILLIAMS WHITE KEMACRYL PAINT[9]

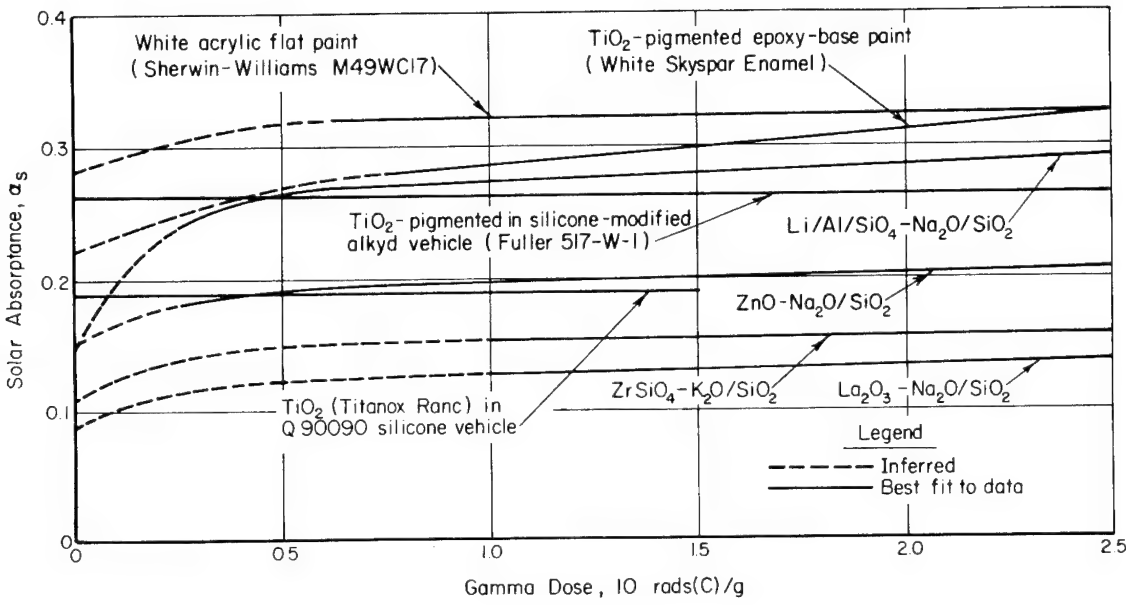

FIGURE B-52. EFFECT OF NUCLEAR RADIATION IN VACUUM ON THE SOLAR ABSORPTANCE OF SELECTED REFLECTOR COATINGS (NEUTRON/GAMMA RATIO IS APPROXIMATELY 10^9)[31]

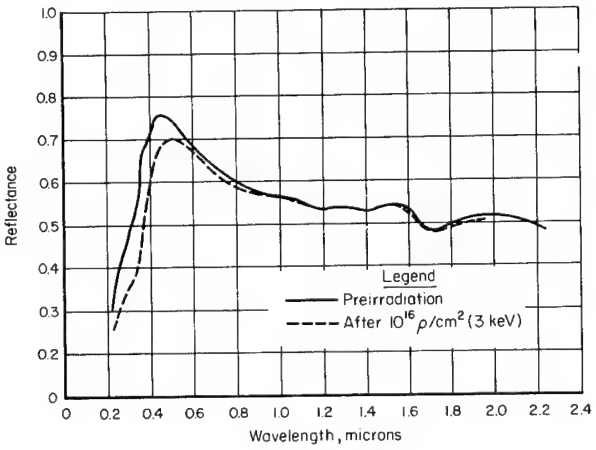

FIGURE B-53. SPECTRAL REFLECTANCE OF MgO/ ACRYLIC (9-4) IN VACUO[34]

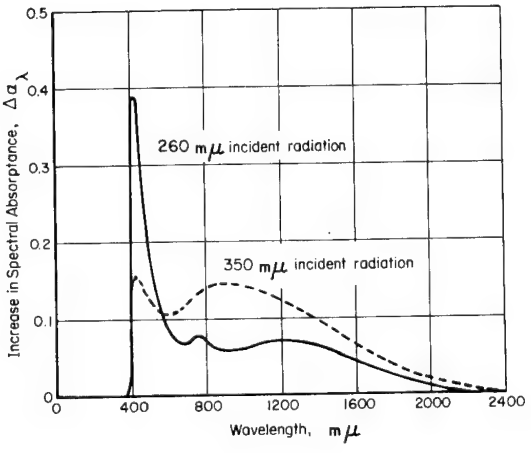

FIGURE B-54. EFFECT OF TWO UV WAVELENGTHS ON THE SPECTRAL ABSORPTANCE OF SKYSPAR COATING[21]

APPENDIX C

TABLES AND FIGURES FOR INORGANIC THERMAL CONTROL COATINGS

TABLE C-1. ENVIRONMENTAL CONDITIONS[40]

Exposure Test Number:	1				2				3				4			
Pigment/Binder;[a]	ZnO/K_2SiO_3				ZnO/K_2SiO_3				Al_2O_3/K_2SiO_3				Al_2O_3/K_2SiO_3			
Specimen Position;[b]	A	B	C	D	A	B	C	D	A	B	C	D	A	B	C	D
Radiation Environment	-	UV	H^+ e^-	H^+ e^- UV	-	UV	H^+ e^-	H^+ e^- UV	-	UV	H^+ e^-	H^+ e^- UV	-	UV	H^+ e^-	H^+ e^- UV
Flux Density ($\times 10^{10}$ particles/cm^2. s)		2.4		1.2		2.4		1.2		2.3		1.1		4.0		0.9
Fluence ($\times 10^{15}$ particles/cm^2)		4.0		2.0		4.0		2.0		6.1		2.9		11.0		2.2
Energy																
Approximate Neutralization, percent		55		100		55		100		30		100		30		100
Proton Specie	H^+															
Irradiation Level																
Total Sun Irradiance/Hour	6															
UN Sun Irradiance/Hour	4															
Irradiance																
Total Sun Hour Equivalents	450															
Total Ultraviolet Sun Hour Equivalent	300															
Vacuum During Measurement	1×10^{-8} Torr															
Vacuum During Exposure	8×10^{-5} Torr															
Specimen Temperature Based on Substrate Measurement and Substrate Control	294 K ± 5 except for Test Number 1, position B and D, where higher temperatures are suspected based on specimen appearance after completion of the test.															

(a) ZnO New Jersey Zinc Co., SP-500, 99.9% pure; 0.25-0.35 μ particle. Pigment/Binder Ratio = 5.2. Pigment ball milled with K_2SiO_3 for 4 hrs, sprayed 6 coats, overnight dry at 20 C, oven cured 1 hr at 150 C, 6-mil coating.

$Al_2O_3(\alpha)$ Linde Division, Union Carbide Co., 99.98% pure, 1.0 μ particle. Pigment/Binder Ratio = 2.0. Pigment ball milled with K_2SiO_3 for 2 hrs, oven cured 1 hr at 150 C, 5-mil coating.

K_2SiO_3 Sylvania Electronic Products (35% solids) PS-7.

(b) Position A No radiation exposure.

Position B Electromagnetic radiation exposure.

Position C Particulate radiation exposure (protons alone or protons plus electrons).

Position D Combined electromagnetic and particulate radiation exposure (with protons alone or protons plus electrons).

TABLE C-2. SUMMARY OF APOLLO 9 THERMAL PROPERTY MEASUREMENTS[32]

Material	Sample Location	Absorptance			Emittance	
		Preflight	Postflight	Change, percent	Preflight	Postflight
Zinc oxide-potassium silicate	Service module					
	Upper left	0.20	0.28	40	0.93	0.93
	Upper right	0.20	0.25	25	0.93	0.93
	Lower right	0.20	0.27	37	0.93	0.93
Titanium dioxide-silicone	Service module					
	Upper left	0.25	0.37	48	0.86	0.88
	Upper right	0.24	0.34	42	0.86	0.88
	Lower right	0.24	0.40	67	0.86	0.87
Chromic acid-anodized aluminum	Lunar-module hatch area	0.70	0.73	4	0.73	0.70
Fused silica-filtered	Lunar-module hatch area	(a)	(a)	(a)	(a)	(a)

(a) Approximately 2-percent decrease in transmittance.

TABLE C-3. RESULTS OF Z-93 TESTS; INITIAL $\alpha_s = 0.147$[21]

Wavelength Region, mμ	Energy Absorbed by Sample, joules/m^2	$\Delta\alpha_s$	ϕ_λ[a], (joules/m^2)$^{-1}$
I (250-312)	3.6×10^8	0.021	0.58×10^{-10}
II (302-324)	1.9×10^8	0.003	0.16×10^{-10}
III (330-380)	6.0×10^8	0.003	0.05×10^{-10}

(a) $\phi_\lambda = \frac{\text{increase in solar absorptance}}{\text{energy dose absorbed}} = \Delta\alpha_s/H_t$

H_t = total energy absorbed.

TABLE C-4. OPTICAL PROPERTIES OF BRIGHT ANODIZED ALUMINUM EXPOSED TO VACUUM-ULTRAVIOLET RADIATION (0.5 mil)[5]

Polishing bath:	Phosphoric Acid/Nitric Acid (95/5)			
Exposure, hours[a]:	0	24	96	192
Total Reflectance, ρ	0.84	0.72	0.66	0.65
Solar Absorption, α_s	0.16	0.28	0.34	0.35
Emittance, ϵ_{Th} 65 C	0.83	0.83	0.83	0.83
α/ϵ Ratio	0.19	0.34	0.41	0.42

(a) To obtain ESH, multiply by 6.

TABLE C-5. EFFECTS OF NUCLEAR RADIATION ON THE OPTICAL PROPERTIES OF BRIGHT ANODIZED ALUMINUM[5]

Thickness, mil	$(\alpha_s)i$	$(\alpha_s)f$	$(\epsilon)i$	$(\epsilon)f$	Thermal Neutron Flux, 10^{14} nvt	Nuclear Rads (C), 10^8
0.15	0.088	0.101	0.70	0.70	2.35	2.93
0.4	0.091	0.123	0.75	0.75	2.35	2.93
0.5	0.126	0.140	0.77	0.78	2.35	2.93
0.6	--	0.129	0.80	0.80	2.59	2.74

TABLE C-6. EFFECTS OF ELECTRON AND UV RADIATIONS ON ANODIZED-ALUMINUM COATINGS AT 77 K[4]

Sample Type	Initial α_s	α_s after 350 ESH	α_s after 5.8×10^{15} e/cm^2	α_s after UV and Electron Radiation
Sulfuric acid anodized aluminum (1199 aluminum)	0.20	0.28	0.20	0.27
Barrier anodized aluminum (1199 Al)	0.17	0.19	0.16	0.20
Aluminum oxide/ potassium silicate	0.11	0.16	0.19	0.24

TABLE C-7. EMITTANCE OF TEFLON OVER VAPOR DEPOSITED ALUMINUM[36]

Thickness, mils	Total Normal Emittance
0.25	0.26
0.50	0.43
1.00	0.53
2.00	0.67
5.00	0.83
10.00	0.89

TABLE C-8. ULTRAVIOLET EXPOSURE OF SERIES EMITTANCE COATINGS[36]

Sample Description	Dosage		Solar Absorptance	
	UV, ESH[a]	X-Ray, MRAD[b]	Before	After
PJ113 on aluminum	3,800	--	0.15	0.15
PJ113 on aluminum	170	10	0.16	0.17
PJ113 on aluminum	1,720	100	0.16	0.18
Polyvinyl butyral (Butvar)	100	10	0.19	0.20
Polyvinyl butyral (Butvar)	1,000	100	0.18	0.20
5-mil Teflon on aluminum	1,150	115	0.21	0.21

(a) ESH refers to equivalent sun hours measured below 3000A.
(b) MRAD = 10^6 rads.

TABLE C-9. CHANGES IN SOLAR ABSORPTANCE ($\Delta\alpha_s$) OF ALUMINIZED AND SILVERED TEFLON WITH PROTON BOMBARDMENT[49]

Coating	Pre-irrad.	Solar Absorptance, α_s After Irradiation Dose, p/cm^2							$\Delta\alpha_s$
		3×10^{12}	5×10^{13}	3×10^{14}	8×10^{14}	3×10^{15}	1×10^{16}	N(a) $\times 10^{16}$	
2-mil aluminized Teflon (TA-2)	0.12	0.12	0.12	0.12	0.12	0.13	0.16	0.18 (1.8)	0.06
5-mil aluminized Teflon (TA-5)	0.13	0.13	0.13	0.13	0.14	0.15	0.18	0.19 (1.7)	0.06
10-mil aluminized Teflon (TA-10)	0.16	0.16	0.16	0.16	0.16	0.17	0.20	0.21 (1.4)	0.05
2-mil silvered Teflon (TS-2)	0.06	0.06	0.06	0.06	0.06	0.07	0.09	0.10 (1.7)	0.04
5-mil silvered Teflon (TS-5)	0.07	0.07	0.07	0.07	0.07	0.08	0.10	0.11 (1.6)	0.04
10-mil silvered Teflon (TS-10)	0.09	0.09	0.09	0.09	0.09	0.10	0.12	0.12 (1.2)	0.03

(a) Irradiation dose given in N $\times 10^{16}$ p/cm^2; N indicated in parentheses.

TABLE C-10. ENVIRONMENTAL STABILITY OF THE OPTICAL SOLAR REFLECTOR MATERIAL(2)

Environment of Interest	Test Conditions: Type of Radiation	Radiation Energy	Integrated Flux	Pressure, torr	Sample Temperature, K	Change in Solar Absorptance
Artificial Electron Belt	Electron	800 keV	10^{16} e/cm^2	$\leq 10^{-6}$	290	0
	Electron	800 keV	10^{15} e/cm^2	$\leq 10^{-6}$	155	0
	Electron plus simultaneous ultraviolet (UV)	800 keV electrons + 3.1 to 6.2 eV ultraviolet	6×10^{14} e/cm^2 plus 436 ESH UV	$\leq 10^{-6}$	300	0
	e + UV	Ditto	.	$\leq 10^{-7}$	77	0
	e + UV	"	3×10^{15} e/cm^2 plus 150 ESH	$\leq 10^{-7}$	300	0
Van Allen Proton Belt	Protons	130 keV	2×10^{15} p/cm^2	$\leq 2 \times 10^{-6}$	290	0
		130 keV	$\geq 5 \times 10^{15}$ p/cm^2	$\leq 2 \times 10^{-6}$	290	0
		176 keV	~5×10^{15} p/cm^2	$\leq 3 \times 10^{-7}$	284	0
		466 keV	~5×10^{15} p/cm^2	$\leq 1 \times 10^{-7}$	284	0
		987 keV	~5×10^{15} p/cm^2	$\leq 3 \times 10^{-7}$	284	0
		500 keV	~6×10^{15} p/cm^2	$<10^{-7}$	77	0
		500 keV	6×10^{15} p/cm^2	$<10^{-7}$	280	0
	p + UV	500 keV	6×10^{15} +150 ESH	--	77	0
	p + UV	500 keV	6×10^{15} +150 ESH	--	300	0
Solar Wind	Proton and H_2^+	2 keV	8×10^{15} p/cm^2	$<10^{-7}$	280	0
	Proton plus simultaneous UV	2 keV protons + 3.1 to 6.2 eV UV	5×10^{15} p/cm^2 plus 255 ESH UV	$<10^{-7}$	280	0
	Proton	1.4 keV	10^{16} p/cm^2	$<10^{-7}$	305	0
	Proton plus simultaneous UV	2 keV protons + 3.1 to 6.2 eV photons	$8 + 10^{15}$ p/cm^2 +1100 ESH UV	$<10^{-7}$	320	0
Solar Ultraviolet	UV	3.1 to 6.2 eV	485 ESH	$<10^{-6}$	290	0
	UV	3.1 to 6.2 eV	436 ESH	$<10^{-6}$	300	0
	UV	3.1 to 6.2 eV	175 ESH	$<6 \times 10^{-8}$	300	0
	UV	3.1 to 6.2 eV	2000 ESH	$<10^{-6}$	294	0
	UV	3.1 to 6.2 eV	2000 ESH	$<10^{-6}$	533	0

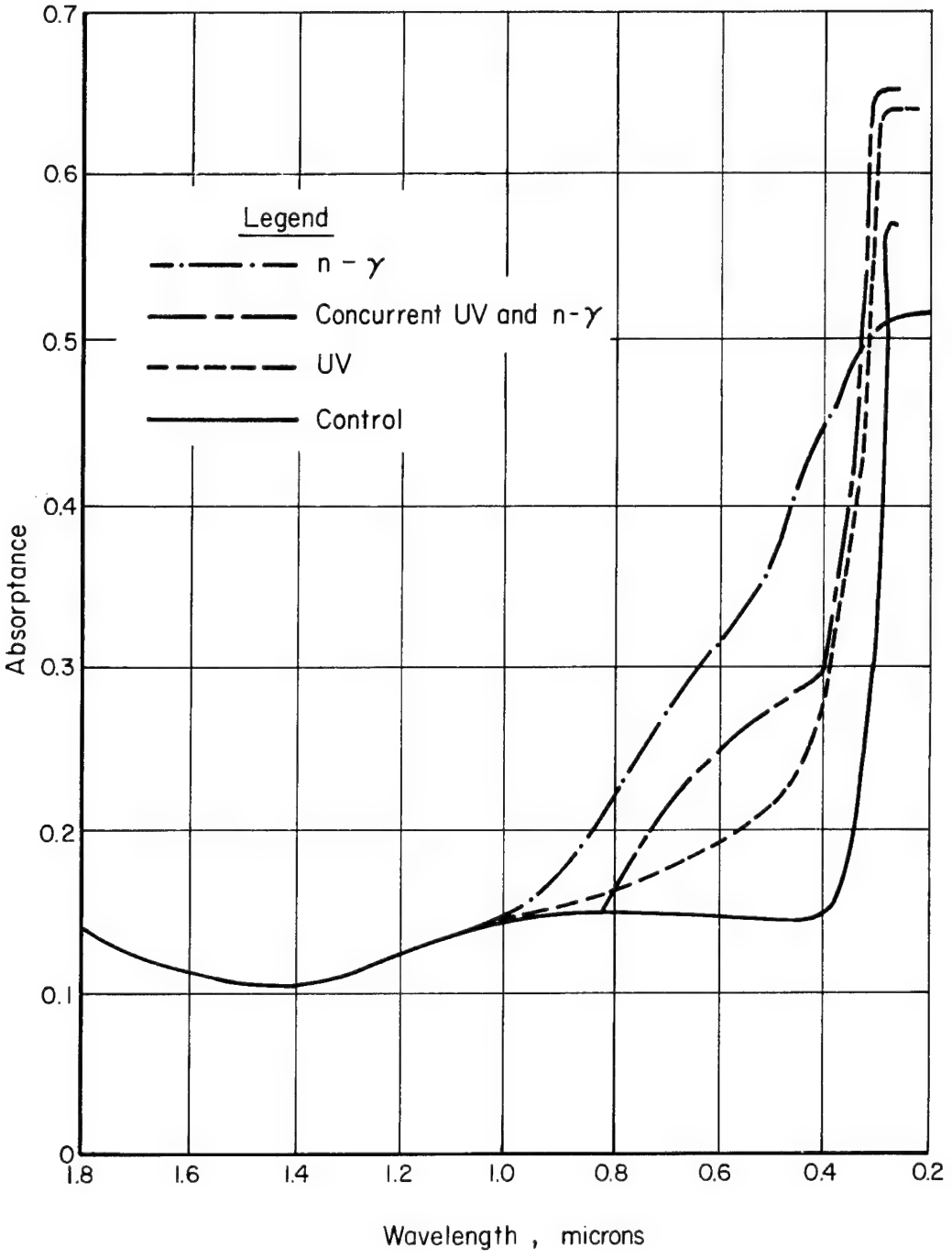

FIGURE C-1. SPECTRAL ABSORPTANCE OF IRRADIATED LITHAFRAX/SODIUM SILICATE PAINT[35]

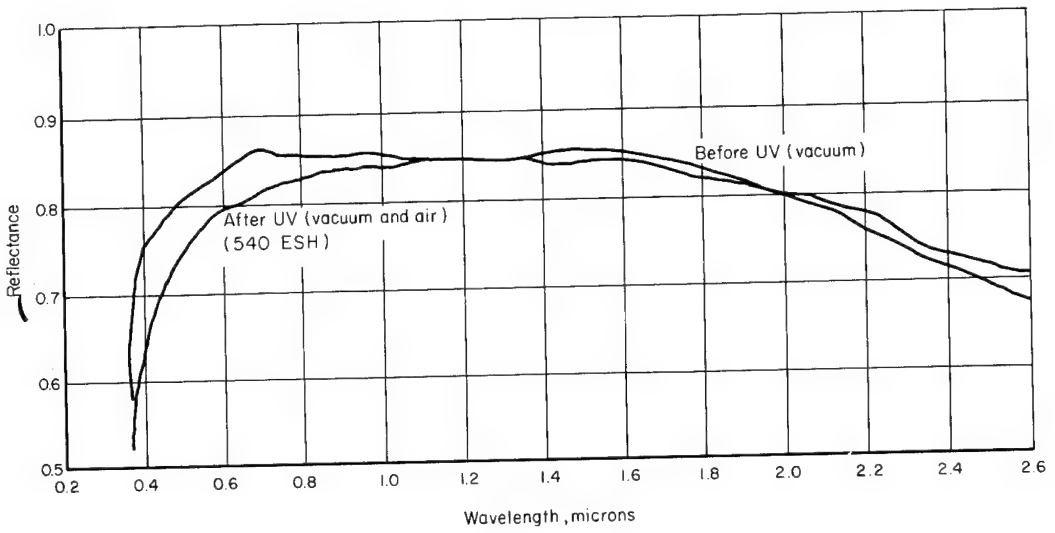

FIGURE C-2. SPECTRAL REFLECTANCE OF HUGHES INORGANIC WHITE COATING[16]

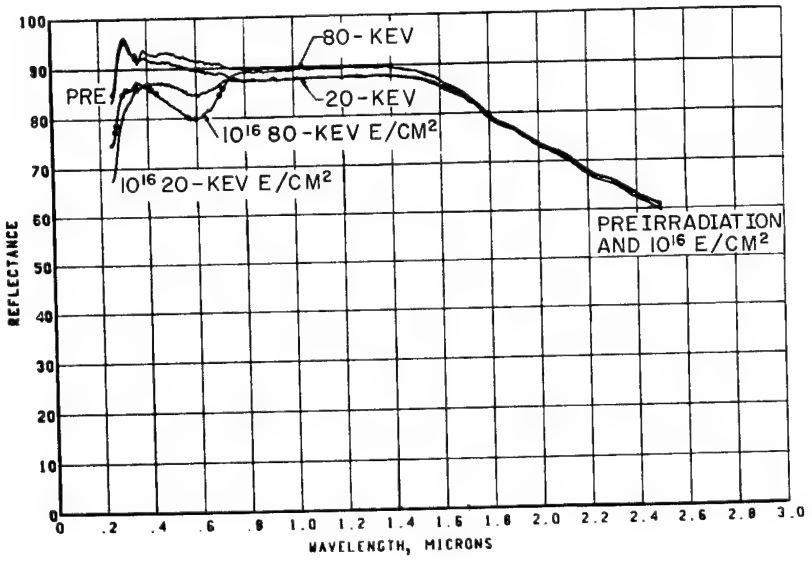

FIGURE C-3. DEPENDENCE OF REFLECTANCE DEGRADATION IN Al_2O_3-K_2SiO_3 UPON ELECTRON ENERGY[27]

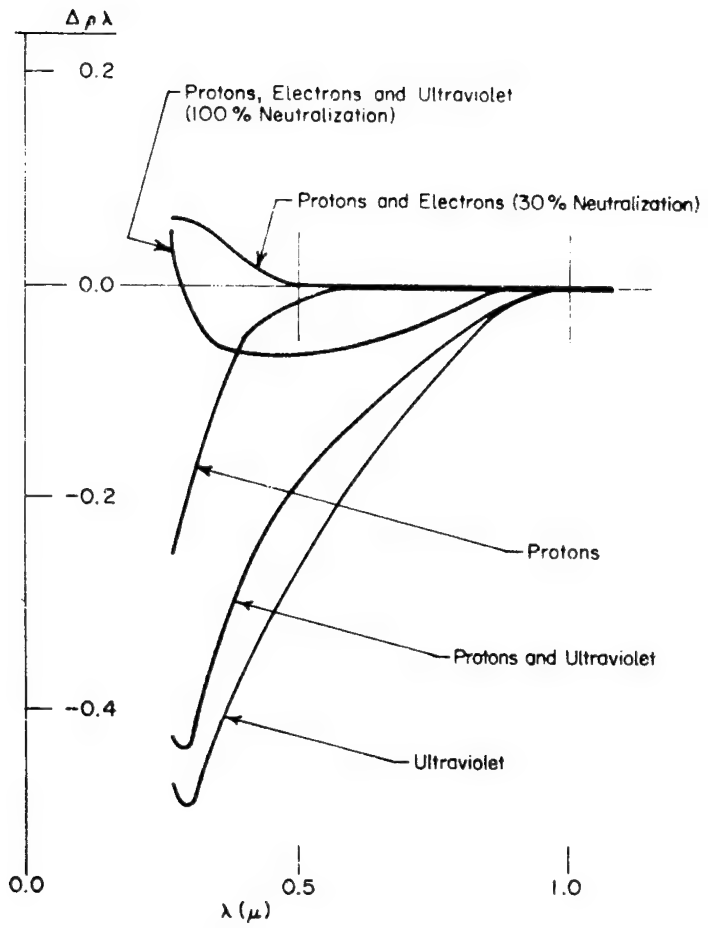

FIGURE C-4. CHANGE IN SPECTRAL REFLECTANCE OF Al_2O_3 IN K_2SiO_3, MEASURED IN SITU[40]

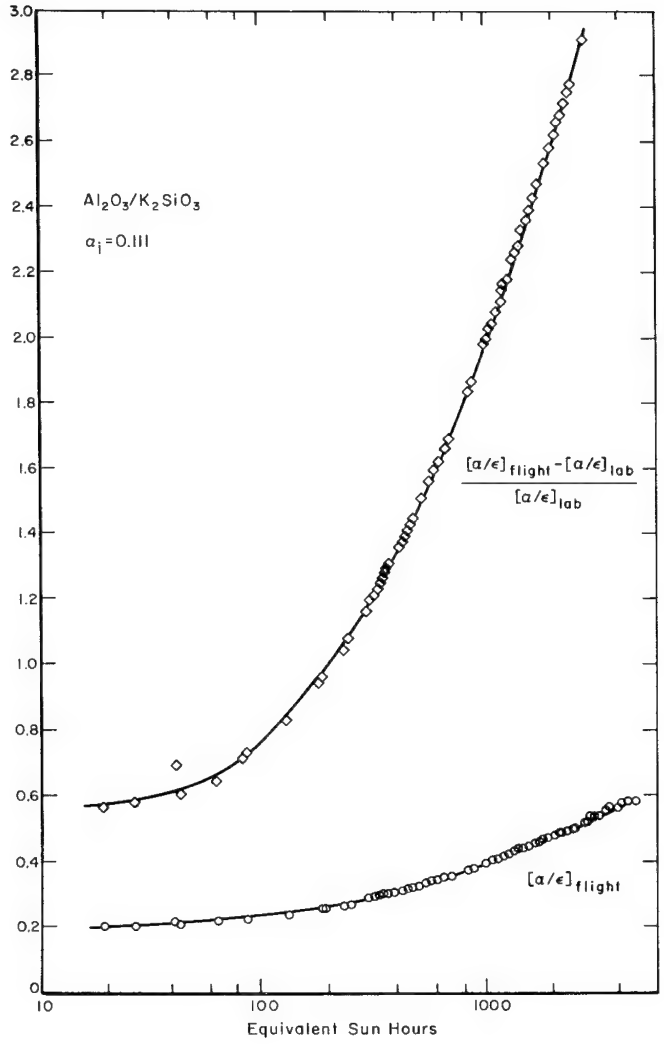

FIGURE C-5. ATS-1 FLIGHT DATA FOR Al_2O_3/K_2SiO_3 COATING[20]

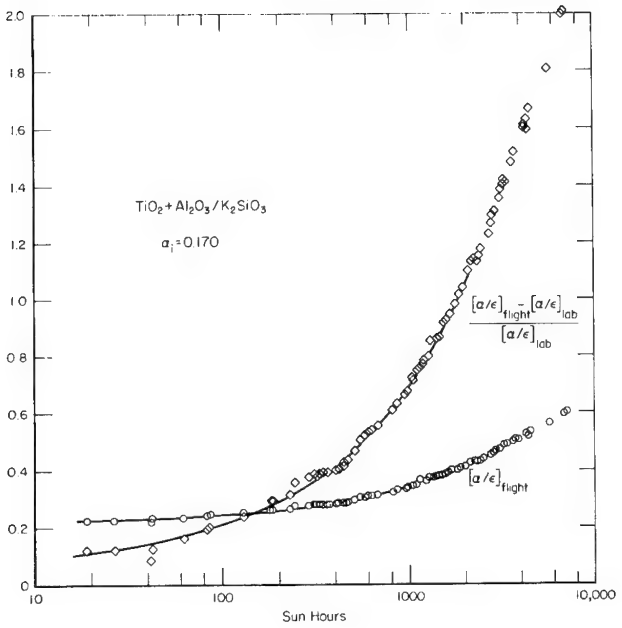

FIGURE C-6. ATS-1 FLIGHT DATA FOR TiO_2/K_2SiO_3 COATING[20]

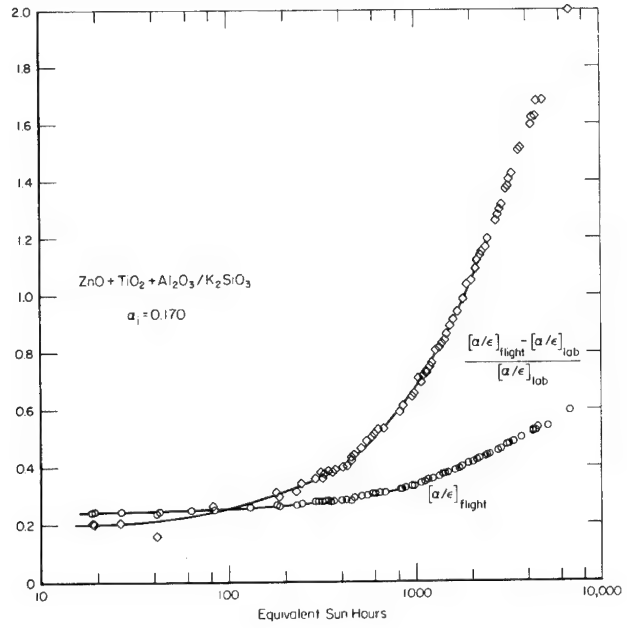

FIGURE C-7. ATS-1 FLIGHT DATA FOR $(ZnO + TiO_2 + Al_2O_3)/K_2SiO_3$ COATING[20]

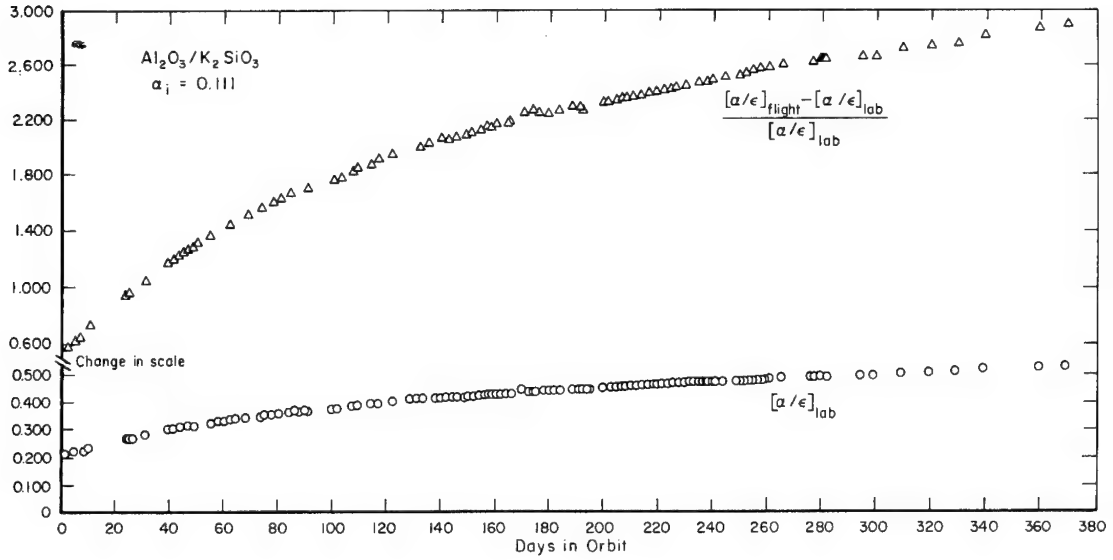

FIGURE C-8. ATS-1 FLIGHT DATA FOR Al_2O_3/K_2SiO_3 COATING[20]

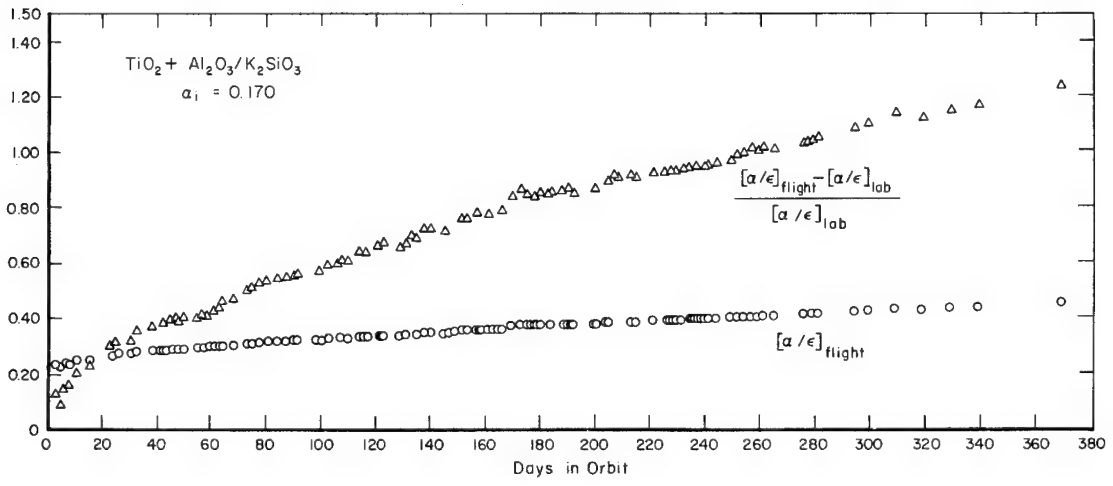

FIGURE C-9. FLIGHT DATA FOR $(TiO_2 + Al_2O_3)/K_2SiO_3$ COATING[20]

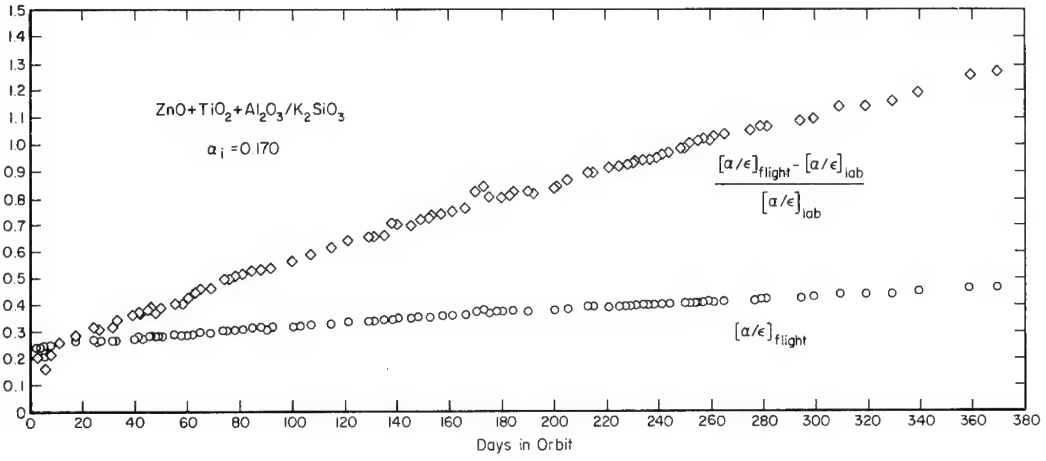

FIGURE C-10. ATS-1 FLIGHT DATA FOR ($ZnO + TiO_2 + Al_2O_3$)/ K_2SiO_3 COATING[20]

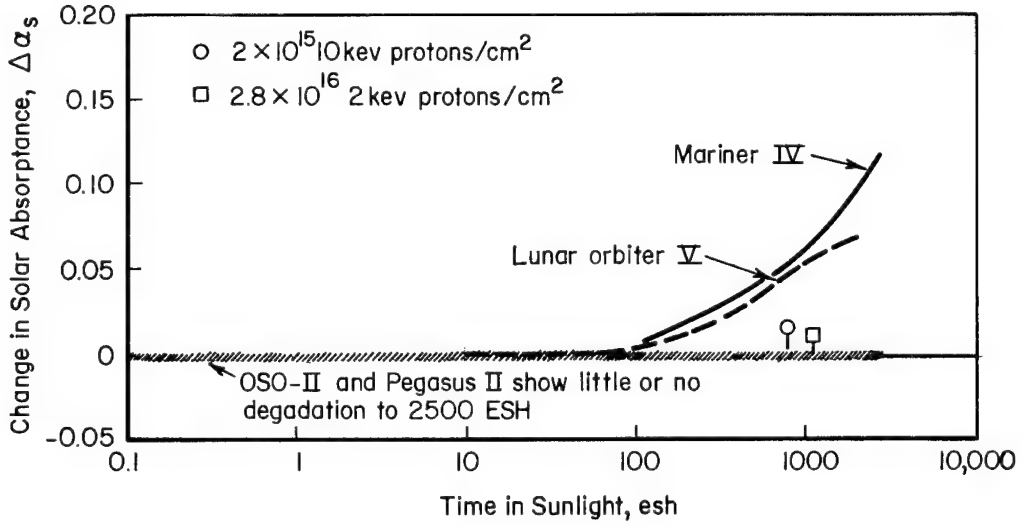

FIGURE C-11. ZINC OXIDE IN POTASSIUM SILICATE (Z-93)[13]

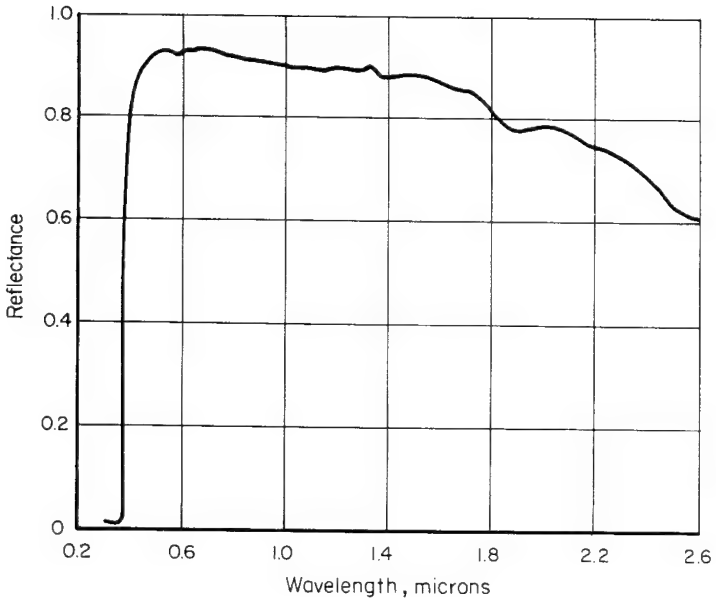

FIGURE C-12. INITIAL REFLECTANCE Z-93 USED ON LUNAR ORBITER[26]

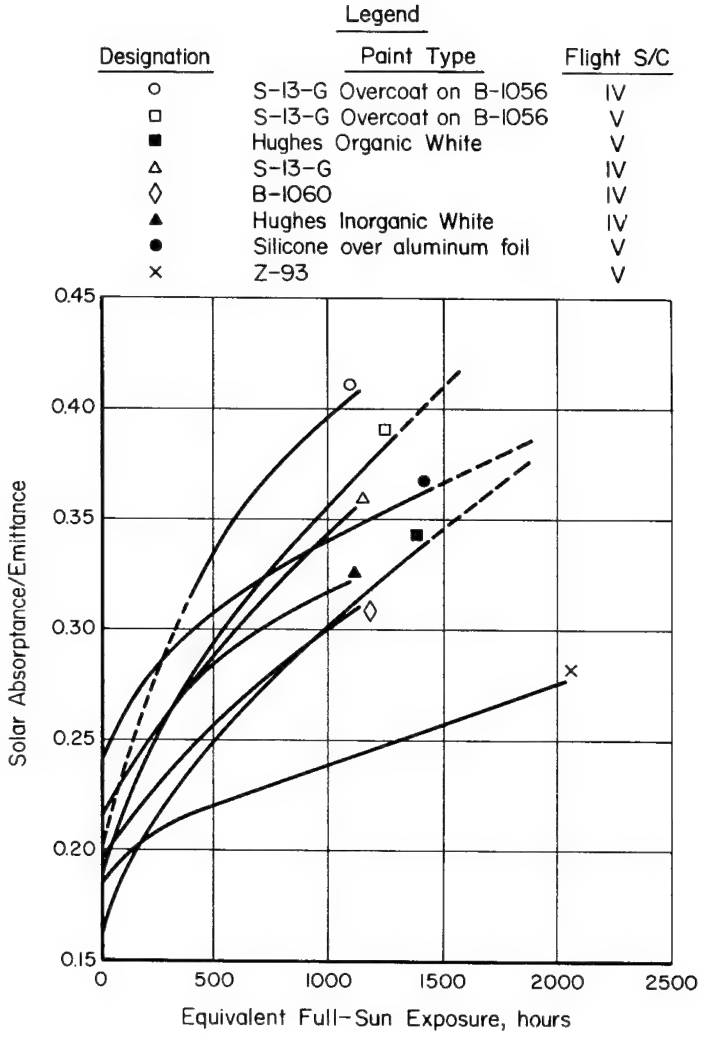

FIGURE C-13. ABSORPTANCE EMITTANCE RATIOS OF THERMAL COUPONS[26]

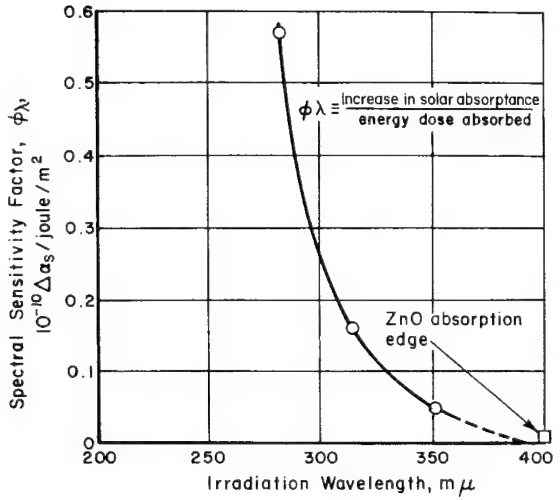

FIGURE C-14. SPECTRAL SENSITIVITY FACTOR VERSUS IRRADIATION WAVELENGTH FOR ZINC OXIDE/POTASSIUM SILICATE (Z-93) COATING[21]

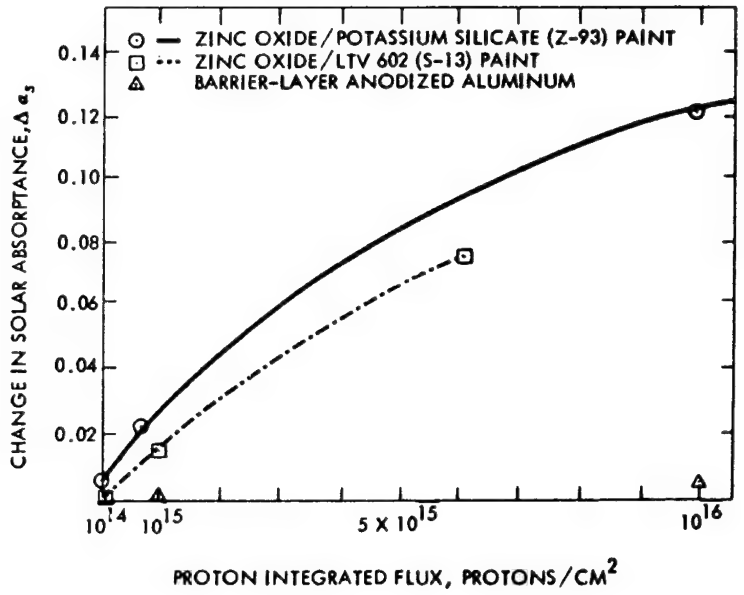

FIGURE C-15. EFFECT OF 8-keV PROTONS ON BARRIER-LAYER ANODIZED ALUMINUM AND SPACECRAFT PAINTS[43]

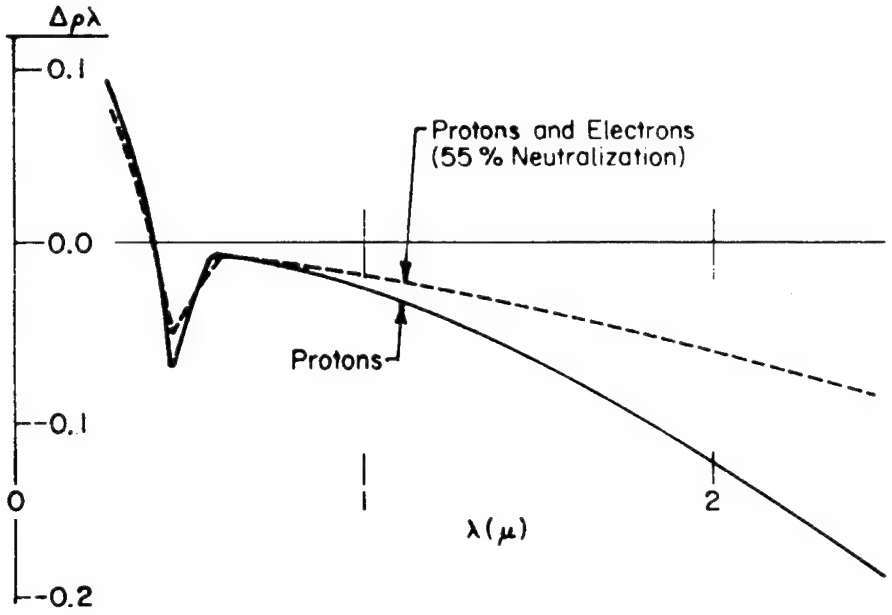

FIGURE C-16. CHANGE IN SPECTRAL REFLECTANCE OF ZnO IN K_2SiO_3 DUE TO PROTONS AND ELECTRONS, MEASURED IN SITU[40]

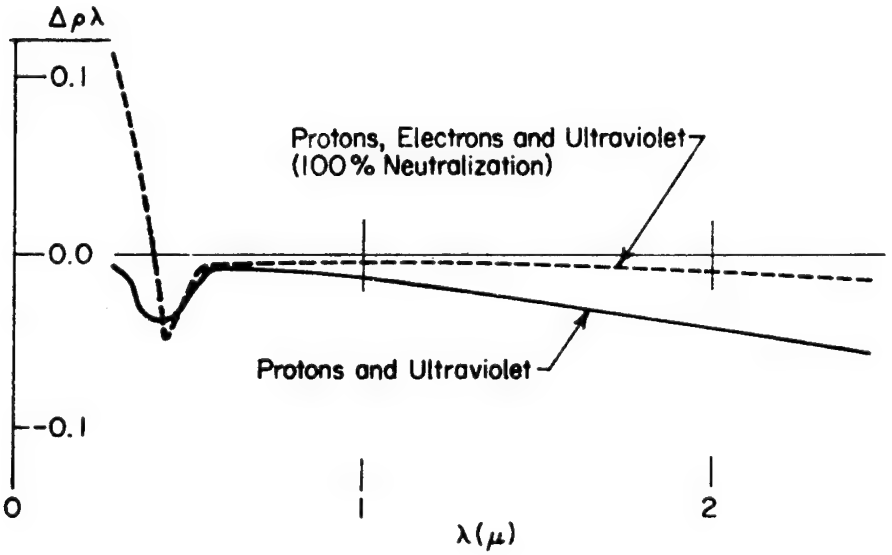

FIGURE C-17. CHANGE IN SPECTRAL REFLECTANCE OF ZnO IN K_2SiO_3 DUE TO PROTONS, ELECTRONS, AND ULTRAVIOLET, MEASURED IN SITU[40]

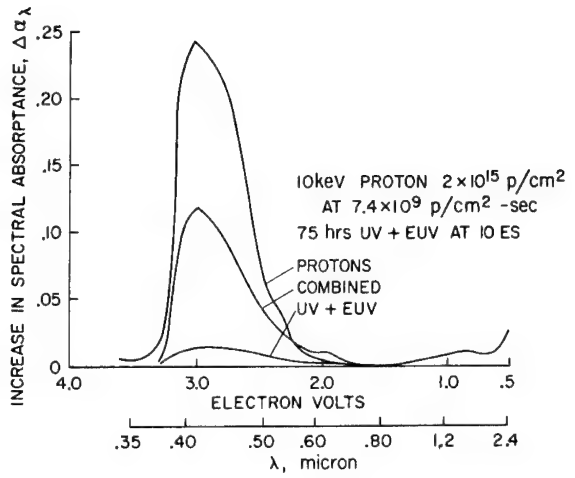

FIGURE C-18. THE INCREASE IN SPECTRAL ABSORPTANCE OF SPECIMENS IRRADIATED WITH COMBINED AND INDIVIDUAL ENVIRONMENTS AT 233 K[45]

EUV = solar vacuum ultraviolet
UV = 0.2 to 0.4 μ

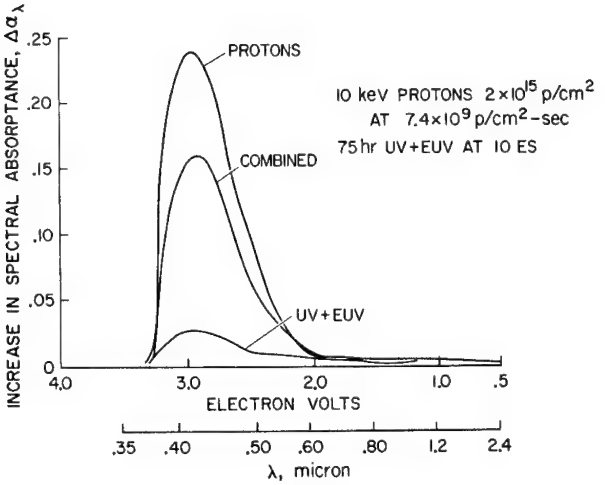

FIGURE C-19. THE INCREASE IN SPECTRAL ABSORPTANCE OF SPECIMENS IRRADIATED WITH COMBINED AND INDIVIDUAL ENVIRONMENTS AT 298 K[45]

EUV = solar vacuum ultraviolet
UV = 0.2 to 0.4 μ

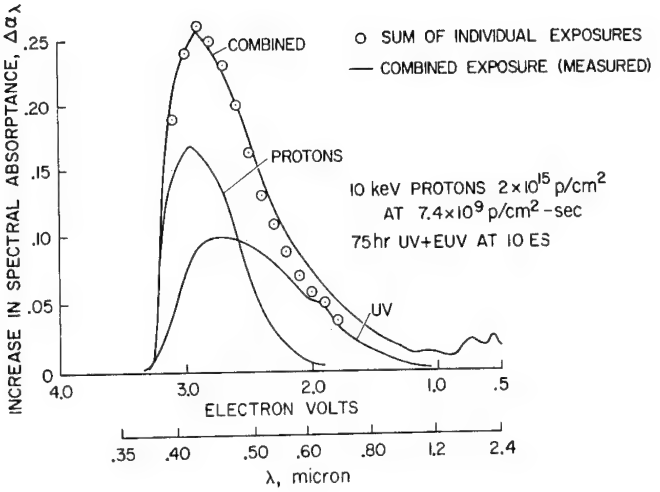

FIGURE C-20. THE INCREASE IN SPECTRAL ABSORPTANCE OF SPECIMENS IRRADIATED WITH COMBINED AND INDIVIDUAL ENVIRONMENTS AT 422 K[45]

EUV = solar vacuum ultraviolet
UV = 0.2 to 0.4 μ

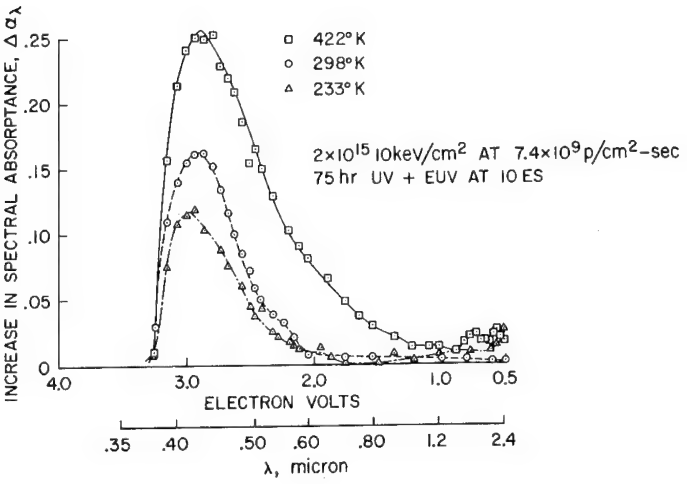

FIGURE C-21. THE INCREASE IN SPECTRAL ABSORPTANCE OF SPECIMENS IRRADIATED BY COMBINED ENVIRONMENTS AT TEMPERATURES OF 233, 298, AND 422 K[45]

EUV = solar vacuum ultraviolet
UV = 0.2 to 0.4 μ

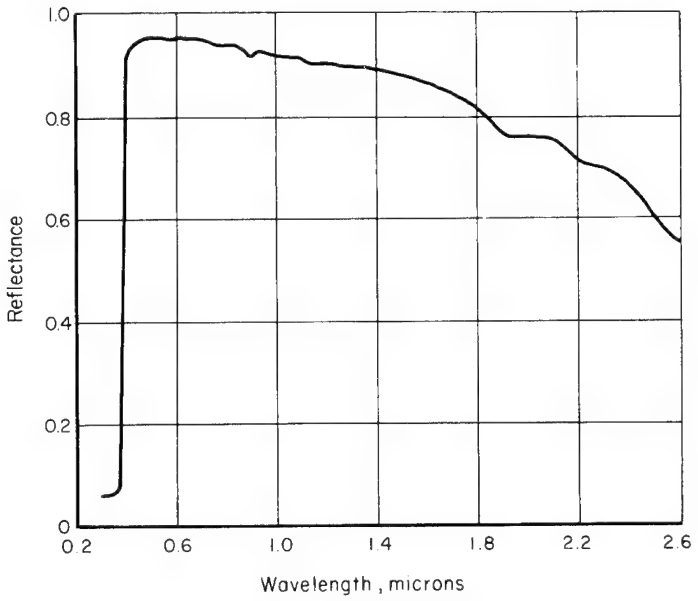

FIGURE C-22. INITIAL REFLECTANCE OF H-2 HUGHES INORGANIC COATING USED ON LUNAR ORBITER IV[26]

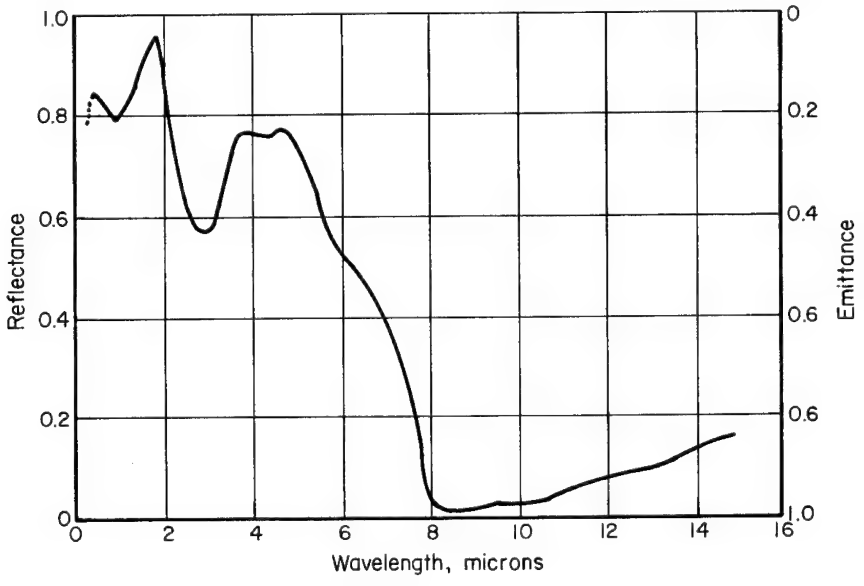

FIGURE C-23. OPTICAL PROPERTIES OF POLISHED ALUMINUM COATED WITH Al_2O_3[5]

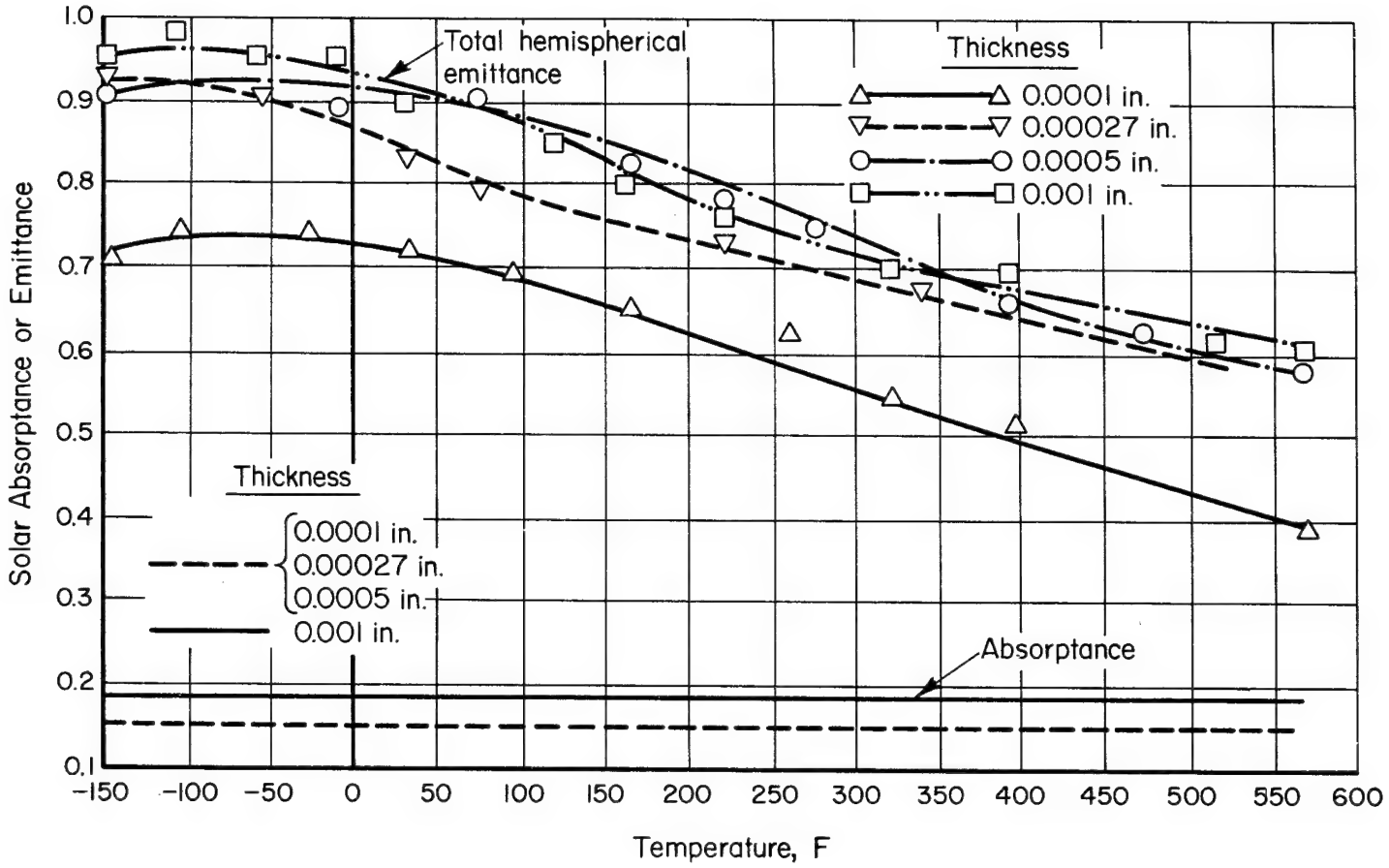

FIGURE C-24. TOTAL HEMISPHERICAL EMITTANCE AND ABSORPTANCE VERSUS TEMPERATURE OF THE Al-Al_2O_3 SYSTEM(5)

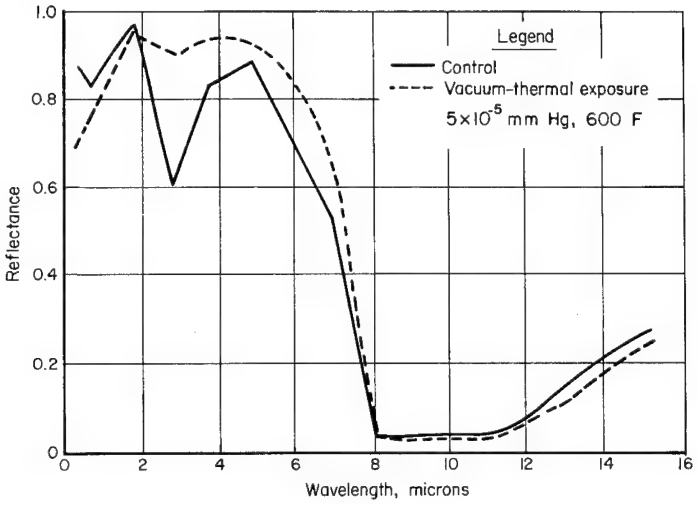

FIGURE C-25. EFFECT OF VACUUM-THERMAL EXPOSURE ON THE WATER-ABSORPTION BAND OF THE Al-Al_2O_3 SYSTEM(5)

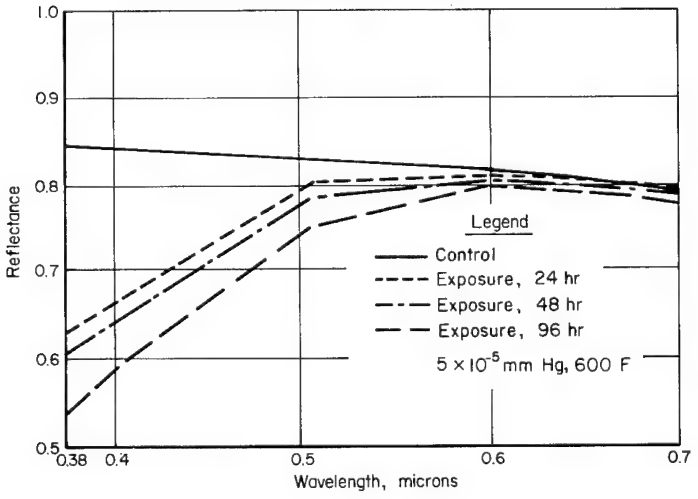

FIGURE C-26. EFFECT OF VACUUM-THERMAL EXPOSURE IN SHORT-WAVELENGTH REGION, 25 MINUTES ANODIZE(5)

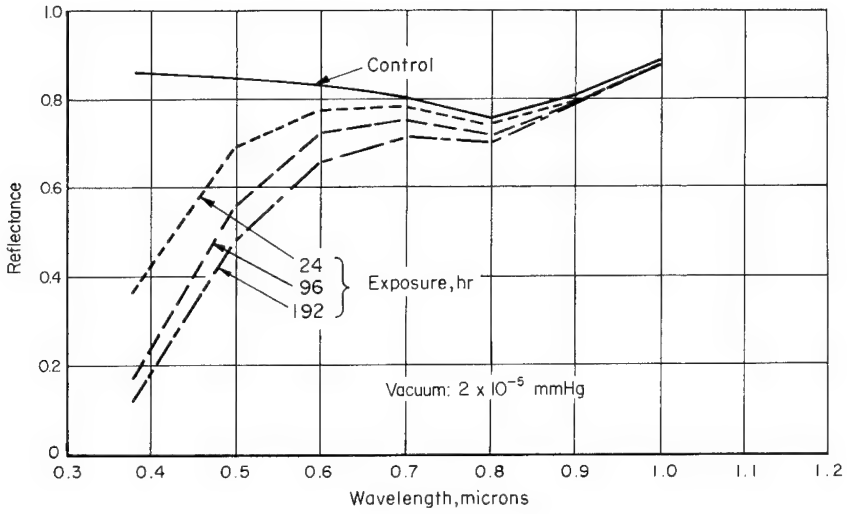

FIGURE C-27. EFFECT OF VACUUM-ULTRAVIOLET EXPOSURE ON BRIGHT ANODIZED ALUMINUM (0.0005 IN.)(5)

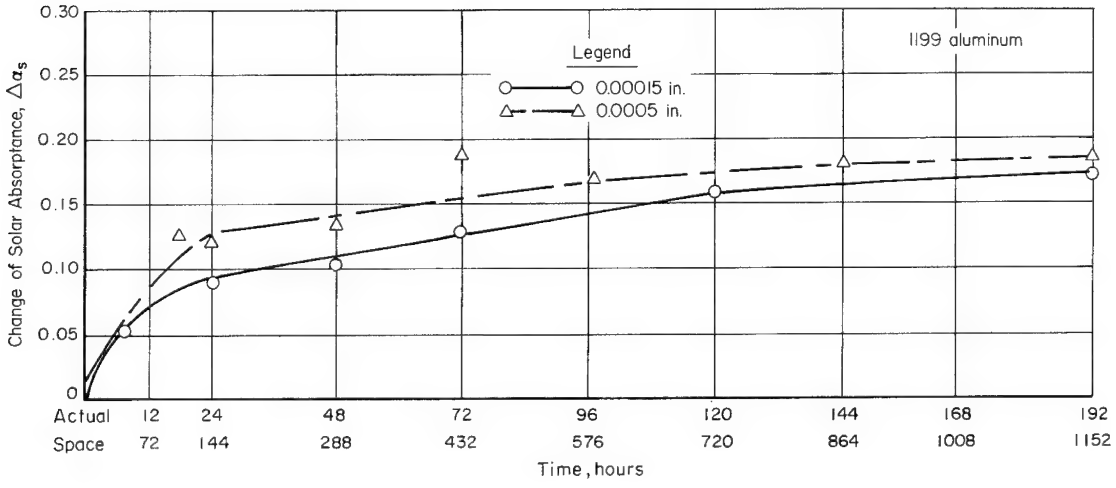

FIGURE C-28. CHANGE IN SOLAR ABSORPTANCE VERSUS TIME FOR VACUUM-ULTRAVIOLET EXPOSURE OF BRIGHT ANODIZED COATINGS(5)

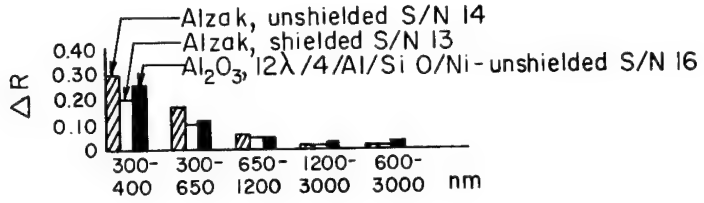

FIGURE C-29. CHANGE IN RELATIVE REFLECTANCE OF ALZAK AND Al_2O_3/Al AFTER 2000 ESH[47]

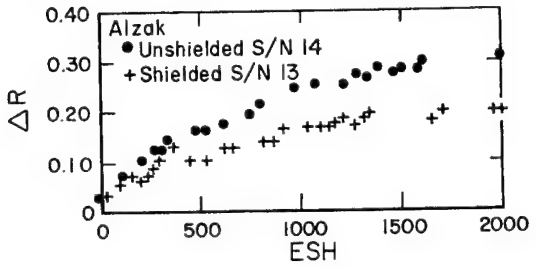

FIGURE C-30. RATE OF CHANGE OF RELATIVE REFLECTANCE OF ALZAK IN THE 300-400 nm BAND AS A FUNCTION OF ESH[47]

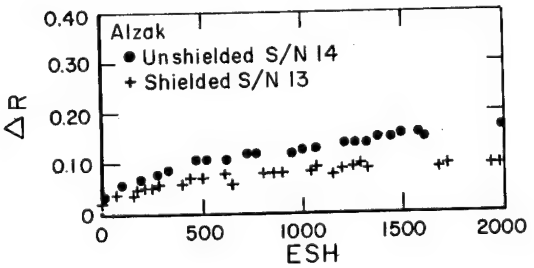

FIGURE C-31. RATE OF CHANGE OF RELATIVE REFLECTANCE OF ALZAK IN THE 300-650 nm BAND AS A FUNCTION OF ESH[47]

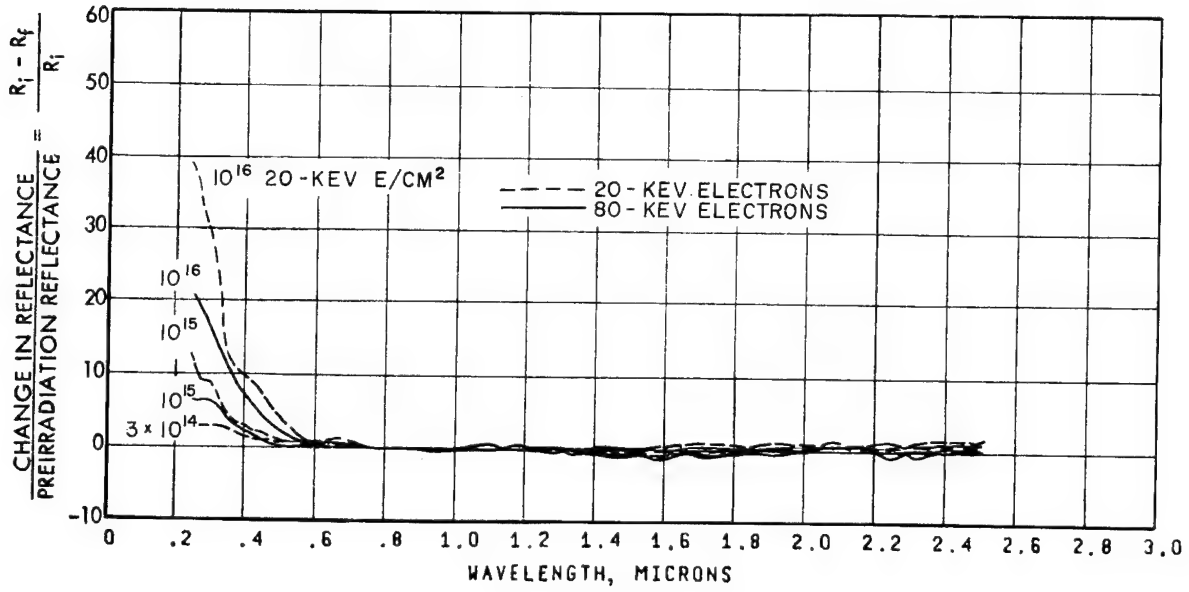

FIGURE C-32. DEPENDENCE OF REFLECTANCE DEGRADATION IN 0.15-MIL ALZAK UPON ELECTRON ENERGY[27]

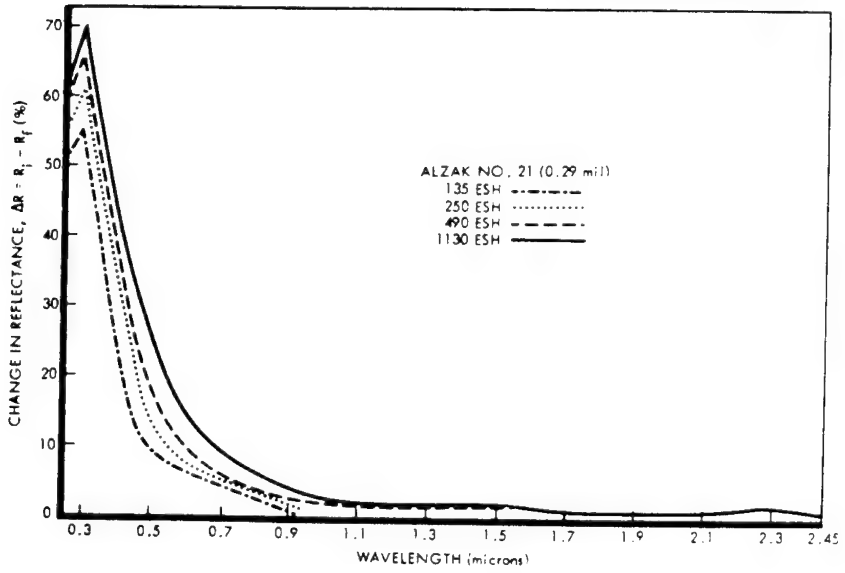

FIGURE C-33. REFLECTANCE CHANGES FOR SAMPLE TYPE ALZAK (0.29 MIL)[25]

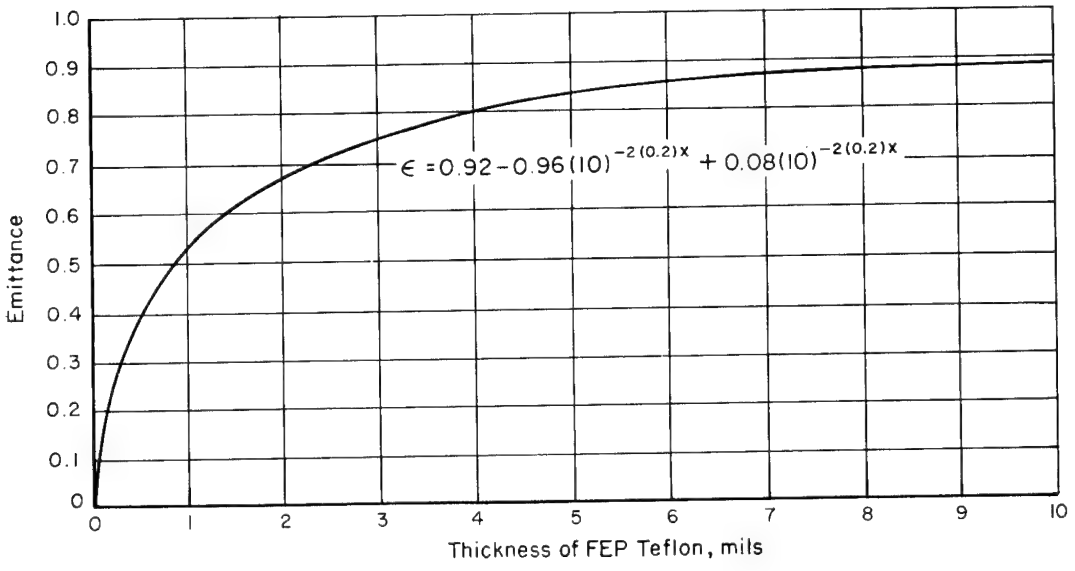

FIGURE C-34. THICKNESS OF FEP TEFLON VERSUS EMITTANCE[36]

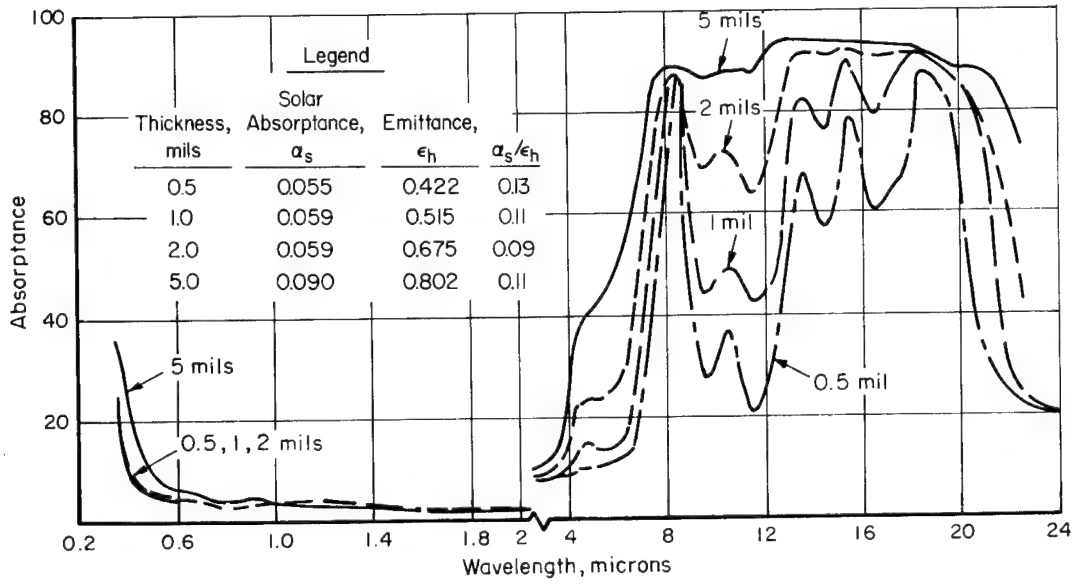

FIGURE C-35. SPECTRAL ABSORPTANCE OF SILVER-COATED TEFLON[36]

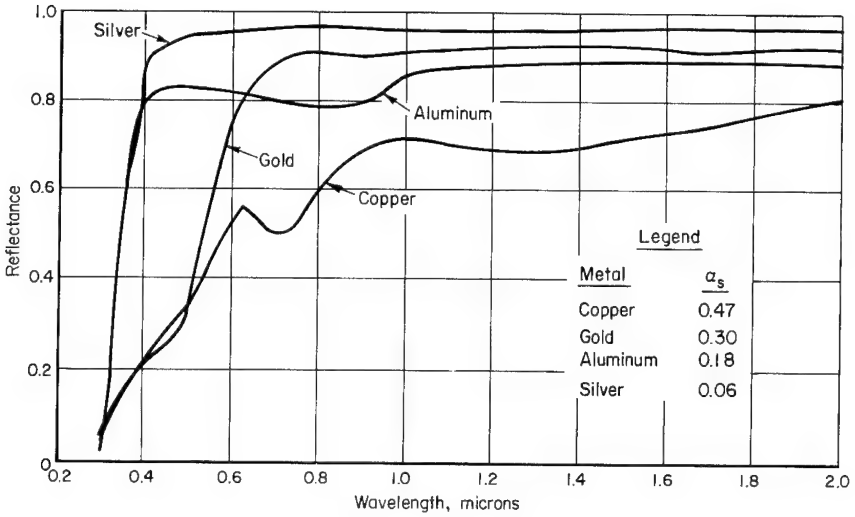

FIGURE C-36. REFLECTANCE OF 0.5-MIL-METALLIZED MYLAR(36)

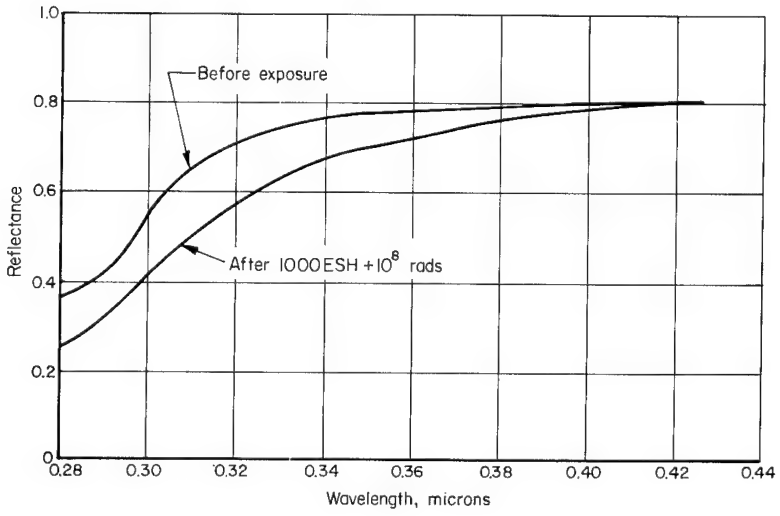

FIGURE C-37. EFFECT OF IRRADIATION ON ULTRAVIOLET REFLECTANCE OF BUTVAR SAMPLE 8-4(36)

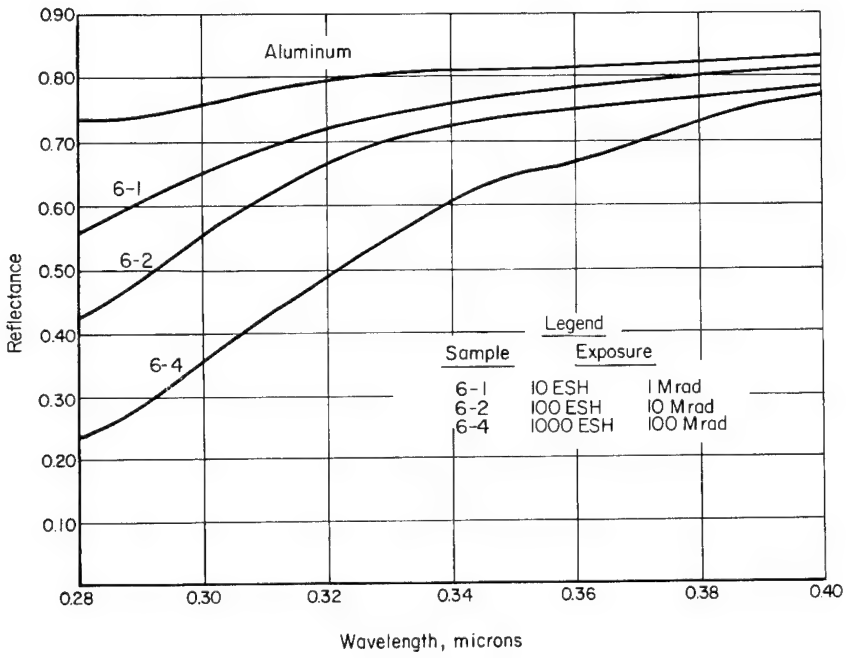

FIGURE C-38. EFFECT OF IRRADIATION ON THE ULTRAVIOLET REFLECTANCE OF SILICONE GE 391-15-170 ON ALUMINUM[36]

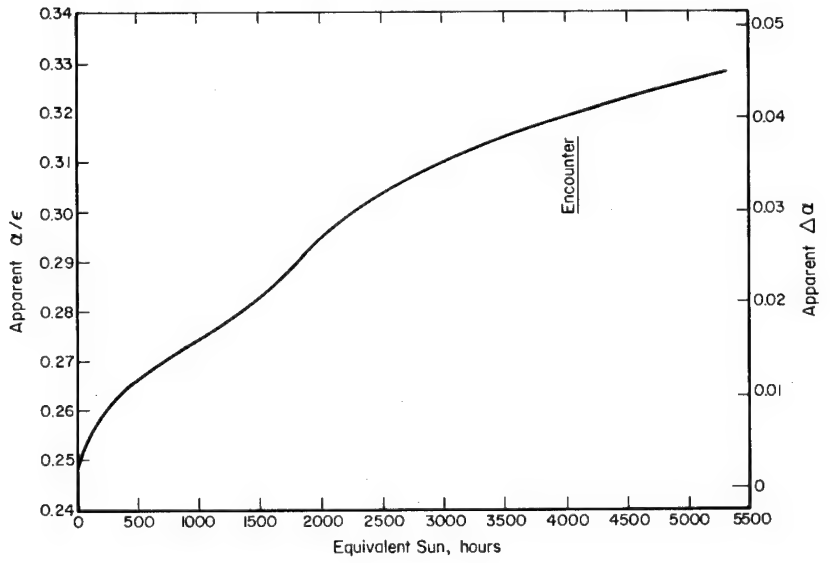

FIGURE C-39. APPARENT α/ε AND $\Delta\alpha$ OF ALUMINIZED 1-MIL FEP TEFLON[18]

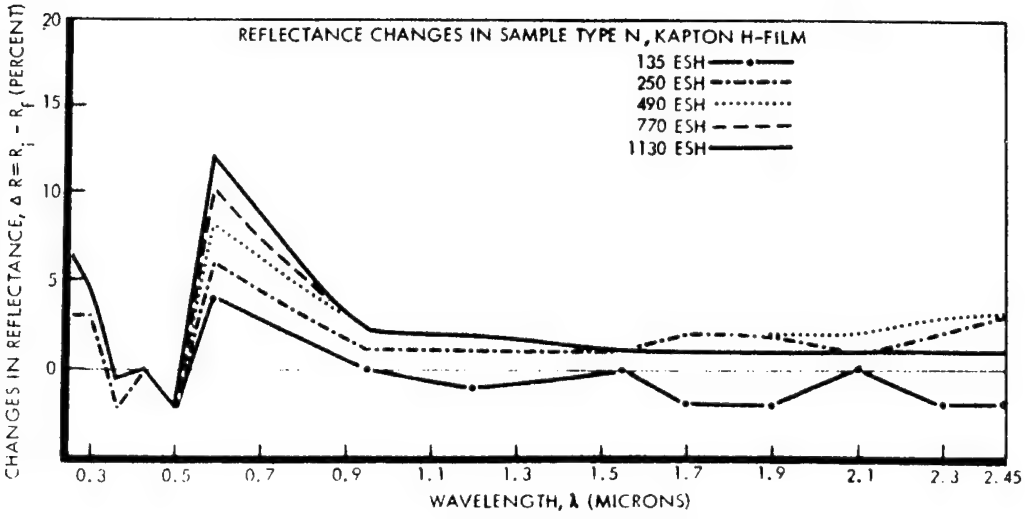

FIGURE C-40. SPECTRAL REFLECTANCE CHANGES IN KAPTON H FILM, FOLLOWING EXPOSURE TO ULTRAVIOLET RADIATION(3)

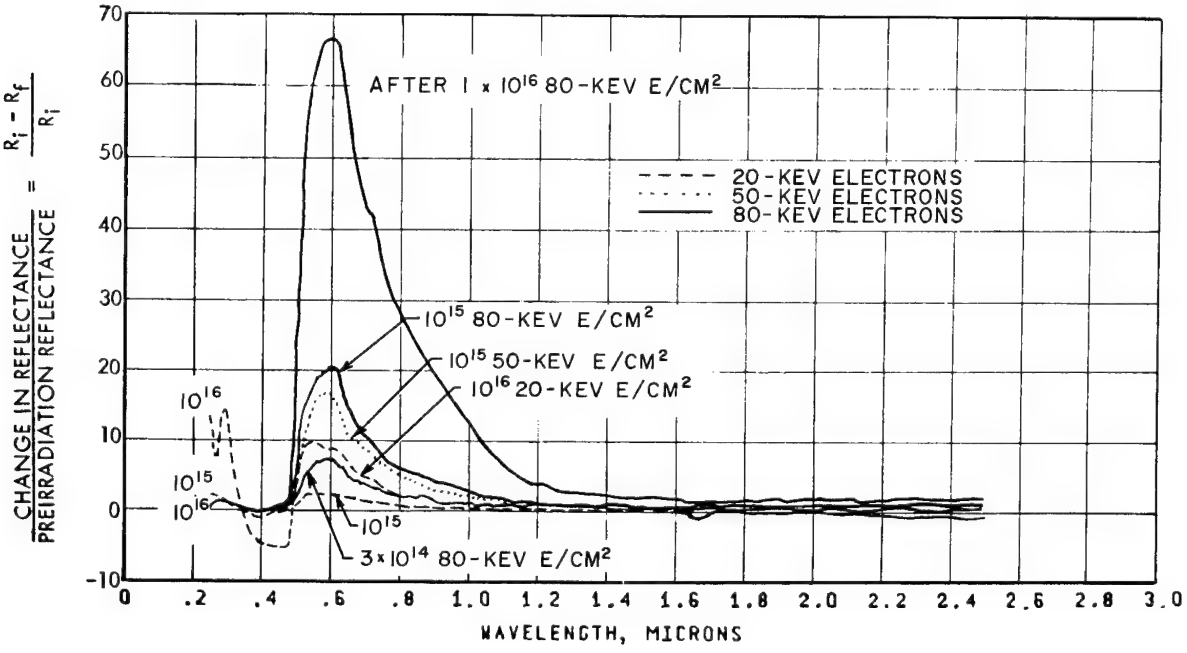

FIGURE C-41. DEPENDENCE OF REFLECTANCE DEGRADATION IN KAPTON H FILM UPON ELECTRON ENERGY(27)

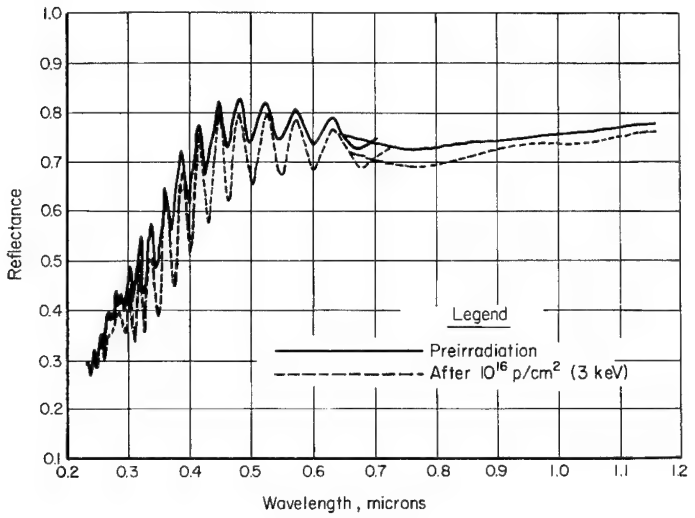

FIGURE C-42. SPECTRAL REFLECTANCE OF SiO-Al-KAPTON (1-3) IN VACUO[34]

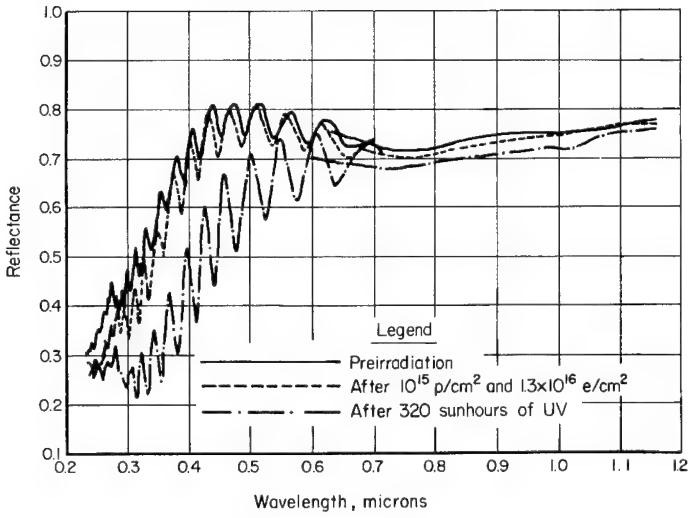

FIGURE C-43. SPECTRAL REFLECTANCE OF SiO-Al-KAPTON (2-1) IN VACUO[34]

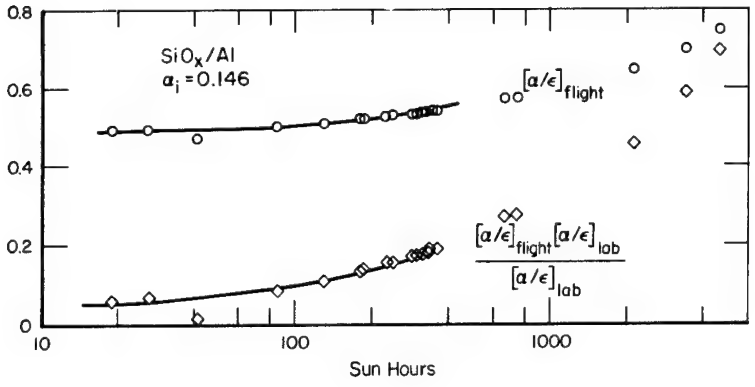

FIGURE C-44. ATS-1 FLIGHT DATA FOR SiO_x/Al COATING[20]

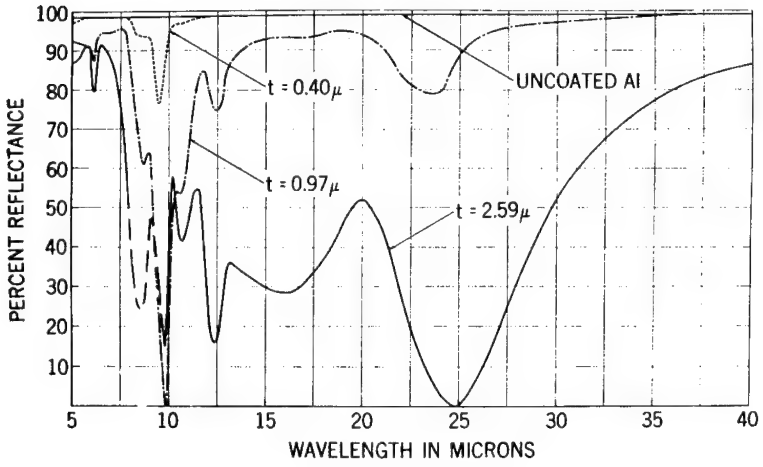

FIGURE C-45. INFRARED REFLECTANCE OF Al AND Al COATED WITH 0.40 μ, 0.97 μ, AND 2.59 μ OF SiO_2[52]

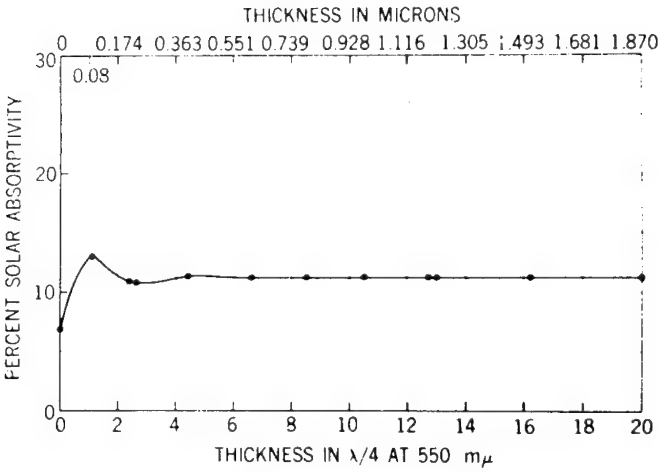

FIGURE C-46. MEASURED SOLAR ABSORPTIVITY OF Al COATED WITH SiO_2[52]

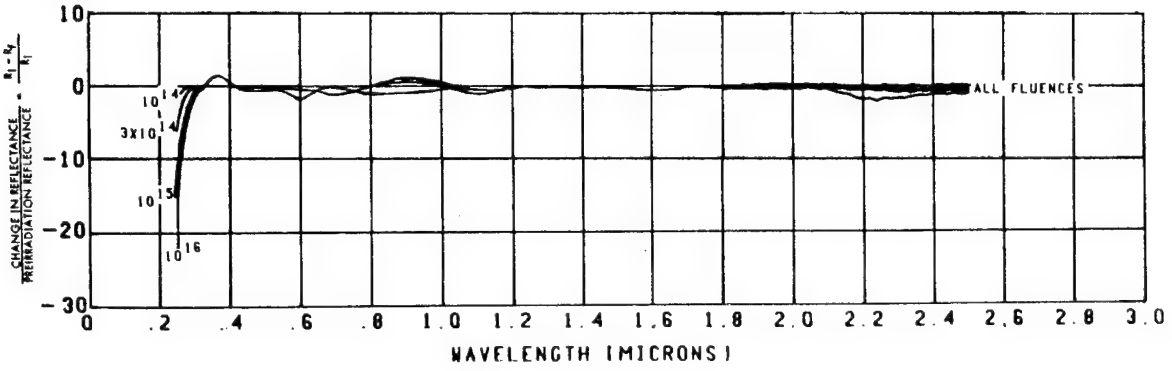

FIGURE C-47. REFLECTANCE CHANGES IN SiO_2 OVER Al DUE TO 20-keV ELECTRON EXPOSURE[27]

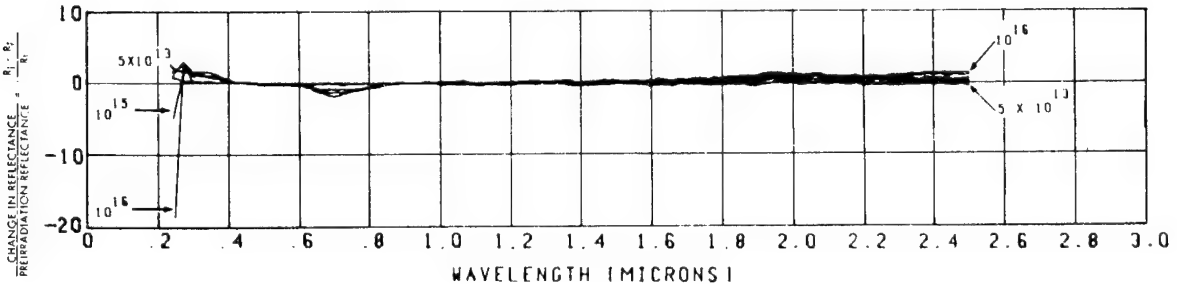

FIGURE C-48. REFLECTANCE CHANGES IN SiO_2 OVER Al DUE TO 80-keV ELECTRON EXPOSURE[27]

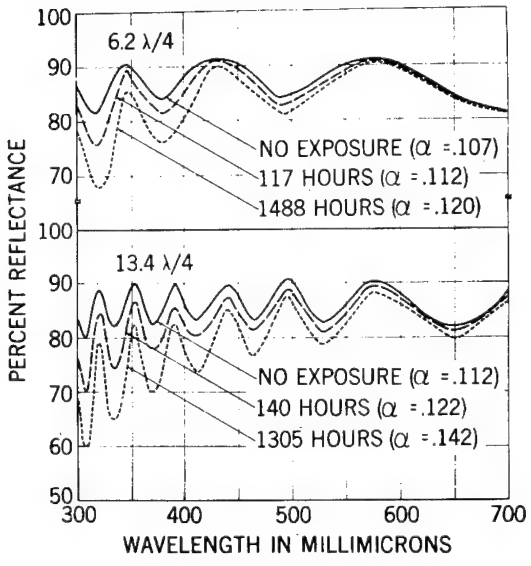

FIGURE C-49. EFFECT OF UV IRRADIATION IN OIL-FREE HIGH VACUUM ON THE REFLECTANCE OF Al COATED WITH 6.2 AND 13.4 QUARTER-WAVELENGTH-THICK FILMS OF SiO_2[52]

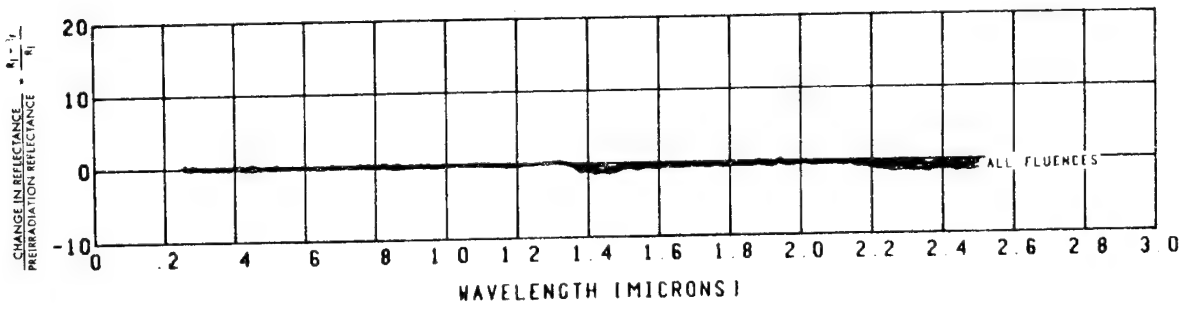

FIGURE C-50. REFLECTANCE CHANGES IN Al_2O_3 OVER Al DUE TO 20-keV ELECTRON EXPOSURE[27]

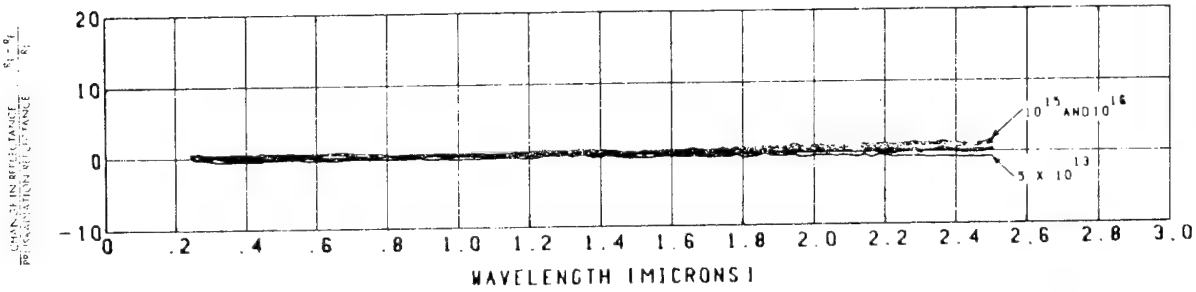

FIGURE C-51. REFLECTANCE CHANGES IN Al_2O_3 OVER Al DUE TO 80-keV ELECTRON EXPOSURE[27]

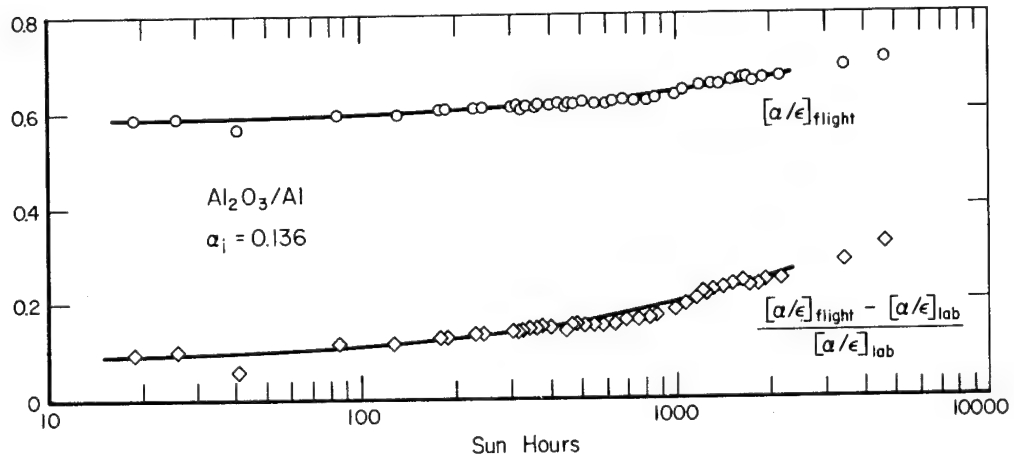

FIGURE C-52. ATS-1 FLIGHT DATA ON Al_2O_3/Al COATING[20]

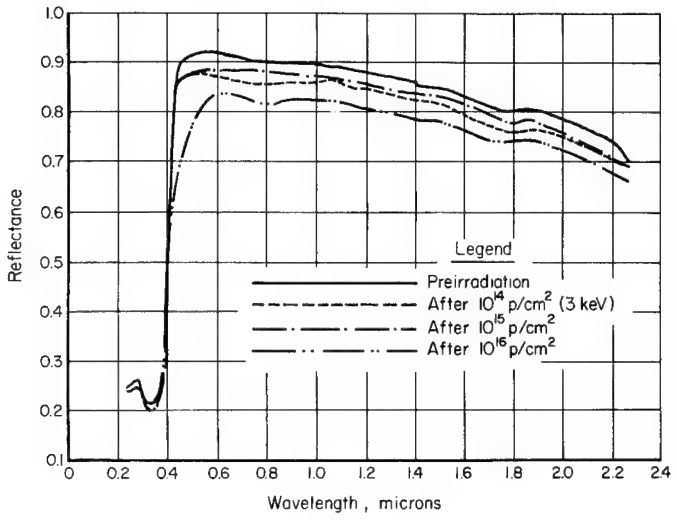

FIGURE C-53. SPECTRAL REFLECTANCE OF 3M202-A-10 (8-1) IN VACUO[34]

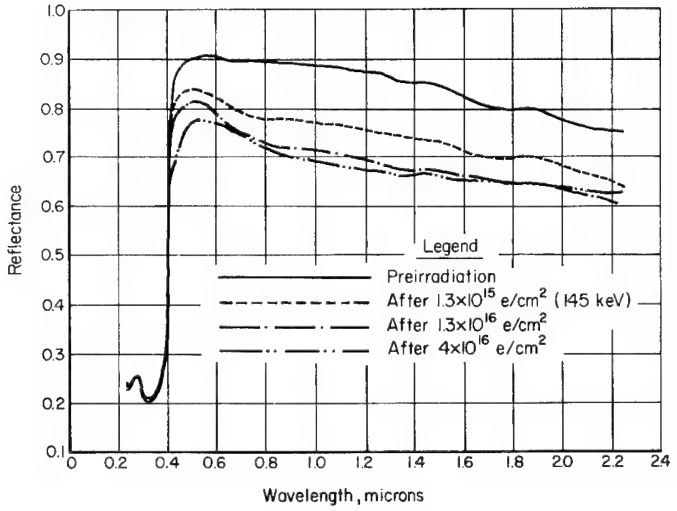

FIGURE C-54. SPECTRAL REFLECTANCE OF 3M202-A-10 (7-1) IN VACUO[34]

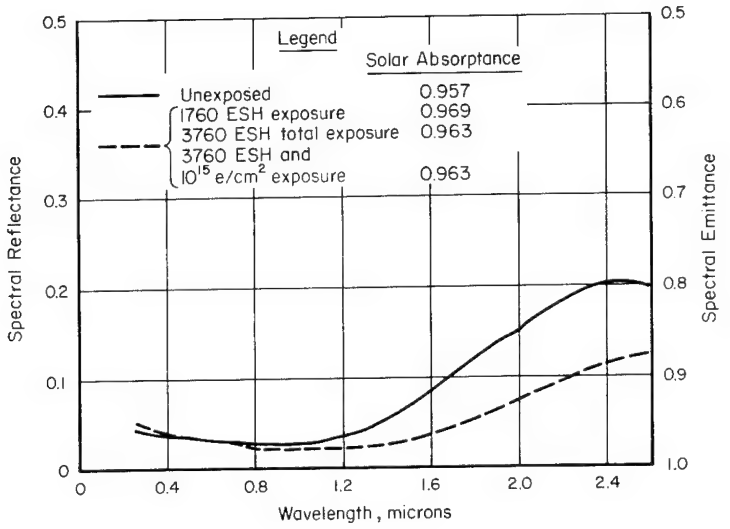

FIGURE C-55. SOLAR ABSORPTANCE OF CoS-DYED ANODIZED ALUMINUM[55]

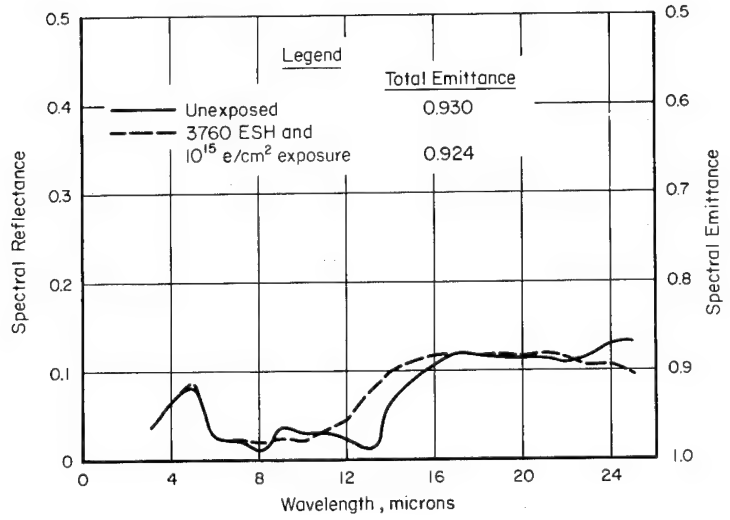

FIGURE C-56. EMITTANCE OF CoS-DYED ANODIZED ALUMINUM[55]

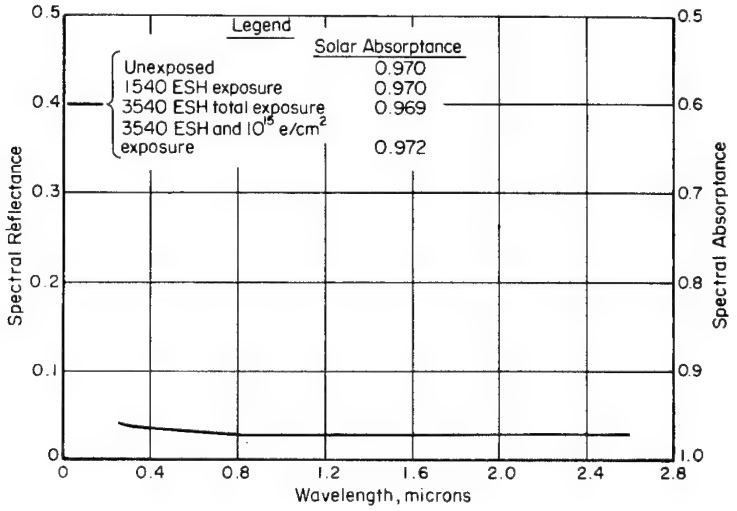

FIGURE C-57. SOLAR ABSORPTANCE OF NiS-DYED ANODIZED ALUMINUM(55)

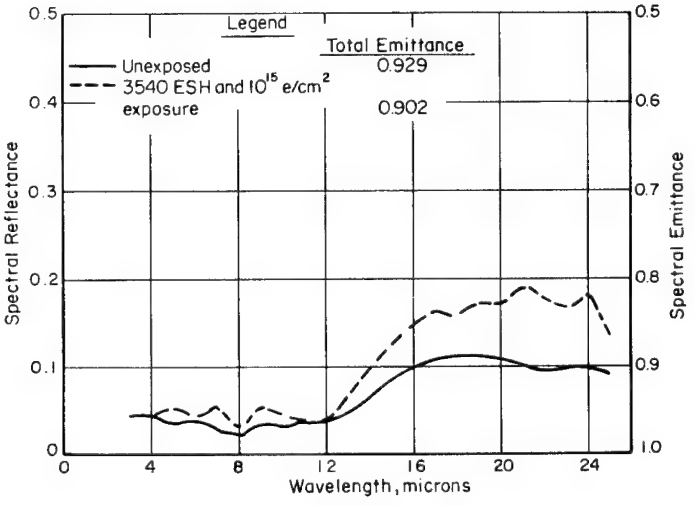

FIGURE C-58. EMITTANCE OF NiS-DYED ANODIZED ALUMINUM(55)

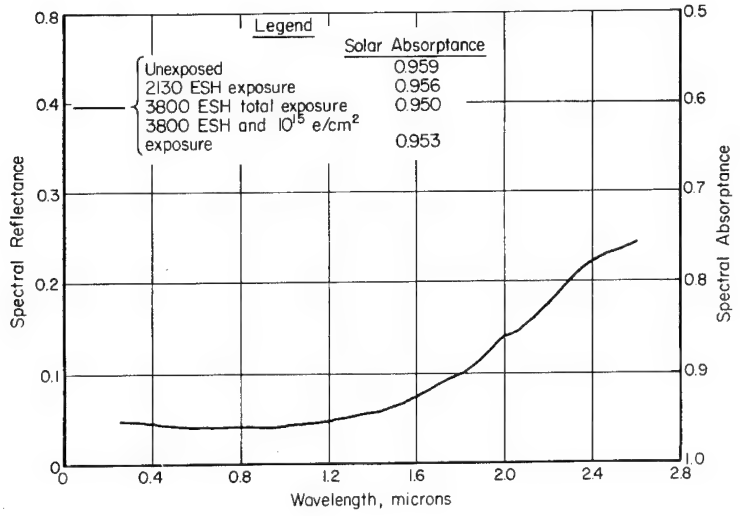

FIGURE C-59. SOLAR ABSORPTANCE OF BLACK NICKEL PLATE ON ALUMINUM(55)

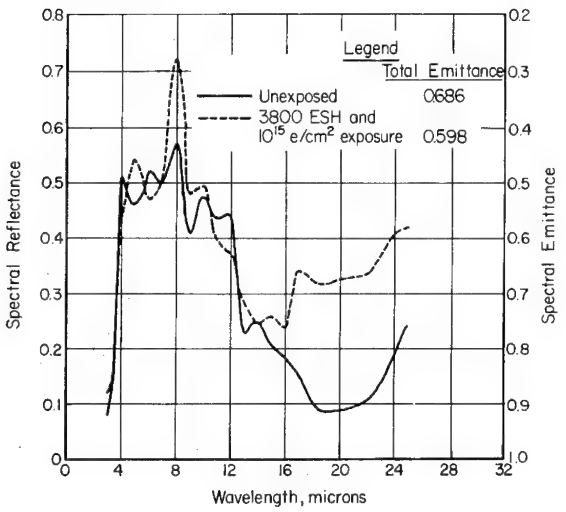

FIGURE C-60. EMITTANCE OF BLACK NICKEL PLATE ON ALUMINUM(55)

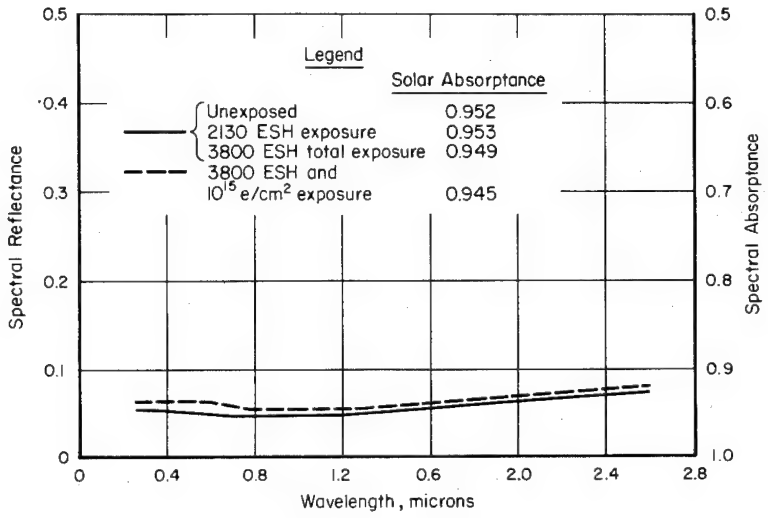

FIGURE C-61. SOLAR ABSORPTANCE OF DU-LITE 3-D ON GRIT-BLASTED TYPE 3-4 STAINLESS STEEL(55)

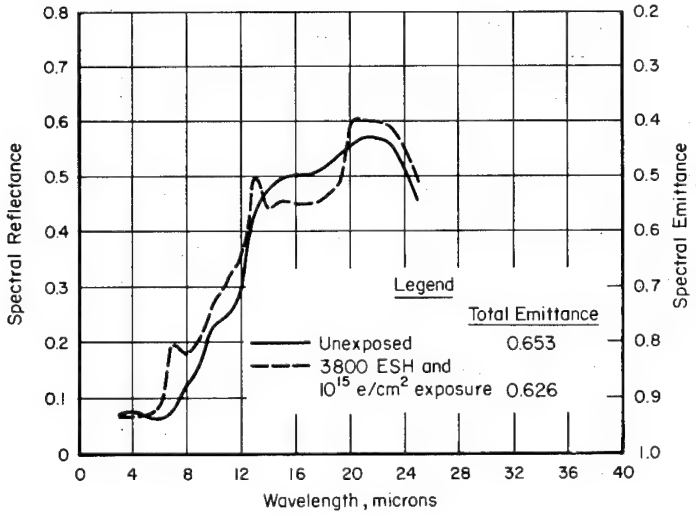

FIGURE C-62. EMITTANCE OF DU-LITE 3-D ON GRIT-BLASTED TYPE 3-4 STAINLESS STEEL(55)

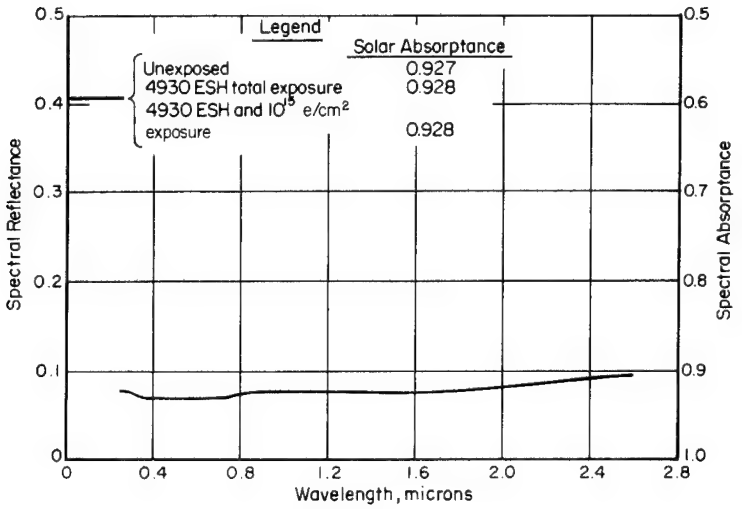

FIGURE C-63. SOLAR ABSORPTANCE OF WESTINGHOUSE BLACK ON INCONEL[55]

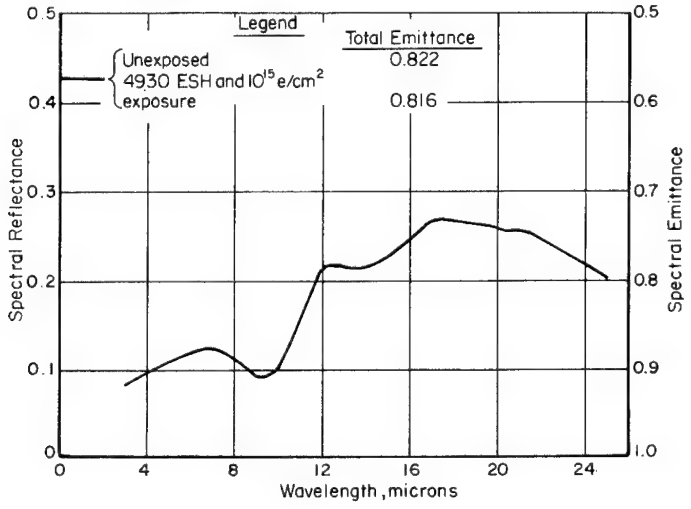

FIGURE C-64. EMITTANCE OF WESTINGHOUSE BLACK ON INCONEL[55]

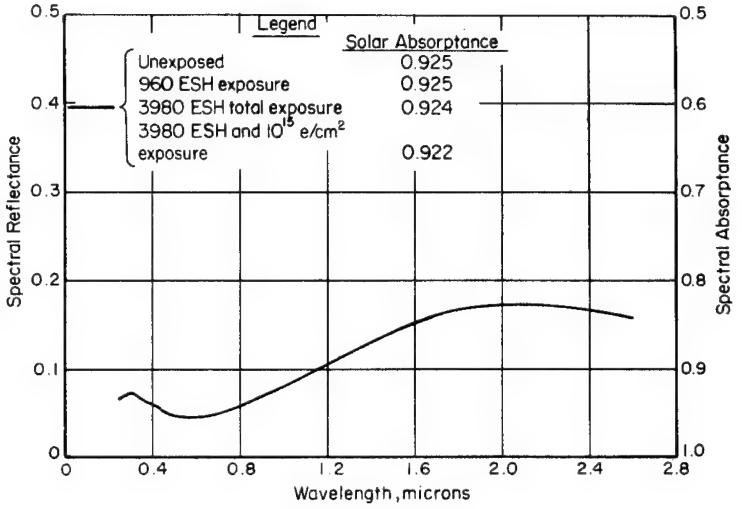

FIGURE C-65. SOLAR ABSORPTANCE OF SODIUM DICHROMATE-BLACKENED TYPE 347 STAINLESS STEEL(55)

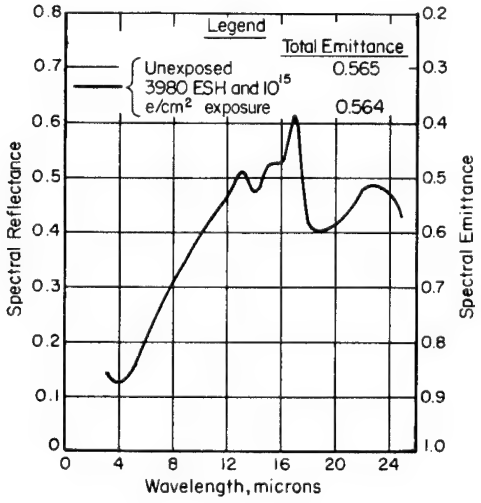

FIGURE C-66. EMITTANCE OF SODIUM DICHROMATE-BLACKENED TYPE 347 STAINLESS STEEL(55)

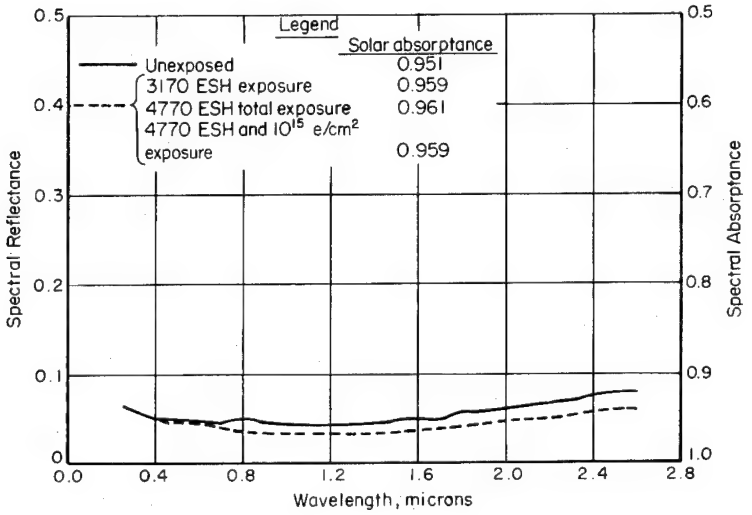

FIGURE C-67. ABSORPTANCE OF SODIUM DICHROMATE-BLACKENED INCONEL(55)

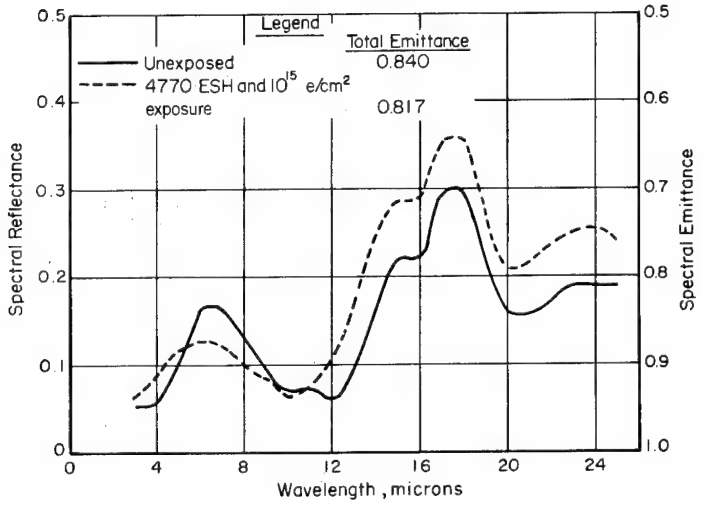

FIGURE C-68. EMITTANCE OF SODIUM DICHROMATE-BLACKENED INCONEL(55)

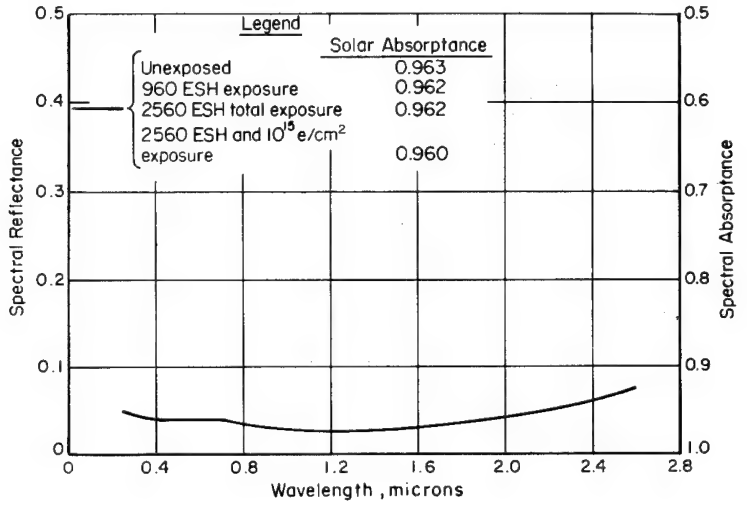

FIGURE C-69. SOLAR ABSORPTANCE OF SODIUM DICHROMATE-BLACKENED INCONEL X[55]

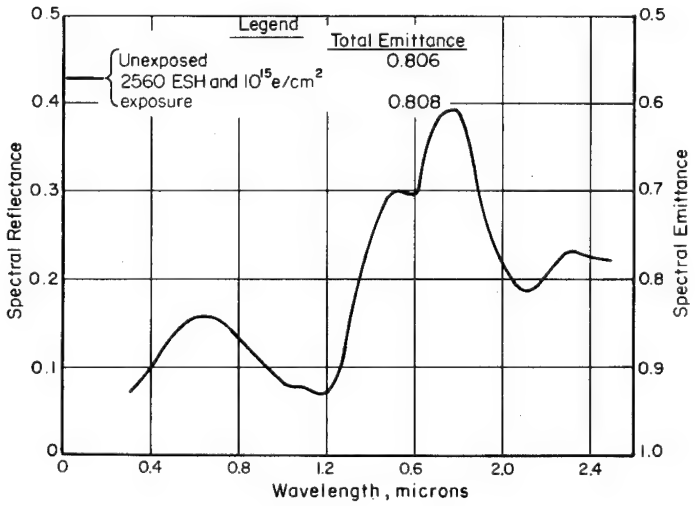

FIGURE C-70. EMITTANCE OF SODIUM DICHROMATE-BLACKENED INCONEL X[55]

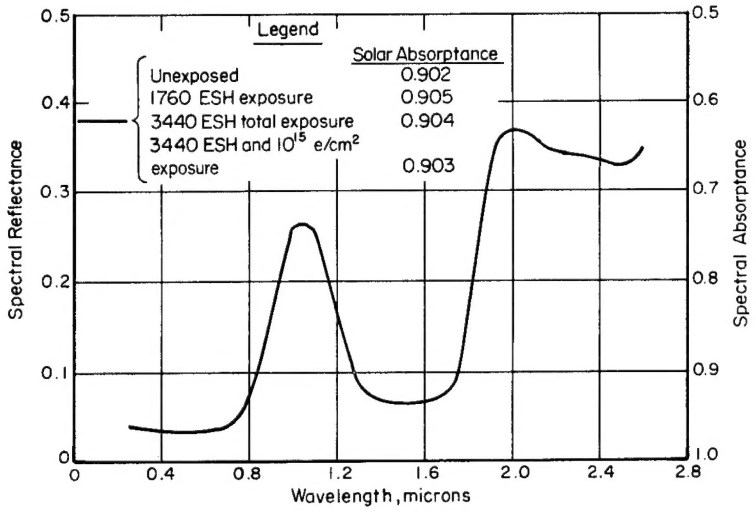

FIGURE C-71. SOLAR ABSORPTANCE OF PYROMARK BLACK ON ALUMINUM[55]

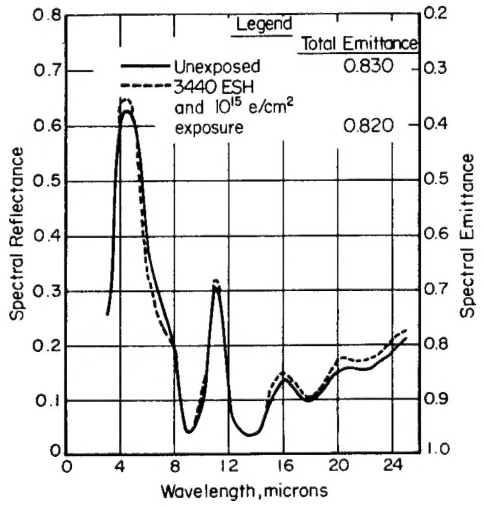

FIGURE C-72. EMITTANCE OF PYROMARK BLACK ON ALUMINUM[55]

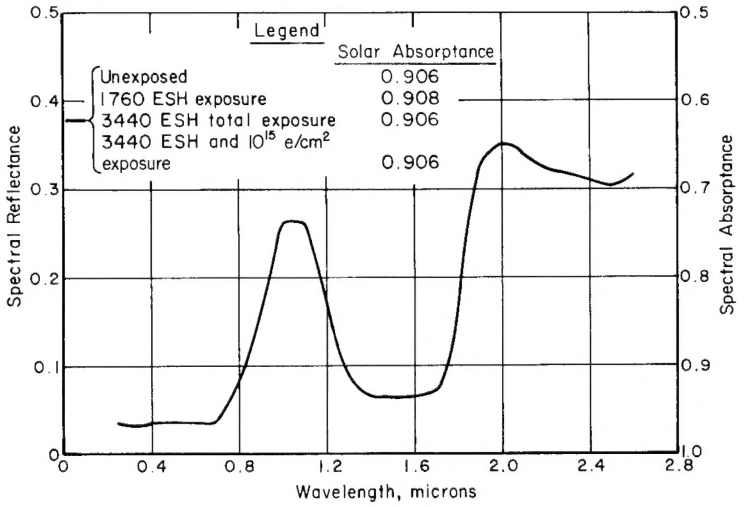

FIGURE C-73. SOLAR ABSORPTANCE OF PYROMARK BLACK ON INCONEL(55)

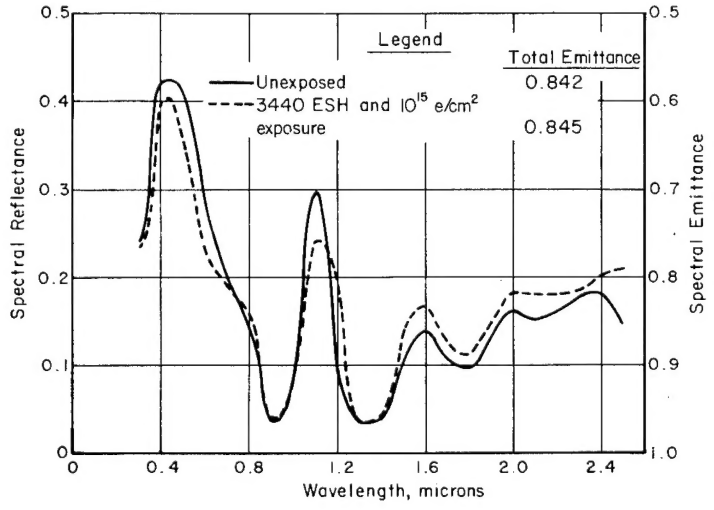

FIGURE C-74. EMITTANCE OF PYROMARK BLACK ON INCONEL(55)

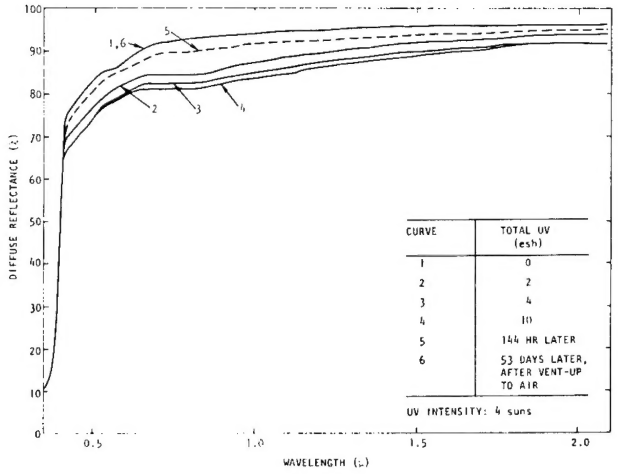

FIGURE C-75. EFFECT OF EXPOSURE TO UV AND RECOVERY (TiO_x-024-G2, NO BINDER)(62)

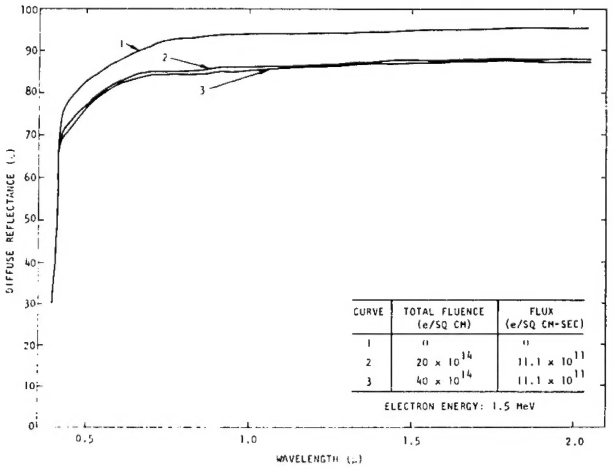

FIGURE C-76. EFFECT OF ELECTRON IRRADIATION ON DRY-PRESSED BINDERLESS SPECIMEN (TiO_x-028-G2)(62)

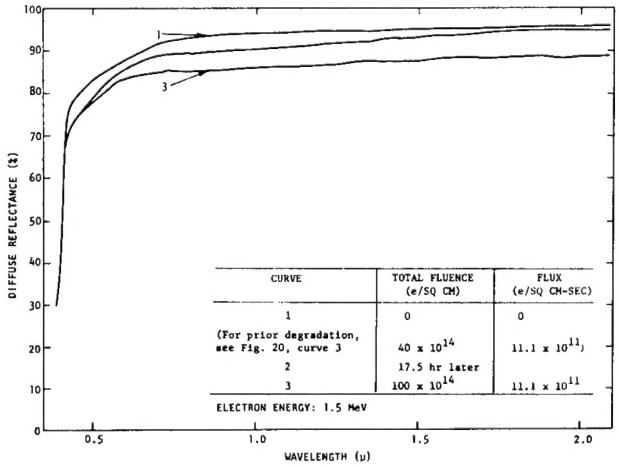

FIGURE C-77. EFFECT OF FURTHER ELECTRON IRRADIATION ON DRY-PRESSED BINDERLESS SPECIMEN (TiO_x-028-G2)(62)

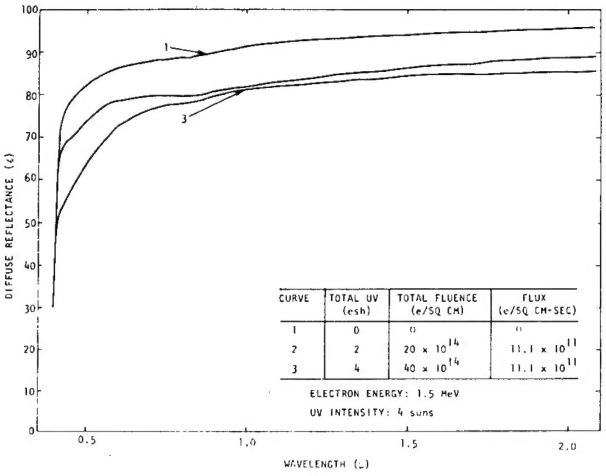

FIGURE C-78. EFFECT OF SIMULTANEOUS UV AND ELECTRON IRRADIATION OF DRY-PRESSED BINDERLESS SPECIMEN (TiO_X-026-G2)[62]

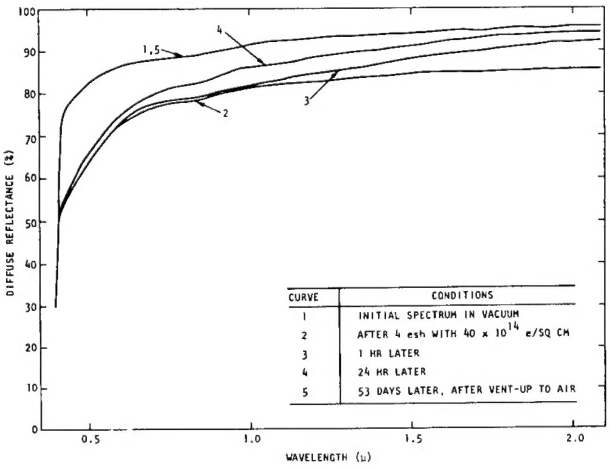

FIGURE C-79. RECOVERY AFTER SIMULTANEOUS UV AND ELECTRON IRRADIATION OF DRY-PRESSED BINDERLESS SPECIMEN (TiO_X-026-G2)[62]

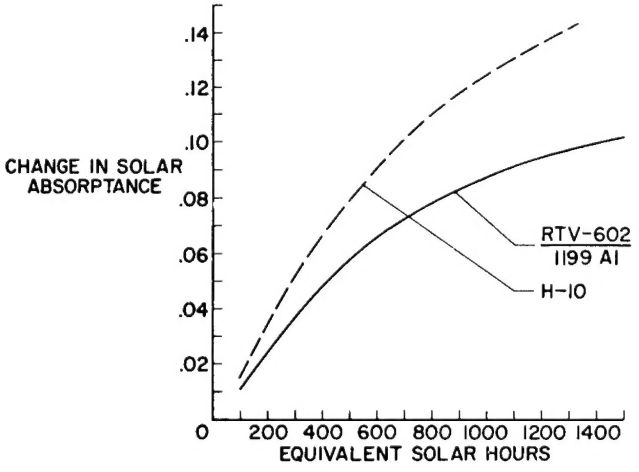

FIGURE C-80. CHANGE IN SOLAR ABSORPTANCE OF H-10 AND RTV-602 OVER 1199 ALUMINUM REFLECTOR SHEET[14]